

DEVELOPMENT OF SUPERIOR ASPHALT
RECYCLING AGENTS

Phase I: Technical Feasibility

Final Technical Progress Report

By
Jerry A. Bullin
Richard R. Davison
Charles J. Glover
Jay Chaffin
Meng Liu
Richard Madrid

July 1997

Work Performed Under Contract No. DE-FC04-93AL94460

For
U.S. Department of Energy
Office of Industrial Technologies
Washington, D.C.

By
Texas Transportation Institute
College Station, Texas

MASTER

DISCLAIMER

This report was prepared as an account of work sponsored by an agency of the United States Government. Neither the United States Government nor any agency thereof, nor any of their employees, makes any warranty, express or implied, or assumes any legal liability or responsibility for the accuracy, completeness, or usefulness of any information, apparatus, product, or process disclosed, or represents that its use would not infringe privately owned rights. Reference herein to any specific commercial product, process, or service by trade name, trademark, manufacturer, or otherwise does not necessarily constitute or imply its endorsement, recommendation, or favoring by the United States Government or any agency thereof. The views and opinions of authors expressed herein do not necessarily state or reflect those of the United States Government or any agency thereof.

This report has been reproduced directly from the best available copy.

Available to DOE and DOE contractors from the Office of Scientific and Technical Information, P.O. Box 62, Oak Ridge, TN 37831; prices available from (615)576-8401.

Available to the public from the U.S. Department of Commerce, Technology Administration, National Technical Information Service, Springfield, VA 22161, (703)487-4650.

DISCLAIMER

Portions of this document may be illegible in electronic image products. Images are produced from the best available original document.

DEVELOPMENT OF SUPERIOR ASPHALT
RECYCLING AGENTS

Phase I: Technical Feasibility

Final Technical Progress Report

By
Jerry A. Bullin
Richard R. Davison
Charles J. Glover
Jay Chaffin
Meng Liu
Richard Madrid

July 1997

Work Performed Under Contract No. DE-FC04-93AL94460

Prepared for
U.S. Department of Energy
Office of Industrial Technologies
Washington, D.C.

In Cooperation with
Texas A&M University
Research Foundation
Texas Transportation Institute
Department of Chemical Engineering

PREFACE

This report documents the technical progress made on the DOE funded project "Development of Superior Asphalt Recycling Agents" for the time period covering August 2, 1993 through November 1, 1996 with emphasis for the latter period from August 1995 to November 1996. Cost sharing for this study is being supplied by the Texas Department of Transportation and the Texas Advanced Technology Program. Bruce Cranford and Merrill Smith are the Program Managers for the DOE Office of Industrial Technologies. Porter Grace and Ken Lucien are the Technical Managers for the DOE Albuquerque Operations Office. Frank Childs, the Project Technical Monitor, is on the staff of Scientech, Inc., Idaho Falls, Idaho. Professors Jerry A. Bullin, Richard R. Davison and Charles J. Glover are the Co-Principal Investigators and are co-authors of this report along with Dr. Jay M. Chaffin, Dr. Meng Liu and current MS candidate Richard Madrid.

Work supported by the U.S. Department of Energy, Assistant Secretary for Energy Efficiency and Renewable Energy, Office of Industrial Technologies, under DOE Albuquerque Operations Office Cooperative Agreement DE-FC04-93AL94460.

Prior work has been reported in two earlier technical annual progress reports:

- (1) Bullin, J. A., et al., Development of Superior Asphalt Recycling Agents, Phase I: Technical Feasibility, DOE/AL/94460-1 (DE95016702), July 1995; and
- (2) Bullin, J.A., et al., Development of Superior Asphalt Recycling Agents, Phase I: Technical Feasibility, DOE/AL/94460-2 (DE97000258), April 1996.

TABLE OF CONTENTS

	Page
Preface	i
Table of Contents	ii
List of Figures	vii
List of Tables	xi
Chapter	
1 Introduction and Literature Survey	1
Physical Property/Chemical Composition Relationship	1
Asphalt Composition and Fractionation Methods	3
Standard Fractionation Methods	3
Supercritical Fractionation	10
Asphalt Aging	12
Recycling Studies	23
Summary	29
2 Executive Summary of Tasks	30
Task 1: Asphalt Fractionation and Source Asphalt Characterization	30
Description and Objectives of Task	30
Important Results	30
Task 2: Aged Asphalt Production	31
Description and Objectives of Task	31
Important Results	31
Task 3: Preliminary Agent Formulation and Blend Testing	32
Description and Objectives of Task	32
Important Results	33
Task 4: Expanded Blend Testing	36
Description and Objectives of Task	36

Important Results	37
Task 5: Rejuvenated Material Aging and Testing	38
Description and Objectives of Task	38
Important Results	38
Task 6: Mixing Rules Development	40
Description and Objectives of Task	40
Important Results	40
Task 7: Lime Additive Testing	42
Description and Objectives of Task	42
Important Results	42
Task 8: Other Additives (Amines) Testing	44
Description and Objectives of Task	44
Important Results	44
Task 9: Processing Schemes Development	45
Description and Objectives of Task	45
Important Results	45
Task 10: Projection Update and Commercialization Plan	45
Description and Objectives of Task	45
Projection Updates	45
Scale-Up and Commercialization Plan	46
Important Results	46
Task 11: Reports	46
Description and Objectives of Task	46
Technology Transfer	46
Reports	46
3 Oxidation Kinetics and an Aging Model for Asphalt Binders	47
Measurement of Oxidation	48
Asphalt Oxidation Kinetics	50
An Aging Model for Asphalt Binders	64

	Correlations for Property Parameters	67
	Feasibility of Evaluating Low Temperature Oxidation Rate by High Temperature Data	71
	Evaluation of the PAV Test	74
	Summary	80
4	Oxidation Kinetics of Asphalt Fractions	82
	Oxidation Kinetics of Generic Fractions	83
	Compositional Analysis of Supercritical Fractions	93
	Oxidation Kinetics of Supercritical Fractions	98
	Compositional Dependence of Asphalt Oxidation	103
	Summary	111
5	Physico-Chemical Correlations of Asphalt Fractions	113
	Hardening Susceptibility HS	114
	Asphaltene Formation Susceptibility AFS and Viscosity-Asphaltene Relationship	118
	Viscosity-Temperature Susceptibility	123
	Summary	128
6	Further Details on the Oxidation Mechanisms of Asphalt Binders	129
	Oxidation Products of the PA and NA Fractions	130
	Oxidation Products of the Supercritical Fractions	134
	Characterization of the Products of Aged NA and PA Fractions	134
	Oxygen Content-Carbonyl Content Correlation for Whole Asphalts	141
	Oxygen Content-Carbonyl Content Correlation for Aged NA and PA Fractions	145
	Summary	149
7	Lime-Treated Tank Asphalt Aging Studies	151
	Experimental Design	151
	Unaged Sample Properties	153
	Aging Studies	154
	Prediction of Ambient Performance	163

Summary	167
8 Recycling Studies	169
First Recycling Study Design	169
First Recycling Study Unaged Blend Properties	171
First Recycling Study Aging Results	171
Significance of Neat AAF-1 Data	179
Second Recycling Study Design	182
Second Recycling Study Unaged Blend Properties	184
Second Recycling Study Aging Results	189
Additional Kinetic Analyses	203
SHRP Performance Grading	206
Summary	211
9 Highly Aromatic Recycling Agents	213
Experimental Design	213
Experimental Methods	214
Recycled Asphalt Blending	214
POV-Aging	215
Results and Discussion	215
Conclusions	221
10 Procession Schemes and Implementation	222
Processing Schemes and Cost	222
Use Existing 3-Stage SCE Unit	223
Construct a 3-Stage Unit	223
Add a 2 or 3-Stage Unit to an Existing 2-Stage Facility	226
Build a 4 or 5-Stage Unit	226
Add a Solvent Extraction Unit to an Existing DAO Unit	227
Implementation	229
References	231
Abbreviations	244

Notation	245
Appendix A: Experimental Methods	246
Supercritical Fractionation	246
Process Description	246
Aged Asphalt Production	249
Pressure Oxygen Vessel (POV)	250
Corbett Analysis	252
Corbett Analysis Using N-Hexane Precipitation and High Performance Liquid Chromatography (HPLC)	252
Fourier Transform Infrared Spectroscopy (FTIR)	253
Dynamic Mechanical Analysis (DMA)	253
Gel Permeation Chromatography (GPC)	254
Microductility Measurements	254
Appendix B: The Use of HPLC to Determine the Saturate Content of Heavy Petroleum Products	255
Appendix C: Supercritical Fractions as Asphalt Recycling Agents and Preliminary Aging Studies on Recycled Asphalts	257
Appendix D: The Effects of Asphaltenes on the Chemical and Physical Characteristics of Asphalt	259
Appendix E: Effects of Asphaltenes on Asphalt Recycling and Aging	261
Appendix F: The Effect of Asphalt Composition on the Formation of Asphaltenes and Their Contribution to Asphalt Viscosity	263
Appendix G: Interstate 45 Recycling	265
Appendix H: Viscosity Mixing Rules for Asphalt Recycling	267
Appendix I: Use of Lime in Recycling Asphalt	269
Appendix J: Economic Summary	270

LIST OF FIGURES

	Page
Figure 3-1. FTIR spectra of unaged and aged SHRP AAA-1	49
Figure 3-2. Carbonyl area vs. aging time for SHRP AAA-1 (C1-C7)	51
Figure 3-3. Carbonyl area vs. aging time for SHRP AAF-1 (C1-C7)	51
Figure 3-4. Carbonyl area vs. aging time for SHRP AAG-1 (C1-C7)	52
Figure 3-5. Carbonyl area vs. aging time for SHRP AAA-1 (C8-C13)	52
Figure 3-6. Carbonyl area vs. aging time for SHRP AAF-1 (C8-C13)	53
Figure 3-7. Carbonyl area vs. aging time for SHRP AAG-1 (C8-C13)	53
Figure 3-8. Oxidation rate vs. aging temperature for SHRP AAA-1	60
Figure 3-9. Oxidation rate vs. aging temperature for SHRP AAG-1	60
Figure 3-10. Hardening susceptibility of SHRP AAA-1	62
Figure 3-11. Hardening susceptibility of SHRP AAG-1	62
Figure 3-12. Graphical demonstration of the proposed aging test	66
Figure 3-13. Isokinetic diagram for the ten asphalts studied	68
Figure 3-14. Activation energy vs. pressure reaction order	68
Figure 3-15. Initial jump pressure factor vs. pressure reaction order	70
Figure 3-16. HS pressure factor vs. pressure reaction order	70
Figure 3-17. Initial jump pressure factor vs. HS pressure factor	71
Figure 3-18. Oxidation rate vs. temperature for five asphalts	73
Figure 3-19. Oxidation rate vs. temperature for another five asphalts	73
Figure 3-20. Aging indices by PAV test and low T, low P aging	80
Figure 4-1. GPC spectra of ANA and APA	84
Figure 4-2. GPC spectra of the five NA fractions	85
Figure 4-3. GPC spectra of the five PA fractions	85
Figure 4-4. Carbonyl area vs. aging time for APA	87
Figure 4-5. Carbonyl area vs. aging time for ANA	88
Figure 4-6. Carbonyl area vs. aging time for GPA	88

Figure 4-7.	Carbonyl area vs. aging time for GNA	90
Figure 4-8.	Arrhenius plots for AAA-1 and fractions	91
Figure 4-9.	Arrhenius plots for the PA fractions	92
Figure 4-10.	Arrhenius plots for the NA fractions	92
Figure 4-11.	GPC spectra of supercritical fractions of AAF-1	96
Figure 4-12.	GPC spectra of AAF-1 fractions	96
Figure 4-13.	GPC spectra of various PA derived from AAF-1	97
Figure 4-14.	GPC spectra of various NA derived from AAF-1	97
Figure 4-15.	GPC spectra of various asphaltenes derived from AAF-1	98
Figure 4-16.	GPC spectra of various saturates derived from AAF-1	99
Figure 4-17.	Carbonyl area vs. aging time for F1F	100
Figure 4-18.	Carbonyl area vs. aging time for F4F	100
Figure 4-19.	Oxidation rate vs. aging temperature for supercritical fractions	102
Figure 4-20.	Oxidation rate vs. aging temperature for AAF-1 fractions	104
Figure 4-21.	The effect of saturate addition on the oxidation rate	108
Figure 4-22.	The effect of asphaltene addition on the oxidation rate	108
Figure 4-23.	CA growth rates of whole asphalts and aromatics fractions	110
Figure 4-24.	CA growth rates of aromatics measured and calculated	110
Figure 5-1.	Hardening susceptibility of NA fractions	115
Figure 5-2.	Hardening susceptibility of PA fractions	115
Figure 5-3.	Hardening susceptibility of AAF-1 fractions	117
Figure 5-4.	Hardening susceptibility of ANA at four temperatures	118
Figure 5-5.	Hardening susceptibility of APA at two temperatures	119
Figure 5-6.	AFS for the five NA fractions	119
Figure 5-7.	AFs for the five PA fractions	120
Figure 5-8.	AFS (slope of asphaltene percentage vs. CA) for AAF-1 fractions	122
Figure 5-9.	Viscosity vs. asphaltene content for NA fractions	122
Figure 5-10.	Viscosity vs. asphaltene content for PA fractions	124
Figure 5-11.	Viscosity vs. asphaltene content for the fractions of AAF-1	125

Figure 5-12.	Viscosity activation energy vs. CA for asphalt fractions	126
Figure 5-13.	Viscosity activation energy vs. CA for AAF-1 fractions	126
Figure 5-14.	Correlation between viscosity model parameters	127
Figure 6-1.	Asphaltene production in aged PA fractions	132
Figure 6-2.	Asphaltene production in aged NA fractions	133
Figure 6-3.	Asphaltene production in aged light fractions of AAF-1	135
Figure 6-4.	Asphaltene production in aged heavy fractions of AAF-1	135
Figure 6-5.	Scheme for the comparison of fractions from various sources	136
Figure 6-6.	GPC spectra of various asphaltenes derived from AAA-1	138
Figure 6-7.	GPC spectra of two kinds of NA derived from AAA-1	138
Figure 6-8.	GPC spectra of various PA derived from AAA-1	140
Figure 6-9.	GPC spectra of various PA derived from AAM-1	140
Figure 6-10.	Oxygen content vs. CA for AAA-1 and AAG-1 at 20 atm	143
Figure 6-11.	Oxygen content vs. CA for two asphalts at multiple T and P	143
Figure 6-12.	Oxygen content vs. CA for five asphalts	144
Figure 6-13.	Oxygen content vs. CA for another five asphalts	144
Figure 6-14.	The effect of RTFOT on AAA-1 oxygen	146
Figure 6-15.	The effect of RTFOT on AAF-1 oxygen content	146
Figure 6-16.	Oxygen content vs. CA for aged AAA-1, ANA and APA	147
Figure 6-17.	Oxygen content vs. CA for aged AAD-1, DNA and DPA	147
Figure 6-18.	Oxygen content vs. CA for aged AAF-1, FNA and FPA	148
Figure 6-19.	Oxygen content vs. Ca for aged AAG-1, GNA and GPA	148
Figure 6-20.	Oxygen content vs. CA for aged AAM-1, MNA and MPA	149
Figure 7-1.	VTS for lime-treated AAA-1 materials	155
Figure 7-2.	Carbonyl growth for untreated tank AAA-1	157
Figure 7-3.	Arrhenius plots for AAA-1 materials	157
Figure 7-4.	Arrhenius plots for AAB-1 materials	161
Figure 7-5.	Arrhenius plots for AAD-1 materials	161
Figure 7-6.	Arrhenius plots for AAF-1 materials	162

Figure 7-7.	Arrhenius plot for all atmospheric untreated AAA-1	162
Figure 7-8.	The dilutory effect of lime on the aging of tank asphalts	164
Figure 7-9.	Lime-treated AAA-1 hardening susceptibility comparisons	164
Figure 8-1.	DLV plot for recycling studies	172
Figure 8-2.	Carbonyl growth for AAF-AB1/ISCF A	175
Figure 8-3.	Arrhenius plots for AAF-AB1/ISCF blends	176
Figure 8-4.	Hardening susceptibilities for AAF-AB1/ISCF blends	176
Figure 8-5.	HS versus saturate content for the first recycling study materials	178
Figure 8-6.	Arrhenius plots for all of the first recycling study materials	180
Figure 8-7.	Arrhenius plot for all atmospheric AAF-1 aging experiments	181
Figure 8-8.	E_{vis} for second recycling study AAA-AB8 blends	186
Figure 8-9.	POV carbonyl growth for untreated AAA-AB8/AAA F3	191
Figure 8-10.	Road condition carbonyl growth for AAA-AB8/AAA F3 blends	191
Figure 8-11.	Arrhenius plots for recycled AAA-AB8/AAA F3 blends	194
Figure 8-12.	The effect of lime on the oxidation rates of recycled asphalts	198
Figure 8-13.	Hardening susceptibilities for recycled AAA-AB8 blends	198
Figure 8-14.	Anomalous HS relationships of lime-treated AAD-AB3 blends	201
Figure 8-15.	Isokinetic plot for all of the materials studied	205
Figure 9-1.	Hardening susceptibilities of TAMU SCFs	218
Figure 9-2.	Hardening susceptibilities of ISCFs	218
Figure 9-3.	HS ratio versus mass percent of recycling agent	220
Figure 10-1.	Conventional 3-stage SCE unit	225
Figure 10-2.	Deasphalting unit with 2 or 3-stage SCE unit	225
Figure 10-3.	Deasphalting unit with solvent extraction unit	228
Figure A-1.	Supercritical unit process diagram	247
Figure A-2.	Legend for supercritical extraction unit diagram	248
Figure A-3.	Pressure oxygen vessel control panel	251
Figure A-4.	Pressure oxygen vessel and control panel	251

LIST OF TABLES

		Page
Table 3-1.	The Tested Aging Conditions	49
Table 3-2a.	CA Growth Rate for All POV-Aged Asphalts for Conditions C1 to C7 . . .	55
Table 3-2b.	CA Growth Rate for All POV-Aged Asphalts for Conditions C8 to C13 . .	56
Table 3-3a.	CA_0 - CA_{tank} of All POV-Aged Asphalts for Conditions C1 to C7	57
Table 3-3b.	CA_0 - CA_{tank} All POV-Aged Asphalts for Conditions C9, C12 and C13, and the Average for Three Pressures	58
Table 3-4.	Kinetic Model Parameters of All POV-Aged Asphalts Studied	59
Table 3-5.	Hardening Susceptibility Parameters for All POV-Aged Asphalts Studied . .	63
Table 3-6.	Critical Time (CT) to Reach 500,000 Poise at Two Aging Conditions	66
Table 3-7.	Pressure Dependence Factors for Each Asphalt Studied	69
Table 3-8.	Oxidation Rates Measured at 140°F and 0.2 atm, Compared to Those Calculated by Two Methods	74
Table 3-9.	Calculated Aging Parameters for Aging at 4 atm Oxygen and 212°F	77
Table 3-10.	Viscosity and Rank of the Ten Asphalts after PAV Test	78
Table 4-1.	Initial Properties of NA, PA Fractions and Supercritical Fractions	83
Table 4-2.	Conditions Applied in the Aging Experiments for NA and PA Fractions and Supercritical Fractions	87
Table 4-3.	CA Growth Rate for NA and PA Fractions at All Conditions	89
Table 4-4.	Kinetic Parameters of NA and PA Fractions and Their Parent Asphalts . . .	89
Table 4-5.	CA_0 - CA_{unaged} for NA and PA Fractions and Their Parent Asphalts at Different Aging Pressures	94
Table 4-6.	Initial Corbett Composition of Supercritical Fractions of AAF-1	95
Table 4-7.	CA Growth Rate for Supercritical Fractions of AAF-1	101
Table 4-8.	Kinetic Parameters of the Supercritical Fractions of AAF-1	102
Table 4-9.	CA_0 - CA_{unaged} for Supercritical Fractions of AAF-1, AAF-1 Generic Fractions and AAF-1 Whole Asphalt	104

Table 4-10.	Oxidation Rates of the Aromatics/Saturates/Asphaltenes Blends of Four Asphalts at Three Temperatures and Pressure 0.2 atm	105
Table 4-11.	Contents of NA and PA in Aromatics Fractions of SHRP Asphalts	111
Table 5-1.	Hardening Susceptibilities HS of SHRP Asphalts and Their NA, PA and Aromatics Fractions	116
Table 5-2.	Comparison of Calculated and Measured AFS of Aromatics Fractions of SHRP Asphalts	121
Table 5-3.	Comparison of Solvation Power Parameters (SPP) of Fractions of SHRP Asphalts	124
Table 6-1.	Information of the Aged NA and PA Fractions for Separation	137
Table 7-1.	Lime-Treated Tank Asphalt Aging Conditions	152
Table 7-2.	Lime-Treated Tank Asphalt Initial Viscosities	153
Table 7-3.	VTS Values of Unaged Lime-Treated Tank Asphalts	155
Table 7-4.	Lime-Treated Tank Asphalt "Initial Jump" Data	158
Table 7-5.	Lime-Treated Tank Asphalt Atmospheric Pressure Activation Energies . .	159
Table 7-6.	Lime-Treated Tank Asphalt Atmospheric Pressure Hardening Susceptibilities	165
Table 7-7.	Lime-Treated Tank Asphalt Extrapolated Road Condition Oxidation and Hardening Rates	166
Table 8-1.	First Recycling Study Rejuvenating Agent Properties	170
Table 8-2.	First Recycling Study Blend Compositions and Viscosities	172
Table 8-3.	First Recycling Study Blend Aging Indexes	173
Table 8-4.	First Recycling Study Aging Parameters	177
Table 8-5.	First Recycling Study Extrapolated Rates	178
Table 8-6.	Relative Rankings of First Recycling Study Asphalts	180
Table 8-7.	Second Recycling Study Material Properties	183
Table 8-8.	Second Recycling Study Aging Conditions	183
Table 8-9.	Second Recycling Study Blend Compositions and Viscosities	185
Table 8-10.	VTS Values for the Unaged Second Recycling Study Blends	188
Table 8-11.	Second Recycling Study PAV Aging Indexes	190
Table 8-12.	Second Recycling Study "Initial Jump" Data	193

Table 8-13.	Second Recycling Study Activation Energies	195
Table 8-14.	Second Recycling Study Road Condition Oxidation Rate Comparisons . . .	197
Table 8-15.	Second Recycling Study Hardening Susceptibilities	199
Table 8-16.	Second Recycling Study Extrapolated Road Condition Hardening Rates . .	202
Table 8-17.	Relative Rankings for Second Recycling Study Blends	204
Table 8-18.	AAF-1 Supercritical Fraction Blend Arrhenius Parameter Comparisons . .	204
Table 8-19.	64°C $G^*/\sin\delta$ Values for Second Recycling Study Blends	207
Table 8-20.	-18°C Bending Beam Parameters for Second Recycling Study Blends . . .	208
Table 8-21.	SHRP Performance Grades for the Second Recycling Study Blends	210
Table 9-1.	Recycling Agent Compositions and Viscosities	216
Table 9-2.	Compositions and Viscosities of Recycled Blends	217
Table 9-3.	HS Values of AAA-AB11 Blends and Chapter 8 Blends	219
Table 10-1.	Conventional 3-Stage SCE Unit Economics	224
Table 10-2.	Deasphalting Unit Plus a 2 or 3-Stage SCE Unit Economics	226
Table 10-3.	4 or 5-Stage SCE Unit Economics	227
Table 10-4.	Conventional DAO Unit Plus Solvent Extraction Unit Economics	230

CHAPTER 1

INTRODUCTION AND LITERATURE SURVEY

It was estimated that as of 1988 well over 10 billion dollars were spent annually in the United States on construction and maintenance of over 2.2 million miles of asphalt pavements (Roberts et al., 1991). Furthermore, it was estimated that over 500 million tons of asphalt and aggregate were consumed in these activities. While newly placed pavements may have desirable properties initially, over a period of many years of service, the physical properties of the asphalt will deteriorate and the pavement will need to be repaired and/or replaced. However, if a large portion of this material could be re-utilized, a tremendous amount of waste, both environmental and economic, could be eliminated.

Even though asphalt recycling has been practiced periodically since the early 1900s, it has not been widely implemented. This has been due to a variety of factors including the relatively cheap cost of asphalt pavements. Economic incentives, which began to appear in the early 1970s with the Arab oil embargo, eased as new reserves were discovered and energy conservation took hold. While these have since been reinforced with the recent tensions in the Persian Gulf area, they have not been sufficient to spawn major recycling efforts. The environmental incentive to recycle has also only recently surfaced, and has not had a major impact. Nevertheless, the major impediment to widespread implementation has been, and continues to be, the general lack of understanding of the interactions not only between a recycling agent and an asphalt, but also of the interactions present in asphalts alone. To attempt to understand the interactions that take place in an asphalt and their effect on asphalt properties, it is necessary to garner a basic understanding of the composition of petroleum residues in general and asphalt in particular.

Physical Property/Chemical Composition Relationship

Although it is desirable to understand how the composition of an asphalt affects its rheological properties (or physical properties), a number of factors have made achieving this understanding very difficult. First, asphalts are a complex mixture of organic molecules derived from petroleum residue. Furthermore, asphalts having widely different compositions may have the same rheological properties.

In addition, asphalts change over time because of oxidative aging. This oxidative process further changes the composition and rheological properties.

Petersen (1984) gave an excellent review on the changes in chemical composition and physical properties of asphalt resulting from oxidative aging. In summary, oxidative aging in both the field and the laboratory increases carbonyl content, asphaltene content, and viscosity and decreases penetration and ductility, which eventually cause the failure of pavement. Unfortunately, quantitative descriptions of the relationships between chemical composition and physical properties vary widely among asphalts and still remain unclear.

During oxidative aging, many changes in asphalt composition, including composition shifts in terms of Corbett fractionation, occur in addition to carbonyl formation. Lee et al. (1973) reported, for four asphalts, that the infrared absorbance in the carbonyl region increases linearly with n-heptane asphaltene content after field and laboratory aging. Furthermore, although each Corbett fraction of an asphalt affects the properties of asphalts before and after aging, the most significant chemical composition changes in terms of Corbett analysis is the transformation of the polar-aromatics fraction to the asphaltene fraction. An excessive amount of asphaltene formation during oxidative aging causes the failure of asphalt binders.

Previous studies have shown that oxidative aging changes the chemical composition and the rheological properties of whole asphalt (Petersen, 1984). Girder (1965) showed by elemental analysis that the asphaltene produced through oxidative aging are chemically different from those originally present by elemental analysis in that the produced asphaltene have lower nitrogen and sulphur content and higher oxygen content. Because of chemical differences, the effect of the produced asphaltene on the physical properties of the asphalt, compared to the original asphaltene, may be different. Anderson et al. (1976) compared the viscosity and n-pentane asphaltene content of 108 different field sections using 8 different asphalts that had been field aged in Utah for seven years. The data were compared with the Hoiberg Model (1944) and did not show good agreement. With laboratory oxidative aging, Plancher et al. (1976) oxidized four asphalts in the presence and absence of lime. The data show that the viscosity at 25°C as a function of n-pentane asphaltene content depended on the crude source, but was independent of lime treatment.

It is highly desirable and very important to develop a rheological model relating the

composition of the unaged and aged asphalt (asphaltene, carbonyl content, or others, if possible) to rheological properties. This model would provide a foundation not only for predicting asphalt behavior during pavement life but also for developing and manufacturing superior asphalt binders with desired rheological properties by manipulating their composition.

Asphalt Composition and Fractionation Methods

Standard Fractionation Methods

Asphalt, as a residue of crude oil distillation, contains all of the high molecular weight, high boiling point materials present in crude oil. Unfortunately, because the residues contain thousands of non-volatile compounds and the extremely powerful analytical tool of gas chromatography cannot be used to fully resolve and identify each individual component. As such, much effort has been expended investigating other methods for determining the chemical composition of asphalt and other heavy petroleum products. Several of these have focused on using purely physical separations to isolate fractions of similar molecular size by gel permeation chromatography, GPC, with limited success correlating fraction distribution to binder properties and pavement performance (Kleinschmidt, 1955; Altgelt and Hirsch, 1970; Bynum and Traxler, 1970; Reerink and Lizenga, 1975; Such and Brule, 1979; Jennings, 1985; Brule et al., 1986; Glover et al., 1987; Davison et al., 1989). However, the correlations between molecular size and performance are complicated by the fact that the large molecules typically are usually of similar chemical functionality and/or reactivity. This is, in general, not true for the other molecular sizes. As such, any truly useful technique must group the components according to chemical functionality or chemical reactivity.

Over the past several decades much effort has been expended to isolate fractions of similar chemical functionality or reactivity from asphalt (Hoiberg and Garris, 1944; Hubbard and Stanfield, 1948; Rostler and Sternberg, 1949; Traxler and Schweyer, 1953; Kleinschmidt, 1955; Corbett and Swarbick, 1960; Corbett, 1969). Nearly all of these efforts have been focused on describing asphalt composition in terms of a relatively few number of pseudo-components or group-type fractions.

Hoiberg and Garris (1944) developed a fractionation method which separates asphalt into hexane insolubles, hard resins, soft resins, oils, and waxes based on solubility and molecular weight differences. Traxler and Schweyer (1953) developed a fractionation procedure intended

as an improvement of the Hoiberg and Garris (1944) procedure. In the Traxler and Schweyer (1953) procedure, the asphalt is dissolved in n-butanol and the insoluble materials are removed. The materials insoluble in the n-butanol are referred to as "the asphaltics". The n-butanol is then removed from the soluble materials. Next, acetone is added and the solution is chilled to -10°F. The acetone insoluble materials, called the saturates (S), are separated from the acetone soluble materials, which are called the cyclics (C). In a later study, Traxler (1960b) further split the asphaltics into asphaltenes (A) and resins (R) based on solubility in n-heptane. Traxler defined a compositional parameter called the coefficient of dispersion "X", which is equal to $(R+C)/(A+S)$, to indicate the colloidal characteristics of an asphalt. A higher value of "X" indicates a better state of dispersion in asphalt. Traxler also found that the degree of hardening as a result of oxidation was related to the coefficient of dispersion for the six asphalts that were studied.

Although the methods of Hoiberg and Garris (1944) and Traxler (1960b) have been utilized to determine asphalt composition, the most well known methods of asphalt fractionation are, by far, those of Rostler and Sternberg (1949) and Corbett (1969). Both of these methods entail performing a binary fractionation of the material based on solubility in some arbitrary solvent, typically a saturated hydrocarbon (n-hexane, n-heptane, i-octane, etc.). The insoluble fraction, if present, is separated by filtration and is referred to as the asphaltene fraction, or simply asphaltenes (AS). The soluble portion of the asphalt is called the maltene fraction. It has been widely reported that the asphaltene fraction contains a large portion of the metals and heteroatoms present in the asphalt (Corbett and Swarbick, 1960; Rostler and White, 1962; Corbett, 1970; Altgelt and Harle, 1975; Corbett, 1979; Savastano, 1991; Stegeman et al., 1992; Jemison et al., 1995; Lin et al., 1995a; Lin et al., 1995b; Lin et al., 1996).

Many of these researchers have also reported that the asphaltenes, both original asphaltenes and those produced by aging or air-blowing, are chiefly responsible for the viscous nature of asphalt. Several of these researchers have investigated the relationship between the viscosity and the asphaltene content in asphalts and asphaltene/solvent mixtures. Eilers (1948) measured the relative viscosities (η_r), which are the viscosity of the solution divided by the viscosity of the solvent (η/η_s), of diethyl ether asphaltenes from several original and air-blown asphalts in carbon disulfide solutions.

The data from all of the solutions were compared with an empirical model Eilers proposed. The data were not well described by the model and Eilers concluded that the deviations between the model and the measured data were associated with the fact that the asphaltenes were non-spherical, deformable particles or are polydisperse in size. Reerink and Lizenga (1973) measured the viscosities of solutions of n-heptane asphaltenes from original and air-blown asphalts dissolved in toluene. The solution viscosities were related to the concentration and width of the molecular weight distribution of the asphaltenes as measured by Gel Permeation Chromatography. The data were compared to the Heukelom and Wijga model (1971) which is a simplification of the Eiler model that assumes a linear relation between the square root of the reciprocal of the relative viscosity, $1/(\eta_r)^{1/2}$, and the particle (asphaltene) volume fraction. Relative viscosities calculated from the model were consistently lower than the measured values.

Sheu et al. (1991) related the n-heptane asphaltene concentration of two Ratawi vacuum residues in toluene to the solution relative viscosity. The authors discussed four different solution viscosity models. The solution viscosity data suggested that the asphaltenes associate to form larger particles as a result of solvation by the solvent phase. They concluded that the Pal and Rhodes (1989) model, Equation (1-1), described the relationship between the relative viscosity, η_r , and the volume fraction of suspending colloidal particles (asphaltene), Φ .

$$\eta_r = \frac{\eta}{\eta_s} = (1 - K\Phi)^{-2.5} \quad (1-1)$$

The solvation constant, K, represents the degree of aggregation of suspended particles. The Pal-Rhodes model assumes that all the particles are solvated by the solvent phase and act like polydisperse hard spheres. No data were reported for maltene/asphaltene systems. Sheu et al. (1991) point out that for non-spherical particles the exponent of -2.5 in the Pal and Rhodes model can be a free parameter to account for the particle asymmetry. Storm et al. (1993) also used the Pal-Rhodes model to describe the relative viscosity/asphaltene concentration relationship of asphalts.

Altgelt and Harle (1975) measured the effect of heptane asphaltene on the viscosity of organic solvents and maltenes. Increasing the asphaltene concentration increased the relative viscosity of the solution. Although no model was developed, the behavior followed a repeatable trend for

blends of asphaltenes and maltenes taken from the same parent asphalt. However, when combining asphaltenes and maltenes from different sources, the data were highly scattered. Evidently, when cross mixing asphaltenes and maltenes, the effect on relative viscosity must not only include the concentration of asphaltenes but also the solvation power of the maltene, which is a function of the composition of the maltene.

Recently, Branthaver et al. (1991) studied the effect of unaged asphaltenes on unaged asphalt relative viscosity. The data at 60°C for unaged asphalts from a variety of crude sources showed very little difference in the *relative* viscosity between asphalts. This result seems to be contradictory to that of Altgelt and Harle (1975) and would seem to indicate that the solvation power of each maltene is similar or the same. The solvation power of the maltene is a function of the composition of the maltene fraction, which changes as the asphalt ages. The changes in composition will be discussed in detail later.

The two major fractionation methods differ in their treatment of the hydrocarbon-soluble fraction (maltenes), but both define a group of materials called saturates (Corbett, 1969) or paraffins (Rostler and Sternberg, 1949) which are highly unreactive and incompatible with the asphaltenes. In the Rostler method, the maltenes are treated with 85%, 100%, and fuming H₂SO₄, successively. The asphaltic materials which react with the various strength sulfuric acid solutions are called the nitrogen bases (N), first acidaffins (A₁), and second acidaffins (A₂), respectively. The compounds which do not react even with the fuming sulfuric acid are called collectively the paraffins (P) fraction. Rostler and White (1962) reported that the nitrogen bases peptize the asphaltenes, the acidaffins act as a solvent for the peptized asphaltenes, and the paraffins cause the asphalt to gel due to their incompatibility with the asphaltenes.

Several researchers have utilized the Rostler fractionation procedure to correlate the composition and the properties of asphalts (Rostler and White, 1962; Halstead et al., 1966; Skog and Zube, 1966; Jamieson and Hattingh, 1970; White et al., 1970; Davidson et al., 1977; Gannon et al., 1980; Rostler and Rostler, 1981; Halstead, 1985). These correlations have typically been done using two compatibility indexes, the Rostler durability parameter (N+A₁/P+A₂) and the ratio of N/P. Generally, asphalts with high Rostler parameters and high N/P ratios have good physical properties mainly because high values of these parameters indicate a high aromaticity in the asphalt and

consequently, highly solubilized asphaltenes. On the other hand, because the Rostler durability parameter is the ratio of the most reactive species to the least reactive species (neglecting asphaltenes), a high value of the Rostler durability parameter also indicates a tendency to react, and thus age. Furthermore, the meaning and validity of the Rostler durability parameter are in question as any possible influence of the asphaltenes is ignored and the contributions of the other fractions are weighted equally. Halstead et al. (1966) did investigate the use of other weightings of the Rostler fractions, but reported that the correlations were generally no better. Another parameter, the Gotolski Ratio, defined as $(N+A_1+A_2)/(P+A)$, has been correlated to field aging (Kemp and Predoehl, 1981). In some cases, the ratios defined based on the Rostler fractions yield good correlations with physical properties. In other studies neither the Gotolski nor the Rostler ratio correlate with performance (Goodrich et al., 1986). The Rostler fractionation method is inherently capable of producing only empirical relationships between pavement performance and composition because the fractionated components have been irreversibly altered in the separation process. Therefore, the properties of the individual fractions are not representative of their properties in the unfractionated asphalt (White et al., 1970).

To eliminate the irreversible changes that the chemical reactivity separation methods produce, several open column chromatographic techniques for asphalt group-type fractionation have been proposed over the past several decades. Corbett and co-workers have been the most active researchers in this regard (Corbett and Swarbick, 1958; Corbett and Swarbick, 1960; Corbett, 1964; Corbett, 1969; Corbett, 1970; Corbett, 1975; Corbett and Merz, 1975; Corbett, 1979; Corbett and Schweyer, 1981; Corbett, 1984). The procedure finally settled on by Corbett (1969) has since been adapted by the American Society for Testing and Materials as the standard method for determining asphalt composition (ASTM D-4124, 1994).

In the standard method, the asphaltenes are separated by precipitation from an n-heptane solution and the maltenes are then separated into saturates (SA), naphthene aromatics (NA), and polar aromatics (PA) by elution chromatography using an open column containing activated alumina. Physically, the asphaltenes are black solids which might resemble coal, the saturates are similar in consistency to petroleum jelly, the polar aromatics are generally black solids at room temperature, and the naphthene aromatics are reddish-brown liquids. The naphthene and polar aromatics are

sometimes lumped together and referred to simply as the aromatics (AR). Generally speaking, the Rostler paraffins are equivalent to the saturates, the nitrogen bases have much in common with the polar aromatics, the second acidaffins are similar to the naphthene aromatics, and the first acidaffins are split between the polar aromatics and the naphthene aromatics. Unfortunately, the Corbett procedure is labor intensive and the separation cut-points can be highly subjective as they are determined by visual inspection. However, this study focused on Corbett-type components over the Rostler components as the Corbett method is simpler. Unfortunately, regardless of which fractionation procedure is utilized, the fractions are operationally defined and are complex mixtures themselves. Moreover, the same fraction from various asphalts may have much different chemical and physical properties and two asphalts with similar fractional composition may behave completely differently (Goodrich et al., 1986).

Corbett-based techniques do have advantages over the Rostler method. In particular, the Corbett method typically produces several grams of each fraction. The "giant" Corbett method utilized by Peterson et al. (1994) is capable of producing several hundred grams of each fraction. The larger sample sizes for the Corbett procedure allow for studies to be conducted on individual Corbett fractions or combinations of Corbett fractions. Several studies have been conducted in this regard (Corbett, 1970; Corbett, 1979; Peterson et al., 1994; Lin et al., 1996; Liu, 1996). The saturates have been shown to lower the viscosity, but are generally believed to be detrimental to viscosity temperature susceptibility, asphalt compatibility and performance in general. The naphthene aromatics help soften the asphalt and bridge the compatibility gap between asphaltenes and saturates. The polar aromatics impart ductility to the asphalt and are chiefly responsible for asphaltene dispersion but contribute negatively towards viscosity temperature susceptibility. Finally, the asphaltenes were shown to be responsible for viscosity building but also contribute to good temperature susceptibility.

More recent studies (Peterson et al., 1994; Lin et al., 1996; Liu, 1996) have focused on determining the influence of the various fractions on the physical properties and aging characteristics of asphalts. Saturates were shown to neither oxidize nor harden. Naphthene aromatics oxidize, but do not harden appreciably. Polar aromatics oxidize and harden rapidly. It should be noted that even though there is a general similarity between the Corbett fractions of different asphalts, the properties

of the fractions often vary widely. Lin et al. (1996) showed compelling evidence that saturates are highly detrimental to the rheological properties of aged asphalts, especially at lower temperatures. Peterson et al. (1994) showed conclusively that although the presence of saturates in blends *without* initial asphaltenes is not detrimental, the presence of saturates in blends *with* initial asphaltenes is highly detrimental to aging performance.

Efforts have also been undertaken to determine Corbett-type fraction composition using the automated, unbiased technique of high performance liquid chromatography (HPLC). In the mid 1970s to early 1980s, petroleum chemists began to use the relatively new analytical technique of (HPLC) for group-type analyses of petroleum and coal derived materials (Suatoni and Swab, 1975; Suatoni and Swab, 1976; Dark and McFadden, 1978; Dark and McGough, 1978; Gayla and Suatoni, 1980). One of the primary advantages of HPLC over open column techniques is the elimination of cut-point subjectivity. Suatoni and Swab (1975) showed that the saturate, aromatic, and polar fractions from different materials with similar boiling points possessed nearly the same refractive index response factor, regardless of crude source. Furthermore, they analyzed several compounds with a wide range of boiling points and they showed that the response factor was a function of residue boiling point range. It has been noted, elsewhere, that the refractive index of the saturates fraction may approach a limiting value (Lundanes and Greibrokk, 1985).

In a later experiment, Gayla and Suatoni (1980) reported that the response factors for saturates obtained from coal liquids with widely varying boiling points were *identical* for three out of the four materials they studied, indicating that calibration of saturate content may be possible. However, other studies have indicated that the best agreement between HPLC saturate content and open column saturate content was obtained when the HPLC saturate content was determined by difference, rather than by direct methods (Dark, 1982; Bishara and Wilkins, 1989; Beg et al., 1990, Ali and Nofal, 1994). In addition, Bishara and Wilkins (1989) reported that the naphthene and polar aromatics for a given material could be determined directly from HPLC calibration but universal calibration was not possible. Recently, Lin (1995) reported data showing the absorptivities of the aromatics fractions change with aging supporting the conclusions of Bishara and Wilkins. However, Lin reported data supporting the claims of Suatoni and Swab (1975), Gayla and Suatoni (1980), and Lundanes and Greibrokk (1985) that saturate calibration may be possible.

More detailed reviews of the methods available for fractionation of asphalts and the general properties of the various fractions were conducted by Altgelt and Gouw (1975), Rostler (1979), and Petersen (1984).

Supercritical Fractionation

There are two general approaches to upgrading the residues from crude oil distillation. These are chemical processes (such as visbreaking, catalytic cracking, and coking) and physical separation processes (such as propane deasphalting and supercritical extraction). Frequently, a combination of these must be used as residues have high asphaltene contents which may result in undesirable coking, and high sulfur and metals contents which will poison catalysts. Supercritical fractionation has been shown to be an especially useful tool for residue upgrading (Gearhart and Garwin, 1976a; Gearhart and Garwin, 1976b; Brons and Yu, 1995; Low et al., 1995). The most well known supercritical fractionation process is the Residuum Oil Supercritical Extraction (ROSE) process licensed by M.W. Kellogg (formerly by Kerr McGee).

Briefly, supercritical fractionation separates the components of a petroleum residue based on their solubility in a supercritical solvent. The solvents of choice for petroleum applications are typically low molecular weight hydrocarbons such as propane, n-butane, i-butane, n-pentane, i-pentane, or a mixture of these. Typically, the selectivity for asphaltene rejection is highest for the lower molecular size solvents, but the versatility of the separations increases with increased solvent molecular size (Gearhart and Garwin, 1976a; Gearhart and Garwin, 1976b; Gearhart, 1980). The solubility of the components in the supercritical solvent is a complex function of both molecular size and chemical functionality of the compounds, the density of the solvent, and the solvent:solute ratio (McHugh and Krukonis, 1986; Stegeman et al., 1992; Jemison et al., 1995; Brons and Yu, 1995; Low et al., 1995). However, the most important factor is the density of the solvent which can be manipulated quite dramatically with only relatively minor changes in the operating temperature or pressure near the critical region.

Most industrial units can be operated as a three-stage process which produce an asphaltene-rich fraction, or "asphaltenes", a saturate-rich fraction known as deasphalted oil, or DAO, and an intermediate fraction known as resins. However, because the process is typically utilized to reject

asphaltenes and produce DAO suitable for use as either lube oil feedstock or catalytic cracker feedstock, most of the industrial units are operated as two-stage units. The use of only two stages negates much of the versatility of the process and, although Gearhart and Garwin (1976) reported that supercritical fractionation could be utilized to produce specification asphalts, only a few studies have been conducted with specific application to studying the properties of asphalt supercritical fractions with the intention of producing superior paving materials.

Stegeman et al. (1992) employed n-pentane as the supercritical solvent to fractionate asphalts. The major problem encountered by these researchers was that a large portion of the feed material (approximately 40%) remained insoluble in n-pentane at the operating conditions and the unit had a tendency to become plugged, requiring much maintenance. In addition, they wanted to fractionate the asphalt into approximately equal-sized fractions for a study of fraction properties. Therefore, they had to perform room temperature separations with n-pentane/cyclohexane mixtures of varying compositions on the heaviest material. They produced a total of eight fractions. To rectify this situation, Jemison et al. (1995) used cyclohexane to perform an initial fractionation of the asphalt in the supercritical unit. This had the desired effect of producing more evenly distributed fraction yields. However, the use of cyclohexane resulted in reduced selectivity and necessitated higher operating pressures and temperatures. These higher temperatures, necessary to achieve the supercritical conditions for the cyclohexane, also led to some thermal degradation of the asphaltic material. Furthermore, an unwieldy total of ten numbered fractions were produced. Jemison (1992) also fractionated reduced crudes using this methodology, but found that the presence of the vacuum gas oils created co-solvency problems.

Stegeman et al. (1992) and Jemison et al. (1995) both showed that the asphaltenes and metals were highly concentrated in a relatively small number of the fractions that they produced, as were the saturates. As one might imagine, the contents of these components were inversely related in the supercritical fractions. They also showed that although there was some concentration, the naphthene aromatics and polar aromatics were fairly evenly distributed throughout the fractions. However, the molecular size of the naphthene and polar aromatics varied quite dramatically from fraction to fraction, reinforcing the fact that separation occurs not only based on chemical functionality, as shown by the concentration of the asphaltene and saturate materials, but also based on molecular size.

Jemison et al. (1995) expanded the study to include aging characteristics. Various fractions were blended to obtain several materials with asphalt-like consistency. The asphaltene and high molecular weight polar-aromatic rich heaviest few fractions and the saturate rich fraction were not included in the blending experiments. A few of the blends consisted of a single fraction. The aging studies were carried out in a pressurized oxygen vessel, POV, (Lau et al., 1992) at elevated temperature and pressure. Poor temperature control prevented determining accurate kinetics, but Jemison et al. (1995) were able to compare performance of the blended and original asphalts based on the hardening susceptibility (HS), discussed later, and the oxidation rate at a given aging temperature. They found that the blended asphalts had hardening susceptibilities superior to those of the original asphalts but the oxidation rates were not appreciably changed. However, the rates for blends made from one asphalt usually were different from the rates for blends made from another asphalt. The implications of this are that the supercritical fractions from an asphalt with a low HS could be blended with fractions from an asphalt with low aging rates (the two are not usually inclusive) to produce a superior asphalt. Although the properties of the single fraction "blends" were worse than the properties for the multiple fraction blends, they were still superior to those of the original asphalt. They attributed the improved properties to the improved compatibility of the blends from reduced levels of asphaltenes and saturates initially present in the blend.

Asphalt Aging

An asphalt begins its irreversible march toward failure as early as the hot-mix plant. In the hot-mix plant, the asphalt is added to the aggregate at very high temperatures in the presence of an impinging flame. At these extreme conditions a certain amount of volatilization takes place which increases the viscosity of the binder. The binder also undergoes chemical changes, particularly at the aggregate/binder interface.

While some hardening does take place in the extreme conditions present in the hot-mix plant, the majority of the changes which take place in the binder, over time, occur after the pavement has been laid. Over the past several decades, much effort has been focused both on describing the aging behavior of asphalts, and on developing aging tests to mimic the aging which occurs over the life time of a pavement. A summary of the asphalt aging literature follows.

An excellent review on the changes in chemical composition, material properties, and measured physical properties caused by oxidative aging is given by Petersen (1984). In terms of chemical composition, oxidative aging in both the laboratory and the field results in an increase in carbonyl content and asphaltene content, and a decrease in compatibility. In terms of physical properties, aging increases viscosity and stiffness, as well as viscosity temperature susceptibility, and decreases penetration and ductility. Overall, aging results in a harder, more brittle cement. Ultimately, the deterioration in the physical properties leads to pavement failure under traffic loads and thermal cycling. The resistance to age hardening under service weathering conditions is generally called durability.

To understand and to model the age hardening process with the hope of finding a way to retard oxidative aging, much effort has been made to track the change in binder properties in service. Brown et al. (1957) periodically measured the softening points, penetrations, and ductilities of two markedly different asphalt types, each used in two different roads, over a testing period of nine years. They found that the change in these properties, namely increase in softening point and decrease in both ductility and penetration, followed a simple hyperbolic law with respect to service time as shown in Equation (1-2).

$$\Delta y = \frac{t}{a_h + b_h t} \quad (1-2)$$

In this equation, Δy represents the property change, t is the aging time in the field, while a_h and b_h are model parameters. Kandhal and Koehler (1984) reported that oxidative aging resulted in progressively lower penetration and higher viscosity. They also reported that these changes could be described by a hyperbolic function of time. Way et al. (1959) also reported that the change of penetration with time followed a hyperbolic form.

As a general model to describe the property change with respect to aging time, Equation (1-2) can be used to predict future service life of the pavement. This is accomplished by measuring data for the early years of a pavement's life and fitting them to the model to obtain the parameters. The rate and ultimate degree of property change over the full life may then be predicted by the equation.

Although this is a model possessing prediction capability, the calculation is based on the assumption that the average weathering condition, particularly the ambient temperature, as well as the traffic load on the specific road would remain not significantly changed from year to year. Furthermore, measurement of the properties of aged samples requires recovery of the binders from field aged pavements, whereby significant error may be introduced due to incomplete recovery and other modes of misoperation (Burr et al., 1990, 1991; Burr, 1993). Also, to collect enough data to fit Equation (1-2), specimens with field aging times of several years are necessary. Clearly using data accumulated during several years to predict additional service life of several years is a high-cost procedure. Finally, even if the quality of the binder has been identified by this method to be inferior, the pavement has already been constructed. It would be much more beneficial to evaluate the quality, particularly the aging quality of the asphalt, before it is selected for a certain pavement project.

The task of evaluating asphalt aging quality in a reasonably short period of time calls for a laboratory test that can be conducted on the original binder. This is why early attempts on developing an asphalt aging test to evaluate long-term durability have been so extensive. Strieter and Snoke (1936) aged 0.635 mm thick asphalt films by exposing them to cyclic treatments of light, heat, refrigeration, and forceful spraying of water. In a modified version (Strieter and Snoke, 1936), the period of refrigeration was omitted, and the specimens were dipped in water instead of spraying. Ebberts (1942) oxidized asphalt films using potassium permanganate. Anderson et al. (1942) proposed two test methods for determining the oxidation stability of asphalts to enable forecast of their road behavior. The first method uses data obtained by means of the loss on heating. In the second method, an asphalt solution in benzene is subjected to the action of oxygen at an elevated pressure, but at a temperature within the range of those found in service. Van Oort (1956) studied the durability of asphalt in the dark. The oxygen uptake and the change in viscosity after exposure was measured with respect to aging time. Both oxygen uptake and viscosity increase showed hyperbolic shapes. Assuming a first order reaction for asphalt oxidation and taking into account the diffusion of oxygen along the asphalt film, a comprehensive theoretical model was proposed for transport and reaction. By comparing the measured time-absorption curve to the theoretical calculation, Van Oort was able to estimate the diffusion coefficient. However, the assumption of first order reaction is arbitrary and may be erroneous, possibly leading to an incorrect estimation of the

diffusion coefficient. Blokker and van Hoorn (1959) reported that the rate of oxidation was much higher in the presence than in the absence of sunlight. However, Blokker and Hoorn also noted that the oxidation prompted by the light was restricted to a depth of about 4 microns. Aiming to measure asphalt durability by its oxidizability, Knotnerus (1972) measured the oxygen absorption of asphalts dissolved in toluene at 303.2 K (30°C). Knotnerus' data also showed the oxygen uptake to be a hyperbolic function of time.

In these works, the researchers did not have a clear objective to develop an aging model, and to interpret the laboratory test results in terms of predicted road performance. The underlying assumption would appear to be that if an asphalt binder ages more slowly at any specified conditions, it will also age more slowly in service. Generally speaking, a more severe aging condition will promote the age hardening process of all the asphalts. However, due to the extreme variability in chemical composition between asphalts, the relative ranking of aging resistance may be different by different test techniques.

In the pursuit of an aging model through laboratory research, the variables important to field aging must be identified. The progress of in-service aging has been found to depend on a number of factors including susceptibility of the binder to aging, void percentage and porosity of the asphalt pavement, ambient temperature, and other factors such as sunlight, the nature of the aggregate and moisture (Verhasselt and Choquest, 1993). It is obvious that perfect laboratory simulation of field aging is almost impossible. However, among the factors listed above, the binder's tendency to age hardening and the temperature at which the binder ages are the dominant factors. Thus, it is a realistic assumption that when other factors remain equal, the aging process is mainly determined by the binder's resistance to oxidative aging and the service temperature. Intuitively, the binder's susceptibility to aging should also be determined by the binder's chemical composition, and therefore highly asphalt dependent. To compare the oxidation of different asphalts, it is necessary to control the oxidation temperature in any aging test. However, oxidation at road-like conditions proceeds at a very slow rate. Therefore, in order to conduct aging tests in a reasonable period of time, elevated oxygen pressure and/or elevated temperature have been investigated in various asphalt aging studies.

Concerns have been raised about the possibility that the reaction mechanism may be changed due to the use of elevated temperature and pressure, particularly aging temperature. It has been

reported by Van Oort (1956) that at temperatures above 373.2 K (100°C), dehydrogenation takes place, as is evident from the water produced. Carbon dioxide may also be formed above this temperature. At lower temperatures, no water or carbon dioxide is formed. Hughes (1962) studied asphalt oxidation at elevated temperatures and found that the oxidation rate-temperature relationship had different patterns for the three temperature ranges: from around 366.5 to 422.0 K, from 422.0 to 505.4 K, and above 505.4 K. Thus it is reasonable to doubt if the reaction mechanism at temperatures far above 366.5 K (200°F) is the same as that below 366.5 K. By studying the asphaltene production patterns when asphalts were aged at different temperatures and comparing them to the asphaltene production pattern of road aged samples, Choquest and Verhasselt (1994) claimed that aging temperatures above 373.2 K in accelerated tests might cause alteration in the reaction mechanism. The conclusion that can be drawn from these previous studies is that the temperature used in a laboratory aging test designed to simulate long-term pavement aging should not exceed 373.2 K (100°C). On the other hand, higher temperatures are essential to simulate the hot-mix process. In fact, both the thin film oven test, TFOT (ASTM D-1754, 1994), and the rolling thin film oven test, RTFOT (ASTM D-2872, 1994) are conducted at significantly higher temperatures and have been shown to approximately describe the "instantaneous" changes in physical properties which occur in the hot-mix plant (Jemison et al., 1991). Unfortunately, both of these aging test are sometimes used to simulate long-term aging as well, with minimal success.

In 1954, Lee and Dickinson (1954) reported the design of a pressure oxygen vessel (POV) to age asphalt films at 20 atm oxygen and 338.2 K for 64 hours. The advantage of this test is the capability to accelerate the aging at relatively low temperatures by using high pressure oxygen. The Frass brittle temperature was measured after POV aging and was correlated to the observed road performance. However, no aging model was proposed. In the same study, it was clearly demonstrated that, compared to the loss of oil through vaporization, the susceptibility to atmospheric oxidation was a much more important factor deciding the durability of the pavement.

Lee (1968) modified the POV test by pre-treating the asphalt using the TFOT to simulate the hot-mix procedure. Lee used 3.2mm asphalt films and aged the asphalts at 338.9 K under 20 atm pure oxygen for 10 days. The properties measured to indicate changes included penetration, softening point, absolute viscosity, asphaltene content, and oxygen content. Six asphalts of different

penetration grades were studied. The viscous hardening in the pressure-oxidation process was found to be a hyperbolic function of time. Lee noted that the degree of hardening was accelerated by a factor of two to five times when aging pressure is increased from 1 atm to 20 atm. Furthermore, Lee concluded that differences exist among asphalts in the rate and degree of hardening during the pressure-oxidation procedure. Therefore, the procedure can distinguish between asphalts that are susceptible to hardening and those that are not. However, Lee did not investigate how the pressure relates to an aging model in terms of its effect on the oxidation kinetics. Because of this, there is no quantitative basis to interpret the test result obtained at higher pressure to the road condition. With eight asphalt cements, Lee (1968) compared field aging data of two years service to the laboratory aging results. He concluded that 46 hours of aging at 338.9 K under 20 atm oxygen with TFOT pretreatment would age an asphalt to the equivalent of about 60 months of actual pavement service in Iowa. In a further study, Lee and Huang (1973) reported that the hyperbolic model could be used to describe the carbonyl content with respect to aging time at the accelerated aging test condition.

All of the test methods described previously involve experiments conducted at only one aging temperature and one oxygen pressure. The main focus has been to develop an operationally simple laboratory test, and to correlate field aging to laboratory aging. Many of these tests were also designed for aging for only one specified time period. Because of a lack of the quantitative understanding of the effects of temperature and pressure on the oxidative aging process, the correlations developed from these tests have always been empirical. To develop an aging model with aging temperature and oxygen pressure being the controlled variables, aging experiments must be conducted at multiple temperatures and pressures.

Some research has been achieved in this direction. Dickinson and Nicholas (1949) developed a comprehensive model to describe asphalt oxidation. Oxygen absorption by asphalt films was measured with both the aging temperature and oxygen pressure being controlled variables. The temperature covered a range from 338.2 to 392.2 K, and the pressure from 0.2 to 1 atm. The model they proposed, which assumes that two simultaneous reactions are occurring, is shown in Equation (1-3).

$$\Delta y = k t + a_n [1 - \exp (-b_n t)] \quad (1-3)$$

The first reaction has a constant rate k , while the second reaction, with model parameters a_n and b_n , is relatively faster, reaching virtual completion after approximately 100 hours. The constant rate was found to be highly sensitive to aging temperature, following an Arrhenius relationship (discussed in detail later) with an activation energy of 29.3 kJ/mol. The sensitivities of parameters a_n and b_n to temperature and pressure were also investigated. The application of this model may be explored. However, since Δy in this study is oxygen absorption, efforts must be made to correlate this chemical measurement to performance related properties.

In Israel, Ishai (1987) suggested a methodology for the analysis of asphalt age-hardening in the time-temperature domain. Penetration aging indices were plotted against exposure time for different aging temperatures. Exposure temperature was also plotted against exposure time to depict curves of the same aging indices. A calibration scheme using field aging data was described. They claimed that the calibrated laboratory aging curves in the time-temperature domains could be used to predict future aging behavior. In the extended study, Ishai et al. (1988) correlated rheological and physico-chemical properties to the long-term asphalt durability evaluated by the time-temperature domain method. The exposure temperatures in the laboratory oven tests ranged from 343.2 to 436.2 K for different time durations of up to 21 days. Again, this study is one of the few systematic research efforts studying the oxidative aging in a multi-temperature context. However, the high end of the temperature used (436.2 and 413.2 K) may alter the mechanisms of the oxidation process. The requirement of the calibration using field aged samples means the method can not be used to evaluate the quality of an asphalt before it is placed on the road.

Verhasselt and Choquest (1991, 1993) and Choquest and Verhasselt (1994) reported an accelerated aging test in which the binder was heated in a rotating stainless steel cylinder in a manner similar to the Rolling Thin Film Oven Test (RTFOT, ASTM D2872). Oxygen was introduced into the cylinder and the aging temperature was controlled between 343.2 and 373.2 K. Aged samples were removed from the cylinder after specific aging times. Asphaltene content, ring-and-ball softening temperature, reciprocal of penetration, and infrared absorption at 1700 cm^{-1} were measured. They developed a model which described the change in properties based on reaction and diffusion in one-dimension, as shown in Equation (1-4).

$$(\Delta y)^2 = k t \quad (1-4)$$

The parameter k is the reaction rate for the particular property. The values of k were obtained for different temperatures and plotted against the reciprocal of aging temperature to estimate the Arrhenius activation energy. The researchers claim that reaction rates at low temperatures may be calculated by extrapolation of the Arrhenius relationship to lower temperatures. Using several years of recorded service temperature and the activation energy, the kinetic mean value of the annual temperature was calculated. It was found that laboratory tests must be conducted at a temperature below 373.2 K (100°C) to simulate the in-service aging of a bituminous binder. At temperatures higher than 373.2 K, the reaction mechanism is different from that which occurs in the pavement. Highly significant linear relationships between the measured properties were reported. However, the method of Verhasselt and Choquest has several flaws. The maximum amount of binder that can be aged is 450 g and the starting thickness of the film on the inner wall is of the order of 2 mm. This means significant error may be introduced in the sample removal step because the aging extent of the sample removed is a strong function of the position within the cylinder (film thickness), particularly at the aging temperature of 343.2 K when the binder is not very fluid. Additionally, the aging time at 343.2 K is reported to be around 240 days, which likely precludes this test from widespread industrial implementation. Finally, the theoretical basis of the model is not correct. Equation (1-4), like other equations such as Equation (1-2), models the data reasonably well. However, the hyperbolic change in properties with respect to aging time does not result from diffusion, but rather from the existence of an initial non-linear rapid reaction which is then followed by the long-term constant rate reaction (Lau et al., 1992; Lunsford 1994). In fact, the carbonyl growth on the surface of an aged asphalt film where diffusion effect has been eliminated still can be fit by a hyperbolic curve for limited number of data. It is a common misunderstanding of many researchers (Blokker and van Hoorn, 1959; Verhasselt and Choquest, 1991) to explain the hyperbolic shape of the aging extent-aging time curves by diffusion effect. Nevertheless, Verhasselt and Choquest's study is quite informative and inventive, particularly in that the activation energy is taken into account to calculate the kinetic mean temperature.

Harnsberger et al. (1991) aged the eight SHRP core asphalts using the thin film accelerated

aging test (TFAAT) at three different temperatures, 358.2, 386.2, and 403.2 K. It was observed that some asphalts had low aging indices that changed very little with increased aging temperature, whereas other asphalts of both low and high aging indices changed dramatically with increased aging temperature. A microstructure model was proposed to explain the phenomenon. These observations are valuable because they indicate (although the authors did not calculate) differences between the activation energies of the asphalts. The aging temperatures of 386.2 and 403.2 K used by these researchers may have been too high and no quantitative model was attempted.

The most interesting and fundamentally important work in recent years in terms of developing an aging model to evaluate long-term aging performance has been accomplished by Lau et al. (1992). Lau et al. (1992) conducted aging studies in a pressure oxygen vessel (POV) operated at 20 atmospheres of pure oxygen. The aging was monitored by measuring the zero shear rate limiting viscosity (η_0), and the infrared absorbance of the carbonyl groups. At 20 atm oxygen pressure and at temperatures from 333 to 366 K, the carbonyl formation rate became constant after an initial, more rapid rate region. For isothermal and isobaric conditions, the carbonyl content (CA) in the constant rate region can be described as a linear function of time, as shown in Equation (1-5).

$$CA = CA_0 + R_{CA} t \quad (1-5)$$

R_{CA} , the rate of increase in carbonyl absorbance, was identified as a measure of the oxidation rate of the asphalt. The carbonyl area (CA) is a measure of the infrared absorbance of various C=O groups in the asphalt including ketones, carboxylic acids and anhydrides (Petersen, 1984). Numerically, the carbonyl area is equal to the integrated area under the infrared absorbance curve between 1650 and 1820 cm^{-1} (Jemison et al., 1992). Lau et al. (1992) also found that the carbonyl formation dependence on aging temperature could be described by the usual Arrhenius reaction kinetics as shown in Equation (1-6).

$$R_{CA} = \frac{dCA}{dt} = A e^{-E/RT} \quad (1-6)$$

The parameters in Equation (1-6) are A, the pre-exponential factor and E_A , the reaction activation

energy. Furthermore, they illustrated that the relative ranking of the oxidation rates of different asphalts may be reversed at different aging temperatures. Finally, they observed excellent linearity between the logarithm of the viscosity and the carbonyl area which they called the hardening susceptibility (HS).

$$\ln \eta^*_0 = \ln m + HS \cdot CA \quad (1-7a)$$

Where m is a model parameter. Differentiating Equation (1-7a) with respect to CA resulted in Equation (1-7b).

$$\frac{d \ln \eta^*_0}{dCA} = HS \quad (1-7b)$$

The linear relationship between the two properties was first identified by Martin et al. (1990) when examining asphalt binders extracted from field-aged pavement samples. This relationship has subsequently been confirmed on laboratory-aged samples, including TFOT and RTFOT-aged samples, been found to be independent of aging temperature below 113°C and has been shown to be highly asphalt specific (Lau et al., 1992; Petersen et al., 1993; Peterson et al., 1994; Jemison et al., 1995; Lin et al. 1996; Huh and Robertson, 1996). The hardening susceptibility is related to the hardening rate as shown in Equation (1-8).

$$\frac{d \ln \eta^*_0}{dt} = \left(\frac{d \ln \eta^*_0}{dCA} \right) \cdot \left(\frac{dCA}{dt} \right) = HS \cdot R_{CA} \quad (1-8)$$

Thus, the hardening rate is determined by both the resistance to oxidation and the resistance to hardening. Obviously, a low value for the HS will help reduce the rate of increase of $\log \eta^*_0$ ($d \ln \eta^*_0 / dt$).

Other physical properties may be used in Equation (1-7) to replace viscosity, as long as the corresponding physico-chemical correlations can be developed. It is commonly accepted that when the physical properties of an asphalt binder deteriorate to a certain degree, the road in which the

asphalt is incorporated will fail. Depending on the failure mode, the critical physical property can be ductility, viscosity and other properties. The strategic highway research program (SHRP, 1992) has identified $G^*/\sin\delta$ and $G^*\sin\delta$ as the properties correlated with rutting and medium temperature fatigue cracking, where G^* is the magnitude of the complex modulus G' and iG'' , and $\tan \delta$, called the loss tangent is the ratio of the loss modulus to the elastic modulus ($\tan \delta = G''/G'$). Results in terms of low frequency limiting viscosity, may be extended to other properties with parallel relationships. This is supported by previous observations that different types of physical properties are uniquely correlated. Ishai et al. (1988) reported that for a given asphalt during oxidative aging, the aging characteristics, expressed by either penetration-viscosity or penetration-softening point relationships, are independent of aging extent and aging temperature and can be represented by a single curve specific for each asphalt.

Typically, the dynamic viscosity in Equation (1-7) has been reported as the dynamic viscosity at a measurement temperature of 60°C ($\eta_{0,60^\circ\text{C}}^*$). The relationship in Equation (1-7) can easily be extended to other viscosity temperatures through the use of a viscosity temperature susceptibility (V.S.) in much the same way as Equation (1-7) can be extended to describe the ductility or some other property. The V.S. can be conveniently expressed by the Andrade (1930), shown in Equation (1-9)

$$\ln \eta_{0}^* = A_{\text{vis}} + \frac{E_{\text{vis}}}{RT} \quad (1-9)$$

In Equation (1-9), A_{vis} is a material constant, R is the ideal gas constant, T is the absolute temperature, and E_{vis} is the viscosity activation energy and describes the sensitivity of the viscosity to changes in temperature. Jemison (1995) argued that E_{vis} was a superior measure of the viscosity temperature susceptibility (V.S.) than traditional methods.

Lunsford (1994) performed additional POV aging studies using the same asphalts as Lau et al. (1992). However, Lunsford also studied the influence of pressure on the oxidation kinetics. The oxidation rates were found to depend on pressure according to a power relationship.

$$R_{\text{CA}} = A' P^\alpha e^{-E/RT} \quad (1-10)$$

Interestingly, the pressure dependence (α) of the asphalts was found to be between 0.25 and 0.29 for all of the asphalts investigated, indicating that a universal pressure correction might exist that would allow aging tests conducted at high pressure to be corrected to ambient conditions. However, activation energies for the asphalts varied from 67 to 81 kJ/mol providing considerable evidence that the relative rates between asphalts would be different depending on the aging test temperature. This was also noted by Lau et al. (1992). Lunsford (1994) also found that CA_0 from Equation (1-5) is temperature independent, within experimental scatter, and pressure dependent.

Liu (1996) studied more asphalts and determined that although the relationship in Equation (1-10) is valid, the approximately equal pressure reaction orders found by Lunsford were fortuitous. Furthermore, Liu discovered that the hardening susceptibility is pressure dependent. Liu reported kinetic pressure reaction orders ranging from 0.33 to 0.58 and activation energies ranging from 83 to 100 kJ/mol. The implications of wide variations in temperature susceptibility and pressure dependence are that the results of any aging test conducted at elevated temperature and/or elevated pressure must be viewed with extreme skepticism. In addition, the hyperbolic nature of the changes in properties cast a negative light on any aging test conducted for a single aging time.

Unfortunately, the "standard" aging test recently developed during the strategic highway research program (SHRP) combines all three factors. The SHRP pressure air vessel (PAV) aging test is conducted at a single high temperature of 100°C and a single high pressure of 20 atmospheres of air for a single period of time of 20 hours (AASHTO PP1, 1994). Recently, Huh and Robertson (1996) conducted PAV aging tests at additional temperatures to investigate the aging properties of the SHRP "core" asphalts. They developed a complicated model to describe the change in viscosity in terms of both the sulfoxide content and the carbonyl content, even though the simple hardening susceptibility relationship suggests that the sulfoxide content can likely be neglected. They, like Lau et al. (1992), Lunsford (1994), and Liu et al. (1996), found that the temperature sensitivity to reaction was different for the different asphalts.

Recycling Studies

The discussion of aging, thus far, has been focused mainly on changes in physical properties and oxidation as the asphalt ages. Another important consideration is the changes in chemical

composition with aging which result from the oxidation. The chemical changes which accompany the physical changes in the binder as it ages are also well known. It has been reported that the content of saturates remains relatively constant during aging, the naphthene aromatic content decreases and the asphaltene content increases. (Corbett and Swarbick, 1958; Corbett and Swarbick, 1960; Corbett and Merz 1975; Shiao et al., 1991). Similar trends in composition for the Rostler fractions have been noted (Rostler and White, 1962; Halstead et al., 1966). This shift in composition results from the naphthene aromatics being converted to polar aromatics and the polar aromatics being transformed into asphaltenes as a result of the addition of oxygen to these molecules. Recent data (Liu, 1996) suggests that the oxidized naphthene aromatics will also eventually form asphaltenes, but only after a very long aging time. The polar aromatics content can either increase or decrease, depending on the relative rates of the conversion of naphthene aromatics to polar aromatics and the conversion of polar aromatics to asphaltenes. The increase in asphaltenes with aging is chiefly responsible for the increase in viscosity with aging (Corbett and Swarbick, 1960; Dunning and Mendenhall, 1978; Lin et al., 1995a; Lin et al., 1996). The conversion of the initial polar aromatics into asphaltenes also results in a loss in ductility. The net result of increased viscosity and decreased ductility is eventual pavement failure and the net effect of the composition changes is that the compatibility, as measured by the Rostler N/P (Corbett P/S) ratio, or the Rostler durability parameter deteriorates with aging. In short, the amount of dispersing media decreases while the amount of material needing to be dispersed increases.

Based solely on these observations it can be theorized that an asphalt recycling agent should have few or no asphaltenes as the aged asphalt already has too many. In addition, because saturates and asphaltenes are highly incompatible (recall asphaltenes are defined as those components insoluble in saturated hydrocarbons), the rejuvenating agent should be low in saturates. Thus, to soften and recompatibilize the asphalt, a rejuvenating agent should be rich in naphthene aromatics. Also, to improve ductility, a rejuvenating agent should be rich in polar aromatics. Indeed, it has been the conclusion of several recycling studies (Davidson et al., 1977; Dunning and Mendenhall, 1978; Epps et al., 1980; Peterson et al., 1994) that a rejuvenating agent should have a controlled composition. Dunning and Mendenhall (1978) suggested limits based on HPLC column composition analysis roughly equivalent to a minimum polar aromatic content of 9%, a minimum naphthene aromatic

content of 60%, and consequently, a maximum saturate content of 31%. Epps et al. (1980) suggested that the rejuvenating agent paraffin content should be under 30%, the N/P ratio should be a minimum of 0.5, and the value of the Rostler durability parameter should be between 0.2 and 1.2. Davidson et al. (1977) have recommended that a reclaiming agent should have an N/P ratio above 1.0 and a value of the Rostler durability parameter preferably between 0.4 and 0.8.

Unfortunately, a wide variety of materials possess N/P ratios and Rostler durability parameters within the ranges suggested by Davidson et al. (1977) and Epps et al. (1980). Furthermore, neither of these groups of researchers gave any specification on rejuvenating agent asphaltene content. Rostler and Rostler (1981), however, did indicate that lower asphaltene content in specially blended or recycled asphalts was desired. Davidson et al. (1977) even argued that reclaiming agents "spiked" with asphaltene were desirable because they allowed for more reclaiming agent to be added without compromising overall blend consistency. Furthermore, it was stated that asphaltene should be used as a bodying agent precisely because they don't affect the durability parameter. The results indicated that increased reclaiming agent content for a given aged asphalt/reclaiming agent blend resulted in improved aging indexes, sometimes dramatically so. Finally, it was argued that using higher viscosity reclaiming agents would allow the use of a single reclaiming agent instead of the combination of a reclaiming agent and a low viscosity asphalt. However, the use of a combination of fresh asphalt and rejuvenating agent is still the preferred method.

Dunning and Mendenhall (1978) opposed the general idea of using a single modifier, although all of the recycled blends they studied were produced using a single modifier. They argued that the use of a single, fixed viscosity modifier does not allow the contractor to compensate for binder variations. In fact, recycling specifications should require the separate addition of recycling agent and add-mix asphalt except in cases where binder homogeneity was not a problem. In a related conclusion, they indicated that the viscosity of a recycling agent should be as low as possible. The ranges suggested were 0.9 to 3.0 dPa·s (poise). The use of a low viscosity agent certainly makes sense from an economic standpoint, as less rejuvenating agent is required.

Newcomb et al. (1984) studied initial blend physical properties, and the properties after RTFOT-treatment for single rejuvenating agent recycled asphalts. They studied one aged asphalt and nine rejuvenating agents ranging in composition from nearly pure saturated oils to what appear to be

moderately high asphaltene content AC-5 grade asphalts. None of the materials had aromatic contents above 70%. They found excellent correlation between aging index and the ratio of the polar aromatics to saturates (P/S) in the modifier. Generally, the agents with higher P/S ratios resulted in blends with lower aging indexes. Noureldin and Wood (1990) also conducted asphalt recycling experiments which indicated that through the proper choice of recycling agent, a binder with excellent hardening properties can be produced. Two of the three recycled blends they investigated had lower TFOT aging indexes than the original virgin asphalt.

While many of the recycling studies have looked at the aging performance of recycled asphalts (Davidson et al. 1977, Newcomb et al., 1984; Noureldin and Wood, 1990; Peterson, 1993; Wisneski et al., in press), few have investigated the oxidation kinetics of recycled asphalts by aging at multiple temperatures and multiple time periods, even though the literature (Lau et al. 1992; Lunsford, 1994; Liu et al., 1996; Liu, 1996) suggests that asphalt aging performance can only be fully understood by studying aging at multiple temperatures and pressures and for multiple aging time periods.

Wisneski et al. (in press) recently reported experiments where two aged asphalts were recycled with three different supercritical fractions. They eliminated one possible source of error by conducting all of their aging experiments at ambient pressure conditions. They found that the hardening susceptibilities of the recycled asphalts were generally no worse than the hardening susceptibilities of the original asphalts. In fact, the hardening susceptibilities for one-half of the blends they investigated were greatly improved over the original binder hardening susceptibilities. Finally, they also investigated the use of lime as an additive for recycling applications. Several researchers (Plancher et al., 1976; Petersen et al., 1987; Wisneski, 1995; Wisneski et al., in press) have studied the effects of lime treatment on the hardening properties of asphalts. Many of these researchers have shown conclusively that lime reduces the hardening, as measured by the aging index, of asphalts (Plancher et al., 1976; Petersen et al., 1987; Wisneski et al., in press) and some have noted changes in chemical properties for lime-treated asphalts (Plancher et al., 1976; Petersen et al., 1987). Wisneski et al. (in press) noted that the addition of the lime to the recycled asphalts resulted in hardening susceptibilities uniformly superior to those of the untreated blends.

The improvement in hardening susceptibility for recycled asphalts reported by Wisneski et al. (in press) confirm the results reported by Peterson et al. (1994) for recycled asphalts. Unfortunately,

poor temperature control did not allow Peterson et al. (1994) to determine accurate aging rates and consequently, accurate kinetics. The conclusions from their study indicated that excessive amounts of paraffins (saturates) were detrimental to the hardening susceptibility of the recycled asphalts but were beneficial to the viscosity temperature susceptibility. Later, Peterson (1994) concluded that to minimize the impact that saturates have on the aging properties of asphalts, a relatively larger proportion of rejuvenating agent should be utilized. Lin et al. (1995b) arrived at this same conclusion based on the analysis of the relationship between viscosity and asphaltene content.

The suggestions of Davidson et al. (1977), Peterson (1993), and Lin et al. (1995b) that a relatively larger portion of softening agent should be utilized raises one final issue that needs to be addressed for asphalt recycling. That issue is the necessity to accurately predict the quantity of softening agent required to restore the consistency of an aged asphalt so that time consuming trial and error blending can be avoided. There are currently two viscosity mixing rules used to predict the necessary amount of recycling agent, in terms of mass fraction (x_{ra}), in order to obtain a certain target mixture viscosity (η_m) when the viscosity of the old asphalt (η_{as}) and the viscosity of the rejuvenating agent (η_{ra}) are known. The first mixing rule is that proposed by Epps et al. (1980).

$$\log_{10}(\log_{10} \eta_m) = x_{as} \log_{10}(\log_{10} \eta_{as}) + x_{ra} \log_{10}(\log_{10} \eta_{ra}) \quad (1-11)$$

This method leaves much to be desired as small errors in terms of $\log \log \eta_m$ can represent large errors in η_m .

Although Epps' rule has received some attention, the rule most commonly used to estimate the quantity of rejuvenating agent necessary to obtain a certain target viscosity for the recycled binder is the procedure specified in ASTM D-4887 (1994). This procedure, also suggested by The Asphalt Institute (1981), uses the graphical representation of the Arrhenius equation (1887) for predicting mixture viscosity.

$$\ln \eta_m = x_{as} \ln \eta_{as} + x_{ra} \ln \eta_{ra} \quad (1-12)$$

Although the Arrhenius equation has been adopted (in nomograph form) as the ASTM standard, the literature indicates that this mixing rule produces poor results in some cases. In one particular study,

Noureldin and Wood (1990) recycled one old asphalt with two low viscosity asphalts and one emulsified recycling agent. They utilized the ASTM mixing rule to determine how much low viscosity asphalt to use, but determined the quantity of emulsified recycling agent "...on the basis of previous recycling projects".

Peterson (1993) used the ASTM mixing rule to obtain initial guesses for the quantity of recycling agent necessary to soften the aged asphalts he studied to 2000 poise. In every case, the resulting blend viscosity was lower than the target viscosity. The resulting viscosities ranged from around 450 poise up to 1230 poise. Peterson rearranged Equation (1-12) to obtain a dimensionless parameter, the dimensionless log viscosity (DLV), which should be linear with respect to the recycling agent content. Although there was tremendous scatter, a second-order polynomial modeled the data more accurately. Dunning and Mendenhall (1978) also reported a viscosity mixing rule of their own.

Irving conducted a survey of equations (Irving, 1977a) that had been proposed to effectively describe the viscosity of binary liquid mixtures. This survey identified more than fifty equations proposed to predict either the dynamic or kinematic viscosity of binary liquid mixtures. Irving also determined the effectiveness of the various mixture equations (Irving, 1977b). Irving concluded that Equation (1-13), the equation proposed by Grunberg and Nissan (1949), was the best overall mixing rule in terms of accuracy and simplicity for predicting the viscosity of non-aqueous binary systems.

$$\ln \eta_m = x_1 \ln \eta_1 + x_2 \ln \eta_2 + x_1 x_2 G_{12} \quad (1-13)$$

The interaction parameter G_{12} is usually considered to be a constant, however, G_{12} may be a function of x_i where x_i may be mole, mass, or volume fraction. Irving determined that the viscosity of a mixture can be predicted to within 30% of the actual viscosity when an average, constant value of G_{12} was used for classes of mixtures (i.e. polar/polar). In addition, Irving's calculations (1977b) indicate that the choice of units for x_i (mole, mass, or volume fraction) make little difference in the accuracy of the model. Mehrotra has used the Grunberg equation to model bitumen/gas (1992) and bitumen/solvent (1990) systems. However, very little effort has been focused on using this equation to predict the viscosity of aged asphalt/softening agent mixtures. The Arrhenius equation (ASTM mixing rule) is a special case of the Grunberg equation with G_{12} equal to zero. Irving (1977b)

concluded that using the Grunberg model with G_{12} equal to zero resulted in errors larger than those obtained using an optimized or average value of G_{12} , if they are available. Large errors may require actual blending to determine a mixture's viscosity.

The objective of this research was to establish the technical feasibility of determining the specifications and operating parameters necessary to produce high quality recycling agents which will allow most, if not all, of old asphalt-based road material to be recycled. Supercritical fractionation of asphalt was utilized to fractionate refinery produced materials, establish operating parameters, and to reblend these fractions to produce superior recycling agents, and systematically study the effect of varying composition on properties. The advanced road aging simulation procedure, developed at Texas A&M, was used to determine the aging characteristics of old asphalt and recycling agent blends so as to relate aging to blend composition.

Summary

The objectives of this project were further broken down into several tasks. Chapter 2 contains a description of the tasks, the objectives of the tasks, and the important results obtained for each task throughout the entire project.

Chapters 3 thru 7 detail work completed in developing a qualitative and quantitative knowledge of asphalt oxidation characteristics, compositional dependence of asphalt properties, and guidelines for producing superior asphalt binders through compositional control. These chapters also detail the development of a kinetic model for asphalt oxidative aging, and present an understanding of the compositional dependence of asphalt oxidation properties as well as other performance-related properties.

Chapters 8 and 9 compare the aging performance of recycled blends produced using commercial recycling agents and industrial supercritical fractions as the rejuvenating agents. The oxidative aging of the recycled blends were evaluated along with the performance of the recycled blends in terms of the strategic highway research program (SHRP) performance grading procedure.

Chapter 10 summarizes the work completed in the areas of processing schemes development, projection updates, and scale-up and commercialization plans. The appendix contains a synopsis of topical publications with a brief introduction as a tie to tasks.

CHAPTER 2

EXECUTIVE SUMMARY OF TASKS

This chapter contains a description of the tasks, the objectives of the tasks, and the important results obtained for each of the tasks conducted during this DOE sponsored research project. The summaries in this chapter are based upon results obtained throughout the project. Most of the work completed during the first two years of this project is described in detail in published topical papers in the open literature and these are summarized in the appendices. In addition, detailed descriptions of work performed during the first two years of the project are given in the first- and second-year project annual reports (refs). Some additional work as well as the experimental procedures, are presented in appendices in detail. Detailed descriptions of work performed during the third year of this project is presented in chapters 3 through 10.

Task 1: Asphalt Fractionation and Source Asphalt Characterization

Description and Objectives of Task

The Contractor shall separate fractions from asphalt to produce candidate fractions for blending to make superior asphalt recycling agents. It is expected that supercritical fractionation of asphalt shall be performed in the Contractor's existing Supercritical Extraction Unit. Asphalt fractions shall be made from several, thoroughly characterized, source asphalts. Also, asphalt fractions shall be obtained from other sources as appropriate, e.g. ROSE fractions from Kerr-McGee, etc.

Appropriate physical and functional properties of the source asphalts shall be analyzed and characterized before performing the fractionations. These tests shall likely include Corbett, Fourier Transform Infrared (FT-IR or simply IR), Gel Permeation Chromatography (GPC), and sufficient aging data to determine the aging characteristics of these asphalts.

Important Results

Four asphalts were chosen to be supercritically fractionated. All four, one obtained from a local hot-mix contractor and three obtained from the strategic highway research program, had all been characterized in detail prior to fractionation. These four asphalts were supercritically fractionated

into seven distinct (eight total) fractions. The results of these experiments largely confirm trends reported previously in the literature. In particular, supercritical fractionation of asphalts can be used to produce materials with predictable chemical and physical properties including group-type compositions, elemental compositions, viscosities, and molecular weights. Several of the supercritical fractions produced in this study have low enough saturate and asphaltene contents, and thus, high enough aromatic contents to restore an aged asphalt to a like-new compositional state. Furthermore, several of the supercritical fractions produced in this study also have viscosities suitable for blending with an aged asphalt to restore it to a like-new consistency. Therefore, supercritical fractionation can be tremendously useful in producing asphalt recycling agents from petroleum residues.

Task 2: Aged Asphalt Production

Description and Objectives of Task

About three asphalts, having significantly different properties, shall be aged in the Pressure Oxygen Vessel (POV) to produce "road" materials of three different viscosities of about 50,000, 150,000, and 500,000 poise at 60°C. Other physical and functional properties shall be determined. These tests are expected to include IR, viscosity, and GPC. Additionally, old highway material, as available and suitable, will be tested.

Important Results

Early in the project, the opportunity to investigate an actual recycling project presented itself. As such, a large quantity of aged pavement was obtained from the construction site. Several tens of kilograms of material were extracted to obtain enough material to conduct a handful of recycling experiments. This highly labor intensive and low yield process was abandoned in favor of laboratory aging of tank asphalts to produce the aged asphalts necessary for this study.

Although the POV could be utilized to produce aged asphalt, the relatively small sample size per tray (up to 5g) limits the amount of material that can be produced in a reasonable amount of time. In addition, to produce large quantities of asphalt in the POV requires combining the material from several trays in a highly labor intensive process. Thus, a new method was developed for the purpose of producing a large quantity of asphalt in an efficient manner.

Initially, an apparatus was constructed consisting of a variable speed motor affixed to a metal frame. Later, a table top drill press was utilized for the aged asphalt production. The motor drives a mixing paddle placed in a half-full can (gallon or quart) of asphalt. The can containing the asphalt is wrapped with a heating tape connected to a variable transformer and a thermocouple actuated on/off controller. House air passes through a surge tank and moisture filter, and then is introduced to the asphalt through a sparging ring made from 1/4 inch stainless steel tubing with nearly uniformly spaced holes. The operating temperature of the air-bubbled (AB) reaction vessel must be high enough for the oxidation to proceed at an appreciable rate, but not so high as to drastically alter the reaction mechanism or reaction products. Additionally, the temperature must be high enough to soften the asphalt so that the asphalt can be well mixed by the mixing paddle. The operating temperature finally used was determined through several preliminary experiments. It was determined that as long as the temperature does not exceed 230°F, the aged asphalt is similar enough to POV-aged asphalt and pavement aged asphalt to warrant its use in recycling studies. Several aged asphalts with a variety of 60°C viscosities were produced in this manner.

Task 3: Preliminary Agent Formulation and Blend Testing

Description and Objectives of Task

The Contractor shall analyze and characterize the appropriate physical and functional properties of the candidate blending fractions obtained from Task 1. Characterization tests shall be selected from Corbett fractionation, FT-IR, GPC, viscosity measurements, and perhaps others.

A spectrum of recycling agents shall be made from the fractions obtained from several source asphalts including several recycling agents formulated from ROSE fractions. At least three viscosity grades of recycling agents (e.g. 5, 25, and 100 poise measured at 60°C) shall be produced by blending the candidate fractions. They shall be comprised of different amounts of molecular size naphthene (NA) and polar (PA) aromatics as well as varying quantities of saturate oil.

A brief test plan for the initial recycle agent screening shall be prepared and discussed with DOE at least two weeks prior to starting the tests. Candidate recycling agents shall be blended with well-characterized, aged road material (from Task 2), and the product "recycled blends" shall be tested for initial physical and functional properties. Tests are expected to include FT-IR and viscosity

from 0-95°C.

After aging the recycled blends using the Pressure Oxygen Vessel (POV) or another method approved by DOE, their physical and functional properties shall be retested. Generally, the tests are expected to be the same as those for the initial properties except for the addition of a ductility test for promising recycle blends.

The effects of the various recycling agents, source materials, and aging on recycle blend properties shall be evaluated. Recycle agents and aged asphalt to be used in subsequent expanded tests shall be selected and the systematic test plan for Task 4 shall be prepared. The overall project status, plans, and market penetration projections shall be reviewed with DOE prior to proceeding with Task 4.

Important Results

The properties of an asphalt binder change over time and specifications based on the initial physical properties do not insure satisfactory performance after the pavement has been placed in service. Therefore, in addition to establishing acceptable initial physical properties, the effect of chemical composition on the oxidation rate of the asphalt binder must be considered. In an effort to address these issues, several different experiments were conducted with the goal of studying the physical properties and aging characteristics of recycled asphalts.

As mentioned in Chapter 1, asphalt composition can best be represented in terms of a few number of pseudo-components or group-type fractions. These fractions are: asphaltenes (AS) and maltenes. The maltenes can then be separated into saturates (SA), naphthene aromatics (NA), and polar aromatics (PA). Several researchers have shown that asphaltenes, both those originally present in the asphalt and those produced by aging, contribute the most to the changes in physical properties of asphalts. Several studies were conducted to determine what factors influence the formation of asphaltenes and the contribution of asphaltenes to an asphalt's rheological properties.

Asphaltenes are products of oxidative aging. A unique relationship called the asphaltene formation susceptibility, or AFS, exists between asphaltene formation and carbonyl formation, which is a measure of the extent of oxidation. The AFS is defined as the partial derivative of asphaltene formation with respect to carbonyl formation. The AFS was found to be independent of saturate

content and type of asphaltene. The AFS was also found to continuously decrease with increased asphaltene content and is a strong function of the composition of aromatics fraction. The contribution that asphaltenes have to the rheological properties was found to be strongly dependent on the asphaltene-maltene interactions. Furthermore, the magnitude of the interaction between asphaltenes and maltenes was found to be a function of temperature and the composition of both asphaltenes and maltenes.

To reduce the detrimental effects that asphaltenes have on an asphalt binder, the AFS should be reduced by adjusting the composition of aromatics. The saturate content also needs to be low because the presence of saturates has been found to magnify the effects that asphaltenes have on the rheological properties of asphalt.

Another study focused on the oxidative aging of asphalt binders, and was extended to their generic fractions and their supercritical fractions to investigate the compositional dependence of asphalt aging properties. The data showed that during oxidative aging PA and NA fractions, as well as supercritical fractions, undergo carbonyl growth profiles similar to those of the whole asphalts. That is, a constant rate region is approached after an initial, more rapid rate period.

The results of this study indicated that the kinetic characteristics of an asphalt are determined by the kinetic characteristics of its fractions as well as the interactions between the fractions. The PA fraction of an asphalt ages faster than its NA fractions. Saturates have only a dilution effect on asphalt oxidation. Asphaltenes may increase the oxidation rate. This means that asphaltenes either oxidize themselves, or they are catalyzing the oxidation of PA and NA fractions. PA and NA fractions age faster in a separated state than in a mixed state.

For supercritical fractions, reactivity increases with the fraction number. This likely results from the elevated polar aromatic content present in the heavier supercritical fractions. In addition, it is theorized that the larger molecular size polar aromatics present in the heavier fractions are more reactive than the smaller polar aromatics present in the lighter supercritical fractions.

For the fractions from the same asphalt source, the molecular size distribution seems to correlate with the reactivities of the fractions. This results from the PA fraction being larger in molecules and aging faster than the NA fraction of the same asphalt. However, for fractions from different asphalt sources, no correlation exists between the molecular size distribution and the

reactivity.

The hardening susceptibility (HS) is one of the important aging properties of an asphalt binder, the HS relationship of the generic fractions and supercritical fractions were examined in detail. This was accomplished by recognizing the fact that the HS relationship is the combined effect of two factors: the viscosity-asphaltene content relationship, which indicates a fraction's solvation power for asphaltenes, and the asphaltene formation susceptibility AFS. These two factors correspond to the first and second terms on the right side of Equation (2-1):

$$\frac{d\ln\eta^*_{0,60}}{dt} = \left(\frac{d\ln\eta^*_{0,60}}{d\%AS}\right) \left(\frac{d\%AS}{dCA}\right) \left(\frac{dCA}{dt}\right) \quad (2-1)$$

For each asphalt, the HS of the NA fraction was smaller than that of the PA fraction, with the HS of the combined aromatics fraction in between. Generally speaking, the generic fractions and supercritical fractions have significantly lower HS values than that of the parent asphalt. The high HS values of the asphalts relative to its fractions is attributed to the coexistence of saturates and asphaltenes in the whole asphalt.

The NA fraction has a bit less solvation power than the PA fraction. However, the effect of a much smaller AFS overrides the effect of a bit less solvation power. Furthermore, the aromatics fraction contains enough PA to yield a solvation power as strong as PA. For supercritical fractions, the AFS increases with fraction number.

Equation (1-9) was used to characterize the viscosity temperature susceptibility of an asphaltic material,

$$\ln\eta^*_0 = A_{vis} + \frac{E_{vis}}{RT} \quad (1-9)$$

In terms of viscosity, the PA fractions are much more sensitive to measurement temperature than the NA fractions. Aromatics fractions are in between. Most supercritical fractions possess E_{vis} lower than the whole asphalt, even after significant aging.

The aged NA and PA fractions were also used to elucidate the oxidation routes of the fractions. The data explicitly show that during the oxidative aging of asphalt binders, polar aromatics

transform to asphaltenes, naphthene aromatics convert to polar aromatics and subsequently oxidize to become asphaltenes. However, for a limited aging extent, it was observed that negligible asphaltenes are produced from naphthene aromatics. Depending on the relative rate of the conversion of polar aromatics to asphaltenes and the rate of the production of polar aromatics from naphthene aromatics, the content of polar aromatics may increase or decrease during the aging process of a whole asphalt.

The newly produced asphaltenes and polar aromatics are smaller in molecular size than those present in the original asphalts. The residual polar aromatics in the aged PA fractions and the residual naphthene aromatics in the aged NA fractions have smaller molecular sizes than those from the parent asphalts.

A superior method was developed for determining the saturate content in heavy petroleum materials such as asphalt, asphalt supercritical fractions, and asphalt recycling agents. Pure saturate fractions isolated from several asphalts and industrial supercritical fractions were analyzed using High Performance Liquid Chromatography (HPLC) to determine if the saturates present in heavy petroleum products are all similar. The refractive index response factor for the saturate fractions isolated from different materials were similar to each other and to the refractive index response factor of petroleum jelly to suggest that petroleum jelly is a suitable calibration standard for HPLC saturate analyses. Furthermore, the automated, unbiased nature of HPLC analysis is superior to the highly subjective open column techniques currently utilized.

Task 4: Expanded Blend Testing

Description and Objectives of Task

The systematic test plan for Task 4 shall be performed with appropriate modifications as test results suggest. Overall, about one hundred recycle blends shall be produced and age-tested with later selections reflecting the results from earlier tests. It is expected that the constituents for the aging-tests of recycle blends shall be made from about nine aged asphalts (three types hardened to three viscosities), and recycling agents from three asphalts plus recycling agents from ROSE fractions of three viscosities with about half a dozen compositions.

Generally, processing considerations shall limit recycle blends to a practical range such as 25%

to 50% recycling agent. Some process development is expected in order to achieve the target viscosity range of 2,000 +1500/-1000 poise at 60°C for each of the recycle blends. Initial mixtures, made using theoretical viscosity calculations, shall be adjusted if the actual viscosity falls outside the target range. After the target viscosity range is obtained, the viscoelastic properties shall be measured over a range of temperature and frequencies to obtain rheological master curves.

Important Results

Two separate recycling studies were conducted. The first recycling study was conducted specifically to compare the performance of commercial recycling agents to the performance of supercritical fractions based on their effects on the aging properties of recycled blends. The viscosity mixing rules described in Appendix H were utilized with some success to predict the quantity of rejuvenating agent required in order to achieve the target viscosities of 2,000 +1500/-1000 poise at 60°C. One aged asphalt was blended with three industrial supercritical fractions, three laboratory produced supercritical fractions, and three commercial recycling agents. The aging indexes after thin film oven test (TFOT) treatment, the aging indexes after pressure aging vessel (PAV) aging, and the extrapolated road conditions hardening rates all indicated that supercritical fractions can be used to produce recycled blends with properties superior to those of the original asphalt. Furthermore, the TFOT and PAV aging indexes from the blends using supercritical fractions were superior to those of the blends produced by using commercial recycling agents. The hardening susceptibilities of the supercritical fraction blends were also generally superior to those of the commercial recycling agent blends. The lower aging indexes for the recycled blends, using supercritical fraction rejuvenating agents, were correlated strongly with the amount of rejuvenating agent in the blend indicating that asphaltene dilution is a key factor in asphalt recycling, as suggested in the literature. The lower hardening susceptibilities, for the recycled blends using supercritical fraction rejuvenating agents, are correlated strongly with both the rejuvenating agent content and the saturate content in the blends. Additionally, the laboratory supercritical fractions were shown to be superior to the industrial supercritical fractions. This can likely be attributed to the narrower cuts produced in the laboratory compared to industrial operation.

The second recycling study investigated more aged asphalts, more rejuvenating agents, more

blend properties, and road condition aging rates. In addition, the recycled asphalts in the second recycling study were graded according to the SHRP performance grading criteria. The data in the second recycling study generally support the conclusions of the first recycling study in regard to the aging properties of recycled asphalts. In particular, the choice of rejuvenating agent can affect both the kinetics and the hardening susceptibility, but the effects were largely as a result of dilution of the aged asphalt. Furthermore, the relative rankings based on PAV aging indexes, and road condition hardening rates for the blends of a given asphalt were usually consistent.

The effect of recycling on the viscosity temperature susceptibility and low temperature rheological properties were also found to be strongly correlated to rejuvenating content. However, dilution was shown to be detrimental to these properties. Even though dilution detrimentally impacted the low temperature rheological properties, the choice of rejuvenating agent rarely changed the low temperature performance grade of the recycled blend. In addition, the performance grades of the recycled asphalts were all superior to the performance grades of the original asphalt. The high temperature specification grades were largely unchanged (except due to too high of an initial viscosity) but in the case of one particular asphalt, recycling improved the low temperature grade by 12°C.

Task 5: Rejuvenated Material Aging and Testing

Description and Objectives of Task

Recycle blends from Task 4 shall be aged in the POV at three temperatures and for three durations. Rheological data shall be obtained as before over a range of temperatures and frequencies. Other characterization tests, such as FT-IR, GPC, etc. will also be conducted.

Important Results

Oxidative aging is one of the major causes of road pavement failure. Through contact with the oxygen in the ambient environment, asphalt binder in the pavement oxidizes. This oxidation process results in an increase in asphaltene content, carbonyl content, and viscosity of the binder. Eventually, the binder becomes too brittle to sustain the damage from traffic load and thermal cycling.

A study on the kinetics of carbonyl formation and physico-chemical correlation was

conducted. Ten asphalts, including seven SHRP asphalts, and three Texas asphalts were aged at a total of 13 aging conditions. The temperature aging conditions ranged from 333.2 K (140°F) to 372.0 K (210°F), and the pressure aging conditions ranged from an oxygen pressure of 0.2 atm to 20 atm.

With an understanding of oxidation kinetics and the physico-chemical correlation, an aging model was proposed. The correlations between the kinetic parameters were investigated. Models were developed to describe the pressure dependencies of the physico-chemical correlation coefficients.

Carbonyl area, as measured by the FTIR, was used as a measure of the oxidation extent for asphalt binders. By measuring the carbonyl growth of the asphalts aged at a combination of temperatures and oxygen pressures, the oxidation rates at the specific conditions and the average value of the initial jump $CA_0 - CA_{\text{tank}}$ at different aging pressures were obtained for each of the asphalts. Generally speaking, the initial jump increased with aging pressure, with the extent being asphalt dependent. Kinetic parameters including activation energy E and pressure reaction order α were estimated through linear regression for the asphalts. The kinetic parameters have been found to be asphalt dependent.

The hardening susceptibility relationship was measured at both high pressure (20 atm) and low pressure (0.2 atm) for the ten asphalts. Data show that the hardening susceptibility is larger for a lower aging pressure, with the extent being asphalt dependent.

A model for the oxidative aging of asphalt binders was proposed. It is based on the understanding that age hardening is the combined effect of the carbonyl growth due to oxidation, and the hardening in physical properties due to the chemical compositional change. A theoretically sound aging test to evaluate low temperature, low pressure aging resistance was described. In the described scheme, the kinetic parameters of a given asphalt were measured to calculate the oxidation rate at the road temperature. The method also requires the measurement of other characteristic parameters for the given asphalt, including the initial jump $CA_0 - CA_{\text{tank}}$ and the HS value at road conditions.

Models were developed to describe the pressure dependencies of the initial jump $CA_0 - CA_{\text{tank}}$ and the HS value. Because the kinetic parameters are asphalt dependent, and because the initial jump $CA_0 - CA_{\text{tank}}$ and the HS value are pressure dependent, any aging test run at a single elevated

temperature and/or pressure, including the PAV test, are not theoretically sound.

Data also show that the RTFOT treatment has a negligible effect on the kinetic behavior of asphalt binders.

Task 6: Mixing Rules Development

Description and Objectives of Task

Current mixing rules predicting the viscosity after combining asphalt in the new and aged conditions is not consistent with observed aging properties. The contractor shall investigate the relationships for mixing new and aged asphalt to improve mixing rules predictions. Based on viscosity, the Contractor shall develop improved mixing rules.

A considerable body of existing data and data obtained in formulating blends in Task 3 and 4 will be used to obtain a correlation of blend viscosity in terms of old asphalt and blending agent viscosities and the weight fraction of each. If possible, this will be refined in terms of other analyses such as Corbett or high pressure liquid chromatography (HPLC).

Important Results

Several aged asphalt/softening agent pairs were blended at multiple levels of aged material content with the sole intent of producing viscosity mixing rules for aged asphalt/softening agent binary systems. Blends were also constructed by “spiking” rejuvenating agents with asphaltenes to determine the effect of asphaltenes on the relationship between blend viscosity and aged asphalt content. Blend viscosity data were also analyzed for specific recycled asphalts produced using asphaltene and saturate free rejuvenating agents in an effort to elucidate the influence of saturates. Finally, a new viscosity mixing rule was developed based on the controlled blending experiments. The new mixing rule shows excellent agreement with data published in the literature.

The relationship between mixture viscosity and aged material mass fraction for nearly all of the asphalt/agent pairs can be described using the Grunberg model for the viscosity of a binary liquid mixture.

$$\ln \eta_m = x_1 \ln \eta_1 + x_2 \ln \eta_2 + x_1 x_2 G_{12} \quad (1-13)$$

The Grunberg model has only one adjustable parameter G_{12} which describes the interaction between blend components. Blends using low viscosity asphalts as the softening agent exhibit significantly different behavior from blends using commercial recycling agents and supercritical fraction recycling agents. The low viscosity asphalt softening agents have viscous interaction parameters near or greater than zero, implying that a blend of aged asphalt and low viscosity asphalt may be more viscous than would be predicted by currently used mixing rules. All of the blends using supercritical fraction and commercial recycling agents had interaction parameters less than zero. Negative interaction parameters are manifested in viscosities below those predicted by the current standard mixing rules.

The value of the interaction parameter G_{12} is a strong function of the viscosity difference between the aged asphalt and recycling agent for either a supercritical fraction or a commercial recycling agent. Normalizing the viscosity in terms of the dimensionless log viscosity (DLV) reduces the difference between recycling agents.

$$DLV = \frac{\ln(\eta_m/\eta_1)}{\ln(\eta_2/\eta_1)} = \left(1 + \frac{G_{12}}{\ln(\eta_2/\eta_1)} \right) x_2 + \left(\frac{-G_{12}}{\ln(\eta_2/\eta_1)} \right) x_2^2 \quad (2-2)$$

In fact, DLV data for all of the recycling agent blends show strikingly little variation between recycling agents regardless of recycling agent composition or aged asphalt used. Surprisingly, even the asphaltene "spiking" experiments indicated no correlation between the group-type composition of the recycling and the interaction parameter. However, the data points from the asphaltene and saturate free rejuvenating agent blends showed more negative deviation than the other blends, indicating that saturates are likely undesirable, but the effect of saturates could not be quantified.

An average normalized interaction parameter was obtained for the aged asphalt/recycling agent mixtures by fitting all of the aged asphalt/recycling agent data. The prediction capability of the DLV mixing rule was verified through comparison to blend viscosity data published in the literature. The data from the literature are remarkably consistent with the mixing rule developed in this study. The DLV mixing rule was then used for the recycled asphalt aging experiments performed in this study. For one set of the recycled asphalt aging studies, the DLV mixing rule was successfully used to obtain the target viscosity for almost half of the recycled asphalts. Although the results were not

as good for the second recycling study, the errors were usually on the side of caution.

Task 7: Lime Additive Testing

Description and Objectives of Task

The Contractor shall investigate the effect of adding lime to the recycle blends to slow oxidation of the asphalt and extend its service life. This may be particularly useful with asphalts that do not otherwise recycle well. Gradient amounts of lime, together with recycle agent, will be used primarily with (but not limited to) asphalts that prove difficult to recycle in Task 4. These recycle blends will be characterized, aged, and evaluated as described in Task 4.

Important Results

Two different studies were conducted to determine the effects of lime treatment on asphalt aging. Because the composition of aged asphalts is different than the composition of virgin asphalts, it was hypothesized that lime treatment might affect the properties of virgin asphalts differently than it would affect the properties of recycled asphalts. As such, lime blending experiments were conducted on both virgin asphalts and recycled asphalts primarily so that the effects of lime treatment might be separated from the effects of recycling.

The first study consisted of two sets of lime-treated tank asphalt experiments. The first set of experiments was conducted on two strategic highway research program (SHRP) asphalts using both calcium oxide, CaO, and calcium hydroxide, Ca(OH)₂, at 0, 1, 2, 5, 10, and 20 percent lime by weight. Although kinetic information could not be obtained from these initial experiments, the experiments did indicate that lime reduced the hardening susceptibilities and selected aging indexes of the asphalts. However, no further conclusions could be made.

The second set of lime-treated tank asphalt experiments involved four SHRP asphalts blended with multiple levels of calcium hydroxide, Ca(OH)₂. Without exception, the addition of lime increased the viscosity of the unaged asphalt. Furthermore, the viscosity increase was directly related to the amount of lime added, as would be predicted by particle suspension models. Lime treatment had little or no effect on the viscosity temperature susceptibility of the unaged asphalt.

The aging data collected in the experiments on lime-treated tank asphalts indicate that the

addition of lime does not affect the "initial jump" of the asphalt. In addition, the data indicate that lime only slightly reduces the oxidation rates of an asphalt, but only as the result of dilution. The reductions in oxidation rates were fairly constant with aging temperature and as such, the addition of lime has no effect on the activation energies of the tank asphalts examined in this study. On the other hand, addition of lime reduced the hardening susceptibilities of the tank asphalts by more than 10%, on average, irrespective of lime content. In other words, the hardening susceptibility was improved by the mere presence of lime and the concentration of lime was not an important factor. Extrapolations indicated that lime-treatment of tank asphalts will probably reduce the hardening rate at road conditions.

The second study consisted of two sets of lime-treated recycling experiments. The preliminary set of experiments were conducted using calcium oxide, CaO, at nominal lime contents of 0, 2, 5, and 10 percent lime. These preliminary experiments indicated that lime treatment was uniformly beneficial to the hardening susceptibility of the recycled asphalts, but only affected the oxidation in a dilutory manner. These preliminary experiments also indicated that the hardening susceptibility was improved by the mere presence of lime and the concentration of lime was not an important factor. As such, a nominal 5 percent lime content was chosen for the second set of experiments. Additionally, re-analysis of the data from the preliminary lime-treated tank asphalt studies and analysis of the costs indicated that calcium hydroxide should be used instead of calcium oxide.

The second set of experiments indicated that lime treatment at a 5 percent level had a profound impact on the properties of recycled asphalts. In particular, the addition of lime caused an almost uniform decrease in the viscosity of the unaged recycled asphalt, which is in stark contrast to the results from the lime treated-tank asphalt studies. This was hypothesized to result from lime effectively interfering with the association of the asphaltenes present in the aged asphalt. Lime also generally improved the reaction activation energy. In agreement with the lime-treated tank asphalt experiments, lime treatment of recycled asphalts was shown to have little or no effect on the viscosity temperature susceptibility of unaged recycled asphalts, and the hardening susceptibilities and road condition hardening rates were lower for the lime-treated samples compared to the untreated samples. The PAV aging indexes of the lime-treated recycled asphalts were also lower than the respective

untreated blends, and the aging index rankings were strongly correlated with the road condition hardening rates. Summarizing, lime was shown to have an almost uniformly beneficial effect on the aging properties of recycled asphalts. Unfortunately, the low temperature creep stiffness and m -values of the recycled mixtures were detrimentally impacted by the presence of lime. Furthermore, because lime treatment reduced the high temperature viscosity and negatively influenced the low temperature rheological properties, it was shown that lime treatment may possibly result in a two grade, or 12°C , decrease in the SHRP performance grade temperature span.

Task 8: Other Additives (Amines) Testing

Description and Objectives of Task

The Contractor shall investigate the effect of adding other components such as amines and other nitrogen-containing additives to the recycled asphalt mixtures to slow oxidation of the asphalt and extend its service life. Small amounts of the test materials, amines, or nitrogen-containing mixtures such as shale oil will be treated by the same procedures as in Task 7.

Important Results

Three amines with dramatically different functionality were blended with two different recycled asphalts at an amine content of 2 percent. Analysis of these experiments eliminated further examination of amine treatment. It was determined that the unpleasant fumes given off during blending may, however unlikely, pose a health hazard. In addition, only a very small amount of amines could be used in recycling applications as the low viscosities of the amines would result in excessive softening of a recycled asphalt. The aging experiments indicated that few, if any, benefits would be realized by the addition of amines to the recycled asphalts. The carbonyl formation rates, activation energies, and hardening susceptibilities were not affected greatly by any of the amine additives. In fact, the data indicate that the kinetics may have been adversely affected by the amines in several cases. If these reasons were not already sufficient to eliminate amines as a recycling addition, the cost of amine treatment was determined to be prohibitively high. Thus, it is clear that lime should be the additive of choice to improve the properties of recycled asphalts.

Task 9: Processing Schemes Development

Description and Objectives of Task

The Contractor shall present the optimum recycling agent compositions to Kerr-McGee, the licensor of the ROSE process, for the purpose of devising practical process alternatives for making superior recycling agents using existing ROSE installations. This information will include crude sources, operating temperatures and pressures, fraction properties and composition. Kerr-McGee in consultation with the Contractor will devise practical and economical operating conditions for obtaining improved agents.

Important Results

The performance of this task was complicated by the sale of the ROSE process to Kellogg, after which we were no longer able to get help from Kerr-McGee. However, from data in the literature and from runs on our supercritical unit, we believe that our cost estimates are accurate. Very good recycling agents can be produced from some crudes as the resin or center cut of a supercritical unit.

Further work has indicated that an even better process would be to recover the aromatics from deasphalted oil (DAO) produced by many refineries using a variety of methods, including supercritical extraction or precipitation by propane or other hydrocarbons. This material is generally about half aromatics and the rest saturates. The aromatics are high in naphthene aromatics and lighter polar aromatics. As such, the aromatic portion is of ideal composition for recycling.

The technology exists for recovering these materials and large plants are operating, primarily to produce lube stocks. The charges to produce recycling agents would be minor.

Task 10: Projection Update and Commercialization Plan

Description and Objectives of Task

Data from the project shall be analyzed and used to predict full-scale commercial operations and economics.

Projection Updates - Data from this research shall be collected and analyzed to confirm or modify proposal estimates of overall market penetration (to the year 2010), process performance,

plant and national energy savings, plant and national emissions reductions, and economic viability. The evaluation of long-term industry trends and the extent of market penetration shall be updated if needed. Differences from economic, energy, and environmental benefits previously predicted shall be noted. The Updates shall be performed annually or more often if new data causes significant changes from those used earlier. DOE shall be notified promptly if test results indicate a significant change in performance projections.

Scale-Up and Commercialization Plan - The Contractor shall prepare a detailed plan for scaling up and commercializing this technology. Assumptions shall be stated and specific roles and commitments from the project industrial participants shall be documented.

Important Results

The most significant factor to affect market penetration is the introduction of SHRP specifications which radically change the measures of asphalt performance. Furthermore, it is intended to extend these specification to recycling. This is likely to have a major negative impact on development of processes to produce recycling agents until this uncertainty is removed.

Cost estimates of large scale production of agents using both supercritical extraction and lube oil extraction technology is presented.

Task 11: Reports

Description and Objectives of Task

The purpose of this task is to provide the management necessary to meet technical objectives within planned schedule and cost, and to fulfill reporting requirements to DOE.

Technology Transfer - The contractor shall take advantage of opportunities for technology transfer, including presentation of papers at technical meetings and publication of journal articles. Prior DOE concurrence shall be obtained on all information prepared for public release. Three weeks lead-time is normally required to obtain DOE patent clearance of material for public release.

Reports - Reports shall be prepared as detailed in the Reporting Requirements Checklist and the Report Distribution List.

CHAPTER 3

OXIDATION KINETICS AND AN AGING MODEL

FOR ASPHALT BINDERS

Oxidative aging is one of the major causes of road pavement failure. Through contact with the oxygen in the ambient environment, asphalt binder in the pavement oxidizes. This oxidation process results in an increase in asphaltene content, carbonyl content, and viscosity of the binder. Eventually, the binder becomes too brittle to sustain the damage from traffic load and thermal cycling.

The concept that asphalt oxidative aging depends on temperature and oxygen pressure is well accepted by most engineers. Some researchers have offered qualitative discussions on this phenomenon (Ishai, 1987; Petersen, 1993). However, a quantitative model for oxidative aging using temperature and oxygen pressure as independent variables, and possessing the ability of predicting the aging extent in terms of aging time is much more desirable. An aging model would be a powerful tool to compare the aging characteristics of different asphalts. An aging model would also provide a theoretical background from which the asphalt community can evaluate current aging tests that are run at conditions of certain specified temperatures and pressures.

Some interesting and fundamentally important progress in pursuing this objective has been made in recent years (Martin et al., 1990; Lau et al., 1992; Lunsford, 1994). In those studies, the effect of oxidative aging was accounted for by two separate factors: the change in chemical composition due to oxidation, and the effect of the chemical composition change on the physical properties of the binder. More specifically, these studies provided a basic understanding of the kinetics of carbonyl formation in asphalt binders during oxidative aging, and the correlation between the carbonyl content and viscosity of a given asphalt. The relations between the aging time, viscosity and carbonyl content are explicitly shown by Equation (1-8) for a measurement temperature of 333.2 K (60°C).

In this chapter, a definitive study on the kinetics of carbonyl formation and physico-chemical correlation is presented. Ten asphalts, including seven SHRP asphalts, AAA-1, AAD-1, AAF-1, AAG-1, AAM-1, AAB-1, and AAS-1, and three Texas asphalts, TX1, Lau4, and TX2 were aged at

a total of 13 aging conditions. The aging conditions are designated as C1 to C13 as listed in Table 3-1 with aging temperature ranging from 333.2 K (140°F) to 372.0 K (210°F), and oxygen pressure from 0.2 atm to 20 atm. Aging condition C9, which is at 0.2 atm and 333.2 K (140°F), is regarded as being comparable to road aging conditions.

In the PAV aging procedure proposed by the Strategic Highway Research Program (SHRP), asphalts are first aged in the Thin Film Oven Test (TFOT, ASTM D-1754) to simulate hot mix aging. To see if this treatment made any difference on the aging characteristics of asphalts, many of the samples which were aged using conditions C1 to C7 were run following the equivalent and quicker Rolling Thin Film Oven Test (RTFOT, ASTM D-2872) (Jemison et al., 1991). Many, but not all, were run with and without oven treatment (i.e. the virgin asphalt and the oven-aged asphalt were run at the same condition).

With an understanding of oxidation kinetics and the physico-chemical correlation, an aging model is proposed in this chapter. The correlations between the kinetic parameters are presented. Models are given to describe the pressure dependencies of the physico-chemical correlation coefficients. These models are then used in a study of the PAV test.

Measurement of Oxidation

Oxidation alters the chemical composition of asphalt binders. Figure 3-1 is the FT-IR spectra of SHRP AAA-1 before and after oxidative aging. As the aging progresses, the bands representing oxygen-containing functionalities are intensified, with those of the carbonyl group and the sulfoxide group increasing the most.

Carbonyl content or carbonyl area (CA) as measured by FT-IR was used as a measurement of oxidation. As seen from Figure 3-1, the sulfoxide band (near wavenumber 1000 cm^{-1}) increases very sharply during the early period of oxidation and then grows much more slowly. This is because sulfoxide is the product of sulfur oxidation which happens rapidly at the beginning of oxidative aging and then reaches a "pseudo-steady state" (Petersen, 1984; Petersen et al., 1993). This means that the sulfoxide band may not be used to measure long-term aging. On the other hand, the carbonyl band (near wavenumber 1700 cm^{-1}) grows persistently during the whole aging process. More importantly, numerous data have shown the linear relationship between carbonyl area and aging time for

Table 3-1. The Tested Aging Conditions

Condition	Temperature	Oxygen Pressure
C1	170°F (349.8 K)	20 atm
C2	180°F (355.4 K)	20 atm
C3	180°F (355.4 K)	10 atm
C4	190°F (360.9 K)	20 atm
C5	190°F (360.9 K)	0.2 atm
C6	200°F (366.5 K)	0.2 atm
C7	210°F (372.0 K)	0.2 atm
C8	140°F (333.2 K)	20 atm
C9	140°F (333.2 K)	0.2 atm
C10	150°F (338.7 K)	0.2 atm
C11	160°F (344.3 K)	0.2 atm
C12	170°F (349.8 K)	0.2 atm
C13	180°F (355.4 K)	0.2 atm

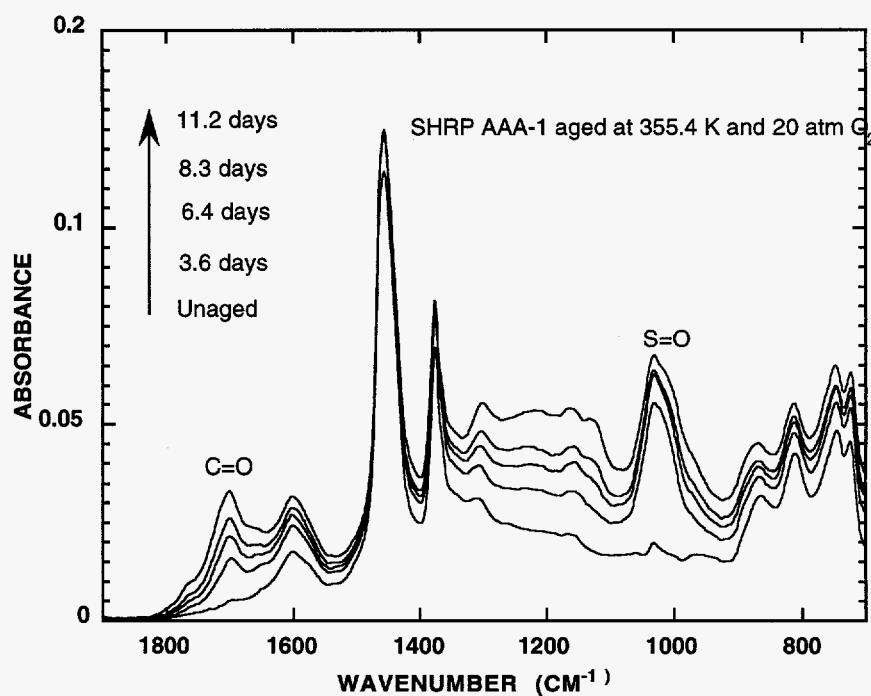


Figure 3-1. FTIR spectra of unaged and aged SHRP AAA-1.

long-term aging, as well as the linear relationship between log viscosity and the carbonyl area (Lee and Huang, 1973; Martin, et al., 1990; Lau et al., 1992; Petersen et al., 1993; Lunsford, 1994; Lin, 1995). For these reasons, carbonyl content has been used as a good measurement of the extent of oxidation.

Asphalt Oxidation Kinetics

Lau et al. (1992) showed that at 20 atm oxygen pressure and at temperatures from 333.2 to 366.5 K (140-200°F) the carbonyl formation rate becomes constant after an initial more rapid rate. These constant rates varied linearly with reciprocal absolute temperature in the usual Arrhenius form:

$$R_{CA} = \frac{dCA}{dt} = A e^{-E/RT} \quad (1-6)$$

For the five asphalts studied, there appeared to be some variation in the slopes of $\ln R_{CA}$ vs $1/T$.

Lunsford (1994) extended Equation (1-6) to

$$R_{CA} = A' P^\alpha e^{-E/RT} \quad (1-10)$$

to include the effect of oxygen pressure. In the constant rate region, carbonyl area CA is

$$CA = CA_0 + R_{CA} t \quad (1-5)$$

However, from the data obtained by Lunsford (1994), no firm conclusion could be drawn as to whether α is asphalt dependent.

In this study, the carbonyl growth profile for a specific aging condition is similar to those observed by other researchers (Lau et al., 1992, Lunsford, 1994); the carbonyl growth approaches a long-term constant rate region after an initial more rapid period. Figures 3-2 to 3-4 show the carbonyl area versus aging time for aging conditions C1 to C7 for three asphalts. Figures 3-5 to 3-7 demonstrate the carbonyl growth of the same three asphalts for aging conditions C8 to C13.

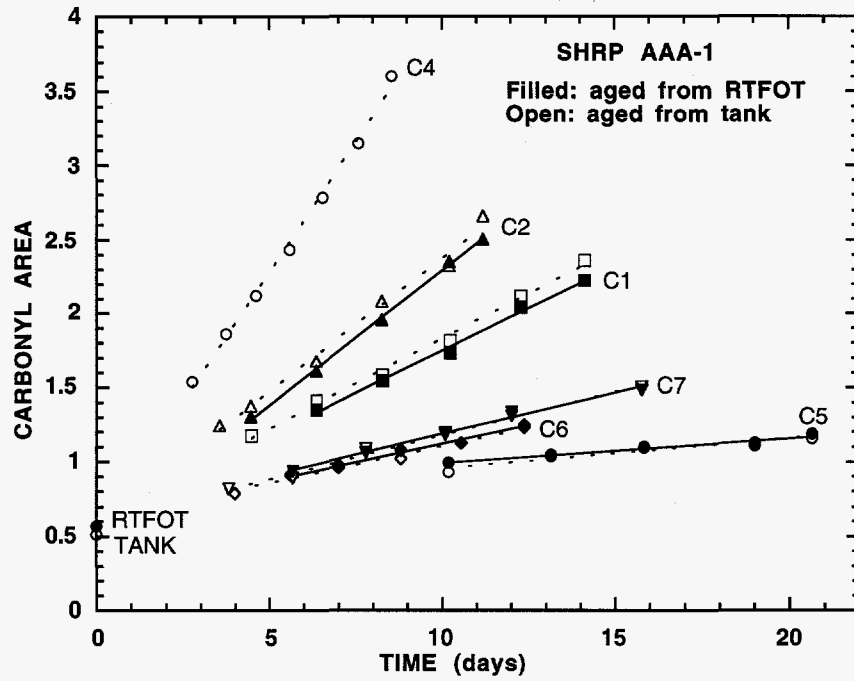


Figure 3-2. Carbonyl area vs. aging time for SHRP AAA-1 (C1-C7).

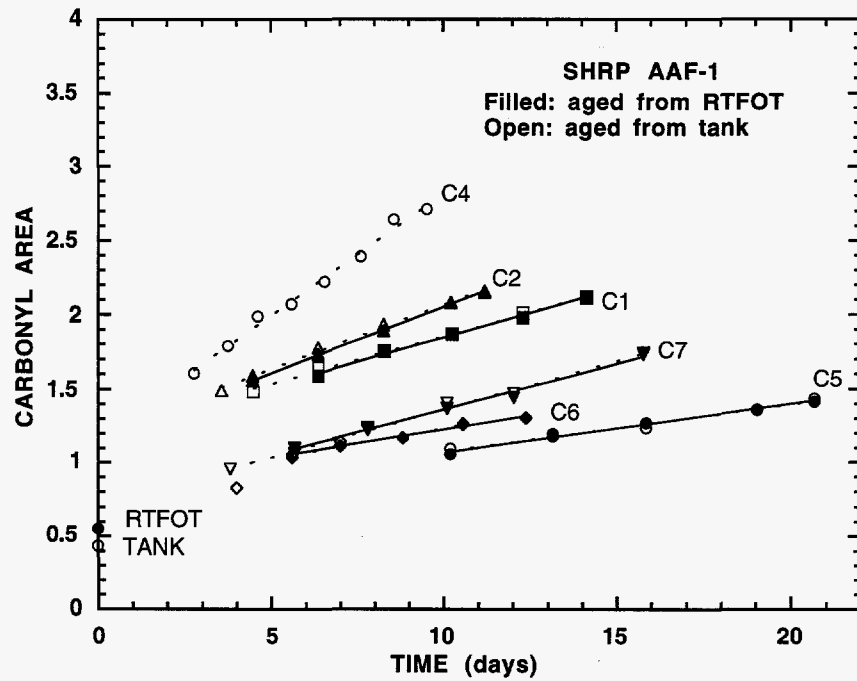


Figure 3-3. Carbonyl area vs. aging time for SHRP AAF-1 (C1-C7).

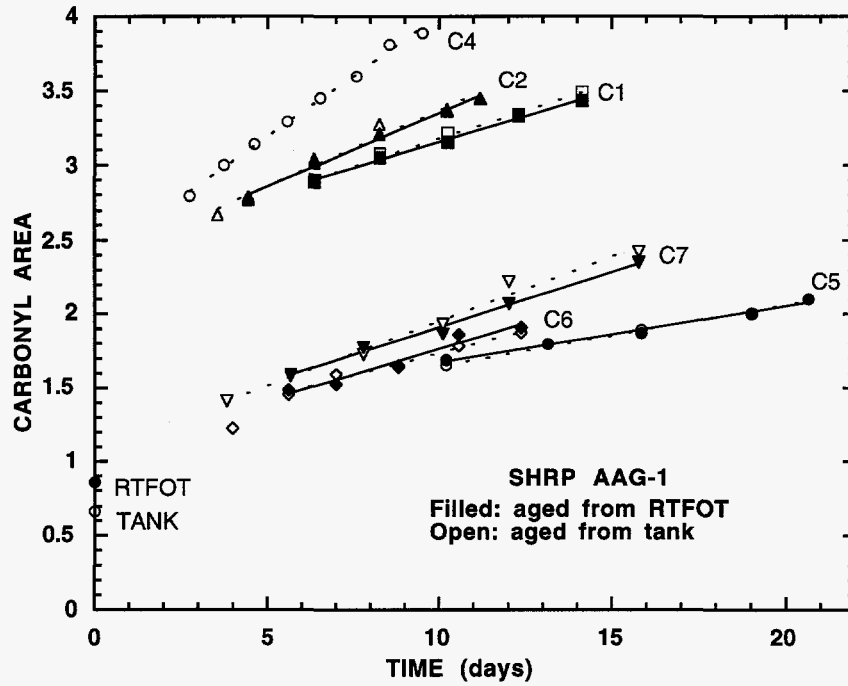


Figure 3-4. Carbonyl area vs. aging time for SHRP AAG-1 (C1-C7).

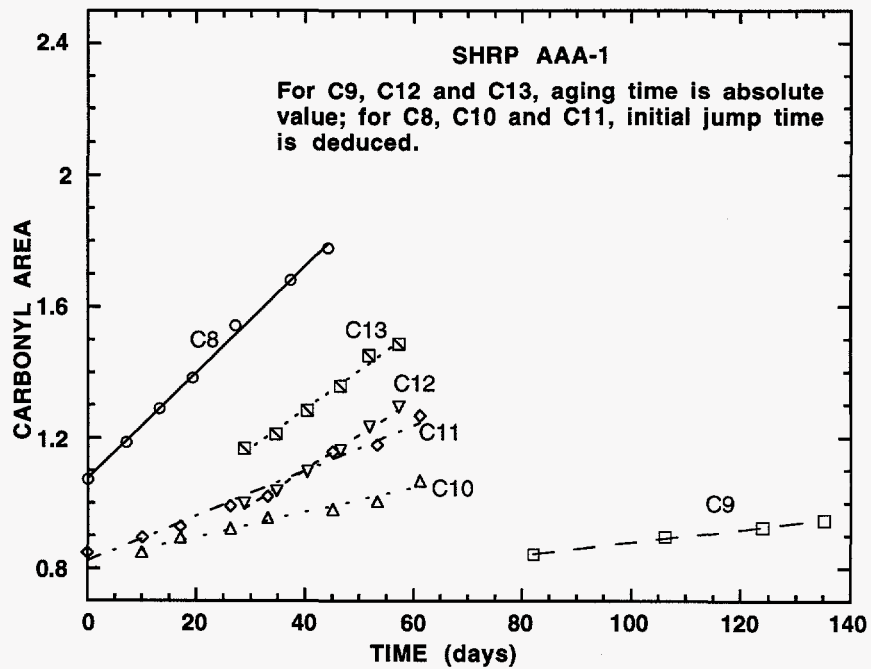


Figure 3-5. Carbonyl area vs. aging time for SHRP AAA-1 (C8-C13).

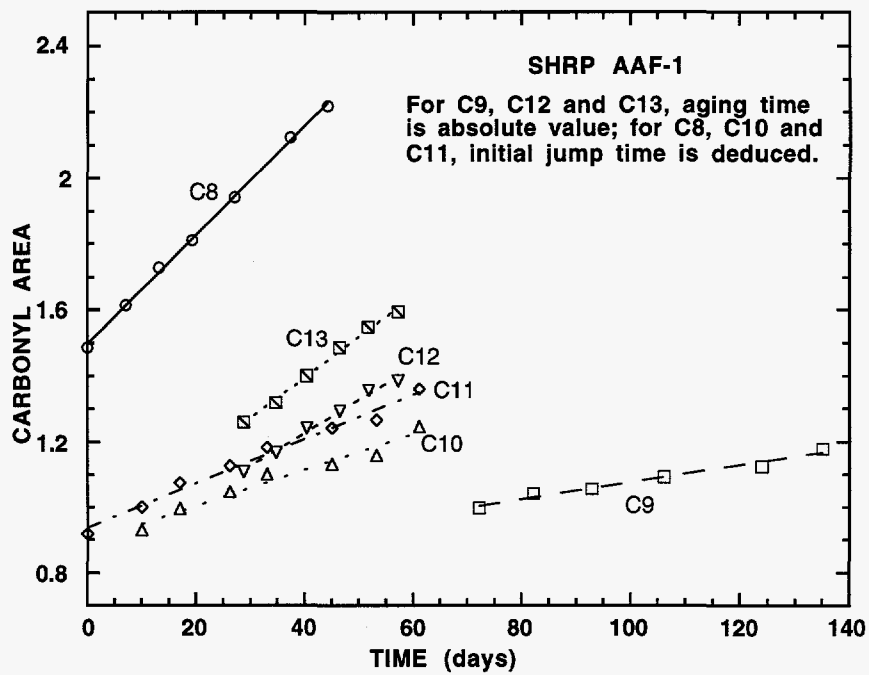


Figure 3-6. Carbonyl area vs. aging time for SHRP AAF-1 (C8-C13).

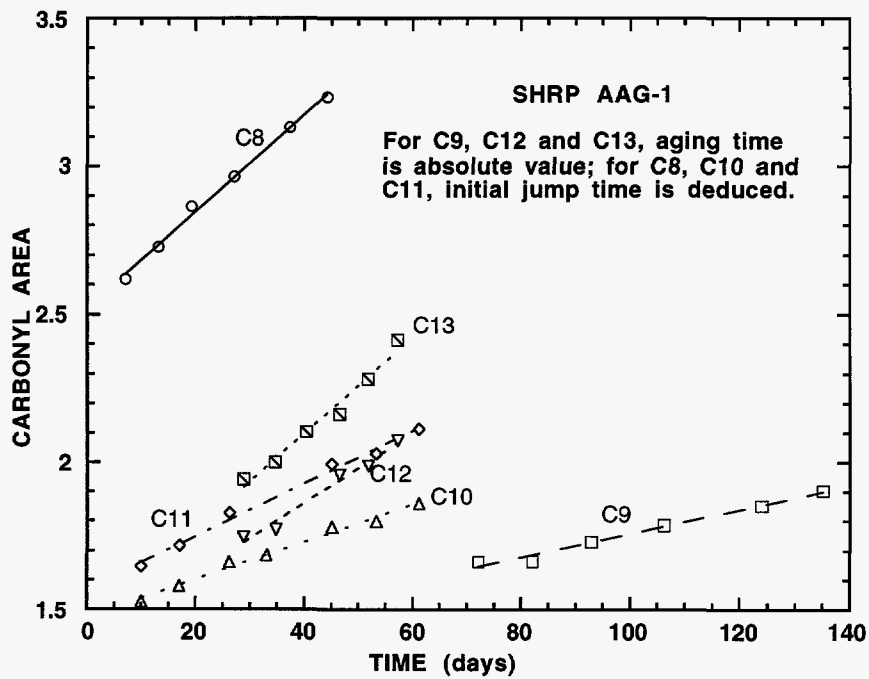


Figure 3-7. Carbonyl area vs. aging time for SHRP AAG-1 (C8-C13).

RTFOT pre-treatment causes negligible change of the kinetic behavior of an asphalt binder. Figure 3-2 shows data for one of the two asphalts that perhaps show some effect of oven aging on the subsequent POV aging, but only at 20 atm. We also see that the initial jump $CA_0 - CA_{\text{tank}}$ is relatively small. In Figure 3-3, there is no evidence of an oven aging effect, but a larger pressure effect on CA_0 is evident. Figure 3-4 also shows no oven test effect but a very large pressure dependent initial jump. In these runs, not all conditions were conducted for both oven aged and virgin material. For those asphalts for which virgin and RTFOT pre-treated samples were studied, both the slopes and intercepts are close for tank asphalts and their RTFOT treated counterparts. We thus conclude that the effect of RTFOT treatment on the kinetic properties is negligible. Since only a limited amount of sample can be collected after the Rolling Thin Film Oven Test, only virgin asphalts were aged for aging experiments using aging conditions C8 to C13. Carbonyl growth with respect to aging time at aging conditions C1 to C7 for the other seven asphalts were also constructed.

Data for aging conditions of C8 to C13 are displayed separately in Figures 3-5 to 3-7 for the sake of clarity. For aging conditions C8, C10 and C11, before the asphalt samples were subjected to the specific conditions of interest, they were aged under conditions with the same oxygen pressures, but at elevated temperatures in order to shorten the time needed to pass the initial jump region. This means that the first samples for these three conditions (aging time shown as 0 in the figures) do not represent the tank asphalt. They are the starting points for the aging under the specific conditions. The slope of a constant rate region regression line is the oxidation rate. However, the intercept point can not be used to calculate the initial jump $CA_0 - CA_{\text{tank}}$ for a specific condition. Similar carbonyl growth plots for the other seven asphalts aged using conditions C8 to C13 were constructed.

Table 3-2a gives the oxidation rates for conditions C1 to C7, and Table 3-2b gives the oxidation rates for conditions C8 to C13. Values of the initial jump $CA_0 - CA_{\text{tank}}$ are listed in Table 3-3a for conditions C1 to C7 and in Table 3-3b for conditions C9, C12, and C13. Equation (1-10) can be linearized for a more convenient determination of the kinetic parameters:

$$\ln R_{CA} = \ln A' + \alpha \ln P - E / RT \quad (3-1)$$

Table 3-2a. CA Growth Rate for All POV-Aged Asphalts for Conditions C1 to C7

Aging Condition ^a :	$R_{CA} \times 10^3$ (CA/day)						
	C1	C2	C3	C4	C5	C6	C7
Asphalt							
AAA-1	121.7	179.5		349.6	19.84	48.68	58.77
AAA-1 R ^b	114.5	181.9			16.29	49.12	54.90
AAD-1	133.3	223.5		403.9	22.53	43.69	60.01
AAD-1 R ^b	124.6	214.1			22.77	35.30	56.80
AAF-1	63.96	86.40		164.3	31.83	41.63	64.98
AAF-1 R ^b	65.84	88.55			32.83	37.75	61.61
AAG-1	74.66	102.0		163.3	41.41	60.17	87.57
AAG-1 R ^b	69.38	99.67			38.04	69.74	74.55
AAM-1	52.31	65.36		111.9	22.36	44.56	56.32
AAM-1 R ^b	50.66	62.15			28.30	45.26	59.33
AAB-1	68.77	132.3		222.2		58.19	80.39
AAB-1 R ^b	67.15	130.9	101.4	220.2		53.95	77.12
AAS-1	60.49			188.8			64.50
AAS-1 R ^b	58.19	105.1	86.59	197.8		46.17	64.72
TX1				229.4			85.39
TX1 R ^b	70.61	132.0	108.5	239.5		62.27	85.27
Lau4		108.0					
Lau4 R ^b	79.22	101.3	76.19	149.3		57.92	79.65
TX2		135.4					
TX2 R ^b	71.27	133.3	108.5	244.4		61.23	75.57

^a See Table 3-1

^b Asphalt pre-treated by Rolling Thin Film Oven Test before aging under the conditions

Table 3-2b. CA Growth Rate for All POV-Aged Asphalts for Conditions C8 to C13

Aging Condition ^a :	$R_{CA} \times 10^3$ (CA/day)					
	C8	C9	C10	C11	C12	C13
Asphalt						
AAA-1	16.17	1.948	3.797	6.907	10.68	11.91
AAD-1	16.54	1.514	3.681	6.378	8.047	12.81
AAF-1	11.35	2.577	5.470	6.741	10.09	12.27
AAG-1	16.48	4.060	6.370	8.979	11.88	16.27
AAM-1	9.579	2.169	4.475	6.393	8.487	9.660
AAB-1	10.63	2.447	4.505	8.100	12.17	15.70
AAS-1	9.306	1.859	4.471	6.515	9.340	14.01
TX1	12.50	2.689	4.843	8.315	9.592	14.39
Lau4	13.10	2.001	5.188	6.753	10.93	14.42
TX2	9.352	2.375	3.773	8.274	11.18	13.16

^a See Table 3-1

Table 3-3a. $CA_0 - CA_{\text{tank}}$ of All POV-Aged Asphalts for Conditions C1 to C7

Aging Condition ^a :	$CA_0 - CA_{\text{tank}}$ (CA)						
	C1	C2	C3	C4	C5	C6	C7
Asphalt							
AAA-1	0.103	0.068		0.024	0.250	0.109	0.082
AAA-1 R ^b	0.092	-0.037			0.320	0.119	0.129
AAD-1	0.225	0.071		0.047	0.271	0.134	0.082
AAD-1 R ^b	0.253	0.040			0.292	0.304	0.150
AAF-1	0.782	0.771		0.742	0.336	0.385	0.279
AAF-1 R ^b	0.755	0.734			0.309	0.415	0.313
AAG-1	1.771	1.686		1.713	0.572	0.473	0.415
AAG-1 R ^b	1.801	1.694			0.630	0.405	0.503
AAM-1	0.780	0.839		0.811	0.402	0.281	0.309
AAM-1 R ^b	0.782	0.829			0.297	0.284	0.273
AAB-1	0.508	0.393		0.395		0.210	0.198
AAB-1 R ^b	0.533	0.412	0.358	0.383		0.259	0.223
AAS-1	0.404			0.342			0.206
AAS-1 R ^b	0.404	0.350	0.291	0.325		0.225	0.202
TX1				0.415			0.176
TX1 R ^b	0.447	0.352	0.356	0.361		0.171	0.190
Lau4		0.593					
Lau4 R ^b	0.501	0.643	0.549	0.706		0.252	0.267
TX2		0.365					
TX2 R ^b	0.371	0.348	0.310	0.280		0.188	0.185

^a See Table 3-1

^b Asphalt pre-treated by Rolling Thin Film Oven Test before aging under the conditions

Table 3-3b. $CA_0 - CA_{\text{tank}}$ of All POV-Aged Asphalts for Conditions C9, C12 and C13, and the Average for Three Pressures

Aging Condition ^a : Asphalt	$CA_0 - CA_{\text{tank}}$ (CA)					
	C9	C12	C13	Average for all Conditions		
				O ₂ Pressure (atm)		
				0.2	10	20
AAA-1	0.175	0.165	0.301	0.183	--	0.050
AAD-1	0.315	0.293	0.246	0.232	--	0.127
AAF-1	0.386	0.390	0.472	0.365	--	0.757
AAG-1	0.690	0.725	0.786	0.578	--	1.733
AAM-1	0.363	0.416	0.510	0.348	--	0.808
AAB-1	0.201	0.226	0.270	0.227	0.358	0.437
AAS-1	0.184	0.239	0.230	0.214	0.291	0.365
TX1	0.163	0.351	0.324	0.229	0.356	0.387
Lau4	0.280	0.261	0.291	0.270	0.549	0.610
TX2	0.176	0.268	0.396	0.243	0.310	0.341

^a See Table 3-1

Because the RTFOT pre-treatment has a negligible effect on kinetic properties as discussed above, data for the RTFOT pre-treated asphalts in Tables 3-2a and 3-3a are used as replicates of the virgin asphalts. In Tables 3-3a and 3-3b, conditions C5, C6, C7, C9, C12, and C13 are at the same aging pressure of 0.2 atm with different aging temperatures. Within experimental error $CA_0 - CA_{\text{tank}}$ appears to be largely temperature independent, except for the relatively larger fluctuation in the values for asphalts AAA-1 and AAD-1, and for condition C13. The scatter between the values of AAA-1 and AAD-1 is partially because these two asphalts have low $CA_0 - CA_{\text{tank}}$. The larger values for condition C13 lead to the speculation that some systematic error may exist at this condition. All the values at different temperatures are included to obtain the average $CA_0 - CA_{\text{tank}}$ for aging pressure of 0.2 atm. These values are listed in the fourth column of Table 3-3b. Average $CA_0 - CA_{\text{tank}}$ values for aging pressures of 10 atm and 20 atm are calculated respectively and are listed in the same table.

The constants in the equation were determined by a multivariable regression using the data in Tables 3-2a and 3-2b and are listed in Table 3-4. Unlike the results obtained by Lau et al. (1992) and Lunsford (1994), a much wider variation in reaction order, α , and activation energy, E, was observed for the larger set of asphalts. For each of the parameters, a 95% confidence limit is also shown. The average error is also given. For most of the asphalts, more than 15 data points were used to estimate the three kinetic parameters. The large number of data points leads to the excellent confidence limits as observed from the table. The variation in the kinetic parameters clearly indicates that the kinetic properties are asphalt dependent.

Figures 3-8 and 3-9 are the Arrhenius plots at 0.2 atm aging pressure for two of the ten asphalts. The oxidation rates listed in Tables 3-2a and 3-2b at pressures other than 0.2 atm were converted to corresponding values for a pressure of 0.2 atm using the pressure reaction order α for each asphalt listed in Table 3-4. These converted rates, together with the measured oxidation rates

Table 3-4. Kinetic Model Parameters of All POV-Aged Asphalts Studied

Asphalt	$\ln A$	E kJ/mol	α	Average % Error ^a
AAA-1	27.9±0.2	92.3±0.7	0.54±0.05	7
AAD-1	29.6±0.2	97.2±0.6	0.58±0.04	6
AAF-1	25.5±0.2	85.4±0.6	0.36±0.04	4
AAG-1	25.0±0.2	83.3±0.5	0.33±0.04	4
AAM-1	25.8±0.2	86.9±0.6	0.33±0.04	5
AAB-1	29.4±0.2	96.6±0.5	0.39±0.03	4
AAS-1	29.0±0.2	95.8±0.5	0.40±0.04	4
TX1	29.2±0.2	95.9±0.6	0.40±0.05	5
Lau4	28.0±0.2	92.6±0.6	0.38±0.05	5
TX2	30.8±0.2	100.7±0.8	0.41±0.06	6

$$a \quad \% \text{Error} = 100 \sqrt{\sum \frac{1}{n} \left(\frac{\text{mea} - \text{cal}}{\text{mea}} \right)^2}$$

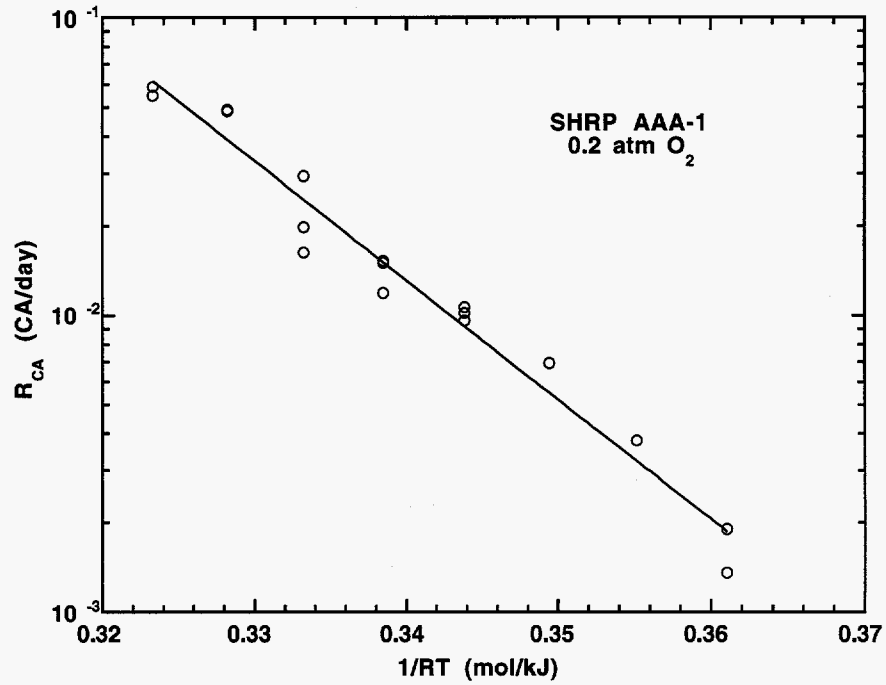


Figure 3-8. Oxidation rate vs. aging temperature for SHRP AAA-1.

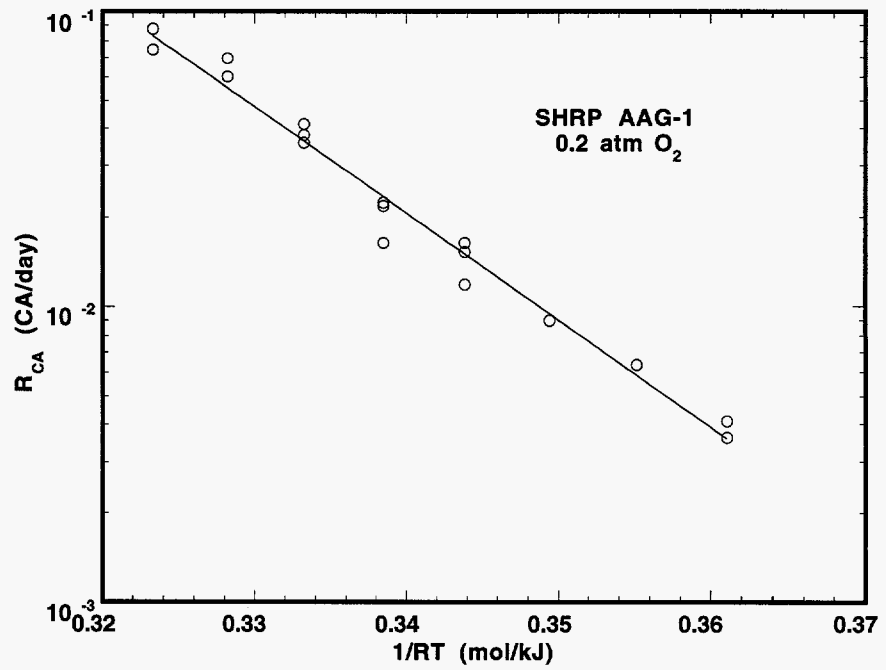


Figure 3-9. Oxidation rate vs. aging temperature for SHRP AAG-1.

at 0.2 atm, were then plotted against the reciprocal of the aging temperature. Despite some scatter of the data due to experimental errors, confidence can be placed in the regression line because of the large number of data points. Arrhenius plots for other asphalts were constructed.

The ultimate reason for pavement failure due to oxidative aging is that chemical compositional changes result in the deterioration of binder qualities. Particularly, the binders become more viscous at high temperature and more brittle at low temperature because of aging. Several authors have demonstrated that during oxidative aging, log viscosity of an asphalt has a linear relationship with its carbonyl content (Lee and Huang, 1973; Martin et al., 1990; Lau et al., 1992; and Petersen et al., 1993). The slope of log viscosity to carbonyl area CA was defined as the hardening susceptibility HS as in Equation (1-7a). HS is asphalt dependent, and has been determined to be independent of aging temperature below 386.2 K (113°C) (Lau et al., 1992; Petersen et al., 1993). No literature discussion exists as to whether HS is aging pressure dependent, although the samples studied by Petersen et al. (1993) were aged at different pressures.

In this study, the hardening susceptibility relationships for the ten asphalts were measured at aging pressures of both 0.2 atm and 20 atm with or without RTFOT pre-treatment. Figures 3-10 and 3-11 are the relationships for two of the ten asphalts. They are representative of the other asphalts. The values of HS and m (defined in Equation (1-7a)) for the ten asphalts at the two oxygen pressures and with or without RTFOT pre-treatment are listed in Table 3-5.

HS is found to be pressure dependent. From Figures 3-10 and 3-11 and the data listed in Table 3-5, significant differences between the hardening susceptibility relationships at the different pressures are observed with HS being larger for the lower aging pressure. This means that at lower aging pressures, the oxidation products are such that the same amount of increase in carbonyl content results in a more significant increase in viscosity.

Compared to the effect of pressure, the effect of RTFOT pre-treatment on the HS relationship is negligible. Nevertheless, in almost all cases, RTFOT pre-treatment increases the HS values, albeit slightly. Since only a limited amount of sample can be obtained after Rolling Thin Film Oven Test and the procedure does require additional time, it is desirable to avoid the RTFOT pre-treatment in an aging test if the evaluation results will not be noticeably different. This is particularly advantageous when multiple asphalts are to be subjected to an aging test.

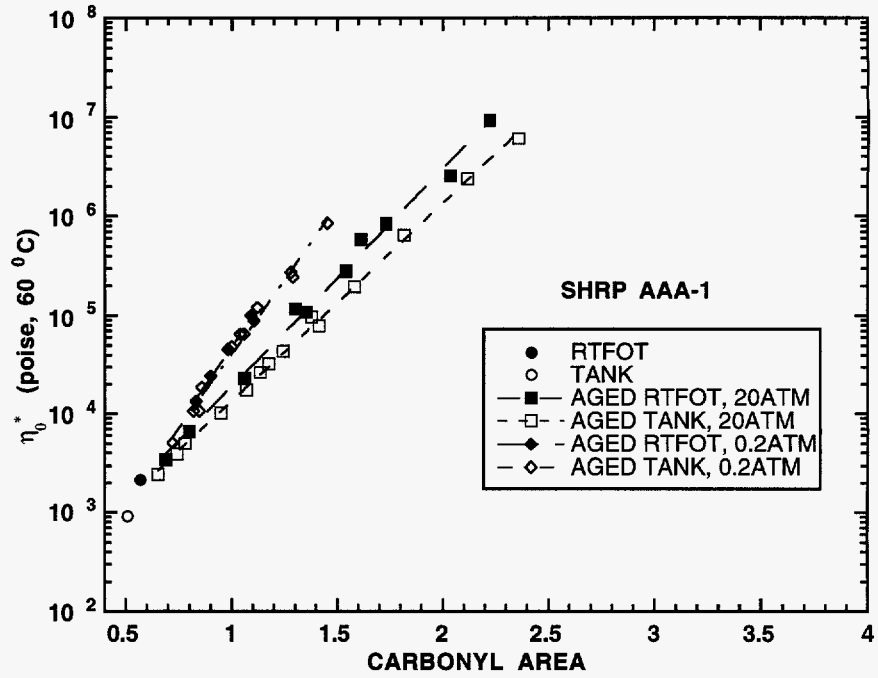


Figure 3-10. Hardening susceptibility of SHRP AAA-1.

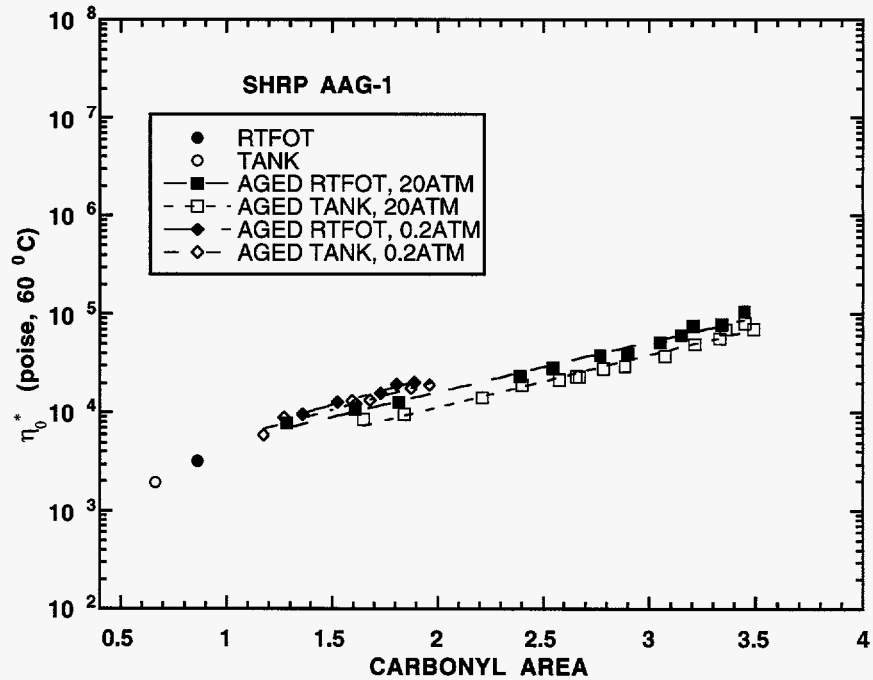


Figure 3-11. Hardening susceptibility of SHRP AAG-1.

Table 3-5. Hardening Susceptibility Parameters for All POV-Aged Asphalts Studied

Asphalt	Aging Pressure=0.2 atm O ₂		Aging Pressure=20 atm O ₂	
	m (poise)	HS	m (poise)	HS
AAA-1	39.77	6.93	134.7	4.61
AAA-1 R ^a	34.69	7.23	119.5	5.06
AAD-1	3.725	8.00	69.69	4.29
AAD-1 R ^a	1.781	8.89	79.71	4.72
AAF-1	345.3	4.47	726.6	3.46
AAF-1 R ^a	429.7	4.62	933.7	3.56
AAG-1	1399	1.35	985.5	1.22
AAG-1 R ^a	1440	1.41	1570	1.16
AAM-1	318.4	4.91	122.6	4.62
AAM-1 R ^a	237.0	5.34	99.43	5.01
AAB-1	87.31	5.86	235.4	4.11
AAB-1 R ^a	78.41	6.18	350.9	4.25
AAS-1	305.6	5.31	417.4	4.38
AAS-1 R ^a	315.5	5.44	717.0	4.47
TX1	66.21	5.45	58.32	4.53
TX1 R ^a	43.91	6.14	192.4	4.13
Lau4	748.0	2.98	773.3	2.51
Lau4 R ^a	765.2	2.99	765.3	2.64
TX2	26.40	7.24	61.43	5.62
TX2 R ^a	14.44	8.30	83.52	5.72

^a Asphalt pre-treated by Rolling Thin Film Oven Test before aging under the conditions

Among the four HS values for each asphalt listed in Table 3-5, the value for the samples aged from virgin tank material at 0.2 atm is the most important information. This is because road aging occurs at 0.2 atm oxygen. Also, since RTFOT pre-treatment will be avoided in our proposed aging test, only HS values for the samples aged without RTFOT pre-treatment will be studied further.

Log viscosity correlates with carbonyl area very well at each pressure (see Figures 3-10 and 3-11). This is true for viscosities as high as 1 Mpoise and as low as the values of the tank asphalts. For all the asphalts, the correlations can be extended to tank asphalts within measurement error. This means that during the aging process, carbonyl area alone can be used as the predictor of viscosity. A recent study by Huh and Robertson (1996) proposed that the viscosity increase during oxidative aging is the sum of both the sulfoxide increase and carbonyl increase. While it is a reasonable assumption that the production of the sulfoxide during the early stages of aging will cause viscosity increase, our data indicate that this effect is virtually negligible.

An Aging Model for Asphalt Binders

The final goal of studying the oxidation kinetics and the physico-chemical correlations of asphalt binders is to develop an aging test that is capable of evaluating road condition aging resistance of the asphalts. In this section, an aging model and a theoretically sound aging test will be proposed. This aging model will also be used to evaluate the PAV test recently developed by the Strategic Highway Research Program.

Combining the results discussed above on oxidation kinetics and the physico-chemical correlation, we have developed an aging model for asphalt binders at a specified aging temperature and oxygen pressure. For the given temperature and pressure, the carbonyl growth in the constant rate region can be calculated by Equation (1-5). The constant oxidation rate in the equation is calculated from Equation (1-10), given the kinetic parameters of the material. The relationship between the carbonyl area and viscosity is governed by Equation (1-7a).

The advantage of the above aging model is that the model parameters CA_0 , m , and HS in Equations (1-5) and (1-7a) are aging pressure dependent but are independent of aging temperature. Thus, they can be measured at temperatures other than the given condition. The kinetic parameters α and E in Equation (1-10), however, still need to be measured by experiment.

Based on this aging model, an aging test to evaluate road condition aging resistance is proposed, which consists of the following steps:

1) Aging experiments at a combination of temperatures and pressures are conducted. At least three experiments are run at an aging pressure of 0.2 atm oxygen.

2) The constant oxidation rates are measured for the multiple conditions. The kinetic parameters are estimated through linear regression.

3) The annual average temperature for a certain pavement location is available. The oxidation rate at this temperature and 0.2 atm oxygen is calculated using the kinetic parameters, or identically, obtained from the constructed Arrhenius plot at 0.2 atm.

4) The average value of CA_0 and the values of m and HS are measured from those aging experiments conducted at 0.2 atm.

5) With CA_0 at 0.2 atm oxygen, measured as in step 4, and oxidation rate at 333.2 K (140°F) and 0.2 atm obtained as in step 3, carbonyl area in the constant rate region is a function of aging time only, as in Equation (1-5). Also, with m and HS at 0.2 atm measured as in step 4, viscosity is a function of carbonyl area only.

6) Assuming a viscosity value at which roads will fail, defined as the critical viscosity, and using the two functions described in step 5, a critical aging time at which the binder approaches the critical viscosity can be calculated. Or, given an aging time, the viscosity of the binder after aging can be predicted using the same two functions in step 5. Either of these two methods can be used to evaluate the aging resistance of the binder of interest.

Figure 3-12 is a graphical demonstration of the steps described above. Equation 3-1 is used to acquire the kinetic parameters. Figure 3-12a display the methods for obtaining the oxidation rate at a given temperature. With CA_0 being measured, Figure 3-12b shows a one-to-one correspondence between aging time and carbonyl area. Since log viscosity has a one-to-one correspondence with carbonyl area as shown in Figure 3-12c, we get a one-to-one correspondence between log viscosity and aging time, as shown in Figure 3-12d. With this relation between log viscosity and aging time, the viscosity value can be predicted for a given aging time, or, for a given critical viscosity, the critical aging time can be calculated.

In Table 3-6, the Critical Time (CT) to reach a viscosity of 500,000 poise are listed for two

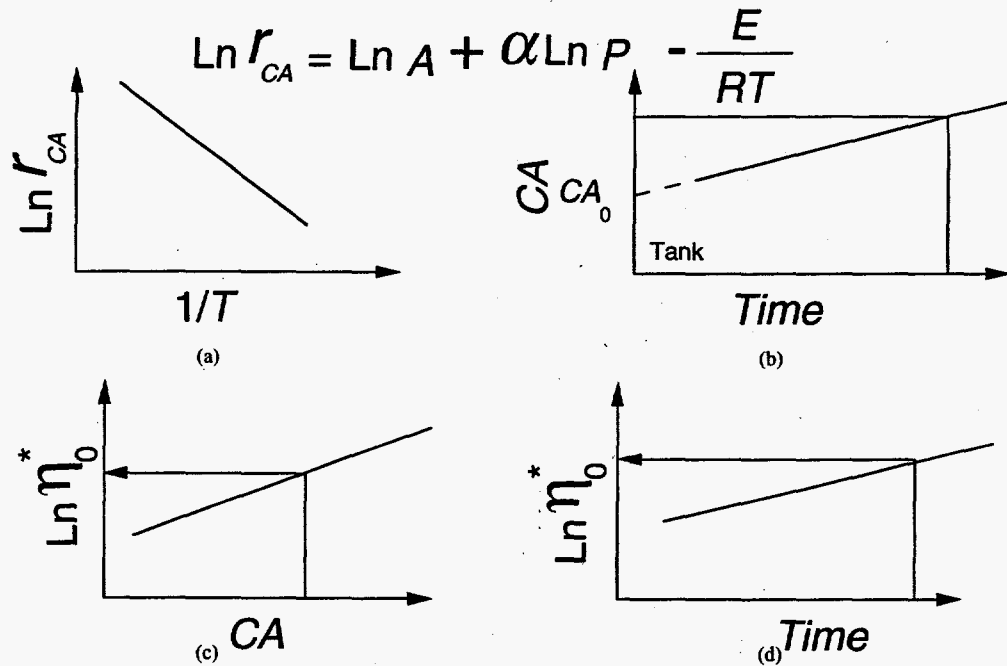


Figure 3-12. Graphical demonstration of the proposed aging test.

Table 3-6. Critical Time (CT) to Reach 500,000 Poise at Two Aging Conditions

Asphalt	R_{CA} ($10^3 \times CA/\text{day}$)		CT (day)	
	0.2 atm 140°F	20 atm 200°F	0.2 atm 140°F	20 atm 200°F
AAA-1	1.88	0.465	356	2.63
AAD-1	1.61	0.565	307	2.11
AAF-1	2.55	0.224	326	3.12
AAG-1	3.58	0.251	868	10.8
AAM-1	2.19	0.174	324	3.15
AAB-1	2.27	0.330	347	2.92
AAS-1	1.91	0.277	389	2.94
TX1	2.33	0.348	397	3.25
Lau4	2.32	0.273	627	5.52
TX2	2.01	0.355	348	2.37

aging conditions for all of the ten asphalts studied. The oxidation rates in the first and second columns are calculated from the kinetic parameters shown in Table 3-4. The m and HS values for samples aged without RTFOT pre-treatment at aging pressures of 0.2 atm and 20 atm listed in Table 3-5, and the average values of $CA_0 - CA_{\text{tank}}$ at aging pressures of 0.2 atm and 20 atm listed in Table 3-3b are used in the calculation. A detailed analysis of the prediction accuracy and the implications of the ranking of the asphalts is given later in this chapter.

Correlations for Property Parameters

In Figure 3-13 the value of $\ln A + \alpha \ln 0.2$ (the value of E/RT where $\ln R_{CA} = 0$ for an oxidation pressure of 0.2 atm) is plotted versus E with remarkable linearity. This figure indicates the existence of an isokinetic temperature (Boudart, 1991) at a pressure of 0.2 atm. For this case, the isokinetic temperature was determined to be 359.8 K (86.6°C).

In Figure 3-14 the activation energy E is plotted versus pressure reaction order α . This figure shows that the asphalts can be divided into two groups. The first group is characterized by high α values (AAA-1 and AAD-1), while for the second group activation energy E increases with pressure reaction order α .

As shown by the data in Table 3-3b, initial jump $CA_0 - CA_{\text{tank}}$ is aging pressure dependent. To investigate this phenomenon, a model proposed to describe the dependency is given as:

$$CA_0 - CA_{\text{tank}} = \beta P^\gamma \quad (3-2)$$

The model parameters β and γ listed in Table 3-7 are obtained using the data in Table 3-3b.

A similar model is proposed to describe the pressure dependency of hardening susceptibility HS :

$$HS = \theta P^\delta \quad (3-3)$$

The model parameters are estimated using the data in Table 3-5 for samples aged without RTFOT pre-treatment. The parameters are listed in Table 3-7.

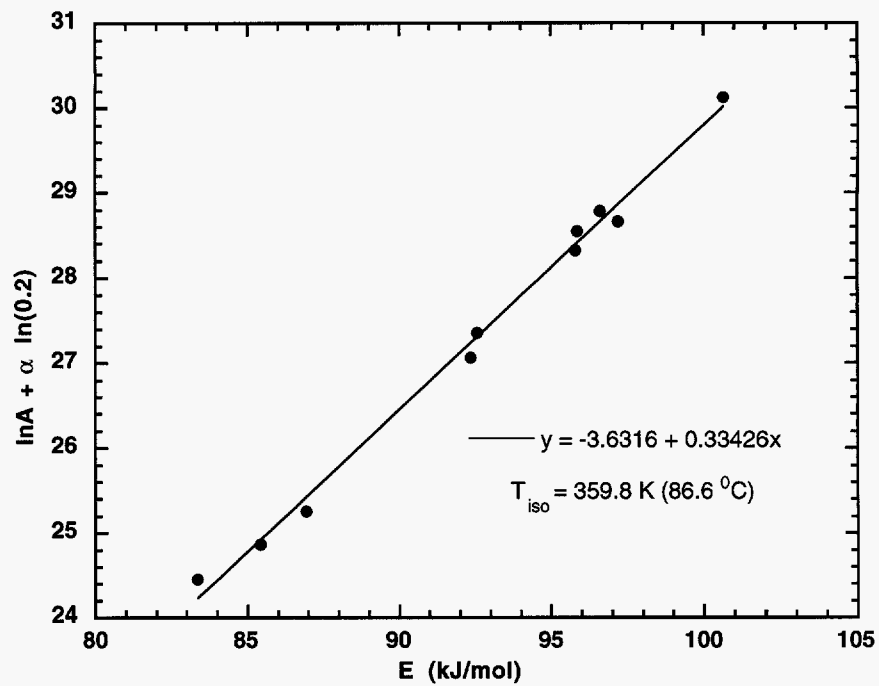


Figure 3-13. Isokinetic diagram for the ten asphalts studied.

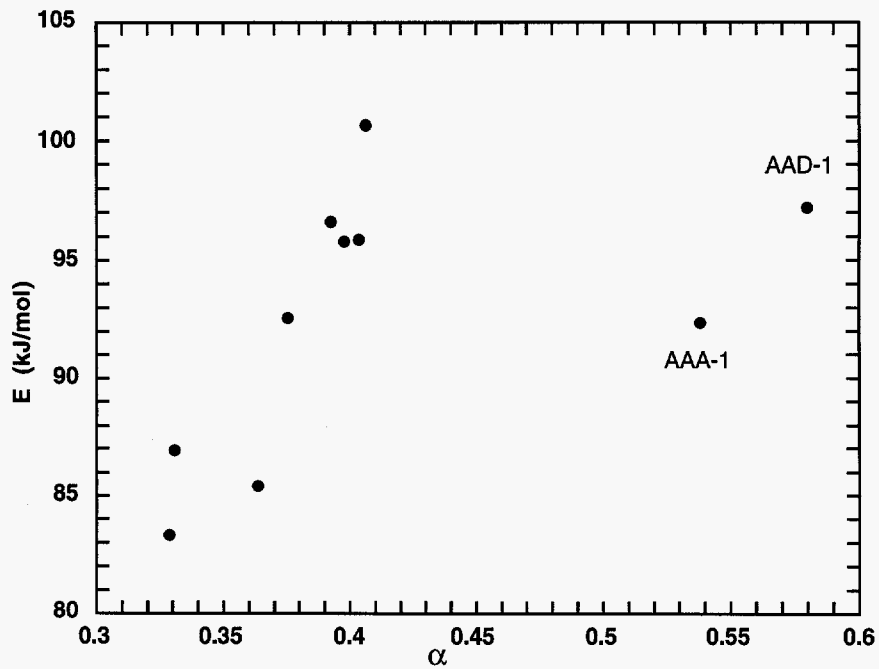


Figure 3-14. Activation energy vs. pressure reaction order.

Table 3-7. Pressure Dependence Factors for Each Asphalt Studied

Asphalt	CA_0-CA_{tank}		HS	
	β	γ	θ	δ
AAA-1	0.116	-0.282	6.01	-0.089
AAD-1	0.188	-0.131	6.44	-0.135
AAF-1	0.471	0.158	4.09	-0.055
AAG-1	0.848	0.238	1.30	-0.023
AAM-1	0.467	0.183	4.81	-0.013
AAB-1	0.279	0.134	5.18	-0.077
AAS-1	0.250	0.103	4.96	-0.041
TX1	0.275	0.114	5.11	-0.040
Lau4	0.360	0.179	2.80	-0.037
TX2	0.271	0.070	6.63	-0.055

In Figure 3-15, initial jump pressure factor γ is plotted against pressure reaction order α . It is observed that γ varies inversely with α . For all the ten asphalts except AAA-1 and AAD-1, initial jump CA_0-CA_{tank} increases with aging pressure. Furthermore, the initial jump values for asphalts with a low α are more sensitive to aging pressure. On the other hand, AAA-1 and AAD-1 have negative γ values. This may be due to measurement errors. Both AAA-1 and AAD-1 are among the asphalts which have the lowest CA_0-CA_{tank} . This makes the measurement errors more noticeable. However, since values for AAA-1 and AAD-1 follow the same trend as other asphalts, these values may be real. If they are correct, then for these two asphalts an increase in aging pressure would result in a decrease in the initial jump. Figure 3-16 compares the effect of aging pressure on oxidation rate and on hardening susceptibility. δ for all the asphalts is negative, which points out that an increase in aging pressure reduces HS values. Furthermore, asphalts with higher α values are more sensitive to pressure in terms of hardening susceptibility. Figure 3-17 is a cross plot of Figures 3-15 and 3-16. In general, γ increases with δ .

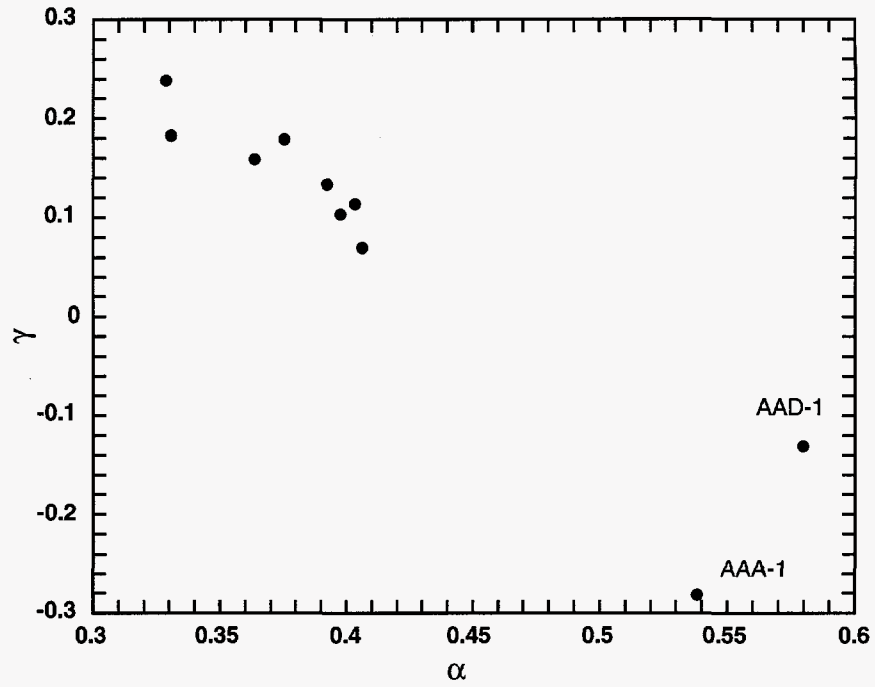


Figure 3-15. Initial jump pressure factor vs. pressure reaction order.

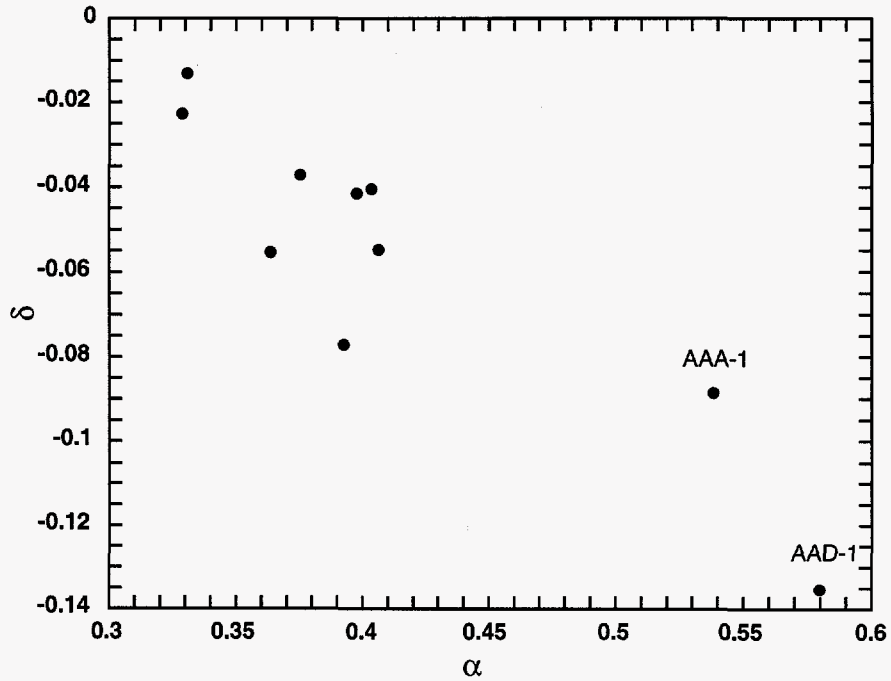


Figure 3-16. HS pressure factor vs. pressure reaction order.

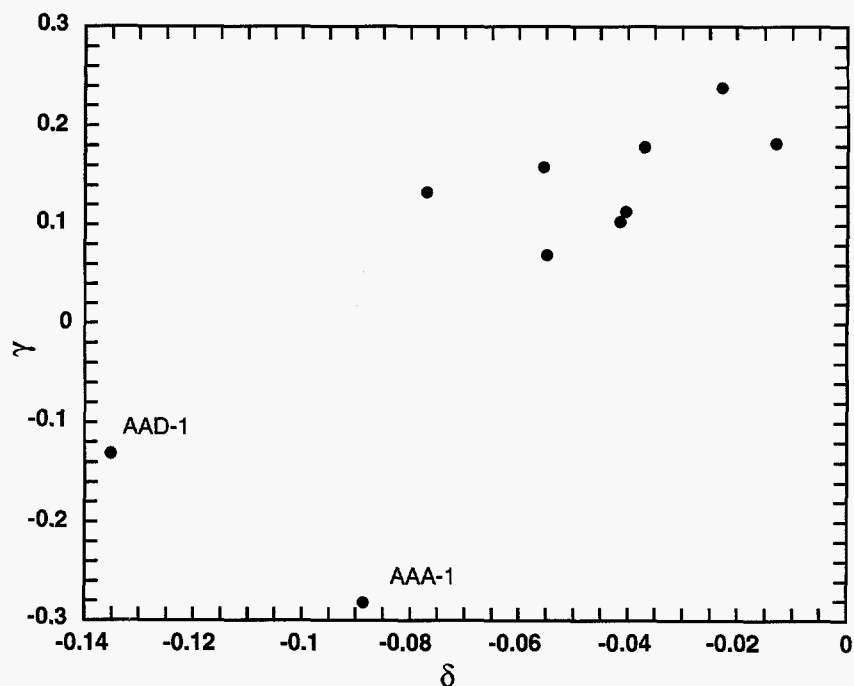


Figure 3-17. Initial jump pressure factor vs. HS pressure factor.

Feasibility of Evaluating Low Temperature Oxidation Rate by High Temperature Data

Extrapolating high temperature data to low temperature conditions is very desirable. Combining Equations (1-5) and (1-7a), a simple relationship between viscosity and the aging time is obtained for the constant rate region:

$$\eta^*_0 = m e^{(HS(CA_0 + R_{CA} t))} \quad (3-4)$$

As explained earlier, this equation implies that the viscosity of an asphalt binder during oxidative aging can be calculated if the parameters m , HS , CA_0 and R_{CA} for the specific aging condition are known. Particularly, in order to evaluate the road aging resistance of a certain binder, the parameter values corresponding to a road aging condition need to be measured. As shown in Table 3-1, asphalts were aged at temperatures as low as 333.2 K (140°F). But it was determined that the aging experiment under the condition of 0.2 atm oxygen and 333.2 K (140°F, C9) would need more than

4.5 months, which is not feasible for industrial applications. It is desirable to obtain these parameters without conditioning aging experiments at low temperatures and low pressures. Because m , HS , and CA_0 are all temperature independent, and only pressure dependent, their values can be measured at pressures of 0.2 atm and temperatures higher than 333.2 K, such as 372.0, 366.5 K and 360.9 K (210, 200, and 190°F). The time required to conduct these aging experiments is three weeks. So the only question is whether R_{CA} can be obtained from high temperature data, which would then call for an extrapolation approach.

However, data show that oxidation rates extrapolated from high temperature data lead to noticeable error. A good candidate method of extrapolation is to use aging conditions at temperatures of 372.0, 366.5, 360.9, 355.4 and 249.8 K (210, 200, 190, 180 and 170°F), all at a pressure of 0.2 atm oxygen. They are conditions C5, C6, C7, C12 and C13 as listed in Table 3-1. Of these temperatures, aging experiments at 372.0, 366.5, 360.9 K (and at 0.2 atm oxygen pressure) require one month. For 355.4 and 249.8 K, the samples can be subjected to 372.0 K and 0.2 atm for 5 days to pass the initial jump region. In this way, oxidation rates at these two temperatures can also be measured with aging times less than 1 month. In this scheme, CA_0 will be taken as the average of the values measured at C5, C6, and C7. Samples aged at all five conditions are sufficient for the measurement of the hardening susceptibility relationship. The low temperature oxidation rate can be extrapolated from the rates measured at the five high temperatures. The rate data for these five conditions in Tables 3-2a and 3-2b are plotted against the temperature in Figures 3-18 and 3-19 for five of the ten asphalts respectively. In Figure 3-19, no rate data at 360.9 K (190°F) are available. By extrapolating the regression line to 333.2 K (140°F) the oxidation rates at 333.2 K and 0.2 atm were calculated. Table 3-8 compares the measured rates and the rates calculated by the two methods at 333.2 K and 0.2 atm. The second column in the table gives the rates extrapolated from the data of the five high temperatures. The rates in column 4 are calculated using the kinetic data in Table 3-4 and Equation 1-10. The percentage errors due to both the methods are also listed in the table. As can be seen from the table, the error of the five temperature extrapolation method is rather significant, particularly for AAG-1, AAM-1, Lau4 and TX2. This is because, oxidation rates at the five high temperatures do not fall on the regression lines very well, which indicates measurement error. Because measurement error can not be avoided, we conclude that the rates extrapolated from

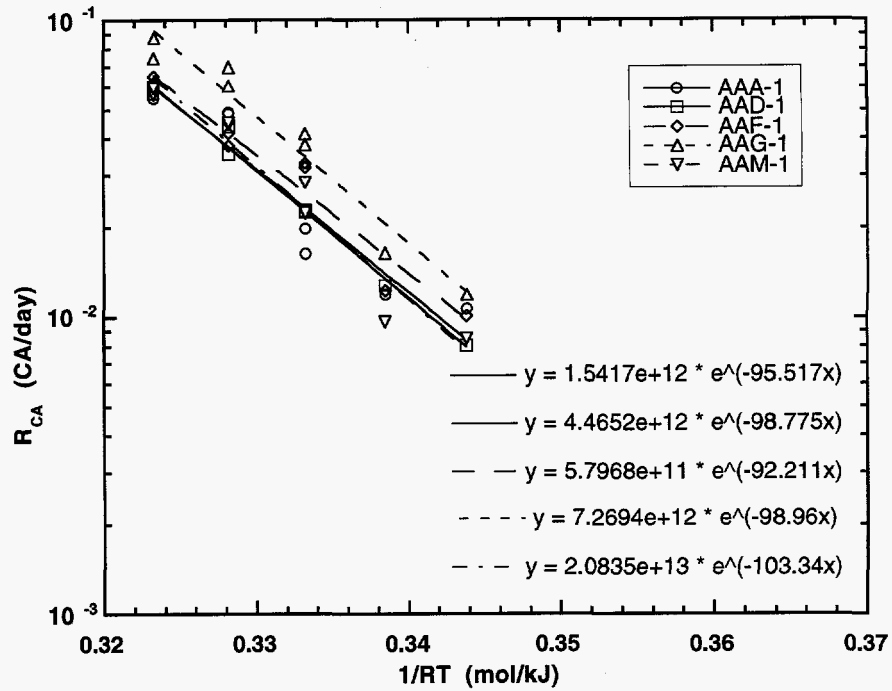


Figure 3-18. Oxidation rate vs. temperature for five asphalts.

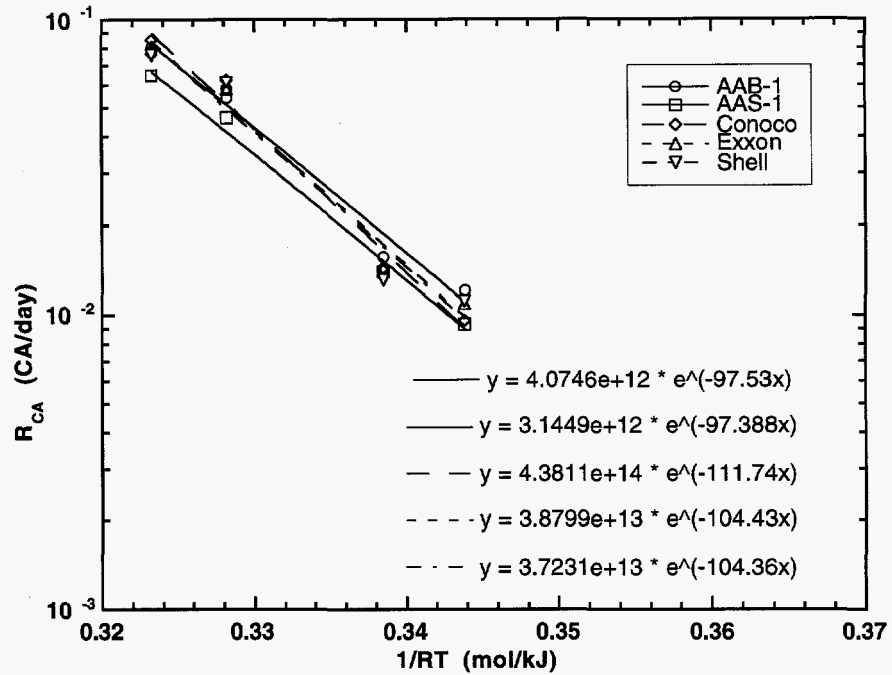


Figure 3-19. Oxidation rate vs. temperature for another five asphalts.

Table 3-8. Oxidation Rates Measured at 140 °F and 0.2 atm, Compared to Those Calculated by Two Methods

Asphalt	R_{CA}^a (CA/day)	$R_{CA}^b \times 10^3$ (CA/day)	%error	$R_{CA}^c \times 10^3$ (CA/day)	%error
AAA-1	1.95	1.62	17	1.88	4
AAD-1	1.51	1.45	4	1.61	7
AAF-1	2.58	2.02	22	2.55	1
AAG-1	4.06	2.21	46	3.58	12
AAM-1	2.17	1.30	40	2.19	1
AAB-1	2.45	2.08	15	2.27	7
AAS-1	1.86	1.69	9	1.91	3
TX1	2.69	1.32	51	2.33	13
Lau4	2.00	1.64	18	2.32	16
TX2	2.37	1.61	32	2.01	15

^a Measured

^b Extrapolated from data of the five high temperatures

^c Calculated from kinetics data in Table 3-4

the five high temperatures are not reliable. However, error in the rates calculated by the kinetic data in Table 3-4 generally is significantly less than that for the extrapolated rates.

Evaluation of the PAV Test

Recently, the Strategic Highway Research Program (SHRP) developed the Pressure Aging Vessel (PAV) test to simulate long-term in-service aging for 5 to 10 years (Button et al., 1993). In the PAV test procedure, asphalt binders are subjected to the Rolling Thin Film Oven Test, followed by 20 hours aging at 20 atm air and a temperature which depends on the climatic regions. The aging temperatures are 363.2, 373.2 and 383.2 K (90, 100 and 110°C). The high temperature, high pressure (4 atm oxygen) condition is used to acquire a reasonable amount of aging during a time period as short as 20 hours. However, assuming an average temperature of 333.2 (60°C) for road aging, which happens at an ambient pressure of 0.2 atm oxygen, one could question the ability of

PAV test to represent road aging accurately.

With an understanding of the aging kinetics, the effects of the selected aging pressure, temperature, and time can be examined. As can be seen from Equation 3-4, in the constant rate region, the viscosity of an asphalt binder is a function of the hardening susceptibility parameters (HS and m), the initial jump $CA_0 - CA_{\text{tank}}$, the oxidation rate R_{CA} , and the aging time t . For the initial jump region, no predictive analytical expression is available. In fact, rates during the initial jump region cannot be used to indicate those during the constant rate region, because the rates at the initial stage are much larger than the constant rates, with the extent being asphalt dependent.

Aging pressure affects the hardening susceptibility, HS, (and m), the initial jump $CA_0 - CA_{\text{tank}}$, and the oxidation rate R_{CA} . As shown in Figures 3-10 and 3-11, and Table 3-5, as well as Equation (3-3), HS decreases with aging pressure. For most asphalts, $CA_0 - CA_{\text{tank}}$ increases with aging pressure. The exceptions, including AAA-1 and AAD-1 among the asphalts studied, may have decreased $CA_0 - CA_{\text{tank}}$ for a higher pressure, but the values of $CA_0 - CA_{\text{tank}}$ are small for these two asphalts. The oxidation rates will increase with aging pressure because of the pressure reaction order. In short, compared to a road condition of 0.2 atm oxygen partial pressure, the 4 atm oxygen pressure in the PAV test decreases hardening susceptibility, increases $CA_0 - CA_{\text{tank}}$ for most asphalts, and raises the oxidation rate, with the extent being asphalt dependent.

Higher aging temperature in the PAV test increases the oxidation rate due to the Arrhenius relationship. Because the activation energy is asphalt dependent, as shown in Table 3-4, the change in oxidation rate caused by the temperature increase will be asphalt dependent too.

The combined effect of aging pressure and temperature is more complicated. Compared to an average road condition of 0.2 atm oxygen and 333.2 K (140°F), the PAV test is run at a high temperature high pressure condition, resulting in a lower hardening susceptibility, a higher $CA_0 - CA_{\text{tank}}$, and a higher oxidation rate. As can be noted from Equation (3-4), a lower hardening susceptibility for one asphalt compared to another leads to a lower increase in viscosity with oxidation, while a higher $CA_0 - CA_{\text{tank}}$, and/or a higher oxidation rate leads to higher increase. If the effects of these factors cancel for two asphalts, then their relative ranking with respect to oxidative hardening after PAV aging compared to that after low temperature, low pressure aging may be close. However, if a higher $CA_0 - CA_{\text{tank}}$ and a higher oxidation rate is the predominant factor for one asphalt,

then that asphalt will be discriminated against by the PAV test (viscosity being unduly high by the PAV test). On the other hand, asphalts which have a lower hardening susceptibility as the predominant effect will be unduly favored by the PAV test.

In order to discuss the effect of aging time, Equation (3-4) is rearranged as:

$$\eta^*_0 = m e^{(HS CA_0 + HS R_{CA} t)} \quad (3-5)$$

The two terms in the exponential, $(HS) (CA_0)$ and $(HS) R_{CA} t$, represent the relative contributions of initial jump and oxidation rate on the viscosity of the aged sample. It needs to be noted that the first term $HS CA_0$ is a constant, while the second term $HS R_{CA} t$ is a linear function of aging time. Because of this, as oxidative aging progresses, the second term becomes relatively more and more significant. Furthermore, this time-dependent relativity is also asphalt dependent. This means that the ranking of the asphalts after PAV aging may differ for varying aging times. In this sense, the selected aging time of 20 hours is merely an arbitrary choice.

To quantify the examination, an effort was made to estimate the aging parameters of the ten asphalts at an oxygen pressure of 4 atm and a temperature of 373.2 K (100°C). The parameters in Equation (3-5) were calculated using the models developed earlier in this chapter. With model Equation (3-2) and the constants listed in Table 3-7, the values of $CA_0 - CA_{\text{tank}}$ for the ten asphalts at an aging pressure of 4 atm were calculated and listed in the second column of Table 3-9. The HS values at an aging pressure of 4 atm were calculated using model Equation 3-3 and the constants in Table 3-7, and the values are listed in the third column of Table 3-9. In addition, the values of the constant m for the aging pressure of 4 atm were interpolated from the data in Table 3-5 assuming a linear relationship between $\ln(m)$ and $\ln(P)$, and are listed in the fourth column of Table 3-9. Finally, the oxidation rate R_{CA} at 4 atm and 373.2 K (100°C) was calculated using Equation (1-10) and the kinetic parameters in Table 3-4. The values of R_{CA} are listed in the last column in Table 3-9.

It should be pointed out that the models for $CA_0 - CA_{\text{tank}}$ and HS, and the linear relationship between $\ln(m)$ and $\ln(P)$, are all based on simplifying assumptions. The model constants are subject to experimental errors. Furthermore, in the PAV test, although the oxygen pressure is 4 atm in the gas phase, the pressure distribution in the asphalt film is not exactly known. Since the film is 3.2 mm

Table 3-9. Calculated Aging Parameters for Aging at 4 atm Oxygen and 212°F

Asphalt	$CA_0 - CA_{\text{tank}}$ (CA)	HS ^b	m^c (poise)	R_{CA}^d (CA/day)
AAA-1	0.589	5.31	101.5	0.336
AAD-1	0.907	5.34	46.63	0.393
AAF-1	1.019	3.78	593.3	0.206
AAG-1	1.843	1.26	1130	0.241
AAM-1	1.043	4.72	191.0	0.170
AAB-1	0.798	4.66	183.6	0.309
AAS-1	0.726	4.69	378.3	0.256
TX1	0.804	4.83	61.08	0.319
Lau4	0.924	2.66	764.5	0.257
TX2	0.717	6.14	49.18	0.333

^a By Equation 3-2 and constants in Table 3-7

^b By Equation 3-3 and constant in Table 3-7.

^c Assume $\ln(m)$ is linear to $\ln(P)$.

^d By Equation 1-10 and constants in Table 3-4.

thick, the diffusion effect may not be negligible. The use of 4 atm in the calculation may lead to error too. For these reasons, the estimated values are only approximations to the real values.

The values of $CA_0 - CA_{\text{tank}}$, m , HS, and R_{CA} obtained above are used to predict the viscosities of the asphalts after aging at the PAV conditions. For comparison, the viscosities of the ten asphalts after PAV test were measured and are listed in the second column of Table 3-10. The ranking of the asphalts by the viscosity values are listed in the third column, with the lowest viscosity being number 1. The viscosity of the asphalts after 20 hours aging at 4 atm and 373.2 K (100°C) were calculated using Equation (3-5), and are listed in the fourth column of the table with the corresponding ranking in the fifth column. Comparing viscosity values in the second column and the fourth column, the predicted viscosities are a bit higher than the measured values, but not by substantial amounts. Most of the viscosities are about several tens of thousands poise. Comparing

Table 3-10. Viscosity and Rank of the Ten Asphalts after PAV Test

Asphalt	VIS _{PAV} (poise)	rank ^a	VIS _{20hrs} (poise)	rank ^b	VIS _{40hrs} (poise)	rank ^c	Hardening rate ^d
AAA-1	9,770	4	10,255	1	45,433	4	1.79
AAD-1	23,070	10	33,810	8	194,020	10	2.10
AAF-1	19,450	8	53,614	10	102,730	8	0.780
AAG-1	7,960	2	14,949	3	19,270	1	0.305
AAM-1	21,390	9	51,419	9	100,560	7	0.805
AAB-1	12,700	6	24,968	6	82,731	5	1.44
AAS-1	20,650	7	30,891	7	84,027	6	1.20
TX1	7,020	1	10,707	2	38,682	3	1.54
Lau4	8,320	3	15,806	4	27,946	2	0.684
TX2	11,400	5	22,159	5	121,820	9	2.05

^a Rank by viscosity measured after PAV test, lowest value being number 1

^b Rank by viscosity predicted for 20 hours aging at PAV conditions

^c Rank by viscosity predicted for 40 hours aging at PAV conditions

^d Hardening rate defined as the product of HS and R_{CA}, all for PAV condition

the rankings, both of the two methods rate AAA-1, AAG-1, TX1, Lau4 and TX2 as the top five asphalts. The other five asphalts are ranked by both of the methods as being the bottom five. They are AAD-1, AAF-1, AAM-1, AAB-1 and AAS-1. With the possible errors cited above, we conclude that the PAV test is predicted reasonably well by the kinetic model.

The viscosities of the asphalts after 40 hours of aging at the PAV conditions were calculated and are listed in the sixth column of Table 3-10. The rank by viscosity is listed in the next column. It should be remembered that the only difference between the data in column four and column six is that the aging time is doubled. It is expected that because of the relative contributions of the two terms in the exponential in Equation (3-5), those asphalts with both higher hardening susceptibilities

and oxidation rates will not perform well by longer aging times. Defining the product of hardening susceptibility and oxidation rate as hardening rate, the final column in Table 3-10 lists the estimated hardening rates of the ten asphalts (the product of columns three and five in Table 3-9). Comparing the ranks in the fourth and sixth columns of Table 3-10, those of AAF-1, AAG-1, AAM-1, AAS-1 and Lau4 are improved by longer aging time. This is because these asphalts have the five lowest hardening rates. On the other hand, the ranks of the five asphalts with the highest hardening rates are deteriorated by longer aging time, except for AAB-1. It is not difficult to imagine that even for longer aging times those asphalts with the highest hardening rates will gradually display higher viscosities. The most noticeable case is asphalt TX2. This asphalt is among the top five (number 5) when the aging time is 20 hours. However, it becomes one of the five worst (number 9) when evaluated at an aging time of 40 hours.

It is clear from the above analysis that the effects of high temperature high pressure condition on the extent of oxidative aging are very asphalt dependent. We thus conclude that the PAV test lacks theoretical support. However, because of the cancellation phenomenon, for most asphalts, data from the PAV test can still be used to indicate long-term aging. On the other hand, for some asphalts, if cancellation does not occur, then they either may be unduly favored or they may be undermined by the PAV test. The above statements are supported by Figure 3-20, which compares the aging indices of the ten asphalts by both PAV test and by 135 days aging at 140°F and air. In terms of ranking by aging index, the PAV test gives similar result as the low temperature, low pressure aging for most of the asphalts. However, asphalt AAF-1 is favored by PAV test, while asphalt AAD-1 is undermined by the PAV test.

The biggest advantage of the PAV test is that it can be performed in a short time. Also, the amount of sample is adequate for various types of physical property tests. Many asphalts can be tested simultaneously. The disadvantage is that the high temperature, high pressure condition and short test time may unduly discriminate against or in favor of some asphalts. At the current time, as no better engineering test exists, it should be taken as a pragmatic method and practiced. However, if time and man power allow, the aging test proposed in the fourth section of this chapter may be used to verify that selected binder do not have inferior aging properties.

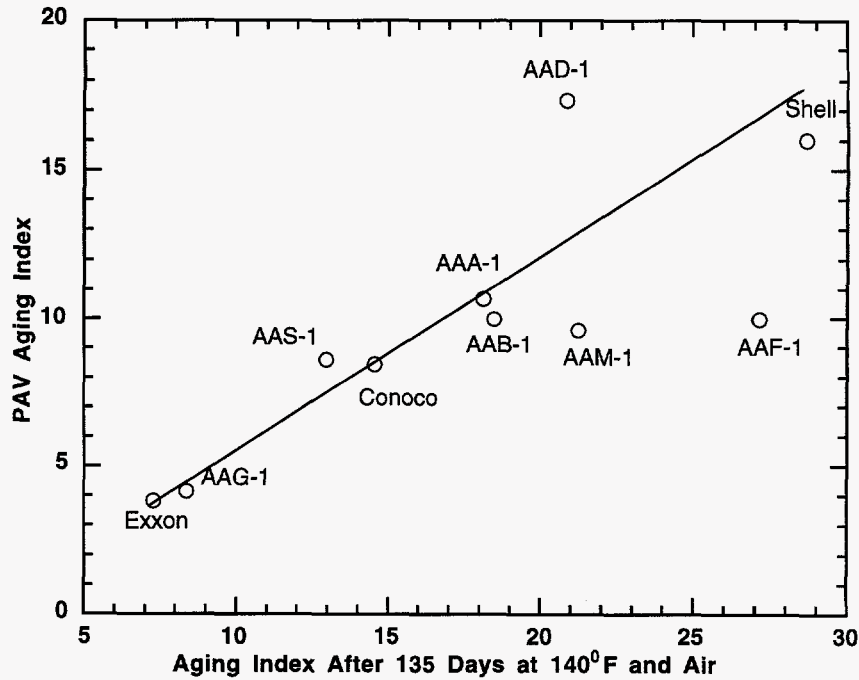


Figure 3-20. Aging indices by PAV test and low T, low P aging.

Summary

Carbonyl area as measured by the FTIR is used as a measure of the oxidation extent for asphalt binders. By measuring the carbonyl growth of the ten asphalts aged at a combination of temperatures and oxygen pressures, the oxidation rates at the specific conditions, and the average value of the initial jump $CA_0 - CA_{\text{blank}}$ at different aging pressures were obtained for each of the asphalts. Generally speaking, the initial jump increases with aging pressure, with the extent being asphalt dependent. Kinetic parameters including activation energy E and pressure reaction order α were estimated through linear regression for the asphalts. The kinetic parameters have been found to be asphalt dependent.

The hardening susceptibility relationship has been measured at both high pressure (20 atm) and low pressure (0.2 atm) for the ten asphalts. Data show that the hardening susceptibility is larger for a lower aging pressure, with the extent being asphalt dependent.

A model for the oxidative aging of asphalt binders was proposed. It is based on the understanding that age hardening is the combined effect of the carbonyl growth due to oxidation and the hardening in physical properties due to the chemical compositional change. A theoretically sound aging test to evaluate low temperature, low pressure aging resistance was described. In the described scheme, the kinetic parameters of a given asphalt are measured to calculate the oxidation rate at the road temperature. The method also requires the measurement of other characteristic parameters for the given asphalt, including the initial jump $CA_0 - CA_{\text{tank}}$, and the HS value at road conditions.

Models were developed to describe the pressure dependencies of the initial jump $CA_0 - CA_{\text{tank}}$, and the HS value. Because the kinetic parameters are asphalt dependent, and also because the initial jump $CA_0 - CA_{\text{tank}}$ and the HS value are pressure dependent, any aging test run at a single elevated temperature and/or pressure, including the PAV test, are not theoretically sound.

Data also show that the RTFOT treatment has a negligible effect on the kinetic behavior of asphalt binders.

CHAPTER 4

OXIDATION KINETICS OF ASPHALT FRACTIONS

In the last chapter, the oxidation and aging kinetics of asphalt binders were discussed. The discussion provided asphalt users and government agencies with a means of evaluating the aging resistance of asphalt binders. On the other hand, for asphalt producers, the more immediate technical issue might be knowledge of the compositional dependence of asphalt properties which will assist in the manufacturing and formulating of superior asphalt binders through compositional manipulation.

The current chapter investigates the compositional dependence of asphalt oxidation. It examines the oxidation kinetics both of asphalt generic fractions and supercritical fractions. This is a direct extension of the kinetic studies conducted on the whole binders described in the last chapter.

In the study of oxidation kinetics of asphalt generic fractions, the naphthene aromatic (NA) fractions and polar aromatic (PA) fractions of five SHRP asphalts (AAA-1, AAD-1, AAF-1, AAG-1 and AAM-1) were separated from their parent asphalts, and aged at multiple conditions. Kinetic parameters of the ten generic fractions were determined, and compared to each other and to those of their parent asphalts. In determining the oxidation kinetics of asphalt supercritical fractions, six supercritical fractions of SHRP AAF-1 (F1F, F2F, F3F, F4F, F6F and F7F), with intermediate contents of NA and PA, were aged at appropriate conditions to obtain their kinetic parameters. The compositional dependence of the reactivity was further studied by analyzing the constituents of the supercritical fractions.

The influence of the asphaltene fraction and the saturate fraction on asphalt oxidation were also investigated. Because asphaltenes exist as solids at room temperature and measurement of the CA values of asphaltenes is extremely difficult, no aging experiments were conducted for the pure asphaltene fractions. As saturates are highly stable at laboratory aging conditions, they were not aged in the pure fraction state either. Instead, aromatics/saturates/asphaltenes blends, with controlled levels of saturates and/or asphaltenes content, were aged at multiple temperatures and atmospheric pressure. The effect of asphaltenes and saturates on the reactivity of the whole asphalt was identified by comparing the oxidation rates of an asphaltic material before and after the addition of any or both of these two fractions.

The next chapter is devoted to the physico-chemical correlations of asphalt generic fractions and supercritical fractions. As we know, aging resistance is a quality affected by both oxidation kinetics, and the resistance to hardening due to the chemical change caused by oxidation. Understanding the compositional dependence of oxidation kinetics and physico-chemical correlations, thus, provides a means of improving the asphalt aging resistance through compositional manipulation.

Oxidation Kinetics of Generic Fractions

Table 4-1 gives the initial CA values of the five NA fractions and the five PA fractions. Although physical properties of the fractions will not be discussed in detail in this chapter, the initial low frequency limiting viscosities of the pure fractions are also listed in the table. They will be referenced to in the next chapter. The initial chemical and physical properties of the six supercritical fractions are also given in Table 4-1. As commonly believed, the PA fraction of an asphalt binder has

Table 4-1. Initial Properties of NA, PA Fractions and Supercritical Fractions

Fraction	Initial CA	Initial Viscosity (poise)	Fraction	Initial CA	Initial Viscosity (poise)
ANA ^a	0.114	24.1	APA	1.230	74,540
DNA	0.117	15.5	DPA	1.604	39,600
FNA	0.158	57.1	FPA	1.200	806,200
GNA	0.215	364	GPA	2.011	2.227M
MNA	0.154	116	MPA	1.312	4.800M
F1F	0.167	<10	F4F	0.489	415
F2F	0.211	13.9	F6F	0.564	5,250
F3F	0.364	89.0	F7F	0.699	74,000

^a ANA represents naphthene aromatics of SHRP AAA-1. Likewise, DNA stands for naphthene aromatics of AAD-1, and APA represents polar aromatics of AAA-1.

much higher carbonyl content than the NA fraction of the same asphalt. Also, as shown in Figure 4-1 for asphalt AAA-1, the PA fraction is much larger in molecular size than the NA fraction of the same asphalt. This is also true for the NA and PA fractions of the other asphalts. These observations support the results reported by other researchers (Corbett 1975; Corbett and Merz, 1975) that the PA fraction is much more reactive than the NA fraction for a given asphalt.

However, a detailed study on the reactivities of these two fractions has not been reported. This is the subject of this section. Furthermore, as shown by the data in Table 4-1, the difference between the NA fractions from various asphalts is noticeable. The PA fractions of the five asphalts also have different properties. Figures 4-2 and 4-3 show the GPC spectra of the five NA fractions and the five PA fractions respectively, which support the differences demonstrated by the data in Table 4-1.

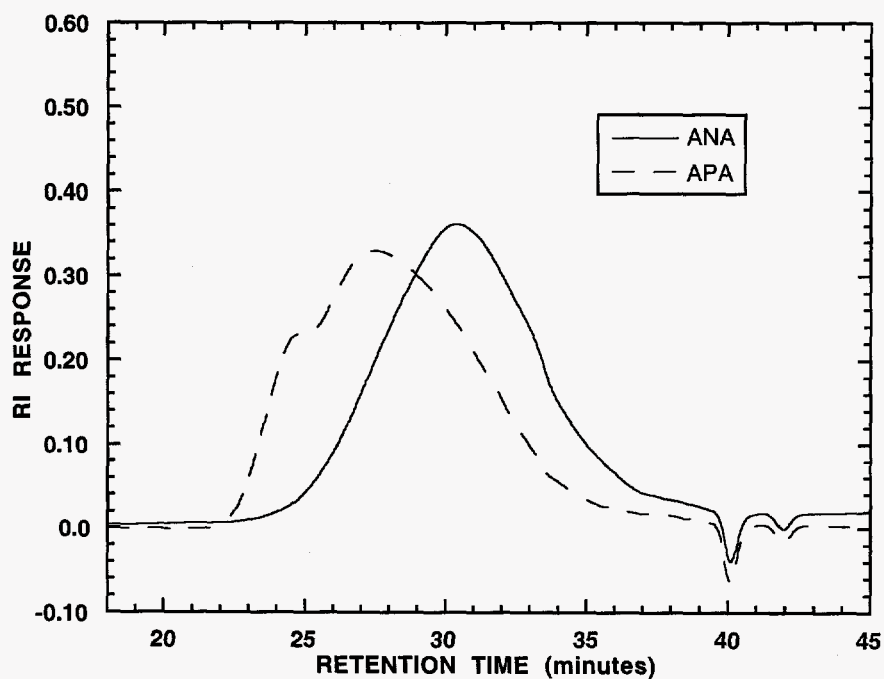


Figure 4-1. GPC spectra of ANA and APA.

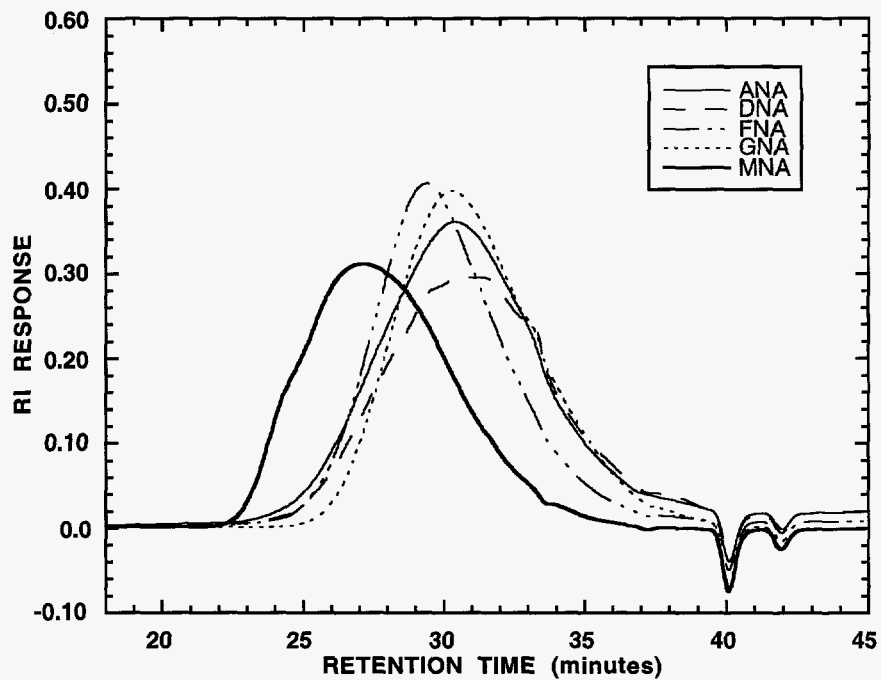


Figure 4-2. GPC spectra of the five NA fractions.

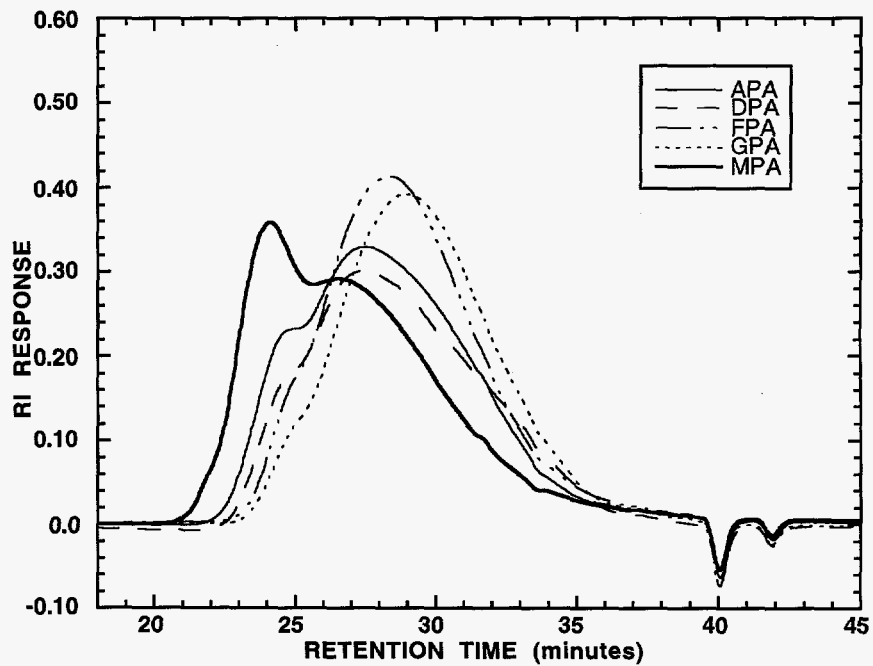


Figure 4-3. GPC spectra of the five PA fractions.

Table 4-2 lists the aging conditions used in the aging experiments for PA and NA fractions. A total of 9 conditions were used, which are designated as C14 to C22 and cover temperatures from 348.2 to 373.2 K (75 to 100°C), with oxygen pressure of 0.2, 10, or 20 atm. The PA fractions were aged at different conditions than the NA fractions because the PA fractions reacted much faster; each fraction was aged using the seven conditions most appropriate for its aging kinetics. In retrospect, an oxygen pressure of 10 instead of 20 atm would have been best for condition C22.

Carbonyl area versus aging time is shown for AAA-1 PA fraction (APA) in Figure 4-4 and for its NA fraction (ANA) in Figure 4-5. Figures 4-6 and 4-7 show similar results for the PA and NA fractions of AAG-1. As observed from the figures, carbonyl growth for a generic fraction follows a similar profile to that of a whole asphalt. That is, the fraction undergoes rapid oxidation initially and then ages at a constant rate for an extended period of time. As shown in Figure 4-5, the initial rapid rate region is almost not noticeable for ANA. This is because the initial jump $CA_0 - CA_{\text{tank}}$ is very low for this fraction. The CA values of the unaged samples and the aging conditions used for the fractions are also shown in the figures. The slope of each aging line is the constant aging rate, and the intercept of the line is CA_0 . As is the case for the whole asphalt, within experimental error, CA_0 is observed to be largely pressure dependent but not temperature dependent. Carbonyl growth of PA and NA fractions of other asphalts have similar profiles.

The constant aging rates of the PA and NA fractions at their respective seven conditions are listed in Table 4-3. Using the rate data in this table and the corresponding temperatures and pressures in Table 4-2, a linear regression was performed for Equation (3-1) to obtain the kinetic parameters of the generic fractions.

Table 4-4 gives the values of the pressure reaction order α and activation energy E for the fractions. For comparison, the values of the five whole asphalts are also listed. It is observed that the kinetic parameters of the generic fractions cover a similar range as the whole asphalts. This means that both the PA and NA fractions, although with distinctly different properties, are still "asphaltic materials" in terms of dependency of reactivity on pressure and temperature. Because the PA fraction oxidizes much more rapidly than the NA fraction of a given asphalt, the carbonyl growth of an asphalt during oxidative aging consists mainly of PA oxidation. If the oxidation rate of an asphalt binder is the sum of its fraction oxidation rates, one would expect that α and E of a whole

Table 4-2. Conditions Applied in the Aging Experiments for NA and PA Fractions and Supercritical Fractions

Condition	Temperature (°C)	Pressure (atm)
C14	85	0.2
C15	90	0.2
C16	95	0.2
C17	100	0.2
C18	75	10
C19	80	10
C20	85	10
C21	90	10
C22	95	20

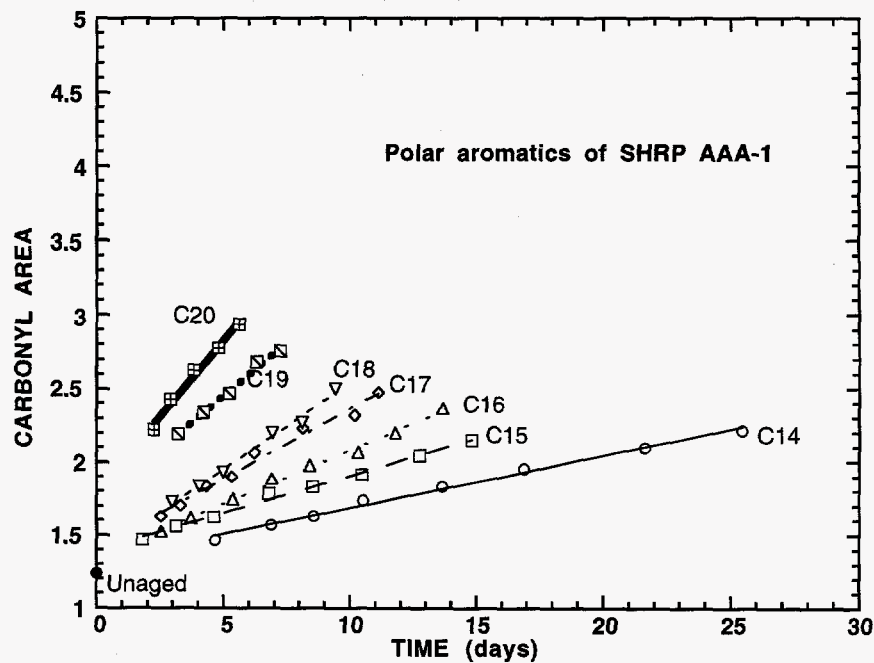


Figure 4-4. Carbonyl area vs. aging time for APA.

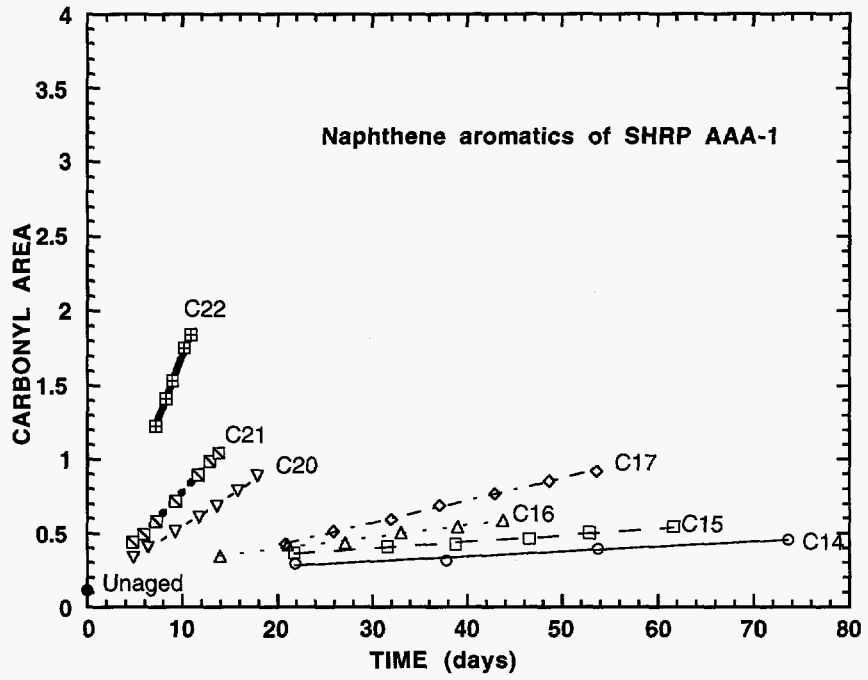


Figure 4-5. Carbonyl area vs. aging time for ANA.

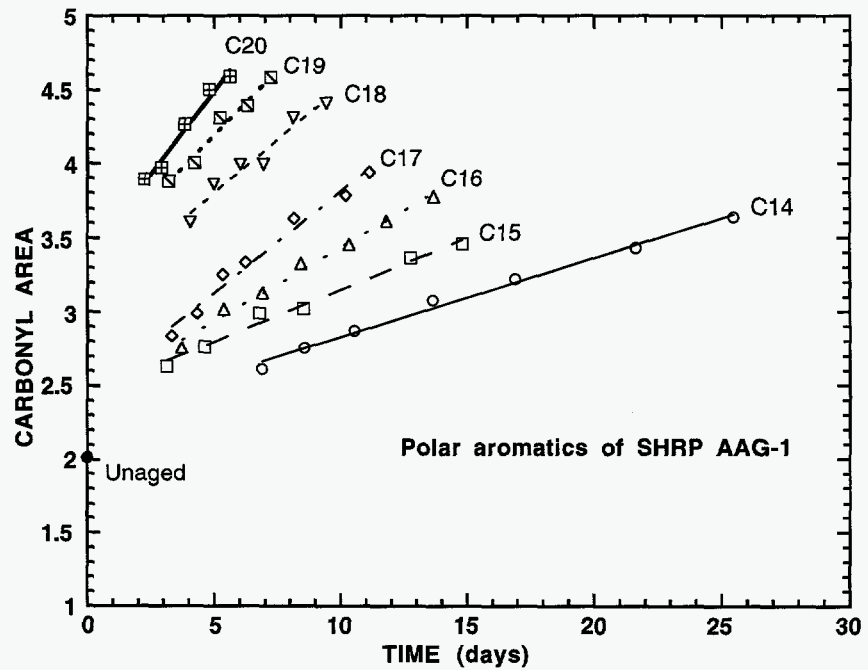


Figure 4-6. Carbonyl area vs. aging time for GPA.

Table 4-3. CA Growth Rate for NA and PA Fractions at All Conditions

Aging Condition ^a :	$R_{CA} \times 10^3$ (CA/day)						
	C14	C15	C16	C17	C18	C19	C20
Fraction							
APA ^b	35.75	51.08	73.15	95.50	117.3	145.2	204.4
DPA	29.89	44.17	60.53	90.23	82.43	112.2	154.4
FPA	45.64	65.76	92.00	118.9	84.89	125.1	220.7
GPA	53.33	70.28	99.08	136.4	143.9	176.3	233.2
MPA	41.14	61.99	86.14	108.6	99.95	122.1	154.0

Aging Condition ^a :	$R_{CA} \times 10^3$ (CA/day)						
	C14	C15	C16	C17	C20	C21	C22
Fraction							
ANA ^b	3.422	4.458	7.911	15.19	41.37	69.23	169.3
DNA	3.041	4.507	6.045	12.05	46.63	78.77	240.7
FNA	7.316	12.16	18.46	25.09	50.57	77.01	145.6
GNA	12.46	18.43	24.75	39.36	69.29	100.3	191.1
MNA	11.11	12.02	17.18	23.71	39.82	58.11	101.9

^a See Table 4-2^b ANA represents naphthene aromatics of SHRP AAA-1. Likewise, DNA stands for naphthene aromatics of AAD-1, and APA represents polar aromatics of AAA-1.**Table 4-4. Kinetic Parameters of NA and PA Fractions and Their Parent Asphalts**

	α			E (kJ/mol)		
	Whole	NA	PA	Whole	NA	PA
AAA-1	0.538	0.658	0.441	92.3	109.6	68.5
AAD-1	0.580	0.744	0.423	97.2	105.7	75.7
AAF-1	0.364	0.471	0.381	85.4	88.1	80.0
AAG-1	0.329	0.435	0.377	83.3	81.7	62.4
AAM-1	0.331	0.372	0.334	86.9	63.2	63.5

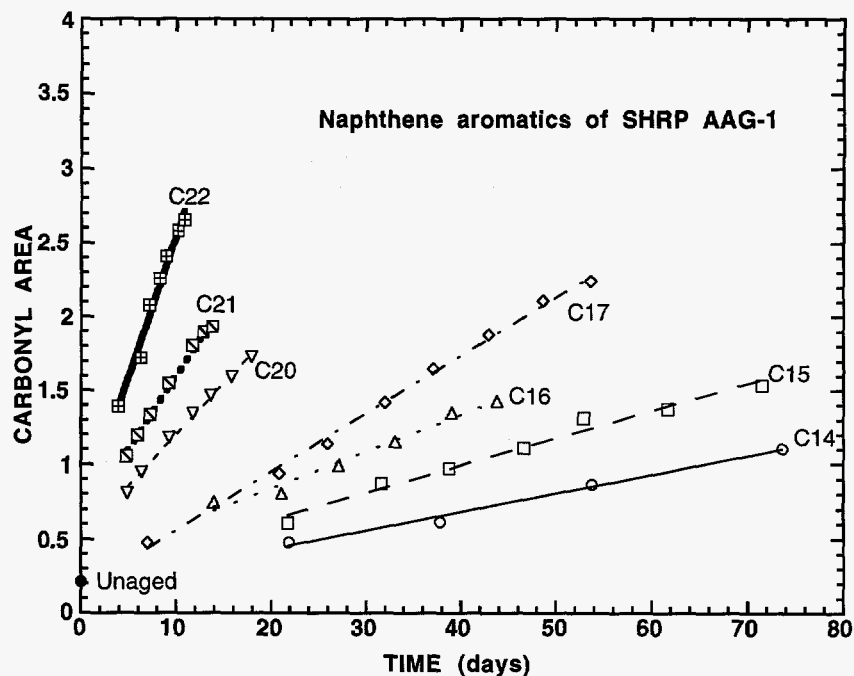


Figure 4-7. Carbonyl area vs. aging time for GNA.

asphalt to be similar to the values of its PA fraction. The data in Table 4-4 contradict this, and strongly suggest that the kinetic characteristics of an asphalt are determined not only by the kinetic characteristics of its fractions, but also by the interactions between the fractions. The interactions may affect the reactivity/accessibility of the reactive sites in a temperature-dependent and/or pressure-dependent manner .

Using the pressure reaction order data in Table 4-4, the aging rates at oxygen pressures other than 0.2 atm can be converted to corresponding rates at 0.2 atm. The Arrhenius plot at 0.2 atm oxygen pressure can then be constructed for each fraction. Figure 4-8 shows the Arrhenius plots for APA, ANA and AAA-1 whole asphalt. Within the temperature range of Figure 4-8, APA has aging rates about five times those of ANA. The whole asphalt, as a mixture of polar aromatics and naphthene aromatics fractions as well as saturates and

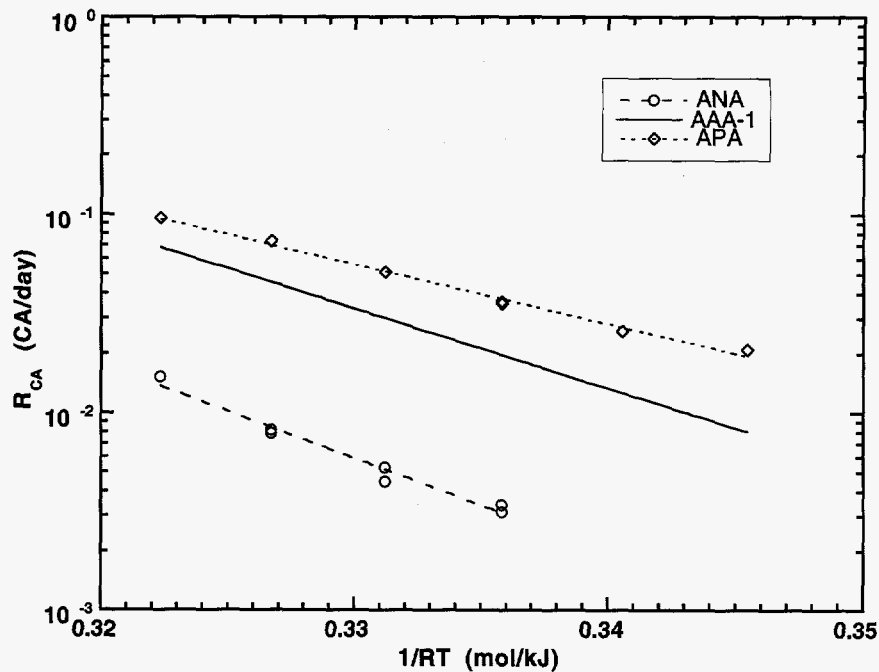


Figure 4-8. Arrhenius plots for AAA-1 and fractions.

asphaltenes, has oxidation rates between the two. Fractions from other asphalts have similar behavior.

Figures 4-9 and 4-10 show the Arrhenius plots of the five PA fractions and the five NA fractions where the reactivities of the pure fractions from different asphalt sources are compared within the temperature range of the figures. Outside the temperature range of the figures, the relative reactivity may change because of the differences in activation energies as listed on Table 4-4. In Figure 4-9, DPA always has the lowest rates, while GPA has the highest rates with the rates of APA, FPA and MPA in between. However, as seen from Figure 4-3, in terms of molecular size, MPA is the largest while GPA is the smallest. This clearly indicates that molecular size alone can not be used to measure the reactivities of asphalt fractions from different sources. This observation is again confirmed by Figures 4-4 and 4-10. While MNA is the largest in molecular size, its reactivity is not the highest. Because, for

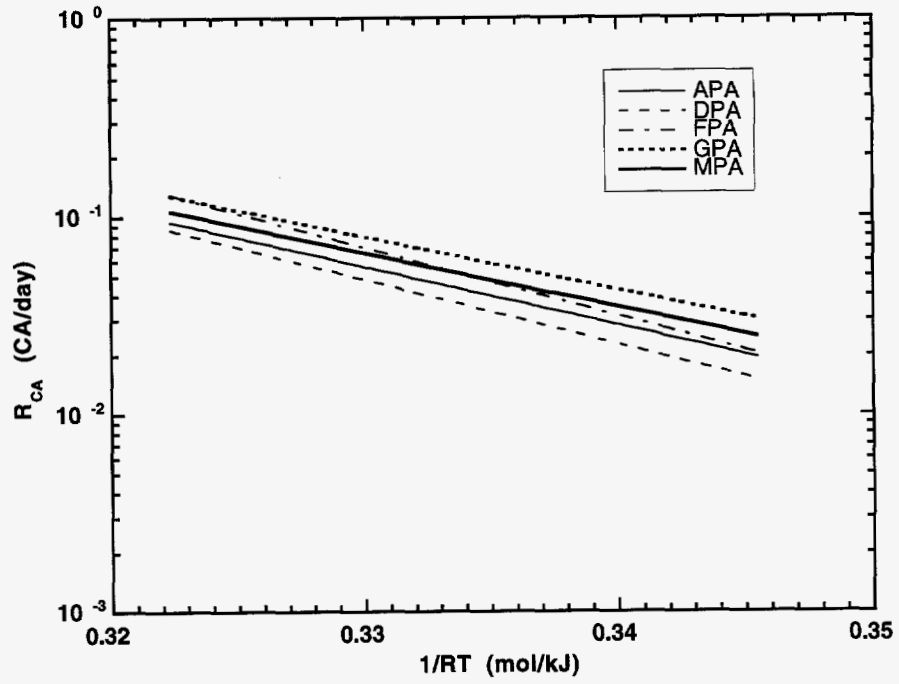


Figure 4-9. Arrhenius plots for the PA fractions.

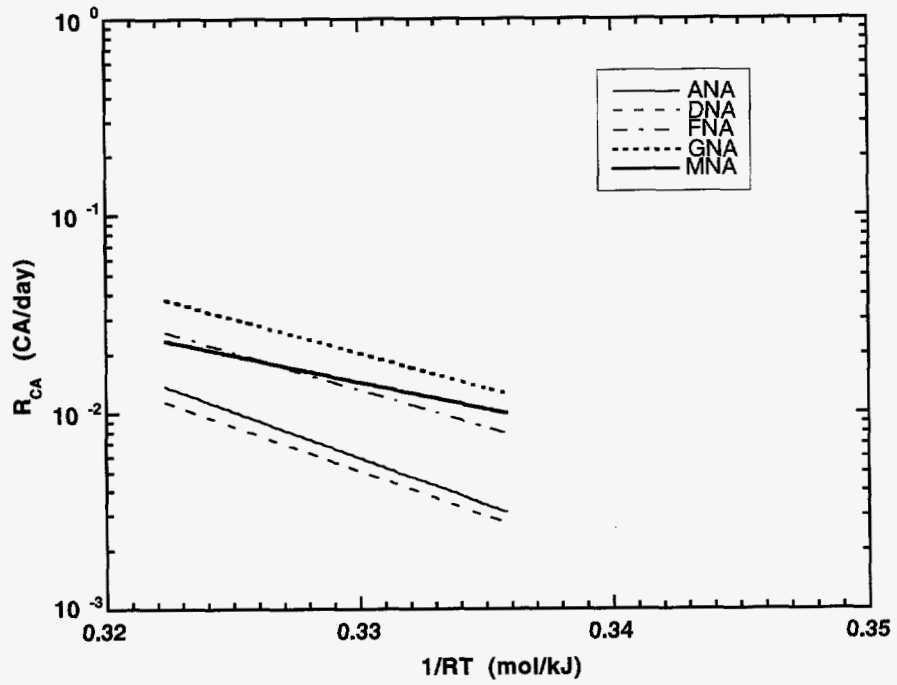


Figure 4-10. Arrhenius plots for the NA fractions.

both PA and NA fractions from different asphalt sources, no correlation exists between the molecular size and the reactivity, any attempt to correlate molecular size to reactivity for whole asphalts will fail. On the other hand, comparing the rank by reactivity for the fractions, both the naphthene aromatics and polar aromatics fractions of AAD-1 are the lowest among the NA group and PA group. For AAG-1, its NA and PA fractions always have the highest rates among the NA group and PA group. This indicates that fraction reactivity is very much asphalt source dependent.

Another important kinetic parameter is CA_0 in Equation (1-5). Table 4-5 shows the average initial jump $CA_0 - CA_{\text{unaged}}$ for the PA and NA fractions and for the whole asphalts at different pressures. Several observations may be made from the data in this table. First, generally speaking, for each asphalt, the NA fraction has a much smaller initial jump than either its parent whole asphalt or its PA fraction, while the initial jump of the PA fraction approximates that of its parent asphalt. Second, for asphalts with low initial jump values, including AAA-1 and AAD-1, their fractions have low initial jump values too. The negative values for these fractions are due to a combination of near zero values and extrapolation error. On the other hand, for asphalts with high initial jump values, including AAF-1, AAG-1, and AAM-1, their fractions have high initial jump values also. Finally, whatever reactions occur that account for the fast initial oxidation, the data in Table 4-5 suggest these reactions are largely associated with the PA fraction.

COMPOSITIONAL ANALYSIS OF SUPERCRITICAL FRACTIONS

As seen from Table 4-1, for the supercritical fractions, the initial carbonyl content increases monotonically with the fraction number. Fraction F1F is the lightest and most pentane soluble, while F7F is the heaviest and least soluble. Not surprisingly, the viscosity increases with fraction number. Furthermore, the chemical composition of the supercritical fractions has a general trend (Stegeman et al., 1992) in that from F1F to F7F, saturate content decreases while asphaltene content increases. Also, naphthene aromatics decrease while polar aromatics increase, although not necessarily monotonically. In the current and the next sections, it will be shown explicitly that the reactivity increases with fraction number.

Table 4-5. CA_0-CA_{unaged} for NA and PA Fractions and Their Parent Asphalts at Different Aging Pressures

	P (atm)				P (atm)		
	0.2	10	20		0.2	10	20
AAA-1	0.168	--	0.050	AAD-1	0.206	--	0.127
ANA ^a	0.090	-0.004	-0.098	DNA	0.053	-0.001	-0.289
APA	0.140	0.400	--	DPA	0.042	0.364	--
	P (atm)				P (atm)		
	0.2	10	20		0.2	10	20
AAF-1	0.339	--	0.757	AAG-1	0.500	--	1.733
FNA	0.096	0.112	0.237	GNA	0.021	0.339	0.425
FPA	0.419	0.709	--	GPA	0.398	1.244	--
	P (atm)				P (atm)		
	0.2	10	20		0.2	10	20
AAM-1	0.308	--	0.808				
MNA	0.190	0.230	0.352				
MPA	0.581	0.858	--				

^a ANA represents naphthene aromatics of SHRP AAA-1. Likewise, DNA stands for naphthene aromatics of AAD-1, and APA represents polar aromatics of AAA-1.

Corbett analyses performed on the six supercritical fractions confirm the observations obtained by previous researchers (Stegeman et al., 1992). Table 4-6 lists the Corbett compositions of the six supercritical fractions. As seen from the table, fractions F1F, F2F and F3F are asphaltene free. Asphaltenes increase from negligible in F4F to 8% in F7F. The saturate content decreases monotonically from 40% in F1F to 5% in F7F. Polar aromatics increase monotonically from 12% to 54%. The content of naphthene aromatics remains stable around 50% for all the fractions. For the six fractions in Table 4-6, the sum of the weight percentages of its four Corbett fractions may be below or above 100. This is because of mass loss during the Corbett separation or residual solvent in the Corbett fractions.

Table 4-6. Initial Corbett Composition of Supercritical Fractions of AAF-1

	F1F	F2F	F3F	F4F	F6F	F7F
SA	39.7	30.7	17.1	10.1	5.86	5.07
NA	48.4	48.8	54.1	51.2	48.9	39.4
PA	12.2	19.0	30.8	40.2	50.1	53.5
AS	0.0	0.0	0.0	0.83	1.27	7.69

Figure 4-11 shows the molecular size distribution of the supercritical fractions. As the fraction number increases, the fraction contains more large-size molecules. This is consistent with the result observed from the Corbett analysis. In Figure 4-12, the GPC spectra of FNA and FPA are compared with those of the supercritical fractions. In terms of molecular size, FPA is the largest, with F7F being very close to it. F1F is the smallest in molecular size, while FNA is close to F2F and F3F.

Figure 4-13 compares the GPC spectra of the polar aromatic portions of the six supercritical fractions along with the polar aromatic portion of the whole asphalt. The molecular size of the PA portions of the supercritical fractions increases with fraction number. Particularly, the PA fractions of F1F and F2F are much smaller than the PA portion of the parent asphalt, while the PA fraction of F7F is larger than the PA portion of the whole asphalt. In this sense, taking FPA as the average polar aromatics, then PA of F1F, F2F and F3F are below average while that of F7F is above average. Those of F4F and F6F are close to average.

Figure 4-14 displays the GPC spectra of the naphthene aromatics portions of the supercritical fractions and that of the parent asphalt. Again, the molecular size of the NA portions of the supercritical fractions increases with fraction number, except that those of F6F and F7F are close to each other. Also, similar to the reasoning above, we may say that NA of F1F and F2F are below the average (FNA), while NA of F6F and F7F are above the average. Figure 4-15 exhibits the GPC spectra of the asphaltenes from F6F, F7F and the parent asphalt

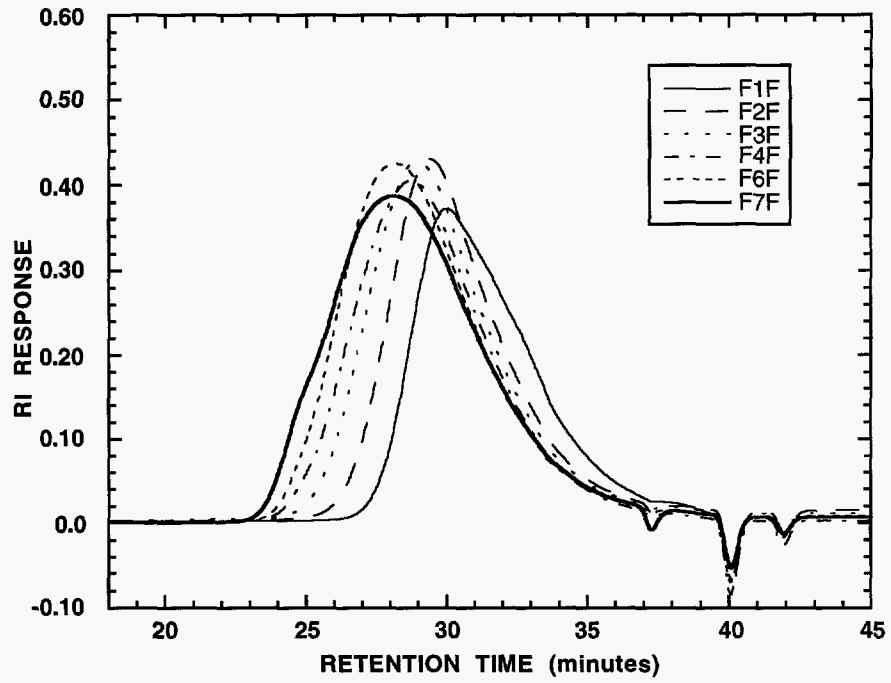


Figure 4-11. GPC spectra of supercritical fractions of AAF-1.

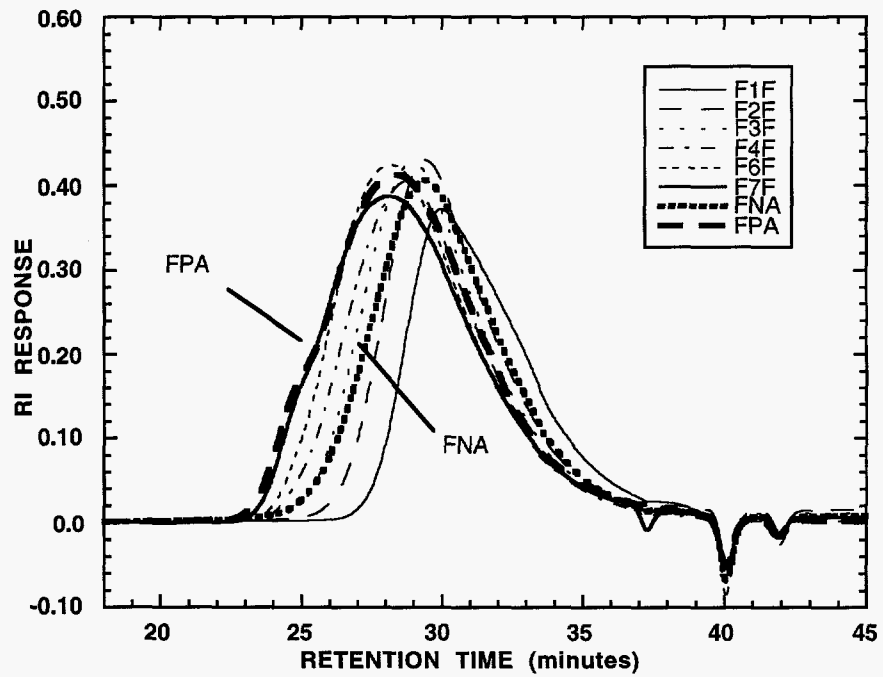


Figure 4-12. GPC spectra of AAF-1 fractions.

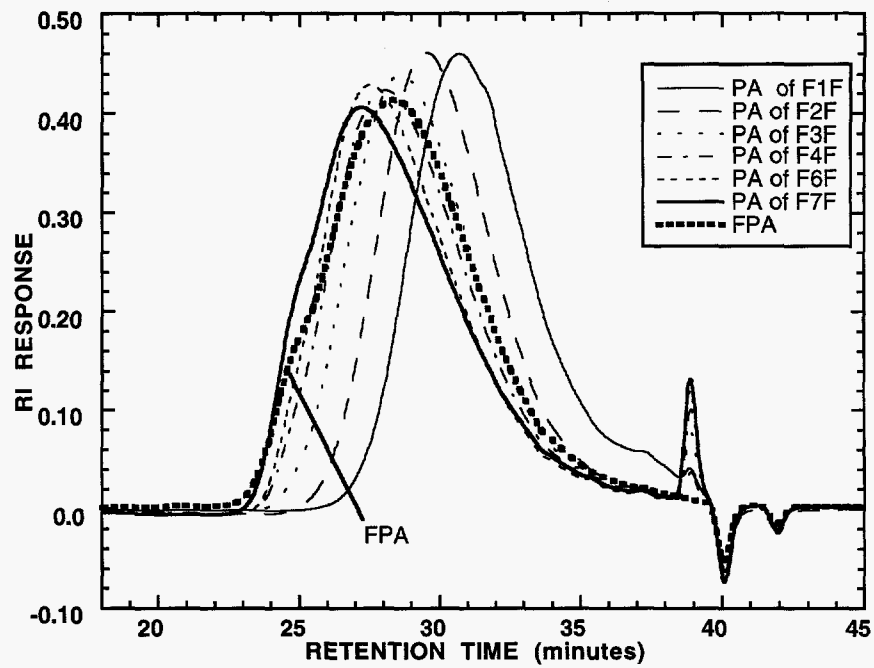


Figure 4-13. GPC spectra of various PA derived from AAF-1.

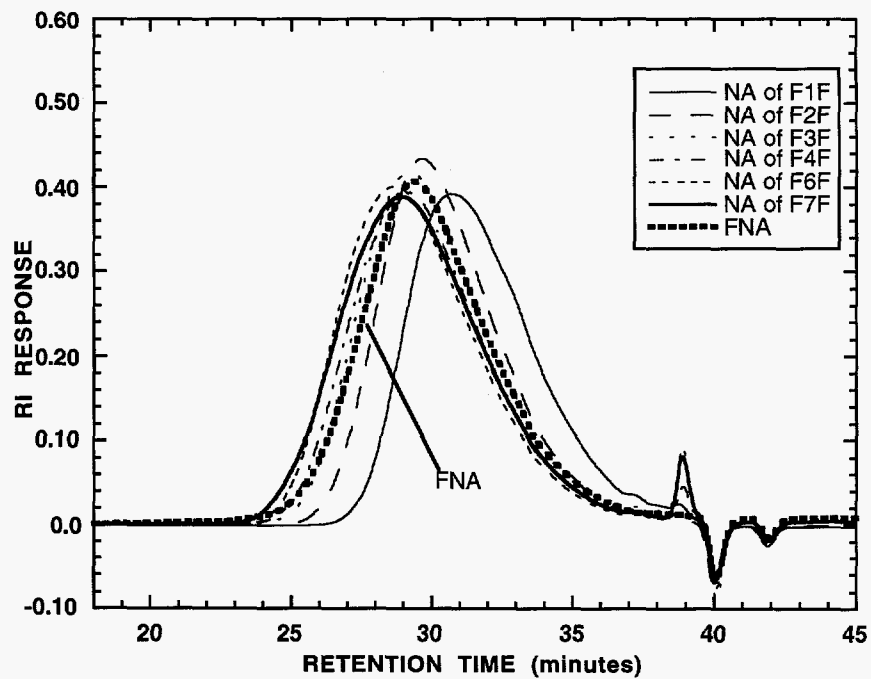


Figure 4-14. GPC spectra of various NA derived from AAF-1.

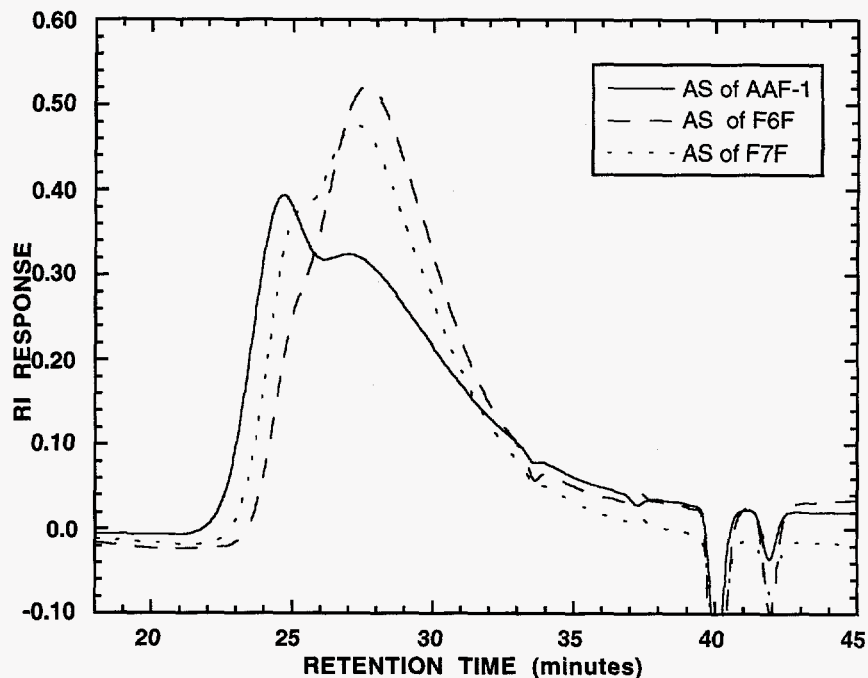


Figure 4-15. GPC spectra of various asphaltenes derived from AAF-1.

AAF-1. Asphaltenes from other fractions are not compared due to the difficulty of collecting enough material for GPC measurement because of the low asphaltene contents of these fractions. As seen from the figure, asphaltenes from F7F are larger than those from F6F. However, both of these two kinds of asphaltenes are smaller in molecular size than those from AAF-1. For reference, the GPC spectra of the saturate portions of the supercritical fractions are shown in Figure 4-16. The SA portion from F1F is the smallest, yet the SA fraction from F7F is not the largest. Instead, all of the SA portions from F2F to F7F are very close.

Oxidation Kinetics of Supercritical Fractions

The aging conditions listed in Table 4-2 were used in the aging experiments of the supercritical fractions. From the compositional analysis of the supercritical fractions, it is reasonable to hypothesize that fractions F1F, F2F and F3F have reactivities comparable to naphthene aromatic fractions, while fractions F4F, F6F and F7F possess reactivities comparable

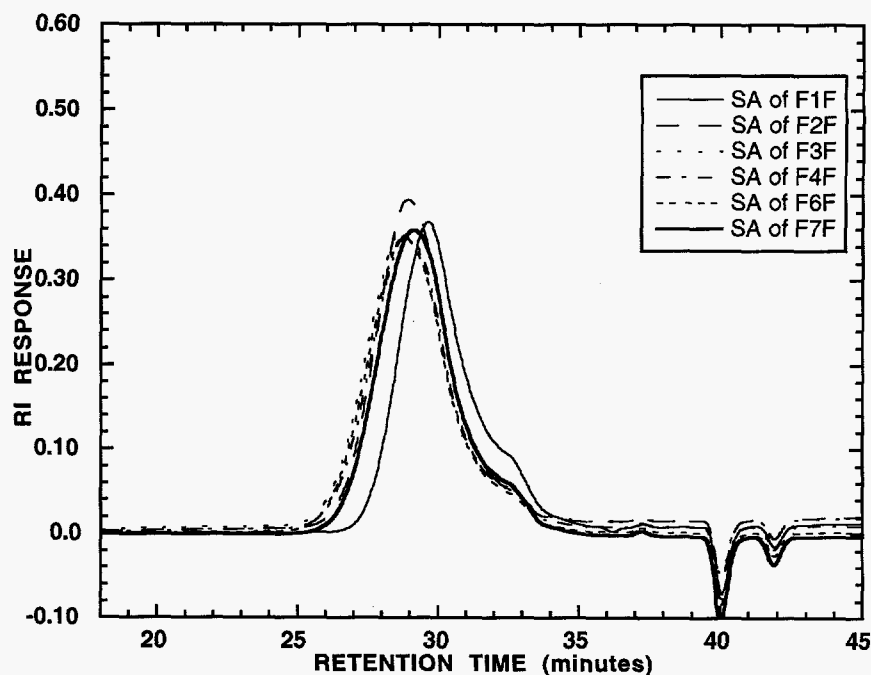


Figure 4-16. GPC spectra of various saturates derived from AAF-1.

to polar aromatic fractions. Because of this, the three light fractions (F1F, F2F and F3F) were aged along with the five NA fractions, while the three heavy fractions (F4F, F6F and F7F) were aged together with the five PA fractions.

Carbonyl area versus aging time is shown for F1F in Figure 4-17 and for F4F in Figure 4-18. As seen from the figures, carbonyl growth for a supercritical fraction follows a similar profile to that of a whole asphalt or a generic fraction. That is, the supercritical fractions undergo rapid oxidation initially, and then age at a constant rate for an extended period of time. The CA values of the unaged samples and the aging conditions used are also shown in the figures. The slope of each aging line is the constant aging rate, and the intercept of the line is CA_0 . As in the case for the whole asphalts, within experimental error, CA_0 is pressure dependent, but not temperature dependent. Carbonyl growth of other supercritical fractions have similar profiles.

Table 4-7 lists the constant aging rates of the supercritical fractions for the respective seven aging conditions. It is observed that for each of the conditions from C14 to C17, and

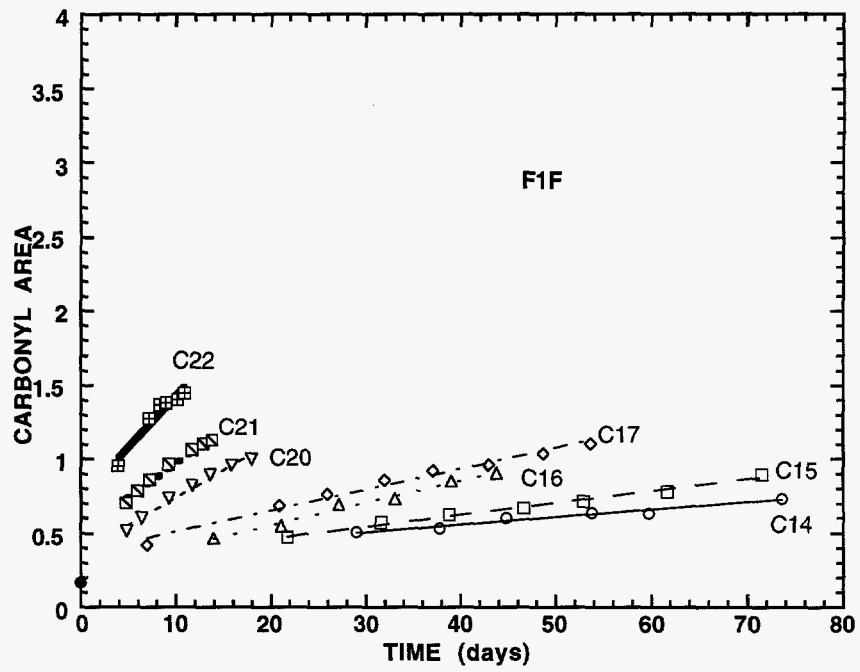


Figure 4-17. Carbonyl area vs. aging time for F1F.

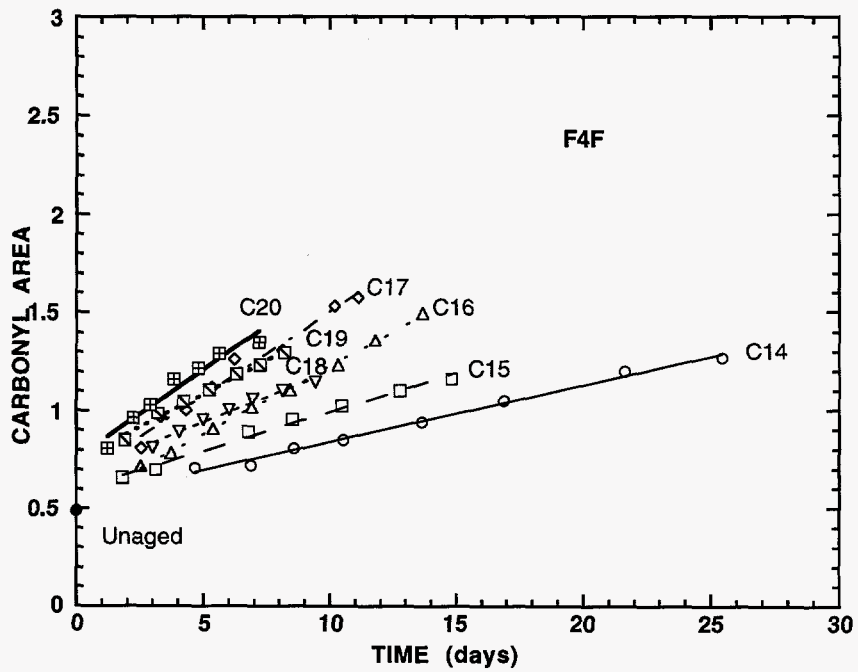


Figure 4-18. Carbonyl area vs. aging time for F4F.

Table 4-7. CA Growth Rate for Supercritical Fractions of AAF-1

	$R_{CA} \times 10^3$ (CA/day)						
	85	90	95	100	75	80	85
T (°C)	85	90	95	100	75	80	85
P (atm)	0.2	0.2	0.2	0.2	10	10	10
Fraction	C14	C15	C16	C17	C20	C21	C22
F1F	4.995	8.004	15.09	14.11	37.23	46.74	69.69
F2F	10.23	13.23	18.21	24.47	66.97	105.2	209.3
F3F	14.35	18.07	23.63	38.80	82.53	145.3	295.7

	$R_{CA} \times 10^3$ (CA/day)						
	85	90	95	100	85	90	95
T (°C)	85	90	95	100	85	90	95
P (atm)	0.2	0.2	0.2	0.2	10	10	20
Fraction	C14	C15	C16	C17	C18	C19	C20
F4F	28.92	39.93	69.72	85.19	52.19	67.96	90.83
F6F	25.26	44.97	62.57	85.92	72.03	87.53	100.7
F7F	34.67	53.34	72.95	93.00	91.05	112.0	142.6

also for C20, the oxidation rate increases from F1F to F7F except for several points due to experimental error. For conditions C21 and C22, the rate increases from F1F to F3F. For conditions C18 and C19, the rate increases from F4F to F7F. In summary, for the same aging condition, aging rate increases with fraction number. Using these rate data and the corresponding temperatures and pressures in Table 4-2, a linear regression was performed for Equation (3-1) to obtain the kinetic parameters of the supercritical fractions. The α and E values of the supercritical fractions are given in Table 4-8. For comparison, the α and E values of AAF-1, FNA and FPA are also listed.

Using the pressure reaction order data in Table 4-8, the aging rates at pressures other than 0.2 atm can be converted to corresponding rates at 0.2 atm. The Arrhenius plots at 0.2 atm oxygen pressure can then be constructed. Figure 4-19 shows the Arrhenius plots for the supercritical fractions F1F to F7F. The rate of F1F at condition C16 is abnormally high and

Table 4-8. Kinetic Parameters of the Supercritical Fractions of AAF-1

	α	E (kJ/mol)		α	E (kJ/mol)
F1F	0.450	62.5	F4F	0.300	76.0
F2F	0.518	71.3	F6F	0.354	72.0
F3F	0.511	80.7	F7F	0.356	64.5
FNA	0.471	88.1	FPA	0.381	80.0
AAF-1	0.364	85.4			

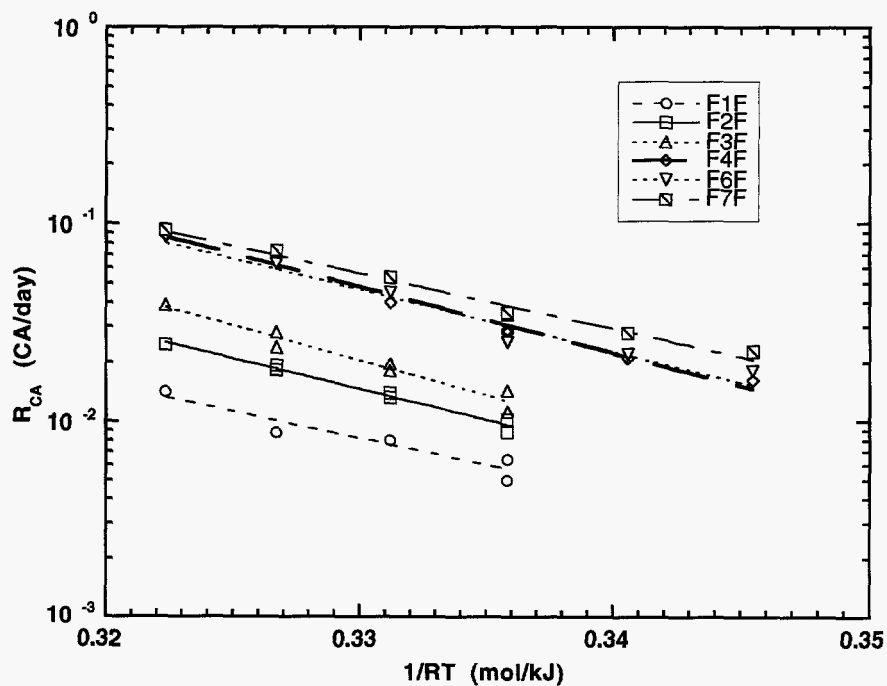


Figure 4-19. Oxidation rate vs. aging temperature for supercritical fractions.

was discarded. Within the temperature range of Figure 4-19, the rates increase from F1F to F7F. The rates of F4F are close to those of F6F for the same aging temperature. There is a noticeable gap between the rates of the group of F1F, F2F and F3F and these of the group of F4F, F6F and F7F. Although the activation energies of the six fractions are different, it is safe to say that even after extrapolation to temperatures as low as the road temperature, the rates of the fractions of the heavy group (F4F, F6F and F7F) would always be higher than those of the light group (F1F, F2F and F3F). In Figure 4-20, the Arrhenius plots of AAF-1, FNA and FPA are shown with those of the fractions. It is observed that the rates of FPA are among the highest while those of FNA are as low as F2F. The line representing AAF-1 lies between the light group and the heavy group. Particularly, F3F oxidizes much slower than AAF-1, and F4F oxidizes faster than AAF-1. This is important because after the analysis of physico-chemical correlations in the next chapter, we will conclude that after a certain amount of oxidation, F3F can be used as an asphalt binder with superior aging properties. Comparing Figure 4-20 to Figure 4-12, we conclude that for fractions from the same asphalt source, a relatively higher molecular size distribution indicates a relatively higher reactivity.

Table 4-9 shows the average initial jump $CA_0 - CA_{\text{unaged}}$ for the supercritical fractions at different pressures. For comparison, the values for AAF-1, FNA and FPA are also listed. For each fraction, the initial jump increases with aging pressure. The initial jump of F4F at 0.2 atm is unusually low and is explained by experimental error. At the same aging pressure (0.2 atm or 10 atm), the initial jump values of the supercritical fractions are between the values of FNA and FPA. At a pressure of 10 atm, a general trend is observed that the initial jump increases with fraction number. This reflects the fact that the polar aromatics content increases with fraction number and that the polar aromatics portion of an asphalt binder is the major part associated with initial jump. However, due to the scatter in the data, the trend is not obvious for the pressures of 0.2 atm and 20 atm.

Compositional Dependence of Asphalt Oxidation

Aging rates measured for the aromatics/saturates/asphaltenes blends are listed in Table 4-10 (Lin, 1995). Materials in the first column were all aged at 372.0 K (210°F). These

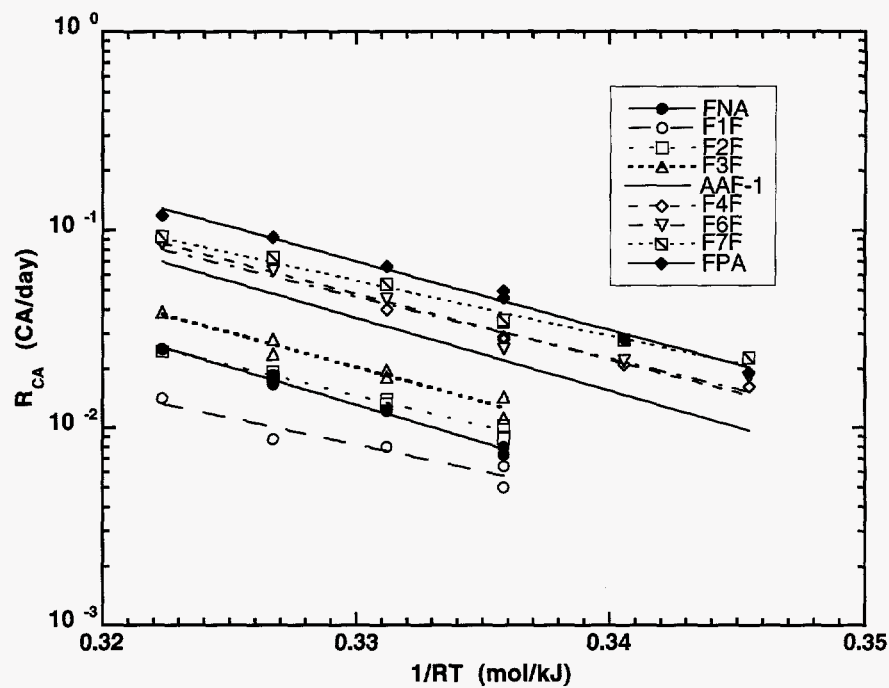


Figure 4-20. Oxidation rate vs. aging temperature for AAF-1 fractions.

Table 4-9. $CA_0 - CA_{\text{unaged}}$ for Supercritical Fractions of AAF-1, AAF-1 Generic Fractions and AAF-1 Whole Asphalt

	Pressure (atm)		
	0.2	10	20
AAF-1	0.339	--	0.757
FNA	0.096	0.112	0.237
F1F	0.155	0.271	0.567
F2F	0.227	0.210	0.451
F3F	0.173	0.205	0.317
F4F	0.092	0.237	--
F6F	0.122	0.374	--
F7F	0.154	0.489	--
FPA	0.419	0.709	--

**Table 4-10. Oxidation Rates of the Aromatics/Saturates/Asphaltenes Blends
of Four Asphalts at Three Temperatures and Pressure 0.2 atm**

Material	T (°F)	$R_{CA} \times 10^3$ (CA/day)	Material	T (°F)	$R_{CA} \times 10^3$ (CA/day)
AR*	210	37.51	AR	190	16.60
AR.SA7	210	34.43	AR.SA7	190	16.01
AR.SA15	210	28.32	AR.SA15	190	12.92
AR.SA20	210	24.11	AR.SA20	190	11.20
AR.AS7	210	44.05	AR	200	23.23
AR.AS7.SA7	210	44.11	AR.SA7	200	21.20
AR.AS7.SA15	210	39.25	AR.SA15	200	16.53
AR.AS15	210	59.07	AR.SA20	200	11.41
AR.AS15.SA7	210	51.27			
AR.AS15.SA15	210	45.21	DR	190	14.09
			DR.SA7	190	14.48
DR	210	36.53	DR.SA15	190	13.81
DR.SA7	210	31.70	DR.SA20	190	11.10
DR.SA15	210	25.43	DR	200	25.01
DR.SA20	210	27.61	DR.SA7	200	17.03
			DR.SA15	200	16.00
FR	210	64.39	DR.SA20	200	15.67
FR.SA7	210	55.51			
FR.SA15	210	50.32	FR	190	26.71
FR.SA20	210	42.85	FR.SA7	190	25.38
FR.AS15	210	71.94	FR.SA15	190	21.59
FR.AS15.SA7	210	62.23	FR.SA20	190	21.60
FR.AS15.SA15	210	47.52	FR	200	30.00

Table 4-10. (Continued)

Material	T (°F)	R _{CA} × 10 ³ (CA/day)	Material	T (°F)	R _{CA} × 10 ³ (CA/day)
GR	210	78.28	FR.SA7	200	35.07
GR.SA7	210	65.50	FR.SA15	200	31.81
GR.SA15	210	63.71	FR.SA20	200	32.00
GR.SA20	210	52.74			
GR.AS7	210	78.10	GR	190	36.62
GR.AS7.SA7	210	78.86	GR.SA7	190	29.10
GR.AS7.SA15	210	73.35	GR.SA15	190	30.80
GR.AS15	210	104.3	GR.SA20	190	25.79
GR.AS15.SA7	210	80.67	GR	200	44.90
GR.AS15.SA15	210	79.46	GR.SA7	200	49.03
			GR.SA15	200	60.00
			GR.SA20	200	41.92

* AR represents AAA-1 aromatics, AR.SA7 represents blend of AAA-1 aromatics with 7% saturates. Likewise, FR is AAF-1 aromatics, and FR.AS15.SA7 is the blend of AAF-1 aromatics with the addition of 15% asphaltenes and 7% saturates. Other samples follow a similar format. The four asphalts are AAA-1, AAD-1, AAF-1 and AAG-1.

include aromatics of AAA-1, AAD-1, AAF-1 and AAG-1 as well as blends of each asphalt's aromatics with controlled levels of saturates and asphaltenes of the same asphalt. Materials in the fourth column were aged at both 360.9 K (190°F) and 366.5 K (200°F). These include aromatics from four asphalts and blends of the aromatics with three levels of saturates of the same asphalt. With the varying levels of both saturates and asphaltenes, it would be an enormous effort to conduct a kinetic study under the conditions applied to the PA and NA fractions. The objective of this set of experiments was not to obtain the kinetic parameters of the blends, but to identify the effects of saturates and asphaltenes on the oxidation of the whole asphalt by comparing oxidation rates. Also, because measurement errors in the CA values are unavoidable and the rates are the slopes of CA versus time, more reliable information can be

obtained by comparing the aging rates before and after saturates/asphaltenes addition as a group rather than by using a single data point.

Figure 4-21 shows the effect of the addition of saturates on the oxidation rate. In the figure, R_{mea} represents the measured aging rate of an aromatics/saturates or aromatics/asphaltenes/saturates blend at a certain aging condition. R_{cal} represents the aging rate of the same blend, calculated from the corresponding aromatics or aromatics/asphaltenes blend, with the assumption that the addition of saturates only has a dilution effect. All the possible cases of comparison in Table 4-10 are included. For example, R_{mea} of AR.SA7 at 360.9 K (190°F) is 16.01×10^{-3} (measured). At that temperature, R_{cal} for AR.SA7 is 93% of the measured rate of AR (16.60×10^{-3}), which means that $R_{cal} = 93\% \times 16.60 \times 10^{-3}$. Likewise, R_{mea} for AR.AS7.SA15 at 372.0 K (210°F) is 39.25×10^{-3} . At the same temperature, R_{cal} for AR.AS7.SA15 is 85% of the measured rate of AR.AS7 (44.05×10^{-3}), which corresponds to $85\% \times 44.05 \times 10^{-3}$. For all the three levels of saturate addition, the percent differences in aging rates are randomly distributed around 0%. The deviation from the 0% line is due to measurement error. Thus, it can be concluded that within experiment error, for saturate addition, any effect other than dilution is negligible.

Data in Table 4-10 can also be used to study the effect of asphaltene addition. Figure 4-22 compares the aging rate of an aromatics/saturates/asphaltenes blend to that before the addition of asphaltenes. For example, the three open circles in the figure are for AAA-1 with 7% asphaltene addition. The values were obtained by comparing the oxidation rates of three pairs of blends. They are (AR, AR.AS7), (AR.SA7, AR.AS7.SA7) and (AR.SA15, AR.AS7.SA15). In each of these three pairs, the second element is a mixture of the first element and 7% asphaltenes. So the rate of the first element is R_b , while the rate of the second element is $R_{b,as}$. It is seen from the figure that, except for two points which are close to 0%, all the other points consistently show an increase in aging rate after the addition of asphaltenes. Furthermore, it is noticed that for the same asphaltene level, AAA-1 shows a more significant increase in rate than AAG-1 and AAF-1, which means that the extent of rate enhancement by asphaltene addition is asphalt dependent. For AAF-1, within experimental error, the effect of asphaltene addition is almost negligible. For AAA-1 and AAG-1, a higher level of asphaltene

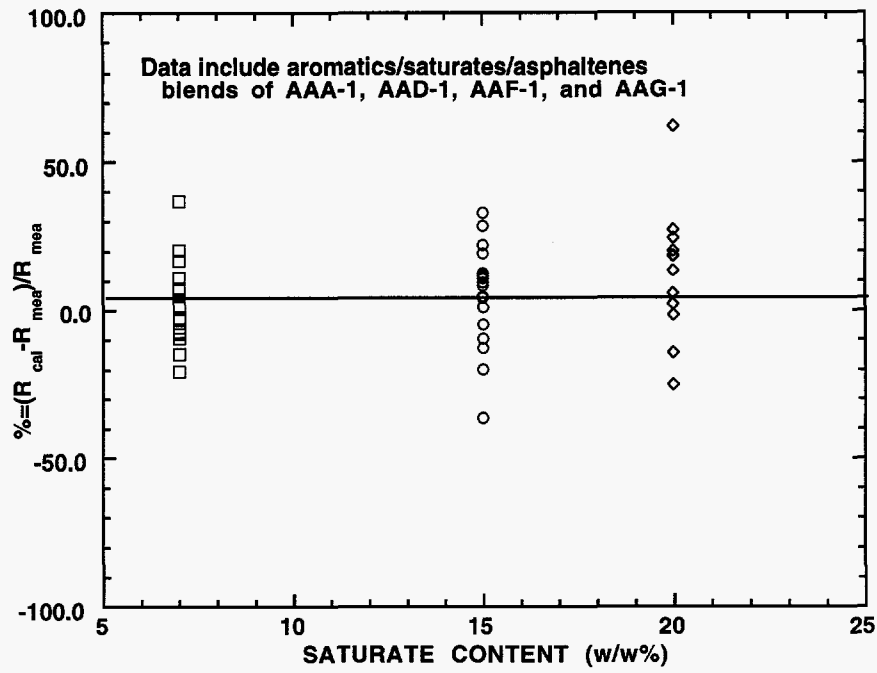


Figure 4-21. The effect of saturate addition on the oxidation rate.

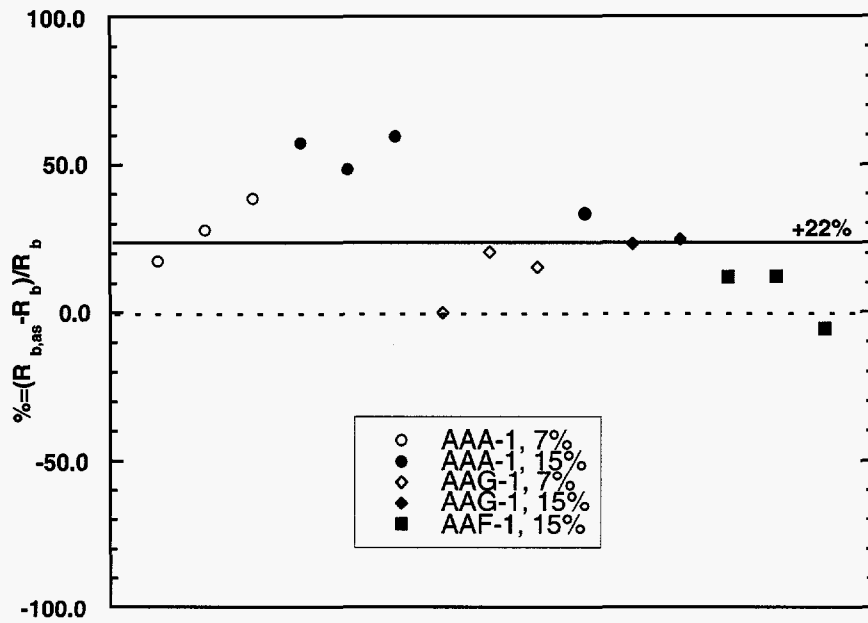


Figure 4-22. The effect of asphaltene addition on the oxidation rate.

content results in a higher rate. The increase in aging rate with asphaltene addition indicates that either asphaltenes are catalyzing the oxidation of PA and NA fractions, or asphaltenes are being oxidized themselves.

The fact that asphaltene content raises aging rates is again demonstrated in Figure 4-23. In this figure, aging rates of aromatics at three aging temperatures and 0.2 atm are compared with those of their parent asphalts. Thus this figure shows that the aging rates of aromatics are almost always no higher than those of their parent asphalts. Because, chemically the difference between aromatic fractions and their parent asphalts is that asphalts contain asphaltenes and saturates while aromatic fractions do not, and the effect of saturates is dilution only, the occurrence of higher rates for the whole asphalts can only be explained by the effect of the asphaltenes. Furthermore, as a group, the three points of AAF-1 are closer to the line, which indicates again that the effect of asphaltene addition is less significant for this asphalt. It may also be concluded that AAA-1 and AAD-1 have the most noticeable effects of asphaltene addition.

Interaction between a PA fraction and NA fraction is illustrated in Figure 4-24. In this figure, calculated aging rates of aromatics are compared to those measured from the aging rates of PA and NA fractions of the same asphalt. R_{mea} is calculated from rates of PA and NA fractions, and the composition data in Table 4-11, assuming that the aging of NA and PA fractions is additive. Since the PA and NA fractions were aged at temperatures different from those at which the aromatics were aged, the kinetic data of the PA and NA fractions in Table 4-4 were used to obtain interpolation values for their rates at the three temperatures (360.9, 366.5 and 372.0 K). Figure 4-24 displays that R_{cal} is consistently larger than R_{mea} by an average of 20%. This suggests that PA and NA fractions age faster in a separated state than in a mixed state. An explanation may be found in the colloidal theory of asphalts, in which the NA fractions would tend to surround the PA portion and thus reduce the accessibility of the reaction sites in the PA portion. As demonstrated in Figures 4-8 and 4-20, the PA portion reacts more easily than the NA portion. This blocking of PA reaction by NA portion results in a net decrease in the aging rate.

As discussed above, other than the fact that saturates only have a dilution effect, the

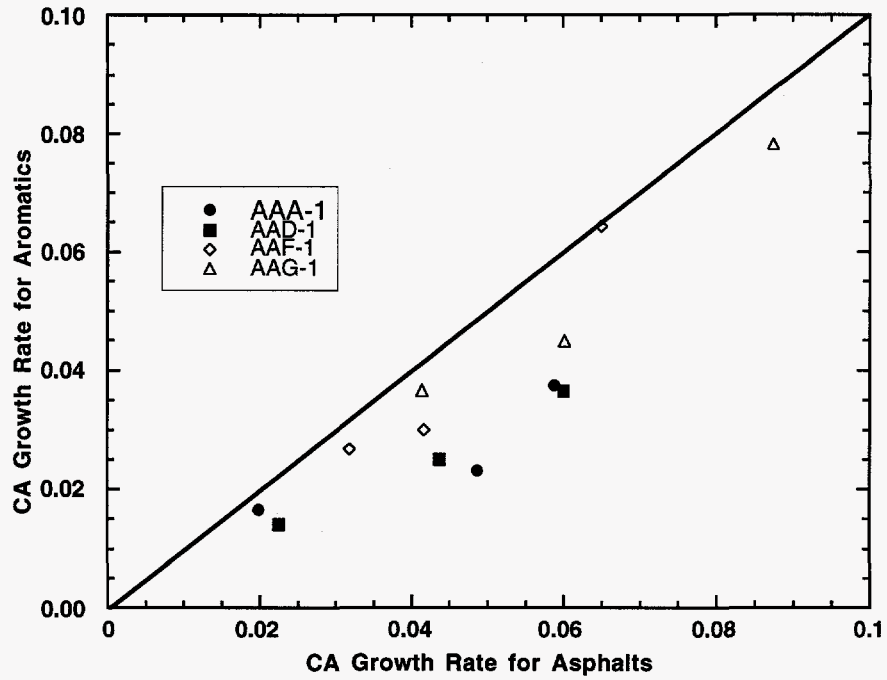


Figure 4-23. CA growth rates of whole asphalts and aromatics fractions.

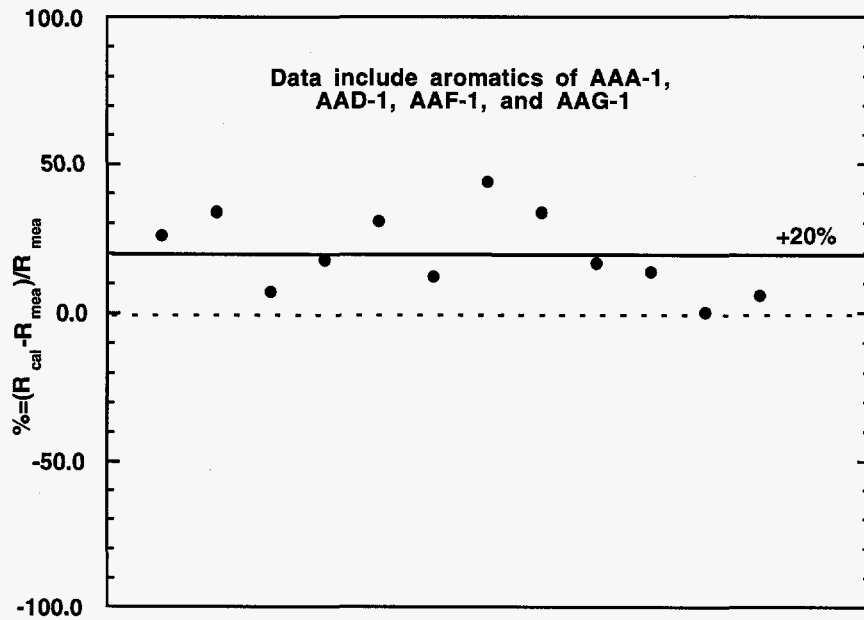


Figure 4-24. CA growth rates of aromatics measured and calculated.

Table 4-11. Contents of NA and PA in Aromatics Fractions of SHRP Asphalts

Asphalt	Naphthene Aromatics (w/w%)	Polar Aromatics (w/w%)
AAA-1	58.6	41.4
AAD-1	55.1	44.9
AAF-1	57.5	42.5
AAG-1	44.0	56.0

other individual fractions play complicated roles in the oxidative aging of an asphalt. The asphaltenes may increase the aging rate while the PA and NA fractions may interact with each other, resulting in an impedance of PA oxidation. It is very likely that interactions between any combination of the asphaltenes, the PA fraction and the NA fraction would have effects on the aging rate of the whole asphalt. All these effects would interact in a temperature-dependent pressure-dependent manner, and thus the kinetic characteristics of the pure generic fractions do not lead simply to the kinetic characteristics of the whole asphalt.

Summary

During oxidative aging, PA and NA fractions as well as supercritical fractions undergo carbonyl growth profiles similar to those of the whole asphalts, that is, a constant rate region is approached after an initial, more rapid rate period. Also, as in the case of whole asphalts, the $CA_0 - CA_{\text{unaged}}$ value for each fraction is pressure dependent, but not temperature dependent.

By measuring the aging rates at a combination of multiple temperatures and pressures, the kinetic parameters of asphalt generic fractions and supercritical fractions were measured.

The kinetic characteristics of an asphalt are determined by the kinetic characteristics of its fractions as well as the interactions between the fractions. The PA fraction of an asphalt ages much faster than its NA fraction. Saturates have only a dilution effect on asphalt oxidation. Asphaltenes may increase the oxidation rate. This means that asphaltenes either oxidize themselves, or they are catalyzing the oxidation of PA and NA fractions. PA and NA fractions age faster in a separated state than in a mixed state.

For supercritical fractions, reactivity increases with the fraction number. This is not only because the heavier fractions contain more polar aromatics, but also because the polar aromatics portion of a heavier supercritical fraction is more reactive than that of a lighter supercritical fraction.

For the fractions from the same asphalt source, the molecular size distribution can be used to indicate the reactivities of the fractions. However, for fractions from different asphalt sources, no correlation exists between the molecular size distribution and the reactivity.

CHAPTER 5

PHYSICO-CHEMICAL CORRELATIONS OF ASPHALT FRACTIONS

Having studied the compositional dependence of the reactivity of an asphaltic material in the last chapter, we now investigate the compositional dependence of the physico-chemical correlations. As pointed out earlier, the age hardening of an asphaltic material is the combined result of the oxidation of the material and the deterioration in physical properties due to the chemical change caused by oxidation. Specifically, the viscosity increases because of the growth in carbonyl content. The slope of log viscosity plotted against the carbonyl area (CA) has been defined as the hardening susceptibility (HS) as in Equation (1-7a). More explicitly, at the measurement temperature 333.2 K (60°C), HS is expressed as:

$$HS_{60} = \frac{d \ln \eta^*_{0,60}}{dCA} \quad (5-1)$$

Lau et al. (1992) showed that HS is a characteristic property of each asphalt binder independent of the aging temperature below 386.2 K (113°C). In this chapter, the HS values of the NA and PA fractions of the five SHRP asphalts studied in the last chapter are obtained and compared to those of their parent asphalts, and the corresponding aromatic fractions when possible. The HS values of the six supercritical fractions of SHRP AAF-1 are also obtained.

To study the HS relationship for these fractions in more detail, the asphaltene content of the samples were measured to determine the asphaltene formation susceptibility, AFS, and viscosity-asphaltene content relationship for the fractions.

Equation (5-1) is expressed in terms of a dynamic viscosity measured at 333.2 K (60°C). To ensure good performance at low temperatures, the viscosity temperature susceptibility (VTS) must be considered. This is conveniently expressed by Equation (1-9):

$$\ln \eta^*_0 = A_{vis} + \frac{E_{vis}}{RT} \quad (1-9)$$

in which, E_{vis} , the viscosity activation energy, is used as a measure of VTS. Because E_{vis} is a material property, it is quite likely that E_{vis} will increase during oxidative aging. This would mean that the hardening susceptibility, HS, would become larger when measured at lower temperatures.

Hardening Susceptibility, HS

As discussed in Chapter 1, the hardening susceptibility, HS, is an important characteristic for a specific asphaltic material. It represents the material's tolerance to hardening due to carbonyl growth caused by oxidative aging. A lower value of this parameter implies a smaller increase in viscosity for the same amount of growth in carbonyl area, which is a favorable property. The results reported by Lau et al. (1992) and other numerous data accumulated in this lab have shown that this parameter is independent of aging temperature. However, the results in Chapter 3 demonstrate that it is dependent on aging pressure. Because road aging is at an ambient pressure of 0.2 atm oxygen, it was decided that for future reference, additional HS measurements would be for samples aged at 0.2 atm. HS values at other pressures may be measured when the pressure dependence becomes the objective of a study.

Figure 5-1 shows the HS relationships for the naphthene aromatic fractions of the five SHRP asphalt. The slopes of the regression lines are the hardening susceptibilities. The measurement temperature of the data in Figure 5-1 is 333.2 K (60°C), so the HS values in the figure are actually HS_{60} . The HS relationship is shown for the five polar aromatic fractions in Figure 5-2 at the measurement temperature of 333.2 K (60°C).

The HS values of the NA, PA, and aromatics fractions as well as those of the original whole asphalts are listed in Table 5-1. For each asphalt, the NA fraction has a smaller HS value than the PA fraction. The aromatic fraction has a HS value between the two. This is reasonable because the aromatic fraction is a mixture of polar aromatics and naphthene aromatics. On the other hand, except for AAG-1, the HS for each of the whole asphalts is larger than those for its PA fraction, NA fraction and aromatic fraction. The exception, AAG-1, however, has a value of HS that is very close to the values for the aromatics and for the whole asphalt. For other asphalts, the reason for the HS value of the whole asphalt being higher than those of its fractions is that the whole asphalt contains saturates and asphaltenes. Although the viscosity of an asphaltic material is reduced by the addition

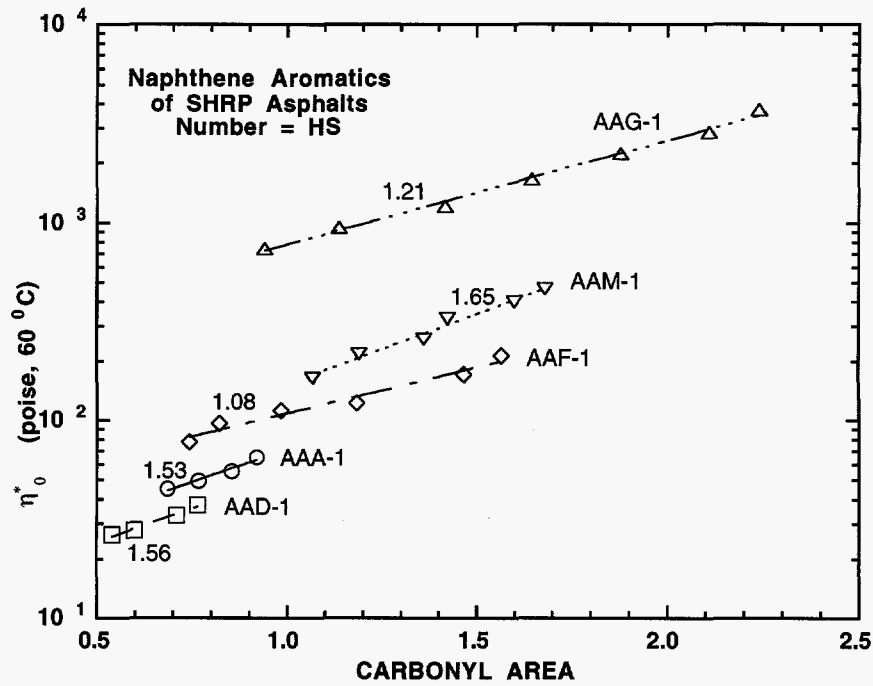


Figure 5-1. Hardening susceptibility of NA fractions.

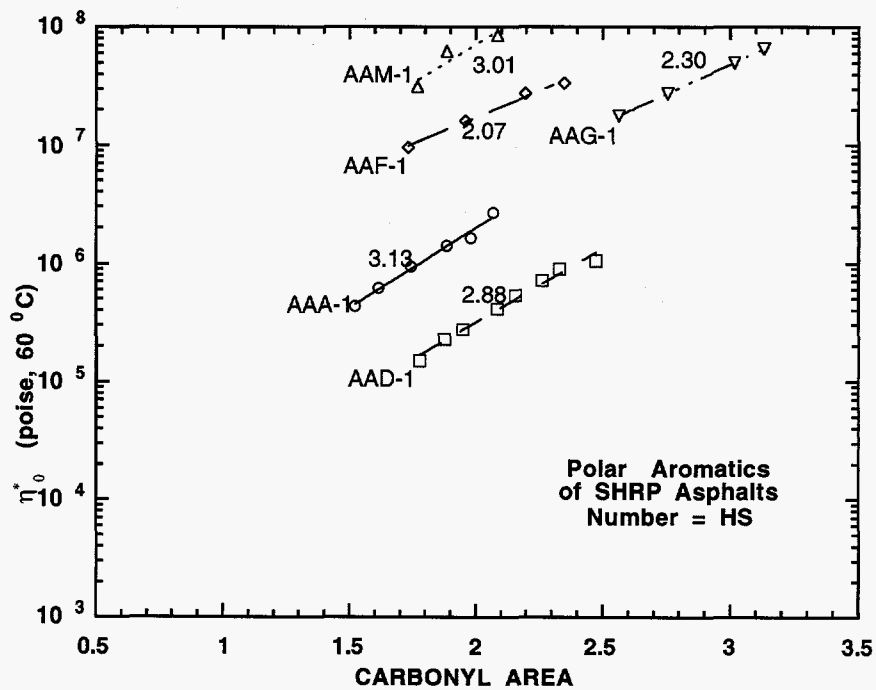


Figure 5-2. Hardening susceptibility of PA fractions.

Table 5-1. Hardening Susceptibilities HS of SHRP Asphalts and Their NA, PA and Aromatics Fractions.

Asphalt	Naphthene Aromatics	Polar Aromatics	Aromatics	Whole Asphalt
AAA-1	1.53	3.13	1.73	6.93
AAD-1	1.56	2.88	2.34	8.00
AAF-1	1.08	2.07	1.60	4.47
AAG-1	1.21	2.30	1.58	1.35
AAM-1	1.65	3.01	--	4.91

of saturates, this may not be true for HS (Lin et al., 1996). On the contrary, because of the incompatibility between the saturates and asphaltenes, the amount of saturates will increase the hardening susceptibility in the presence of asphaltenes, such as in the case of a whole asphalt. Unlike the PA, NA and aromatic fractions, the whole asphalt contains both saturates and asphaltenes. During oxidative aging, the asphaltene content increases along with carbonyl growth. The presence of the saturates and asphaltenes in the original unaged asphalt renders the material intolerant to newly produced asphaltenes, and thus results in a larger HS than its fractions. Furthermore, for different asphalts, HS values vary much more for whole asphalts than for their fractions. There are two reasons for this. First, HS values for NA fractions, PA fractions, and aromatics are already low. And secondly, there is a considerable variation in asphaltene and saturate content for the whole asphalts.

Figure 5-3 compares the HS of AAF-1 whole asphalt with those of its fractions, including its NA, PA and five supercritical fractions, and aromatics. The data for F1F are not shown because this fraction is mostly saturates and very light aromatics, and is extremely soft. To accurately measure the viscosities of the aged and unaged samples of this fraction, a measurement configuration different from that used for other samples is required. Obviously, the whole asphalt has a much higher HS value than its fractions. This is entirely because of the presence of asphaltenes and saturates together in the whole asphalt. The HS values of the supercritical fractions generally increase with fraction number, as the content of polar aromatics increase and the content of naphthene aromatics decrease in the materials. Fraction F3F is an exception. However, the HS of F3F is still smaller than either

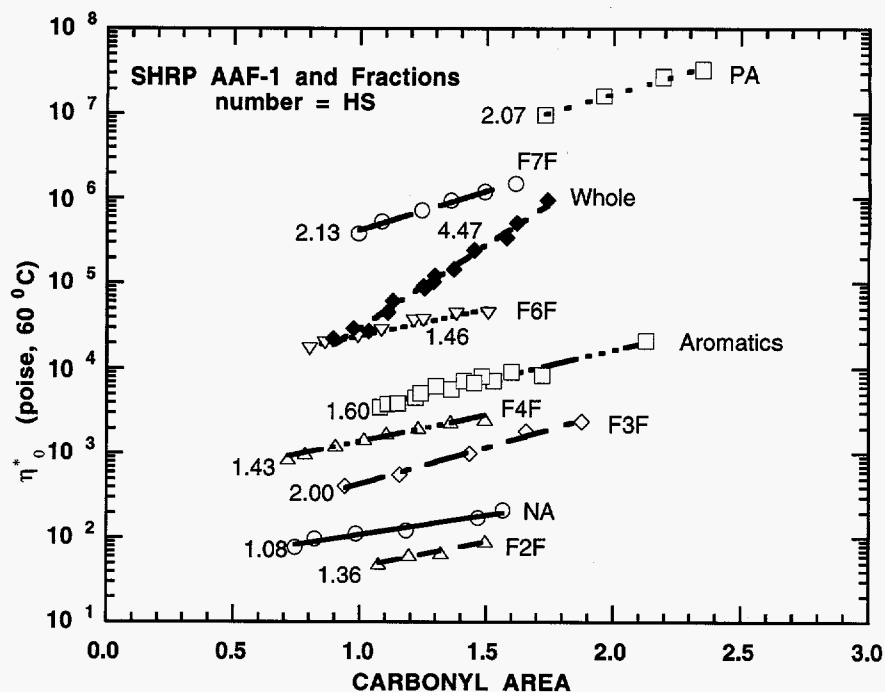


Figure 5-3. Hardening susceptibility of AAF-1 fractions.

the polar aromatics fraction or F7F, and lower than that of the whole asphalt. As discussed in Chapter 4, F3F has a lower reactivity than AAF-1. The combined effect would be that F3F has a much slower age hardening rate than AAF-1. F7F has a slightly larger HS value than the polar aromatics fraction because F7F not only is largely polar aromatics, but also contains a certain amount of asphaltenes. This indicates that for a mixture of NA and PA fractions to achieve a low HS value, more naphthene aromatics are needed than polar aromatics.

Figure 5-4 displays the change in HS values when different measurement temperatures are used. In fact, hardening susceptibility increases as measurement temperature decreases. It indicates that the viscosity is more sensitive to carbonyl growth for lower measurement temperatures. It further implies that for the same range of measurement temperature (298.2 to 346.7 K, 25 to 73.5°C in the figure), the difference between the viscosities at high temperatures and those at low temperatures will become greater as the material undergoes oxidation and the carbonyl area increases.

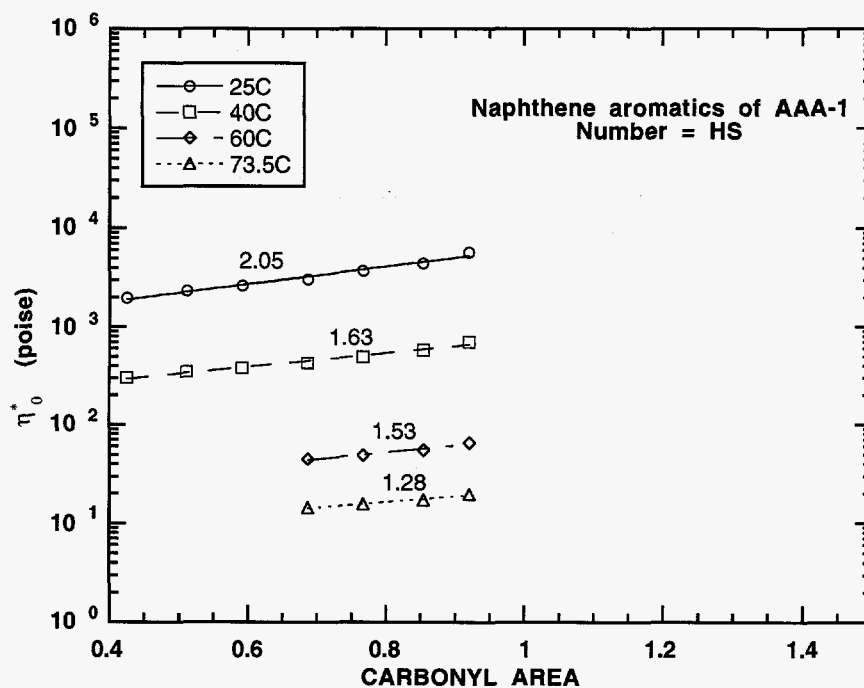


Figure 5-4. Hardening susceptibility of ANA at four temperatures.

This can be graphically observed from the Figure 5-4. The regression lines diverge as oxidative aging progresses, which is in the direction of increasing carbonyl area. The HS lines at two different temperatures are shown for the PA fraction of AAA-1 in Figure 5-5. Again, an increase in HS value for the lower measurement temperature and the divergence of the lines in the direction of increased CA are observed. Figures 5-4 and 5-5 demonstrate that the viscosity temperature susceptibility is an important characteristic property of asphaltic materials and needs further research.

Asphaltene Formation Susceptibility, AFS, and Viscosity-Asphaltene Relationship

Figure 5-6 shows the asphaltene-carbonyl area relationship for the five NA fractions. For each material, the asphaltene-formation susceptibility (AFS) is the slope of the line. The asphaltene-carbonyl area relationship is shown in Figure 5-7 for the five PA fractions. As seen from these two figures, naphthene aromatics have a significantly lower AFS value than polar aromatics of a given

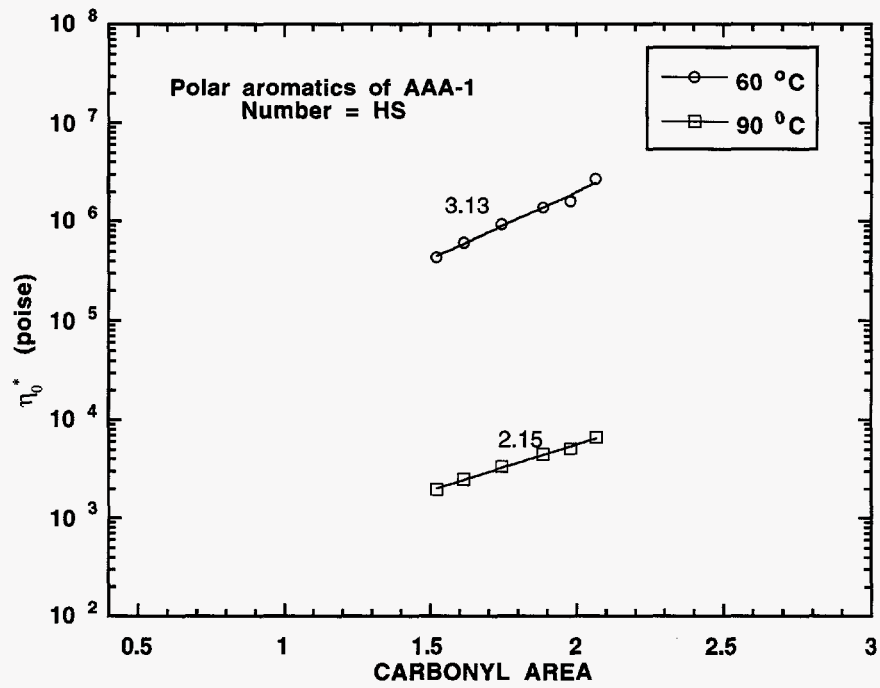


Figure 5-5. Hardening susceptibility of APA at two temperatures.

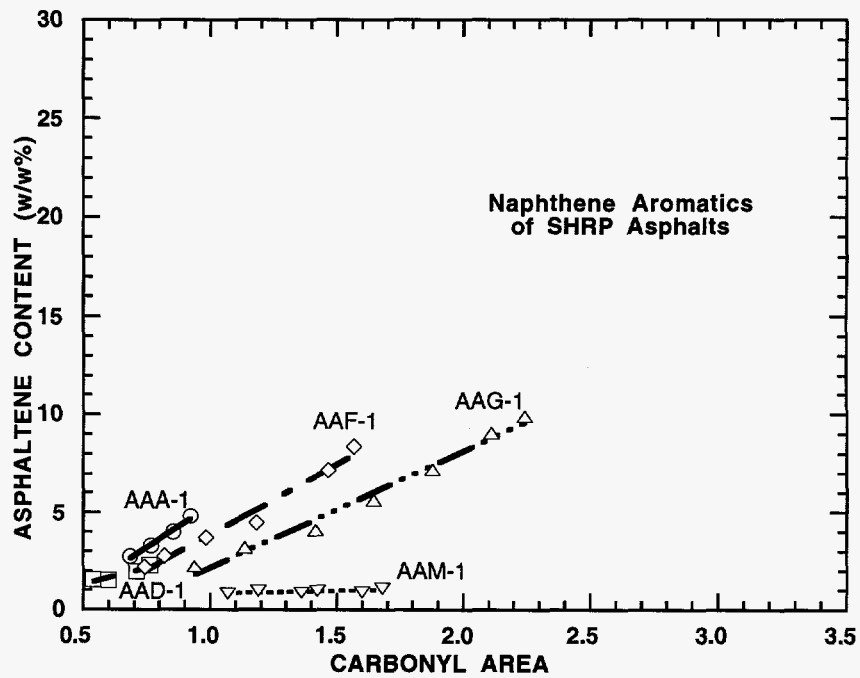


Figure 5-6. AFS for the five NA fractions.

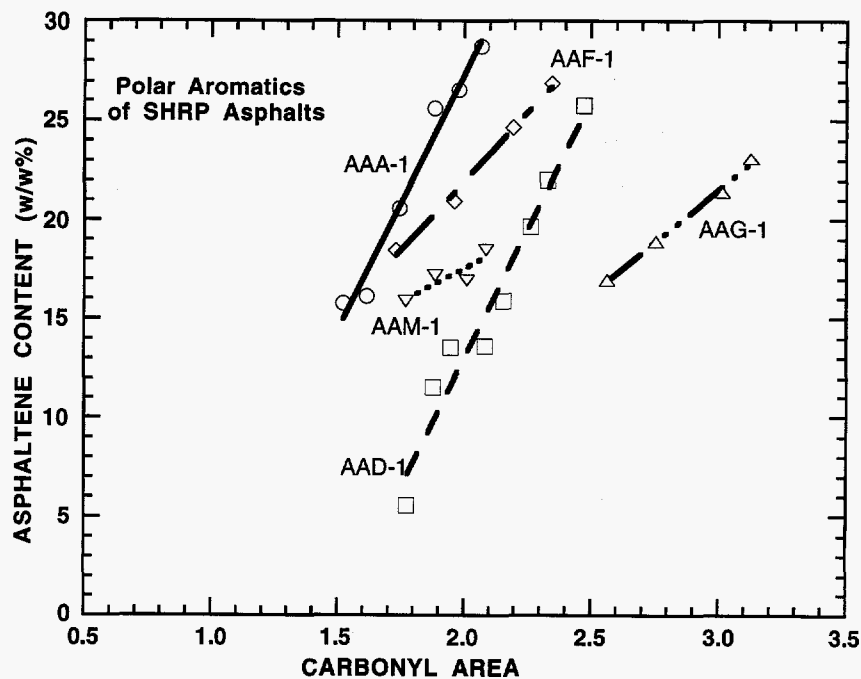


Figure 5-7. AFS for the five PA fractions.

asphalt. Asphalt AAM-1 is special in that both of its NA and PA fractions have a much lower AFS than others of the same kind of fraction (NA or PA). The explanation is that relatively fewer asphaltenes are produced during oxidation of MNA and MPA, although carbonyl growth still occurs. Thus, the oxidation product of MNA either still remains in the NA fraction or more likely becomes MPA. The oxidation product of MPA will largely be heavy PA, rather than asphaltenes. However, as displayed in Figures 5-1 and 5-2, the hardening susceptibilities of MNA and MPA are comparable to the fractions of other asphalts. This means that although the material produced during oxidation of MNA and MPA may not be asphaltenes, it is still a viscosity builder. On the other hand, the PA fractions of AAA-1 and AAD-1 have much larger AFS than the PA fractions of other three asphalts. Asphaltenes are more easily produced by these two PA fractions.

Table 5-2 lists the AFS values of the NA, PA, and aromatics fractions of the five asphalts. Also in the table are the values for the aromatic fractions calculated from the data of the NA and PA

Table 5-2. Comparison of Calculated and Measured AFS of Aromatics Fractions of SHRP Asphalts

Asphalt	Calculated Aromatics AFS ^a	Aromatics AFS ^a	Naphthene Aromatics AFS ^a	Polar Aromatics AFS ^a
AAA-1	15.80	15.13	8.72	25.83
AAD-1	13.62	19.72	3.44	26.12
AAF-1	10.04	11.75	7.25	13.82
AAG-1	8.57	9.55	5.99	10.59
AAM-1	3.75	--	0.26	6.75

^a Mass-weighted (see Table 4-11) sum of the measured NA AFS and PA AFS values

fractions of the same asphalt assuming that the AFS is additive. The composition data in Table 4-11 for the aromatic fractions in terms of contents of naphthene aromatics and polar aromatics are used in this calculation. The calculated values are lower than the measured values except for AAA-1, but, for this asphalt, the calculated and measured AFS for aromatics are close. Again, this can be explained by the relative reaction rate of the two pure fractions. As discussed in Chapter 4, the reaction rate of the polar aromatics fraction is higher than that of the naphthene aromatics fraction of the same asphalt. Therefore, during the aging of the aromatics fraction, despite the blockage effect discussed in Chapter 4, most of the carbonyl growth and consequently most of the asphaltene content increase comes from the polar aromatics portion. Thus, the AFS of an aromatic fraction is closer to that of polar aromatics.

Figure 5-8 shows the AFS (slope of asphaltene content vs. CA) for the fractions of asphalt AAF-1. A general trend of increase in AFS with fraction number is observed due to increasing content in polar aromatics.

Figure 5-9 is a plot of viscosity versus asphaltene content for the five naphthene aromatics fractions. The slopes of the regression lines represent the abilities of the aromatic media to dissolve the asphaltenes. In this report, the slope is called the solvation power parameter. A small solvation power parameter corresponds to a small increase in log viscosity for a given amount of asphaltene production and represents a strong solvation power. Lin et al. (1995a) used a modified Pal-Rhodes

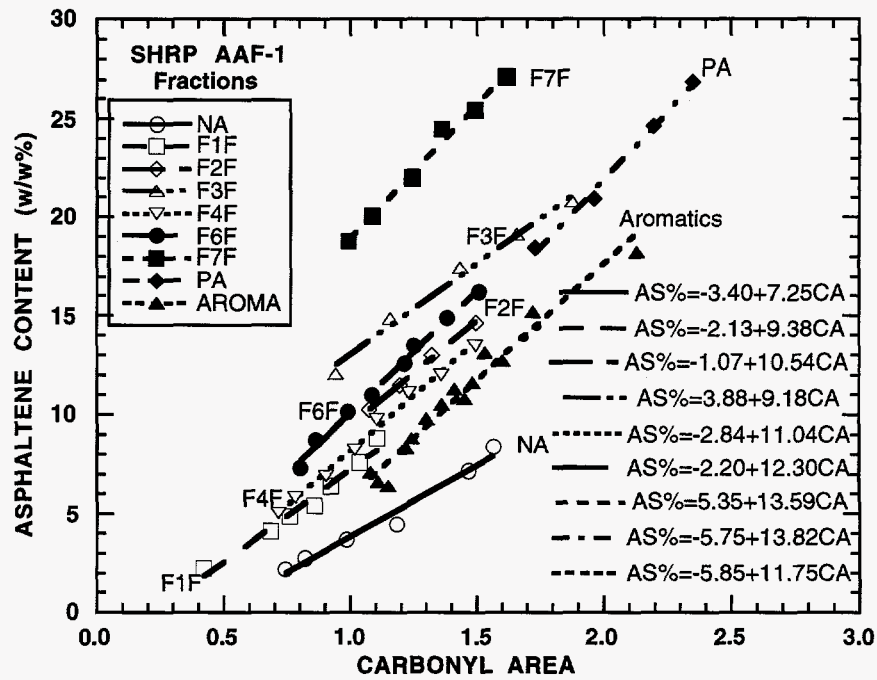


Figure 5-8. AFS (slope of asphaltene percentage vs. CA) for AAF-1 fractions.

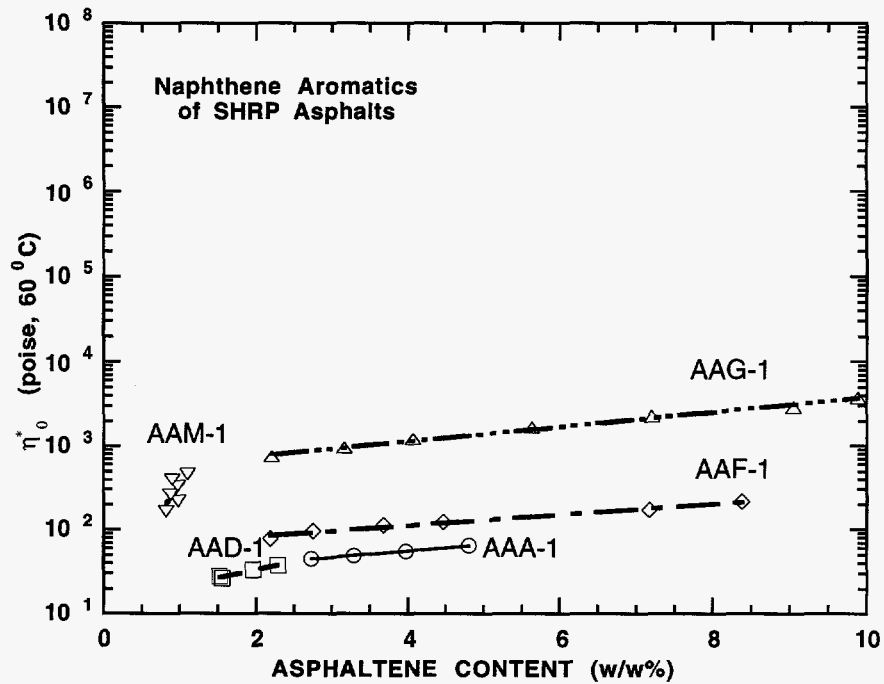


Figure 5-9. Viscosity vs. asphaltene content for NA fractions.

model to describe the effect of the asphaltene content on the viscosity. However, the range of asphaltene content was much larger in their study than that shown in Figure 5-9. The regression lines in Figure 5-9 can be viewed as local approximations of the modified Pal-Rhodes model. The viscosity-asphaltene content relationship is shown for the five PA fractions in Figure 5-10. Again, the NA and PA fractions of AAM-1 have relatively large solvation power parameters, because the heavy polar aromatics produced by the oxidation of MNA and MPA are not measured as asphaltenes. Nevertheless, these heavy polar aromatics are viscosity builders.

Table 5-3 lists the solvation power parameters of NA, PA and aromatics fractions of the five asphalts. It is noticed that for asphalts AAF-1 and AAG-1, the solvation power parameters of the three fractions are close. However, for asphalts AAA-1 and AAD-1, the solvation power parameters of the PA and aromatics fractions are close, but both are a smaller than those of the NA fractions. For these two asphalts, the PA fractions have a stronger solvation power (smaller solvation power parameter) than the NA fractions. There are many reasons for the solvation power parameter of the aromatic fraction to be close to that of the PA fraction. It is possible that the oxidation of the aromatics fraction is mostly the oxidation of its PA portion. Also, the aromatics fraction may possess a solvation power approximate to that of the pure PA fraction as long as it contains a sufficient amount of polar aromatics.

Figure 5-11 plots the viscosity versus asphaltene content for fractions of AAF-1. AAF-1 has nearly identical solvation power parameters for its NA, PA and aromatics fractions. All the solvation power parameters of the supercritical fractions of AAF-1 are close to these values, with F3F being an exception, which was also referred to in the discussion of the HS values of AAF-1 fractions.

From the analysis of the AFS and the solvation power parameters, it is seen that polar aromatics may have a stronger solvation power than naphthene aromatics, but naphthene aromatics have a much smaller AFS. As a combined effect, naphthene aromatic fractions have lower HS values than the polar aromatic fractions, which is desirable.

Viscosity-Temperature Susceptibility

In order to describe viscosity-temperature susceptibilities (VTS) of the fractions, the two-parameter Andrade equation, Equation (1-9), was used. Viscosities of a specific sample were

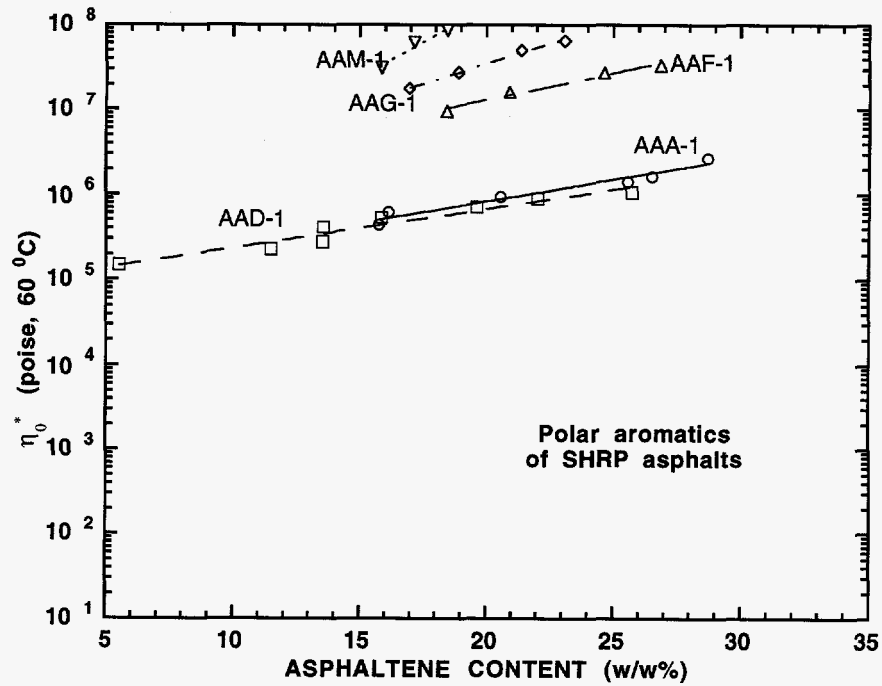


Figure 5-10. Viscosity vs. asphaltene content for PA fractions.

Table 5-3. Comparison of Solvation Power Parameters (SPP) of Fractions of SHRP Asphalts

Asphalt	Naphthene Aromatics SPP	Polar Aromatics SPP	Aromatics SPP
AAA-1	0.177	0.118	0.117
AAD-1	0.430	0.105	0.118
AAF-1	0.148	0.148	0.131
AAG-1	0.200	0.216	0.164
AAM-1	2.696	0.388	--

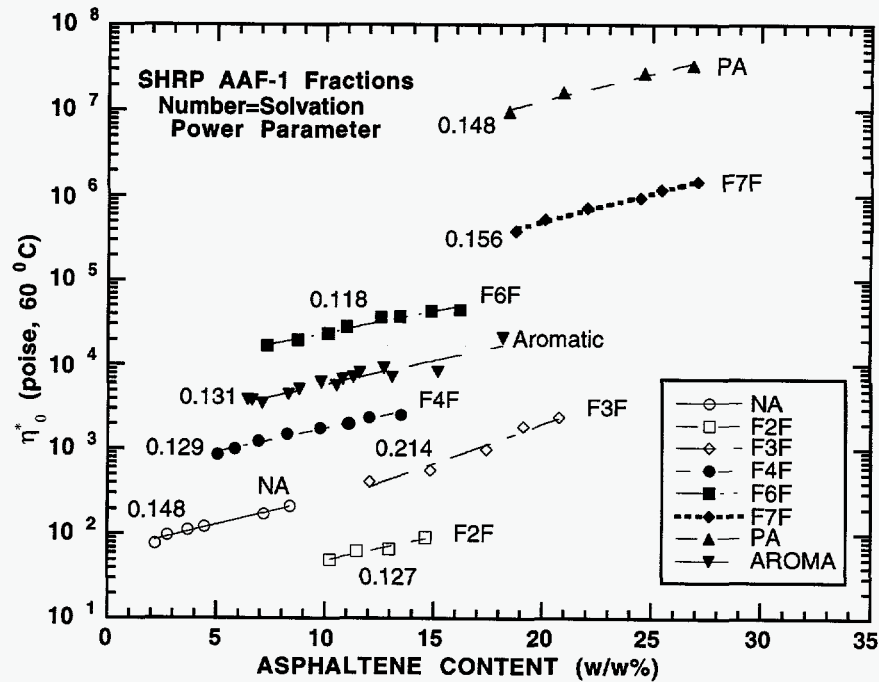


Figure 5-11. Viscosity vs. asphaltene content for the fractions of AAF-1.

measured at multiple temperatures to obtain its E_{vis} . A large E_{vis} of an asphaltic material means that its physical properties, particularly its viscosity, is sensitive to the environment temperature, which is not favorable. During the oxidative aging of an asphaltic material, both the carbonyl content and the asphaltene content increase progressively, resulting in the deterioration of its VTS properties. Figure 5-12 shows an increase in E_{vis} with respect to carbonyl growth for the NA fractions, PA fractions and aromatic fractions of the five asphalts. For all the fractions, the changes in E_{vis} during the aging experiment are around or below 20 kJ/mole. On the other hand, the differences between the E_{vis} of NA fractions of different asphalts may be as high as 50 kJ/mole. This indicates that the absolute value of E_{vis} is more important than its change due to oxidative aging. It is observed that E_{vis} of the NA fractions fall between 90 kJ/mole and 160 kJ/mole, while E_{vis} of the PA fractions fall between 170 kJ/mole and 260 kJ/mole. For each asphalt, the NA fraction has a much smaller E_{vis} than its PA fraction, with the aromatic fraction in between. This trend is again shown by Figure 5-13 where

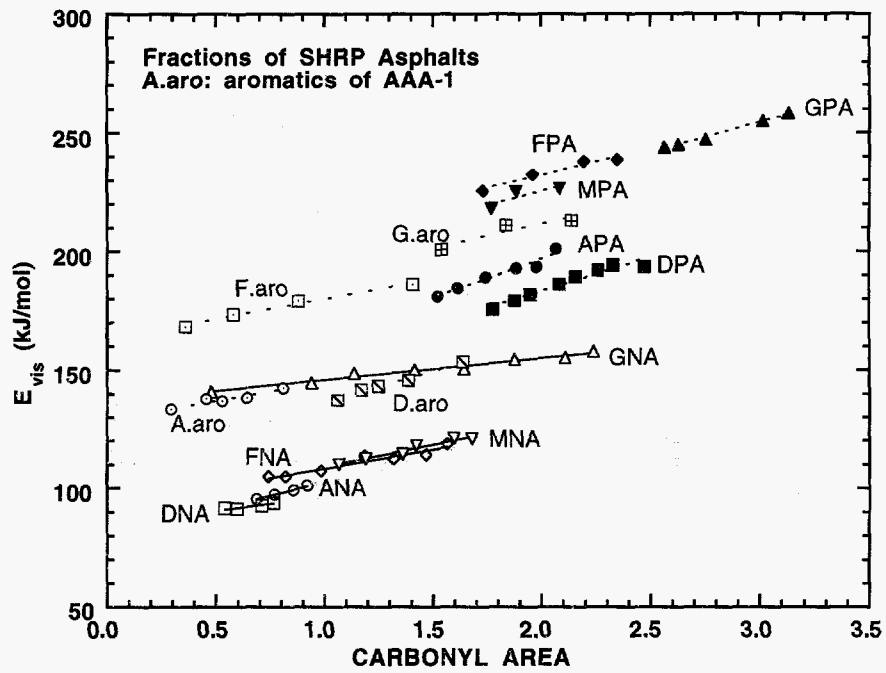


Figure 5-12. Viscosity activation energy vs. CA for asphalt fractions.

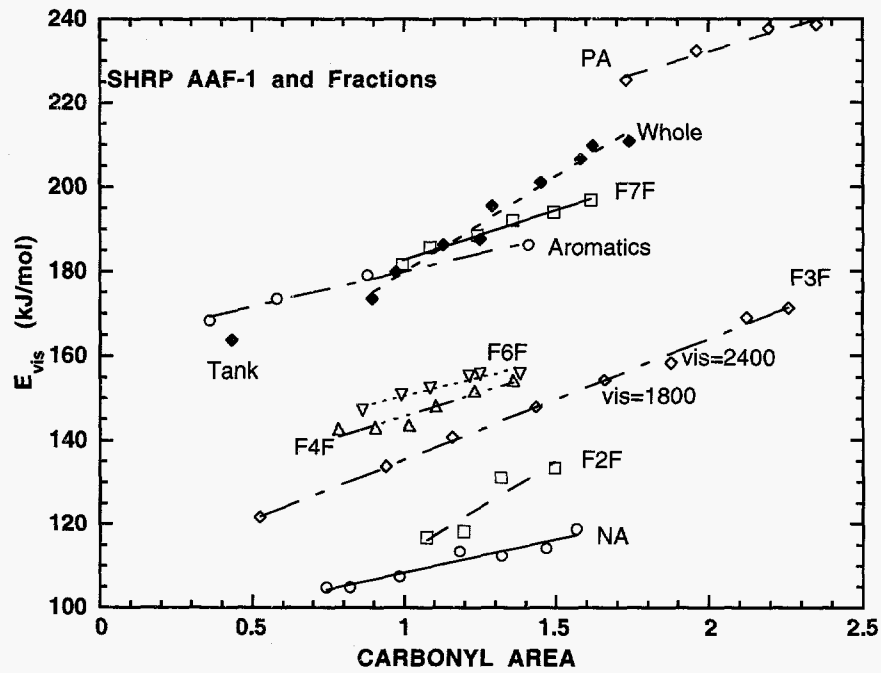


Figure 5-13. Viscosity activation energy vs. CA for AAF-1 fractions.

E_{vis} is plotted versus carbonyl area for AAF-1 fractions. As the fractions contain more polar aromatics, E_{vis} becomes larger. This means that a high content of naphthene aromatics is desirable. Particularly, when F3F is aged to a viscosity level of a typical AC-20 asphalt, its E_{vis} is lower than AAF-1 tank asphalt which is an AC-20. Furthermore, comparing AAF-1 whole asphalt and F3F, the former has a larger increase in E_{vis} with the same amount of carbonyl growth. This means, in terms of temperature susceptibility, the binder produced by oxidizing F3F to a specification viscosity level is better than the parent asphalt AAF-1. Recalling that F3F has a much lower HS and less reactivity than AAF-1, lower VTS is the third superior property possessed by F3F.

Figure 5-14 shows a remarkable relation between A_{vis} and E_{vis} in Equation (1-9). If true, this figure indicates the presence of a viscosity isokinetic temperature for all materials (a temperature at which all materials have the same viscosity value). The reason for the displacement between the polar aromatics line and the other lines is as follows: The polar aromatic fractions as well as fractions F6F and F7F are so hard after aging that the measurement of the low temperature viscosities becomes a

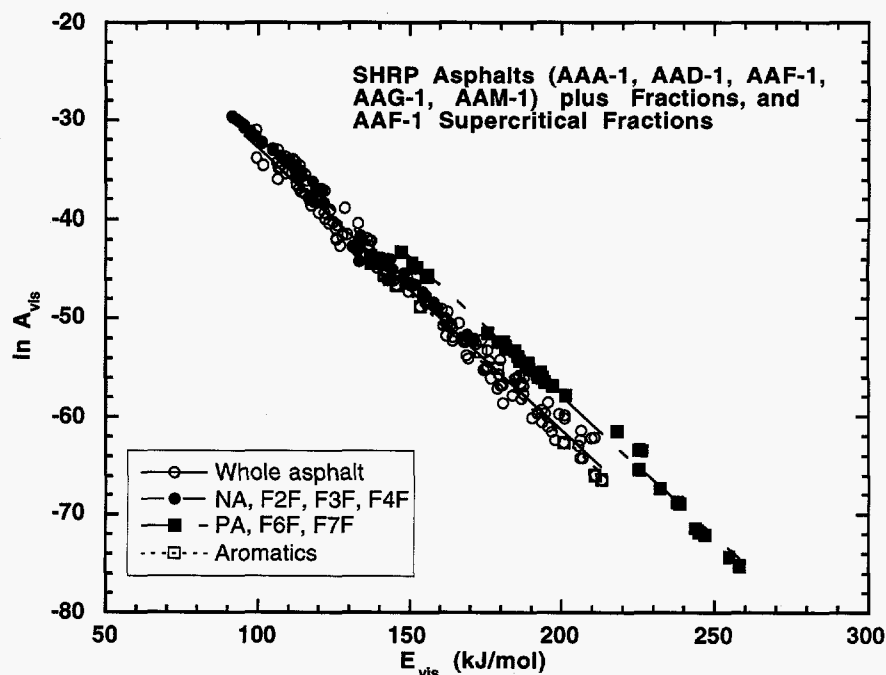


Figure 5-14. Correlation between viscosity model parameters.

problem. For these samples the range of measurement temperature was from 333.2 to 363.2 K (60 to 90°C) while for the other samples, the measurement temperature was from 283.2 to 363.2 K (10 to 90°C). Thus, the Andrade Equation is only an approximation with E_{vis} varying with temperature. The discrepancy resulting from the difference between the two temperature ranges is about 20 kJ/mole. Taking this bias into account, the discussion made on Figure 5-13 is still valid, that is, the PA fractions have much larger E_{vis} than the NA fractions.

Summary

For each asphalt, the hardening susceptibility HS of its NA fraction is smaller than that of the PA fraction, with that of the aromatics fraction being in between. All these fractions have much smaller HS than that of the parent asphalt. Supercritical fractions possess lower HS than the original asphalt.

The NA fraction has less solvation power than the PA fraction. However, the effect of a much smaller AFS overrides the effect of less solvation power. Furthermore, the aromatic fraction contains enough PA to yield a solvation power as strong as that of the PA fraction. For supercritical fractions, the AFS increases with fraction number.

In terms of viscosity, the PA fractions are much more sensitive to measurement temperature than the NA fractions. Aromatics fractions are in between. Most supercritical fractions possess E_{vis} 's lower than the whole asphalt, even after aging. Fraction F3F has a particularly desirable E_{vis} after being aged to the viscosity of an AC-20 asphalt. F3F has a much lower HS than the parent asphalt AAF-1.

CHAPTER 6

FURTHER DETAILS ON THE OXIDATION MECHANISMS OF ASPHALT BINDERS

This chapter contains the results of studies of asphalt oxidation mechanisms from two separate perspectives: one on the oxidation products of asphalt fractions, and the other on the uptake of oxygen by asphaltic materials undergoing aging as correlated to carbonyl growth. The materials used in both of these efforts are the asphalts and asphalt fractions studied in Chapters 3, 4, and 5.

In the study of the oxidation products of asphalt fractions, the objective was to clarify the compositional change of the Corbett fractions during aging, and the characteristics of the products from aged fractions. As discussed in the previous chapters, asphalt properties are the manifestations of its chemical composition. However, during the oxidative aging, in terms of Corbett composition, there is a shift from aromatics (either NA or PA) to asphaltenes. Thus, the asphalt binder is a dynamic system in the aging process. There may exist a favorable composition for a binder to possess desirable physical and chemical properties at the unaged state. But after oxidative aging the composition will be changed, and so will be the future performance. What needs to be considered for a superior binder in terms of compositional manipulation is the optimal initial composition which ensures a desirable performance during the service life. A study of the oxidation products of the fractions will give us better understanding of the interchange between the Corbett fractions during the aging process.

To accomplish such a study, the aged PA fractions studied previously were precipitated to acquire the aging-produced asphaltenes, and the residual polar aromatics. The aged NA fractions were also precipitated to obtain the aging-produced asphaltenes, if any, and were further separated, using the Corbett procedure, to obtain the aging-produced polar aromatics and the residual naphthene aromatics. GPC measurements were used to characterize these produced asphaltenes and polar aromatics together with the residual polar aromatics and naphthene aromatics. The spectra of these materials are compared to those of the NA, PA, and asphaltene fractions of the parent asphalts. For the six supercritical fractions of AAF-1, only asphaltene precipitation was performed.

The second attempt to understand the asphalt oxidation mechanism is to correlate the oxygen up-take to the increase in carbonyl content. Although carbonyl area CA has been used in this dissertation as a measurement of oxidation extent, the more direct perception of asphalt oxidation would be the uptake of the oxygen. Numerous data were collected to examine if any correlation exists between the increase in the oxygen content (weight percent) and carbonyl growth during the oxidation of asphaltic materials, and if the correlation is aging temperature or aging pressure dependent. The correlations between the oxygen weight percentage and the carbonyl area were obtained for the ten asphalts studied in Chapter 3, and for the NA and PA fractions studied in Chapter 4. By comparing the correlation coefficients of a whole asphalt and those of its NA and PA fractions, an understanding of how much of the total oxygen up-take forms C=O may be acquired.

Oxidation Products of the PA and NA Fractions

During the oxidative aging of an asphalt binder, its composition in terms of Corbett fractions changes. It is well accepted that the asphaltene content increases, and the saturate fraction is the most stable. Obviously, the increase in asphaltene content is the result of the oxidation of the aromatics. However, the aromatics fraction contains both the NA and PA fractions. As shown in Chapters 4 and 5, the NA and PA fractions have far different reactivities and physico-chemical properties. It is desirable to clarify the transformation routes between the NA fractions, PA fractions, and the asphaltenes. According to the data obtained by Corbett (1975) and Corbett and Merz (1975), in the aging process, asphaltenes increase while naphthene aromatics and polar aromatics decrease. The naphthene aromatics change to polar aromatics, and they, in turn, to asphaltenes.

Rostler and White (1962) proposed a method to separate an asphalt into five fractions. The five fractions are asphaltenes, nitrogen bases, 1st acidaffins, 2nd acidaffins and paraffins. Rostler and White observed that, during the aging process, the paraffins and 2nd acidaffins change very little. Nitrogen bases change to asphaltenes, and the first acidaffins convert to the nitrogen bases. However, they also concluded that the newly formed portions of the nitrogen base fraction, originating from the 1st acidaffins, do not change to asphaltenes. In terms of Corbett's fractions, the last observation would suggest that naphthene aromatics are oxidized to polar aromatics, but they always stay in the polar aromatics portion, and will not subsequently change to asphaltenes. This is

in direct contradiction with Corbett's observations.

Choquest and Verhasselt (1994) separated asphalts into four fractions: asphaltenes, resins, cyclics, and saturates. They reported that aging results in little change in saturates, a decrease in cyclics, and an increase in asphaltenes. In conflict with Corbett's observation, an increase in the resins, which correspond to polar aromatics in Corbett's terminology, was reported. This was also shown by Glover et al. (1987).

To elucidate whether naphthene aromatics are converted to polar aromatics and subsequently to asphaltenes, and why at one time, or for some asphalts, the polar aromatics content increases during aging, and in other cases it decreases, the aged NA and PA fraction were analyzed by asphaltene precipitation and by the Corbett procedure to examine the compositional transformation. First, the asphaltene contents of the PA fractions, aged at 368.2 K (95°C), were measured. These asphaltene content data have been used in Chapter 5 to evaluate the asphaltene formation susceptibilities (AFS) of the PA fractions. In this chapter, asphaltene content is plotted against aging time to explicitly display the increase in asphaltene content as the oxidative aging progresses. Likewise, the asphaltene content were measured for the NA fractions aged at 373.2 K (100°C), and were plotted against the aging time. Second, about 5 grams of NA fractions aged at different conditions was collected and mixed to a homogenous state. Corbett analysis was performed on the aged NA fraction (one for each of the five asphalts) to measure the content of asphaltenes, polar aromatics and naphthene aromatics. Similarly, about 5 grams of aged PA fractions was collected. Asphaltene content was measured by precipitation, and the residual polar aromatics were recovered.

Figure 6-1 shows the asphaltene production in the PA fractions aged at 368.2 K (95°C) and 0.2 atm oxygen. Data of AAM-1 PA fraction were not available. Also, as shown in Figure 6-1, the asphaltene content in the unaged PA fractions is not negligible. This may be explained by two factors. First, because the polar aromatics fractions are very reactive, asphaltenes may be produced during the final recovery process. It is also true that the polar aromatics materials have been heated repeatedly for the preparation of samples to be aged. However, special attention was paid to the heating temperature and heating time to minimize any property change due to repeated heating during sample preparation. Considering the temperature and time duration of the final recovery process, it is much more likely that the asphaltenes are produced in this procedure. Second, in the asphaltene

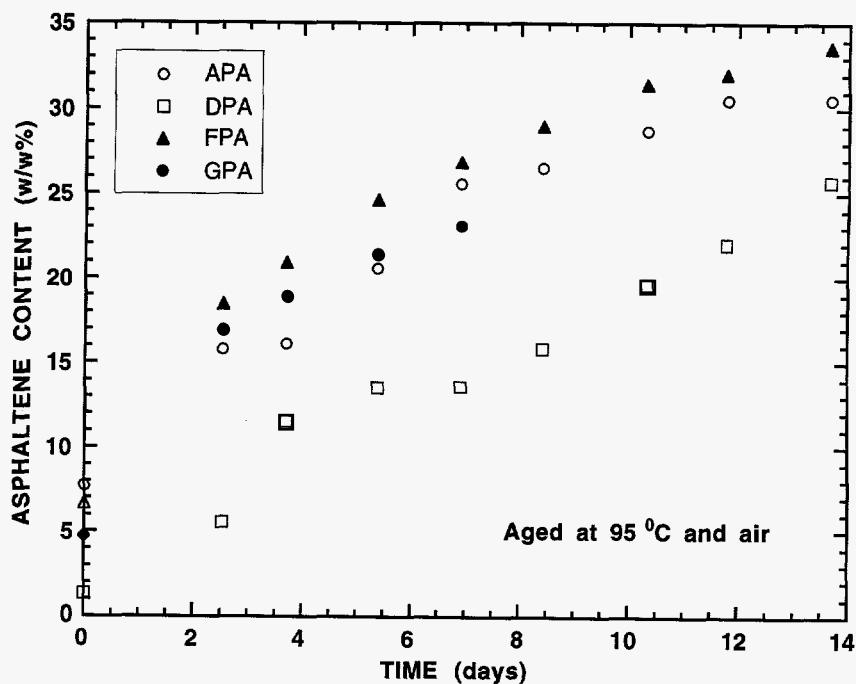


Figure 6-1. Asphaltene production in aged PA fractions.

precipitation method, the measured asphaltene content is affected by the solvation power of the soluble phase. This implies that after the removal of the asphaltenes, the heavy portion of the polar aromatics fraction may precipitate when solvent (hexane) is added. Or, it may be a combination of the two factors.

The increase in asphaltene content with respect to aging time is shown in Figure 6-2 for the five NA fractions aged at 373.2 K (100°C) and 0.2 atm. It is noticed that no appreciable asphaltenes are produced for a time period as long as twenty days. For an extended aging time, there is a gradual increase in asphaltene content, at an increased production rate. This strongly indicates a two-reaction in series mechanism for the oxidation of the NA fractions. The naphthene aromatics are first oxidized to become polar aromatics. This is why at the beginning stage no asphaltenes are produced. However, with further oxidation, the produced polar aromatics transform to asphaltenes. For the produced polar aromatics, the rate of production from the naphthene aromatics is higher than the rate

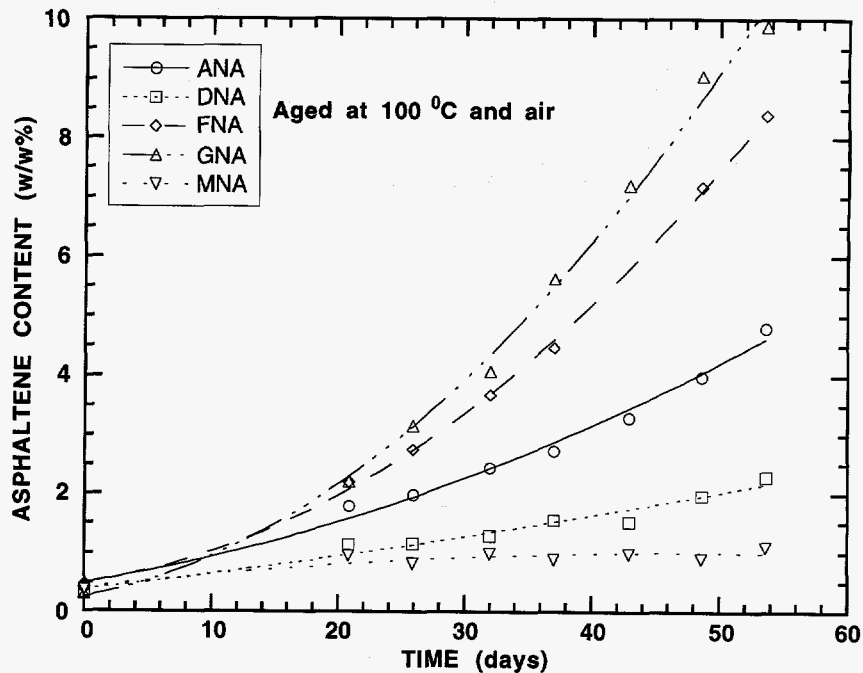


Figure 6-2. Asphaltene production in aged NA fractions.

they convert to asphaltenes, resulting in the accumulation of the polar aromatics and an increase in the rate of asphaltene production. Figure 6-2 thus is an evidence that naphthene aromatics are converted to polar aromatics, and they in turn transform to asphaltenes. Although it would be highly valuable if the polar aromatics content of the aged NA samples could be measured and plotted against aging time, the separation time, as well as the sample amount required, prevent any real attempt to accomplish this.

Figure 6-2 also demonstrates that MNA is special in that no noticeable amount of asphaltenes are present even after 55 days aging at 373.2 K (100°C) and 0.2 atm. For this asphalt, it would be correct to say that the naphthene aromatics change to polar aromatics, and always remain as polar aromatics.

Furthermore, recalling the data in Chapter 3, after aging at 373.2 K (100°C) and 0.2 atm for two weeks, normal asphalt binders will approach viscosities as high as 1 million poise (AAG-1 and

Exxon are a bit lower than that). But as shown in Figure 6-2, with that amount of aging time, no appreciable asphaltenes have been produced in all the five aged NA fractions. So the observation whether polar aromatics produced in an aged NA fraction will or will not subsequently convert to asphaltenes depends on the aging extent of the samples studied by the researcher. This is why Rostler and White (1962) reported that the newly produced polar aromatics do not change to asphaltenes. On the other hand, in Corbett's air-blowing study (Corbett, 1975), the oxidation was much more severe, and the transformation of the newly produced polar aromatics to asphaltenes was observed.

From the above analysis, whether an increase or decrease in polar aromatics content would be observed in the aging process depends on the relative rate of the production of polar aromatics from naphthene aromatics, and the rate of the conversion of polar aromatics to asphaltenes.

Oxidation Products of the Supercritical Fractions

Figure 6-3 shows the asphaltene production in supercritical fractions F1F, F2F, F3F and in FNA aged at 373.2 K (100°C) and 0.2 atm. The delay in the production of asphaltenes which is obvious in the plot for FNA is not present in the plots for F1F, F2F and F3F. This is because all three supercritical fractions already contain a certain amount of polar aromatics at the beginning of aging and these polar aromatics can immediately age to asphaltenes. The asphaltene content is plotted against aging time for the supercritical fractions F4F, F6F, F7F, and for FPA aged at 368.2 K (95°C) and 0.2 atm in Figure 6-4.

Characterization of the Products of Aged NA and PA Fractions

As demonstrated earlier in this chapter, asphaltenes are produced during the oxidation of NA and PA fractions. The portion left in the aged PA fraction after the removal of the newly produced asphaltenes is still polar aromatics, which can be referred to as the residual polar aromatics. For the aged NA fractions, it has been suggested that polar aromatics are produced. But no newly produced polar aromatics have been collected. In this study, enough of the various kinds of fractions were obtained to measure their GPC spectra. Figure 6-5 is the scheme of the materials for comparison.

In order to obtain enough of the aged NA and PA fractions so that the materials for comparison, as listed in Figure 6-5, are adequate for GPC measurements (0.2 grams), for each asphalt

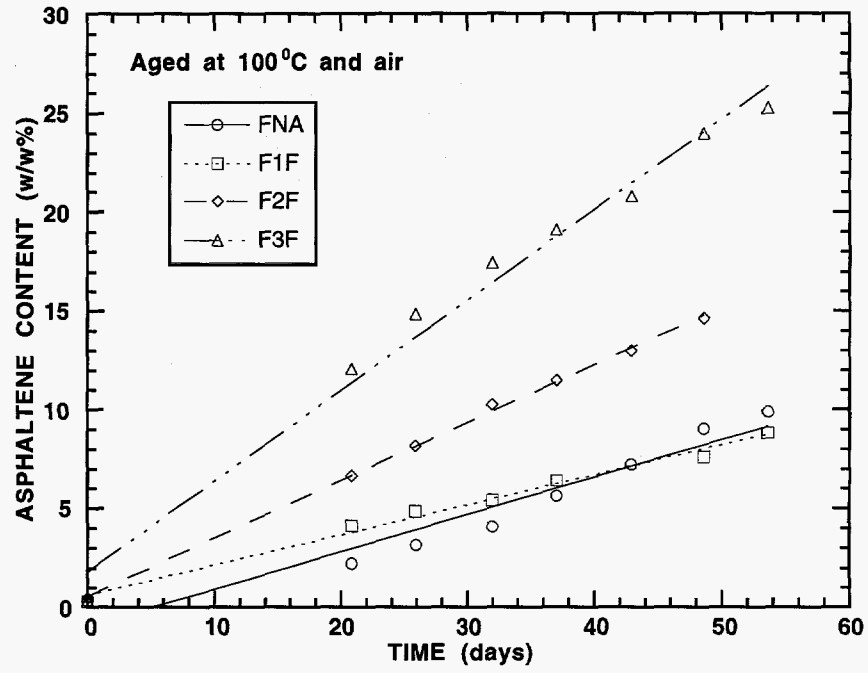


Figure 6-3. Asphaltene production in aged light fractions of AAF-1.

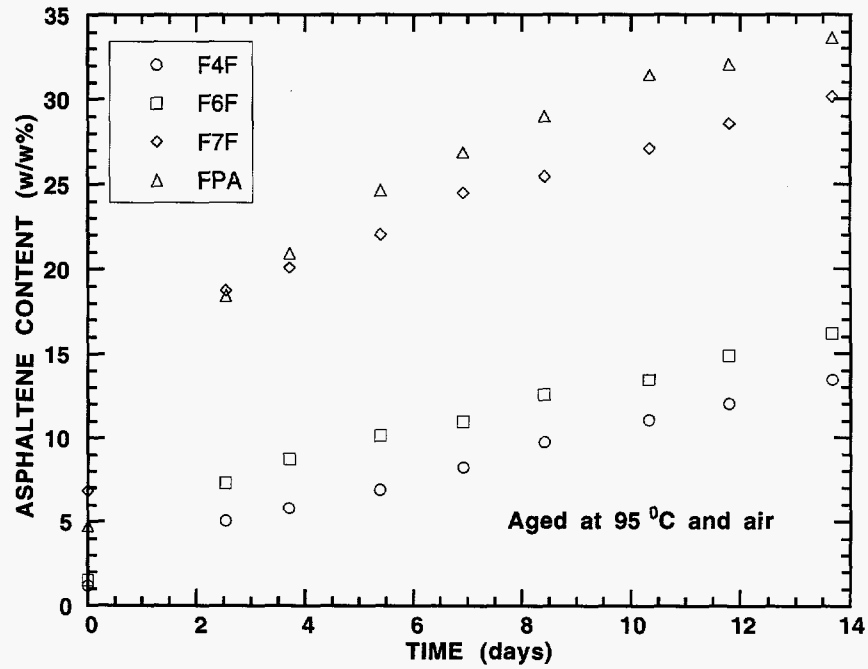


Figure 6-4. Asphaltene production in aged heavy fractions of AAF-1.

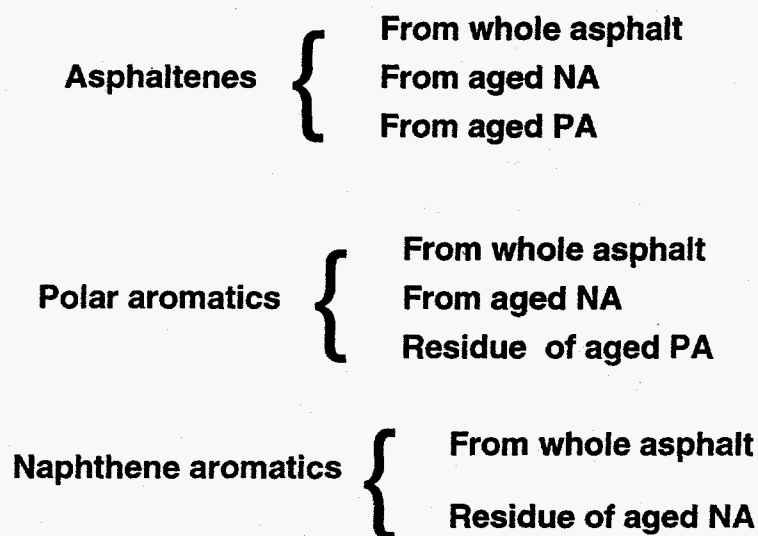


Figure 6-5. Scheme for the comparison of fractions from various sources

the NA samples aged at different temperatures and pressures were collected and mixed as one homogenous aged NA sample. The carbonyl area values for these five aged NA fractions were measured. An equivalent time to reach these values of carbonyl area at the aging condition of 373.2 K (100°C) and 0.2 atm were calculated for each aged NA fraction. Then, Corbett analysis was performed for these five aged NA fractions. The composition of these fractions are listed in Table 6-1 along with the other information. As shown by the data in the table, the collected fractions have equivalent aging times of around 40 days. However, for the aged PA fractions, to mix the collected samples to a homogenous state would require excessive heating, or a recovery process, which needs to be avoided. For this reason, no carbonyl area data for the five aged PA fractions are available. The contents for the produced asphaltenes and residual polar aromatics of the five aged PA fractions are shown in the same table.

Table 6-1. Information of the Aged NA and PA Fractions for Separation

	Quantity	CA	t ^{equ}	w/w%		
				NA	PA	AS
ANAAM ^a	5.81	0.816	46	76.8	13.9	2.67
DNAAM	5.67	0.754	54	68.3	24.3	1.99
FNAAM	5.88	1.17	38	63.3	25.9	3.74
GNAAM	4.80	1.57	36	61.9	27.9	3.65
MNAAM	6.02	1.15	30	55.5	25.9	--
APAAM	6.42	--	--	--	64.6	31.8
DPAAM	5.25	--	--	--	62.3	32.2
FPAAM	4.69	--	--	--	72.1	23.7
GPAAM	4.30	--	--	--	75.6	21.2
MPAAM	4.70	--	--	--	89.4	--

^a ANAAM represents the mixture of aged ANA samples. Likewise, APAAM represents the mixture of the aged APA samples.

Figure 6-6 compares the GPC spectrum of asphaltenes from AAA-1 to those of the newly produced asphaltenes in aged ANA and APA. The molecular sizes of the three asphaltene fractions are such that those from aged ANA < from aged APA < from unaged AAA-1. This suggests that the asphaltenes from aged NA fractions are less detrimental than the asphaltenes from the aged PA fractions and the asphaltenes originally present in the whole asphalts. The difference between the molecular sizes of the three types of asphaltenes of other asphalts are similar. Comparison for asphalt AAM-1 is not available because the asphaltene content in aged MNA is extremely low.

The GPC spectra are shown in Figure 6-7 for the naphthene aromatics of AAA-1 and the residual naphthene aromatics of aged ANA. The residual naphthene aromatics from aged ANA are smaller in molecular size, which is a reasonable observation. It indicates that even within the pure naphthene aromatics fraction there are still a light portion and a heavy portion. The heavy portion is larger in molecular size and more reactive. The heavy portion gets oxidized first and becomes polar aromatics. The residual naphthene aromatics, which now is mostly the light portion, have a smaller

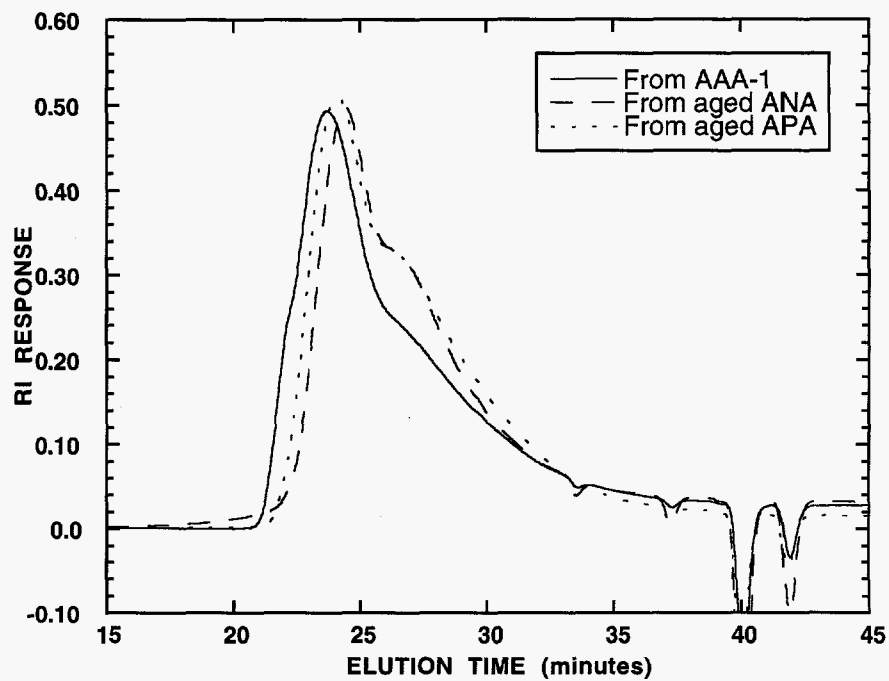


Figure 6-6. GPC spectra of various asphaltenes derived from AAA-1.

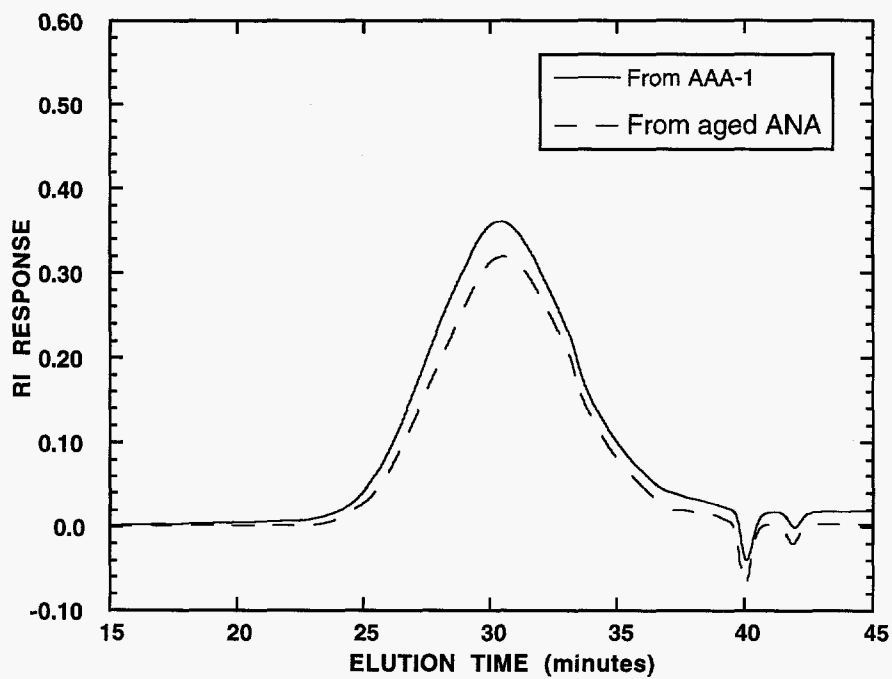


Figure 6-7. GPC spectra of two kinds of NA derived from AAA-1.

molecular size. The difference between the two types of NA fractions of the other asphalts are similar.

Figure 6-8 compares the polar aromatics of AAA-1 to those from the aged PA fraction and the aged NA fraction of this asphalt. Again, it is understandable that the molecular size of the polar aromatics from the whole asphalt is larger than that of the residual PA of the aged PA fraction, because the heavy portion has transformed to asphaltenes. This figure also shows that the polar aromatics converted from naphthene aromatics are smaller in molecular size than the other two types of polar aromatics, and is the least reactive. The ranks in molecular size for the three types of polar aromatics of other asphalts are similar to those of AAA-1.

The spectra of the three types of polar aromatics of AAM-1 are displayed in Figure 6-9. Similar to other asphalts, the polar aromatics from the whole asphalt is larger in molecular size than the polar aromatics from the aged NA fraction. But the polar aromatics from the aged PA fraction is larger than that from the whole asphalt, which for other asphalts is smaller. This is because, as pointed out earlier, during the oxidation of AAM-1, aromatics transform to heavy aromatics, rather than asphaltenes. The oxidation product of the polar aromatics, although heavier, remains in the polar aromatics fraction, resulting in an overall increase in the molecular size of the polar aromatic portion.

From the above analysis, it is clear that the asphaltenes and polar aromatics produced during the oxidation of naphthene aromatics are smaller in molecular size than the asphaltenes and polar aromatics that appear in the parent asphalt. The asphaltenes produced in the aged PA fraction are also smaller in molecular size than the original asphaltenes. It has been shown that a high content in both asphaltenes and saturates is detrimental to the quality of the binder (Lin et al., 1995b). Because of this, removal of the asphaltenes and saturates from the asphalt binder will improve the quality, except that the aromatics portion may not be able to meet the consistency requirements. However, because the asphaltenes and polar aromatics newly produced from aged naphthene aromatics and aged polar aromatics are smaller in molecular size, and thus also less reactive. Air-blowing of an aromatics portion to a certain viscosity level to meet consistency requirements may be a good method to produce superior asphalts. This indirectly coincides with the results obtained in Chapter 4 and 5 for F3F.

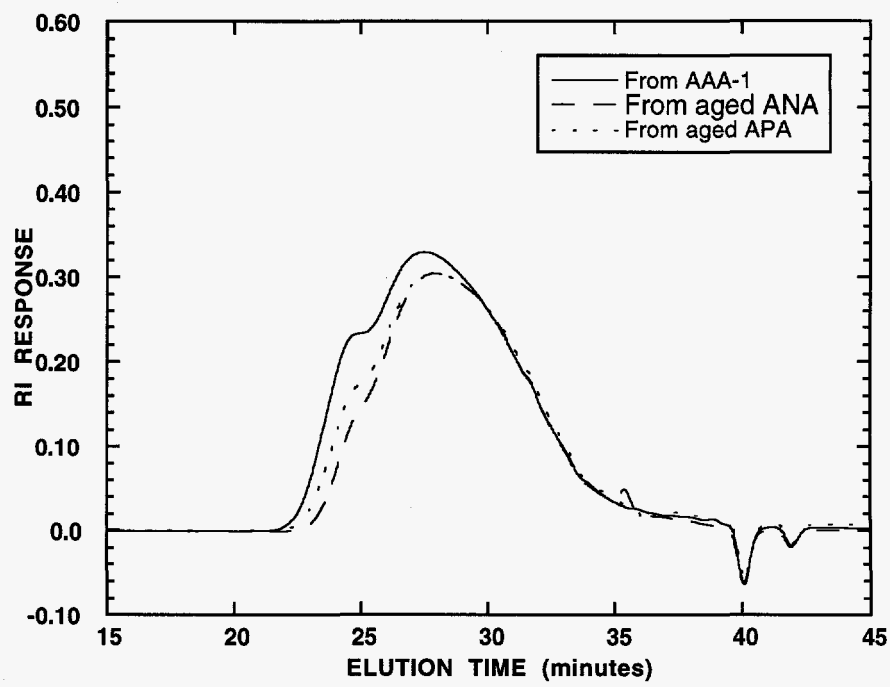


Figure 6-8. GPC spectra of various PA derived from AAA-1.

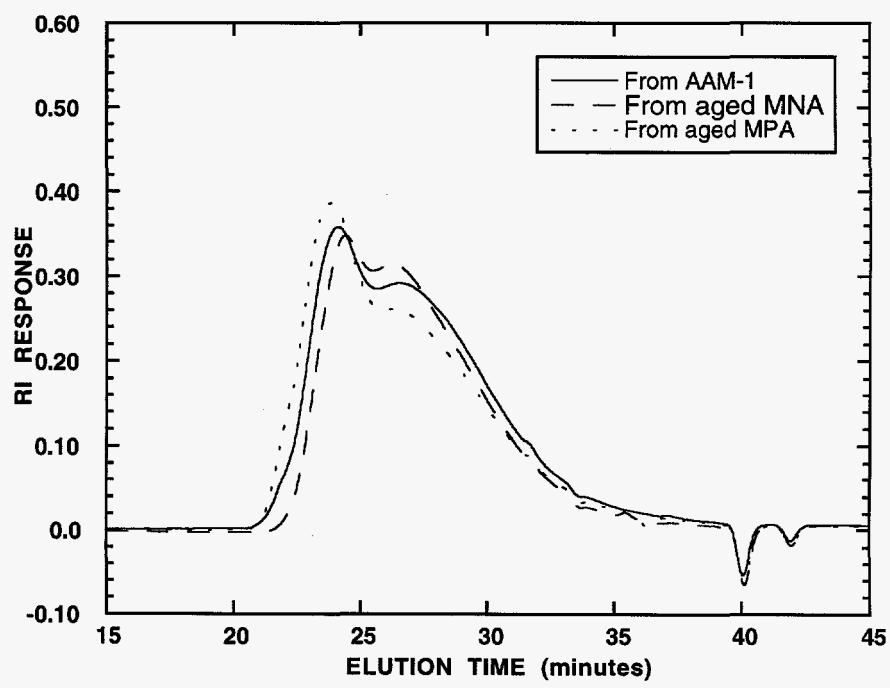


Figure 6-9. GPC spectra of various PA derived from AAM-1.

Oxygen Content-Carbonyl Content Correlation for Whole Asphalts

When asphalt binders are oxidized, both the carbonyl content and asphaltene content are increased. The increase in the amount of asphaltenes is due to the oxidation of some portion in the maltene phase which becomes more polar and less soluble in the solvent. The carbonyl growth results from the creation of functionalities with C=O. In this dissertation, carbonyl area has been used as the measure of the extent of oxidation extent. The main reasons are that the measurement technique for CA is well developed (Jemison, 1992), and that carbonyl area CA correlates with both the aging time and viscosity in a reasonable manner. However, both the increase in asphaltene content and carbonyl growth are the result of oxygen uptake by the reactive portion in the asphalt. Because of the success in modeling the asphalt aging behavior in terms of carbonyl area, a research objective to correlate carbonyl area to oxygen content (weight percentage) was initiated.

Petersen (1986) reported that the functionalities produced during aging and containing oxygen are ketones, carboxylic acids, anhydrides and sulfoxide. Among them, sulfoxide are produced during a short period of time at the beginning. The other three functionalities all have C=O present. It is the generation of these functionalities that causes the carbonyl growth. However, each oxygen atom corresponds to one C=O in ketones, while, in carboxylic acids, two oxygen atoms correspond to one C=O. For anhydrides, the ratio is three oxygen atoms for two C=O, or, an average of 1.5 oxygen atoms for one C=O. Clearly, for the same amount of oxygen up-take measured by the increase in oxygen weight percentage, the amount of C=O created will be dependent on the kind of the functionality containing C=O, or more precisely, on the distribution of the total amount of C=O in the three kinds of the functionalities. Identically speaking, for the same amount of carbonyl growth, the increase in oxygen weight percentage will be different depending on the product distribution. For the same amount of carbonyl growth, the increase in oxygen weight percentage when the oxidation product is only ketones will be double of that when the product is only carboxylic acids. So, if there is any correlation between the oxygen weight percentage and carbonyl area, the correlation coefficient would provide information on the relative distribution of the oxidation products among the three kinds of C=O containing functionalities.

To investigate the correlation between the oxygen content and CA, the oxygen weight percentages of relevant samples studied in the previous chapters are measured. The CA values of

these samples are available, and do not need additional measurements. Furthermore, if a correlation does exist, its dependence on aging time and/or aging pressure needs to be examined.

In Figure 6-10 oxygen content by weight percentage is plotted against carbonyl area for asphalt SHRP AAA-1 aged at 20 atm oxygen and 349.8, 355.4 and 360.9 K (170, 180 and 190°F), as well as for asphalt SHRP AAG-1 aged at 20 atm and 349.8 and 360.9 K (170 and 190°F). All of the samples were aged at a pressure of 20 atm, at multiple temperatures, and an excellent linear correlation between the oxygen content and the carbonyl content is evident. This figure demonstrates that at a specific aging pressure, the correlation is aging-temperature independent.

In Figure 6-11, the data of both of the two asphalts aged at 0.2 atm and multiple temperatures are added to the plots shown in Figure 6-10. However, each regression line in this figure is of the whole set of samples for each asphalt. This figure shows that at the aging pressure of 0.2 atm, the correlation is also temperature independent. Furthermore, since the regression lines for both of the asphalts represent samples aged at both 0.2 atm and 20 atm, we thus conclude that the linear correlation between oxygen content and carbonyl content is also independent of aging pressure.

With the verification that the linear correlation between the oxygen content and the carbonyl area is independent of aging temperature and aging pressure, the measurement of oxygen weight percentage was extended to the other seven asphalts studied in Chapter 3. Figure 6-12 shows the oxygen weight percentage-carbonyl area correlations for five of the ten asphalts studied in Chapter 3. For the sake of comparison, asphalts AAA-1 and AAG-1 from Figure 11 are also included in this figure. Figure 6-13 shows the correlations for the other five asphalts. The oxygen weight percentage for the tank asphalts are also displayed in the figures, which are all around 1.0%. As seen from Figure 6-13, the correlations for the five asphalts are surprisingly close. However, the five asphalts shown in Figure 6-12 have much different oxygen content-carbonyl content behavior. Thus, it would not be beneficial to suggest a universal correlation line for all the asphalts. The difference between the asphalts in Figure 6-12 indirectly confirms the wide diversity in the crude source of the SHRP core asphalts. Observing the correlation coefficients, asphalt AAG-1 has the smallest while asphalt AAD-1 has the largest. This suggests that the oxidation products for AAG-1 in long term aging are relatively high in ketones or anhydrides, and for AAD-1 there are high levels of carboxylic acids or anhydrides.

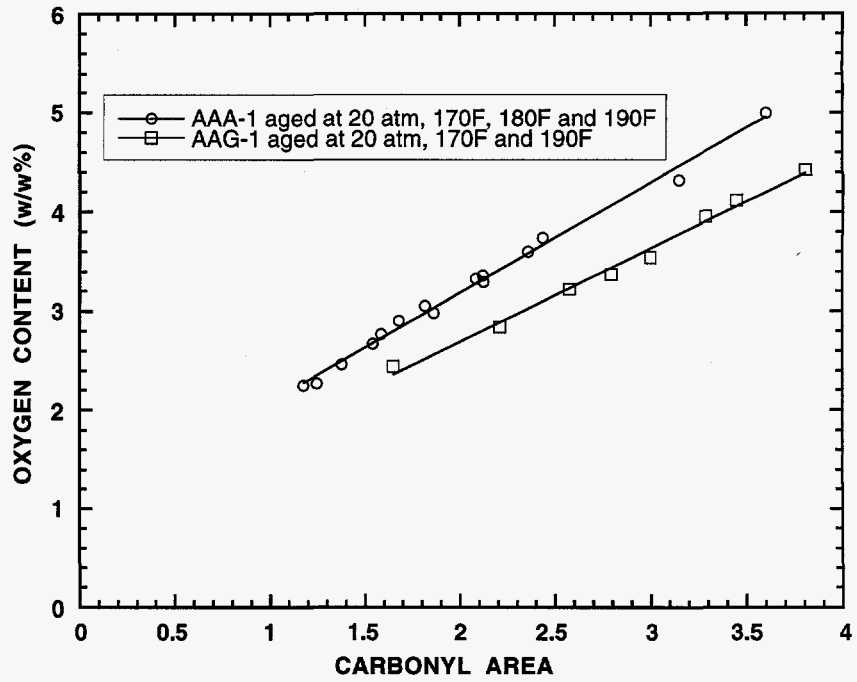


Figure 6-10. Oxygen content vs. CA for AAA-1 and AAG-1 at 20 atm.

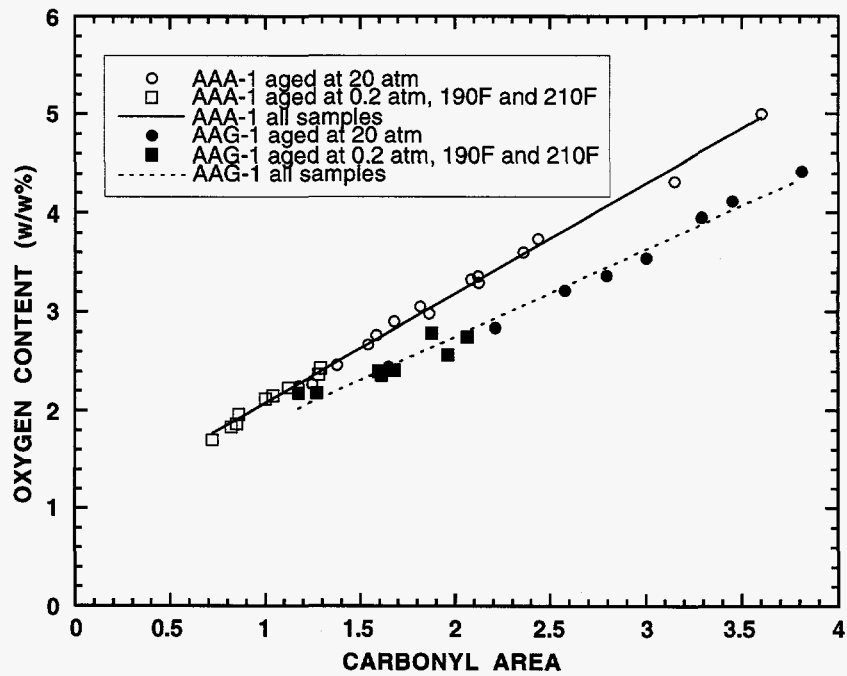


Figure 6-11. Oxygen content vs. CA for two asphalts at multiple T and P.

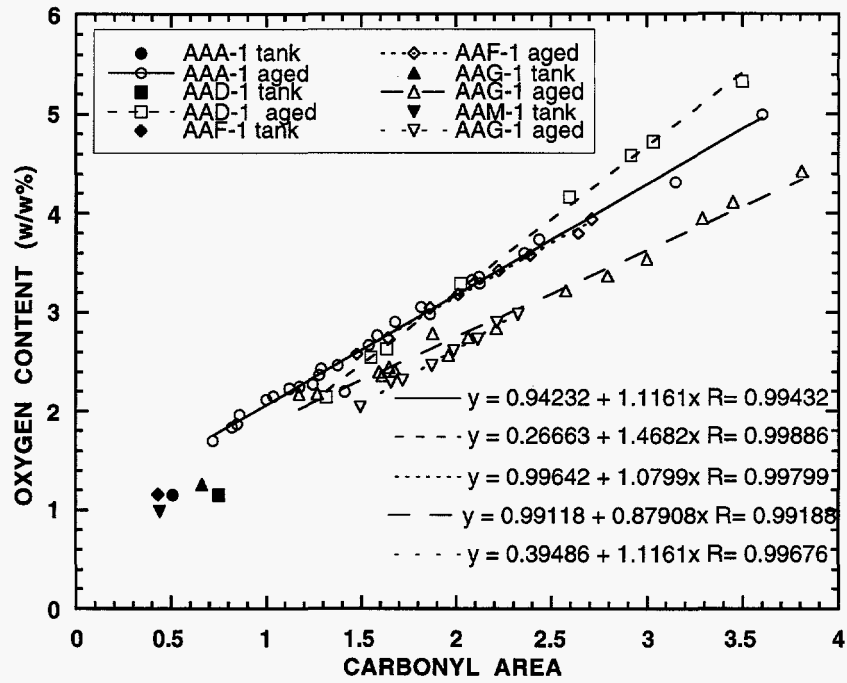


Figure 6-12. Oxygen content vs. CA for five asphalts.

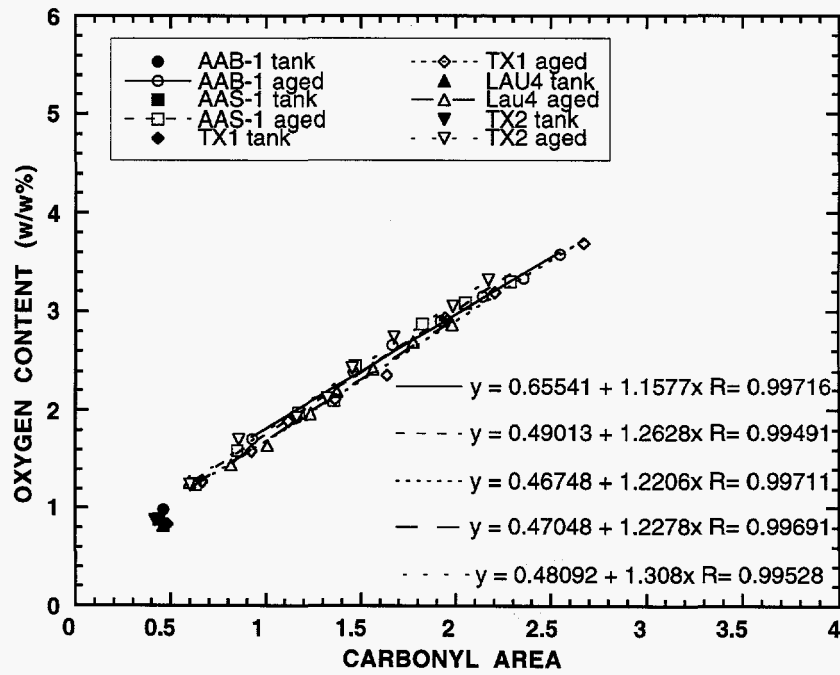


Figure 6-13. Oxygen content vs. CA for another five asphalts.

The linear correlation between the oxygen weight percentage and the carbonyl content indicates that parallel observations, in terms of oxygen content, can be derived from the results obtained in previous studies when carbonyl area is used as the measurement of oxidation extent. Furthermore, since the linear correlation is independent of aging temperature and aging pressure, the kinetic parameters for the asphalts obtained in Chapter 3 are the same when oxygen content is used as the measurement of oxidation extent.

In order to investigate if the Rolling Thin Film Oven Test (RTFOT) has any effect on the oxygen content-carbonyl content correlation, data for samples of AAA-1 and AAF-1, aged after RTFOT treatment, are measured and compared to the data of these two asphalts reported above, as shown in Figures 6-14 and 6-15. From these two figures, we conclude that the RTFOT treatment has no substantial effect on the oxygen content-carbonyl content correlation.

Oxygen Content-Carbonyl Content Correlation for Aged NA and PA Fractions

To further study the oxygen content-carbonyl content correlation of asphalt binders during oxidative aging and to gain more understanding of the asphalt oxidation mechanisms, the oxygen weight percentages of aged NA and PA fractions of the five SHRP asphalts were measured. These fractions have been used in Chapter 4 for the study on the oxidation kinetics of asphalt generic fractions.

The oxygen content-carbonyl content data of the NA and PA fractions along with their parent asphalts are plotted in Figures 6-16 to 6-20 for SHRP asphalts AAA-1, AAD-1, AAF-1, AAG-1 and AAM-1. Data for the unaged samples are also shown on the figures. As we know, for each asphalt, the carbonyl content has the rank of NA fraction < whole asphalt < PA fraction. It is clear from the figures that this order is also true for their oxygen contents.

Figures 6-16 to 6-20 demonstrate that the oxygen weight percentage-carbonyl area correlations exist for aged NA and PA fractions. For all five asphalts except AAM-1, the slopes of the whole asphalt is smaller than those for both its NA and PA fractions; for AAM-1, the slopes of the three are close.

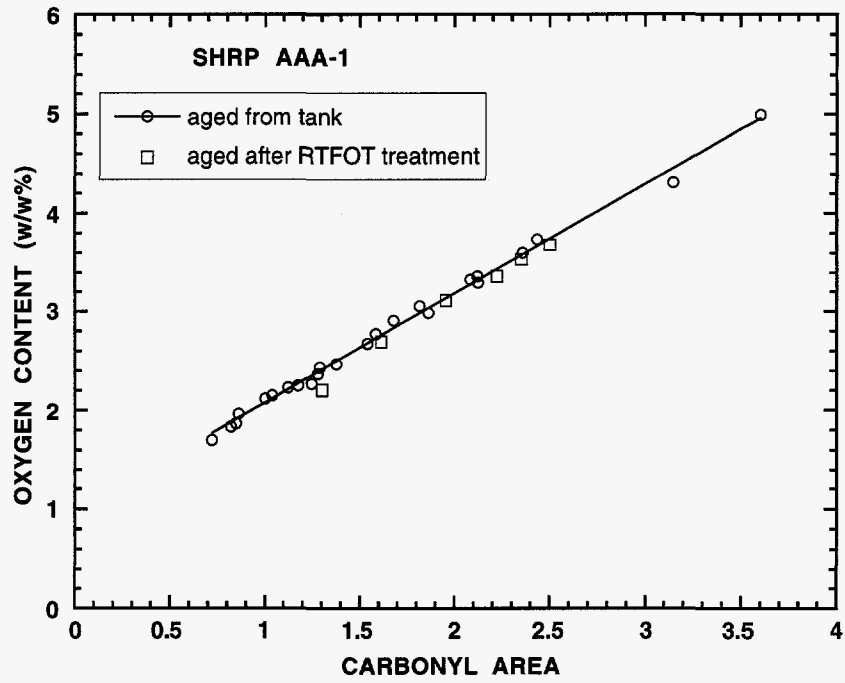


Figure 6-14. The effect of RTFOT on AAA-1 oxygen content.

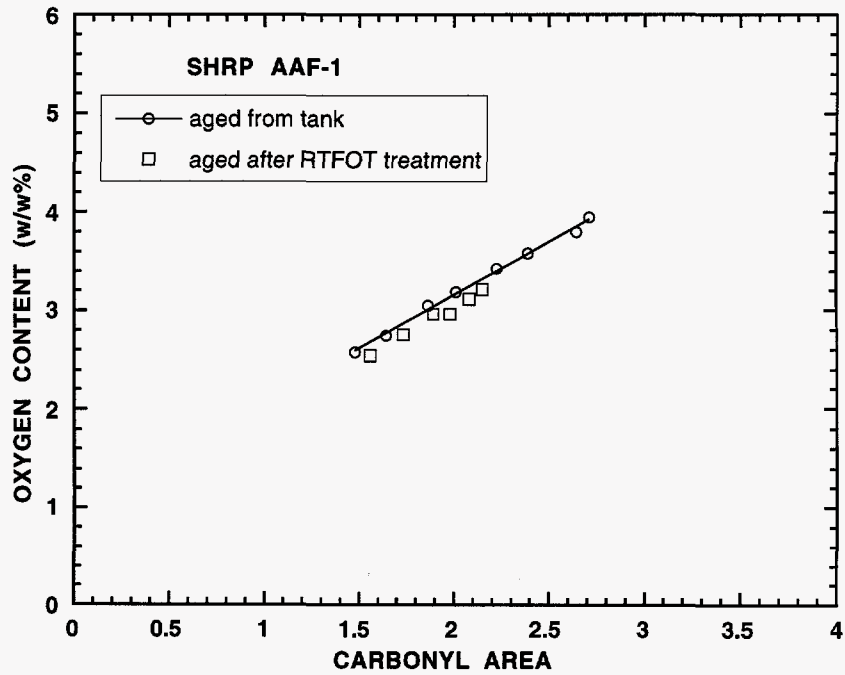


Figure 6-15. The effect of RTFOT on AAF-1 oxygen content.

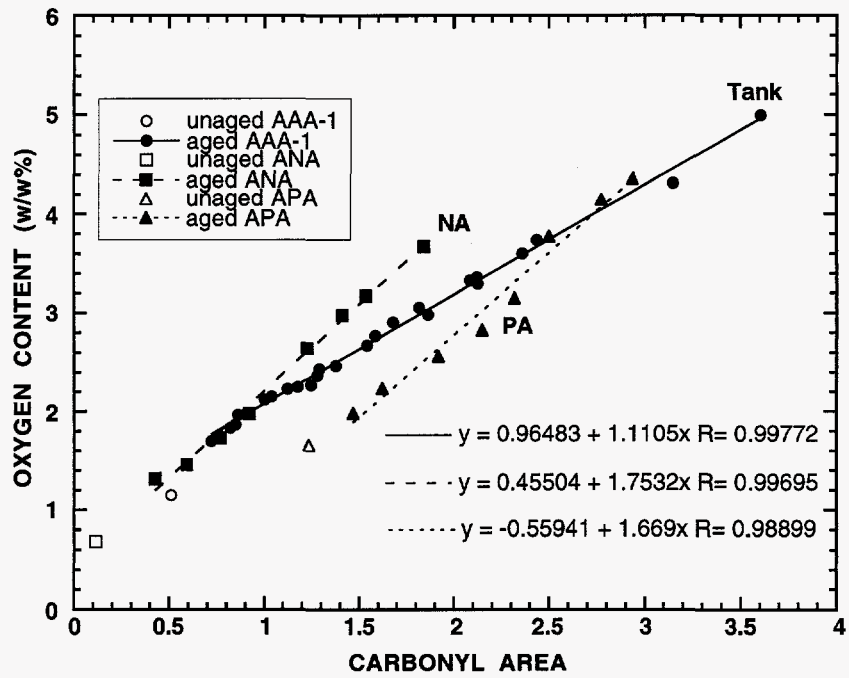


Figure 6-16. Oxygen content vs. CA for aged AAA-1, ANA and APA.

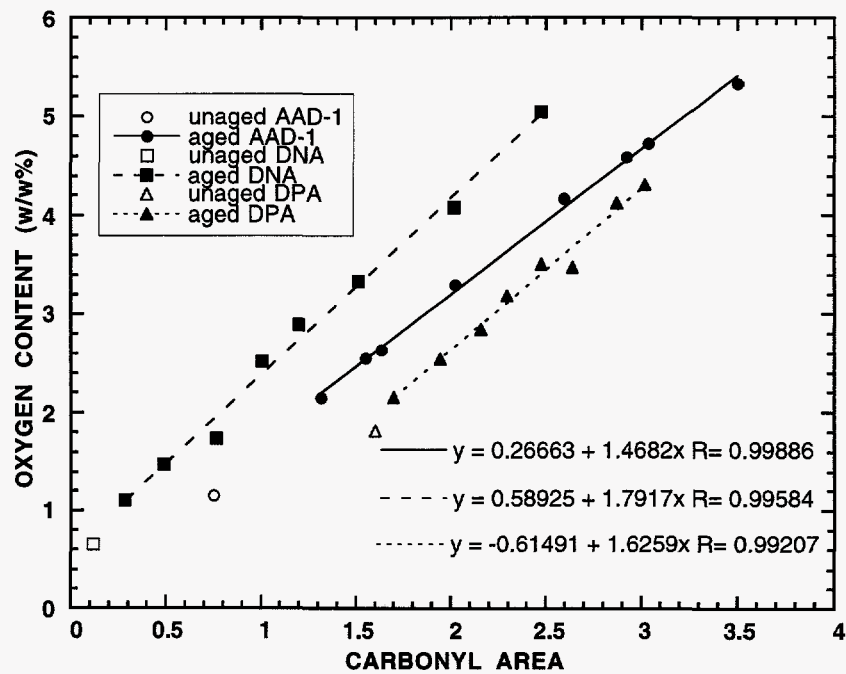


Figure 6-17. Oxygen content vs. CA for aged AAD-1, DNA and DPA.

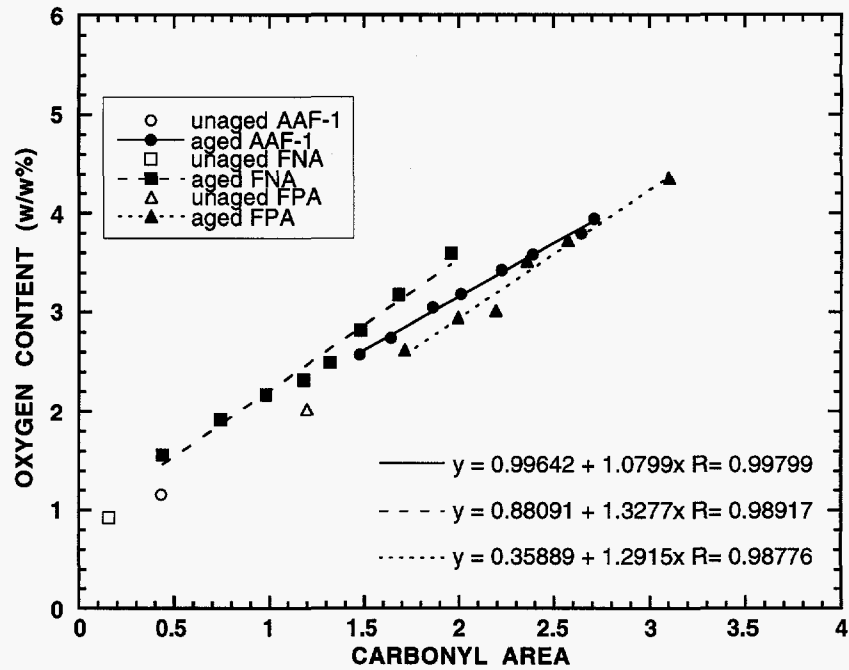


Figure 6-18. Oxygen content vs. CA for aged AAF-1, FNA and FPA

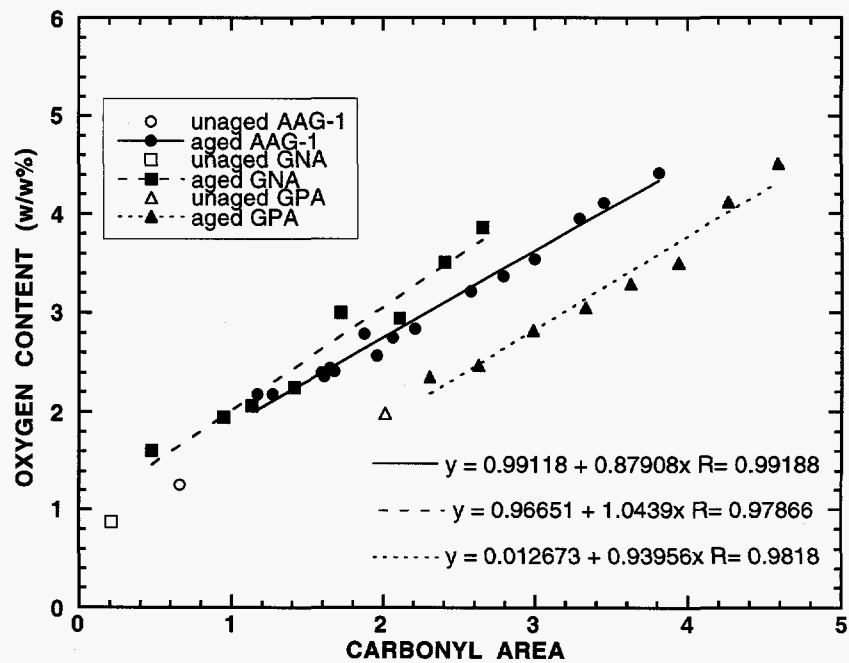


Figure 6-19. Oxygen content vs. CA for aged AAG-1, GNA and GPA

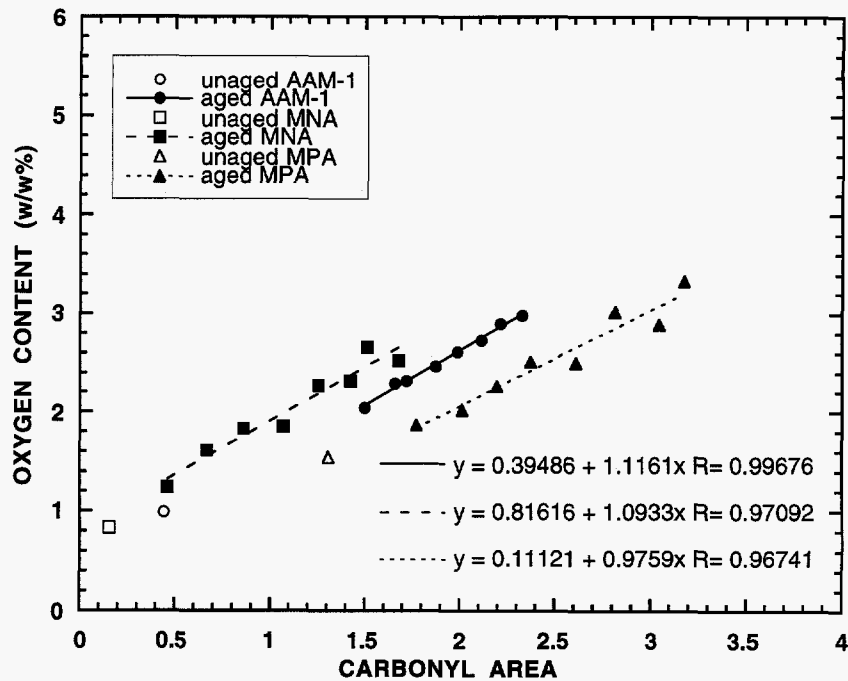


Figure 6-20. Oxygen content vs. CA for aged AAM-1, MNA and MPA

Summary

During the oxidative aging of asphalt binders, polar aromatics transform to asphaltenes, naphthene aromatics convert to polar aromatics and subsequently oxidize to become asphaltenes. Within a limited extent of aging, it may be observed that negligible asphaltenes are produced from naphthene aromatics. Asphaltene content will always increase, while the saturate content is the most stable. Naphthene aromatics will always decrease. Depending on the relative rate of the conversion of polar aromatics to asphaltenes and the rate of the production of polar aromatics from naphthene aromatics, the content of polar aromatics may increase or decrease.

The newly produced asphaltenes and polar aromatics are smaller in molecular size than those present in the original asphalts. The residual polar aromatics in the aged PA fractions and the residual naphthene aromatics in the aged NA fractions have smaller molecular sizes than those from the parent asphalts.

A linear correlation between the oxygen content and the carbonyl content which is independent of aging temperature and aging pressure has been developed for all the ten asphalts studied in Chapter 3. The data show that the oxidation products for AAG-1 in long term aging are relatively high in ketones or anhydrides, and for AAD-1 they are higher in carboxylic acids or anhydrides. The distribution of the created C=O bonds in the three kinds of C=O containing functionalities for other asphalts are in between. The correlation between the oxygen weight percentage and carbonyl area CA were also measured for the NA and PA fractions of the five SHRP asphalts. The slopes for the whole asphalts are smaller than those of the fractions. This likely is due to the presence of asphaltenes in the whole asphalt which apparently produce more carbonyl per unit of oxygen than other species.

CHAPTER 7

LIME-TREATED TANK ASPHALT AGING STUDIES

Several researchers (Plancher et al., 1976; Petersen et al., 1987; Wisneski, 1995; Wisneski et al., in press) have studied the effects of lime treatment on the hardening properties of asphalts. Many of these researchers have shown conclusively that lime reduces the hardening of asphalts, as measured by the aging index, (Plancher et al., 1976; Petersen et al., 1987; Wisneski et al., in press), and some have noted changes in chemical properties for lime-treated asphalts (Plancher et al., 1976; Petersen et al., 1987). However, very few studies have been conducted with the intention of determining the impact of lime treatment on the aging kinetics of asphalts. Wisneski et al. (in press) collected data suggesting that lime treatment may slightly improve the oxidation kinetics of recycled asphalts, but temperature control problems prevented them from determining if lime treatment also improved the kinetics of tank asphalts. Finally, they also concluded that lime can have a substantial beneficial influence on the hardening susceptibilities (HS) of both tank asphalts and recycled asphalts.

The experiments described in this chapter were primarily undertaken to determine what effects lime has on the oxidation and hardening characteristics of tank asphalts so that comparisons could be made to lime-treated recycled asphalt aging. The experiments described in this chapter are more extensive than those conducted by Wisneski (1995) in that more asphalts were included and more aging temperatures were utilized.

Experimental Design

Lime in the form of calcium hydroxide, Ca(OH)_2 , was blended with SHRP AAA-1, AAB-1, AAD-1, and AAF-1. These asphalts were selected because large quantities of these asphalts had been aged for the recycling studies described in Chapter 8. Furthermore, SHRP AAA-1 and AAF-1 had been studied by Wisneski et al. (in press), and they could be used for comparison. The lime was added to the four asphalts to obtain nominal lime contents of 0, 2, 5, and 10% lime by weight. Thus, a total sixteen different materials (4 asphalts \times 4 lime levels) were involved in the experiments described in this chapter. Approximately 50 g of each blend was produced by hand stirring the lime into the asphalt.

The primary properties of interest were the viscosities ($\eta_{0,60^{\circ}\text{C}}^*$) of the unaged samples and the viscosities and carbonyl areas of POV-aged samples. Rheological measurements were also performed at 0, 10, 25, and 40°C on the unaged materials to determine what effect, if any, the lime has on the viscosity temperature susceptibility (VTS) of the unaged samples.

The aging conducted in these lime experiments was limited to POV aging. Six trays, each containing $1.5 \pm 0.1\text{g}$ of asphalt, were POV-aged at five different temperatures using atmospheric air. Atmospheric air pressure was used in order to simplify the kinetic rate expression and to eliminate one possible source of experimental error. The aging temperatures utilized in these experiments were 80, 85, 90, 95, and 100°C. As described above, this is an improvement over the three aging temperatures that Wisneski (1995) utilized. The data published by Liu et al. (1996) were utilized to determine both the length of time necessary to overcome the “initial jump” and the predicted oxidation rate at each temperature. On the basis of these calculations, appropriate aging times and sampling intervals were determined for each aging temperature. The aging times and aging intervals for each temperature are listed in Table 7-1.

Table 7-1. Lime-Treated Tank Asphalt Aging Conditions

Aging Temperature (°C)	Initial Sampling Time (days)	Sampling Interval (days)
80	12	4
85	10	3
90	10	3
95	5	2
100	5	2

The samples were aged in a rotation due to space considerations in the POVs. All of the AAA-1 and AAB-1 samples were placed in the POV on day one. As the first set of AAA-1 and AAB-1 samples were removed, the (last set of) AAD-1 and AAF-1 samples were rotated in. This rotation of samples greatly reduced the total aging time required but resulted in the complete loss of

rate data for the AAD-1 and AAF-1 samples at 95°C when the temperature bath stirring motor failed on the second to last day of aging. The failure of the stirring motor caused a temperature gradient to develop in the bath resulting in uncertain initial jump aging times. This uncertainty could not be accurately corrected for mathematically. Although the rate data for these samples could not be used, the HS points were not affected because the HS is temperature independent over the range of temperatures utilized in these experiments.

Unaged Sample Properties

The viscosities of the unaged materials are shown in Table 7-2. The data in this table indicate for all asphalts that the addition of lime raises the viscosity of the asphalt monotonically with increasing lime content. The literature are somewhat divided as to what effect lime should have on the viscosity of the asphalt. If the lime particles do in fact act as particles, then the viscosity-particle concentration relationship should be modeled by the Pal-Rhodes model (Pal and Rhodes, 1989; Lin et al., 1995a) which predicts that viscosity increases with particle concentration.

Table 7-2. Lime-Treated Tank Asphalt Initial Viscosities

Asphalt	$\eta_{0,60^\circ\text{C}}$ (dPa·s)				
	Nominal Ca(OH) ₂ Content (wt%)	0	2	5	10
AAA-1		1200	1580	1670	1940
AAB-1		1400	1920	2010	2170
AAD-1		1490	1970	2290	2440
AAF-1		2800	3200	3680	4400

In fact, looking at recent lime-treated asphalt experiments, Wisneski (1995) reported data showing a general trend that lime, both CaO and Ca(OH)₂, caused an increase in the viscosity of unaged AAA-1 and AAF-1. On the other hand, Petersen (1982) reported that mixing lime with asphalt resulted in a steady decrease in the 25°C viscosity with time. However, Petersen's

experiments were complicated by solvent dissolution and recovery steps, which may severely alter the viscosity of the samples (Burr et al., 1990; Burr et al., 1991; Burr et al., 1994).

The viscosities (η^*_0) for the 2, 5, and 10% unaged samples were also higher than the viscosities for the 0% samples at viscosity measurement temperatures of 0, 10, 25, and 40°C. However, the viscosities at some temperatures did not increase monotonically with lime content, likely due to random errors associated with the time-temperature-superposition (Ferry, 1985). Figure 7-1 is a plot of viscosity as a function of measurement temperature for the AAA-1 unaged samples. Clearly, over the range of the viscosity measurement temperatures examined in these experiments, the data in Figure 7-1 are well described by the Andrade equation (Andrade, 1930).

$$\ln \eta^*_0 = A_{\text{vis}} + \frac{E_{\text{vis}}}{RT} \quad (1-9)$$

In Equation (1-9), A_{vis} is a material constant, R is the ideal gas constant, T is the absolute temperature, and E_{vis} is the viscosity activation energy and describes the sensitivity of the viscosity to changes in temperature. Jemison et al. (1995) argued that E_{vis} was a superior measure of the viscosity temperature susceptibility (VTS) than traditional methods. The value of E_{vis} can be obtained directly as the slope of the exponential fit of the data as shown in Figure 7-1 for AAA-1. Similar figures were constructed for the other asphalts. The E_{vis} values for the materials examined in this study are tabulated in Table 7-3. The data in Table 7-3 may show slight bias towards an increasing E_{vis} with the increasing lime levels, especially for AAF-1. This increased E_{vis} will magnify viscosity difference between the lime-treated and untreated asphalts at lower temperatures. Thus, lime *may* be detrimental to the asphalt in terms of the potential for low temperature cracking. However, it should be noted, that the E_{vis} differences between the lime-treated and untreated samples are, in general, much smaller than the E_{vis} differences between asphalts. As a result, one can conclude that lime treatment will not cause a relatively good asphalt (in terms of E_{vis}) to become a relatively poor asphalt.

Aging Studies

After POV aging, carbonyl area measurements were performed on all of the samples, and

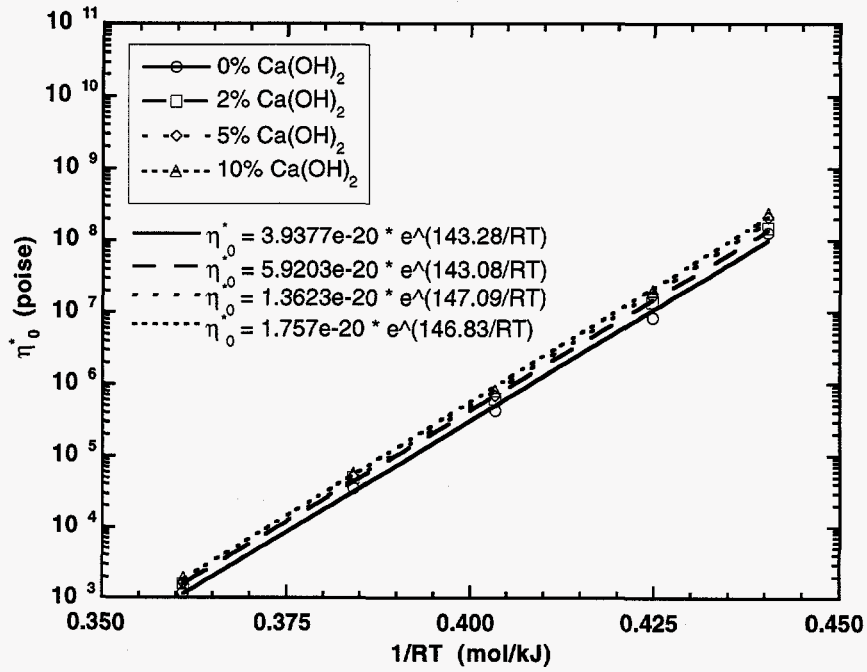


Figure 7-1. VTS for lime-treated AAA-1 materials.

Table 7-3. VTS Values of Unaged Lime-Treated Tank Asphalts

Asphalt	E_{vis} (kJ/mol)				
	Nominal $\text{Ca}(\text{OH})_2$ Content (wt%)	0	2	5	10
AAA-1		143.3	143.1	147.1	146.8
AAB-1		161.9	166.6	168.4	169.7
AAD-1		150.0	151.1	152.2	154.7
AAF-1		174.6	182.0	188.7	188.4

viscosity ($\eta_{0,60^\circ\text{C}}$) measurements were performed on at least one-third of the samples. Carbonyl measurements were also performed on the unaged asphalt samples. The carbonyl grows as a linear function of aging time, as shown in Figure 7-2 for the untreated AAA-1. Similar figures were constructed for the other materials. The only possible exceptions are the 80°C aging profiles for AAA-1 with 10% lime and AAD-1 with 2% lime. From Chapter 1, in the constant rate region, the carbonyl data can be fit by linear regression to obtain the carbonyl formation rates (R_{CA}) and extrapolated carbonyl areas (CA_0) according to Equation (1-5).

$$CA = CA_0 + R_{CA} t \quad (1-5)$$

The data indicate that the initial aging times used in these experiments were sufficient to overcome the initial non-linear aging which occurs in the "initial jump" region. The poor fits for the two noted exceptions are probably the result of sample inhomogeneity or systematic problems encountered during the aging at 80°C. Potential problems are evident from the rate data discussed later.

The data in Figure 7-2 show the expected trends that CA_0 is relatively temperature independent (Liu et al., 1996). The average CA_0 values for each asphalt is shown in Table 7-4 along with the carbonyl area for the unaged sample (CA_{unaged}) and the difference between the two, or the so-called "initial jump". The data in Table 7-4 indicate that the value of the "initial jump" is relatively unaffected by the presence of lime, within experimental error. Additionally, the "initial jump" values of 0.175, 0.247, 0.239, and 0.314 for the untreated samples compare favorably to the "initial jump" values of 0.183, 0.227, 0.232, and 0.365 reported recently by Liu (Table III-3b, Liu, 1996).

The carbonyl formation rates for the AAA-1 materials are plotted in Figure 7-3 together with the experimental atmospheric rate data reported by Liu (1996) and Chaffin (1996). The distinction about experimental atmospheric rate data is important, because Liu conducted several experiments at elevated pressures and corrected the rates to atmospheric conditions. By only including the experimental atmospheric data to generate the solid line shown in Figure 7-3, one potential source of error, pressure correction, has been removed.

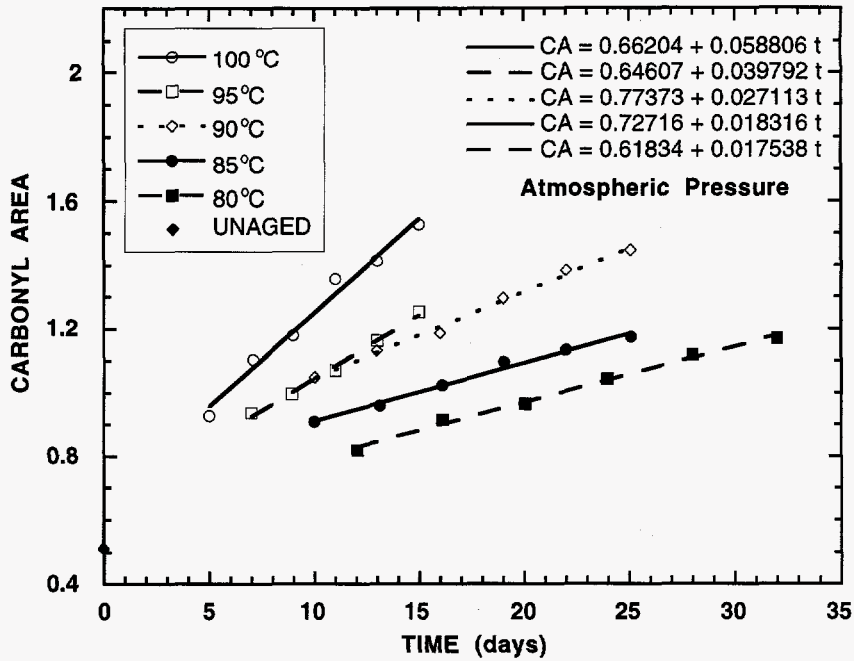


Figure 7-2. Carbonyl growth for untreated Tank AAA-1.

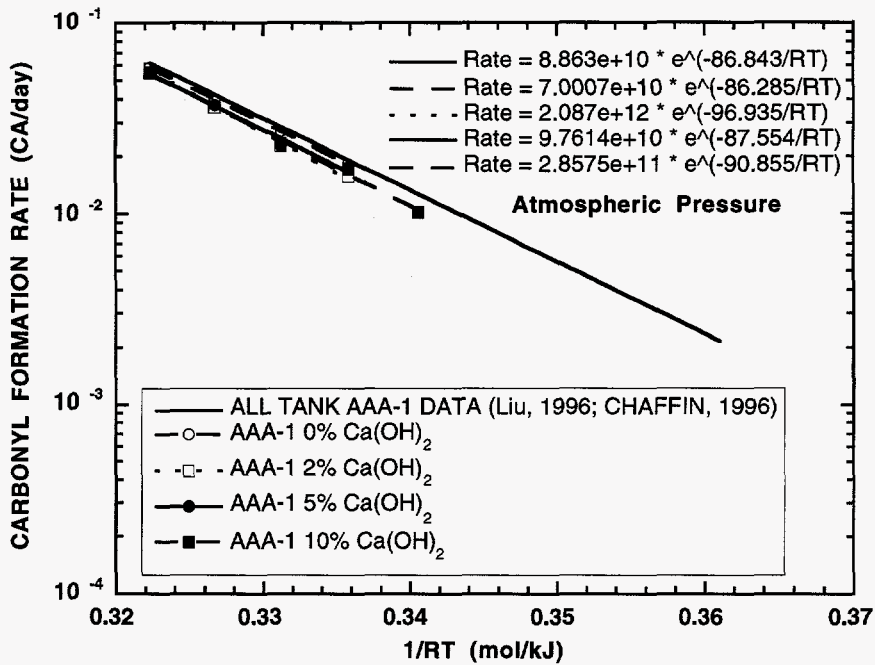


Figure 7-3. Arrhenius plots for AAA-1 materials.

Table 7-4. Lime-Treated Tank Asphalt "Initial Jump" Data

Material	CA _{0, ave}	CA _{unaged}	CA ₀ - CA _{unaged}
AAA-1 0% Ca(OH) ₂	0.686	0.510	0.175
AAA-1 2% Ca(OH) ₂	0.661	0.520	0.141
AAA-1 5% Ca(OH) ₂	0.663	0.514	0.149
AAA-1 10% Ca(OH) ₂	0.680	0.500	0.180

AAB-1 0% Ca(OH) ₂	0.717	0.470	0.247
AAB-1 2% Ca(OH) ₂	0.657	0.495	0.162
AAB-1 5% Ca(OH) ₂	0.700	0.495	0.205
AAB-1 10% Ca(OH) ₂	0.732	0.493	0.239

AAD-1 0% Ca(OH) ₂	0.966	0.727	0.239
AAD-1 2% Ca(OH) ₂	0.956	0.733	0.223
AAD-1 5% Ca(OH) ₂	0.936	0.730	0.206
AAD-1 10% Ca(OH) ₂	0.944	0.719	0.226

AAF-1 0% Ca(OH) ₂	0.777	0.463	0.314
AAF-1 2% Ca(OH) ₂	0.936	0.468	0.369
AAF-1 5% Ca(OH) ₂	0.758	0.474	0.284
AAF-1 10% Ca(OH) ₂	0.776	0.470	0.306

As expected, the carbonyl rate data for the SHRP AAA-1 materials are well described by the Arrhenius reaction kinetics model expressed in Equation (1-6).

$$R_{CA} = A e^{-E/RT} \quad (1-6)$$

Recalling, A is the pre-exponential factor, E is the reaction activation energy, R is the ideal gas constant and T is the absolute temperature. Figure 7-3 is an example of an Arrhenius plot, the slope of each line is the activation energy, E, for that particular material. The long solid line in Figure 7-3 was generated using the atmospheric data collected in this study and the atmospheric data published by Liu (1996) for the SHRP AAA-1 tank (0% lime) asphalt (data omitted for clarity).

As discussed above, there seemed to be a consistent trend that the 80°C rates were significantly higher than the rest of the rates would suggest for several of the materials. The 80°C data points were not used in the regressions after this inconsistency was noted. The data in Figure 7-3 indicate that the AAA-1 carbonyl rates obtained in this study alone yield an activation energy nearly equal to that obtained using all of the atmospheric rate data available. Figure 7-3 also indicates that the presence of lime does not affect the activation energy of the asphalt. The activation energies for all materials discussed in this study are shown in Table 7-5.

Table 7-5. Lime-Treated Tank Asphalt Atmospheric Pressure Activation Energies

Asphalt	E (kJ/mol)					
	Nominal Ca(OH) ₂ Content (wt%)	0 ^a	0 ^b	2	5	10
AAA-1		86.8	86.3	96.9	87.6	90.9
AAB-1		90.3	77.2	84.7	91.3	89.1
AAD-1		92.6	95.8	67.9	83.7	70.9
AAF-1		80.1	81.4	95.5	80.1	70.7

^a All experimental atmospheric data Liu (1996) and this work

^b This study only

The Arrhenius plot for AAB-1, Figure 7-4, indicates that the activation energy may be affected by lime treatment if the comparison is made strictly on the basis of aging data collected in this study. However, if the comparison is made to the solid line constructed using all of the experimental atmospheric data available, the activation energy appears to be unaffected by the presence of lime. This illustrates the significant complications and errors that may arise from trying to determine kinetic information from only four or five aging temperatures. In fact, the Arrhenius plots for AAD-1 and AAF-1 shown in Figures 7-5 and 7-6, respectively, further remind one about the significant errors which may arise from determining kinetics from only a small number of data points.

For AAD-1, the activation energies for the tank and 5% lime-treated materials are similar to each other and the activation energy determined using all of the AAD-1 atmospheric rate data available. The activation energies for the 2% and 10% lime-treated materials are similar to each other but they are more than 25% different from the AAD-1 tank data. Similar trends are also seen for SHRP AAF-1. It is highly unlikely that such observations indicate real phenomena. The long solid line for the SHRP AAF-1 untreated asphalt (0% lime) also includes data collected in the studies described in Chapter 8.

The activation energy differences for the AAD-1 and AAF-1 materials may be the result of the aging rotation in the POVs. However, if one analyzes the data which make up the solid lines in Figures 7-3 to 7-6, it is clear that there can be considerable scatter in the data. For example, Figure 7-7 shows the scatter in the experimental atmospheric data used to generate the overall activation energy for SHRP AAA-1. This indicates that in order to get a "true" activation energy it is imperative to conduct many, many aging experiments, especially if the goal is to accurately predict the ambient aging performance of an asphalt. However, it is impractical to collect that many experimental rates for each material and conclusions (right or wrong) must be drawn from a relatively few number of data points and previous experience. Thus, the weight of the data indicate that lime probably has no effect on the reaction activation energy even though a few of the data points indicate otherwise.

Figures 7-3 to 7-6 show that the lime treatment generally causes the carbonyl formation rates to decrease. Furthermore, the data indicate that the carbonyl rate decreases with increasing lime

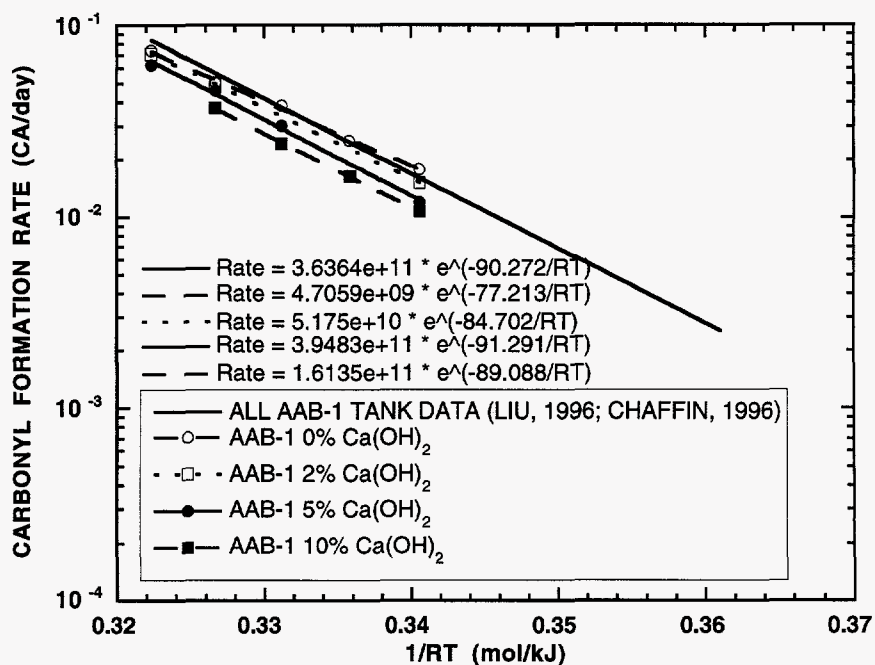


Figure 7-4. Arrhenius plots for AAB-1 materials.

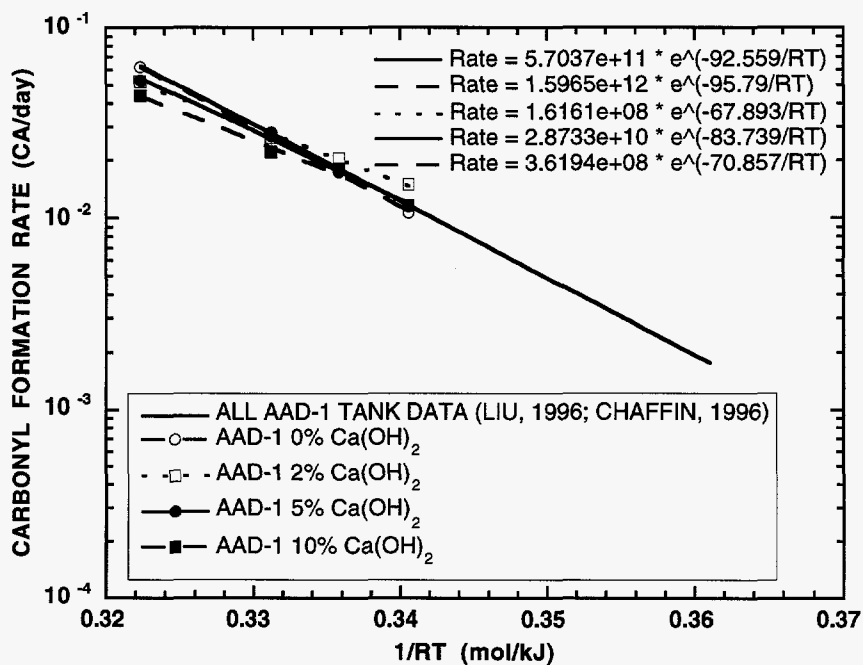


Figure 7-5. Arrhenius plots for AAD-1 materials.

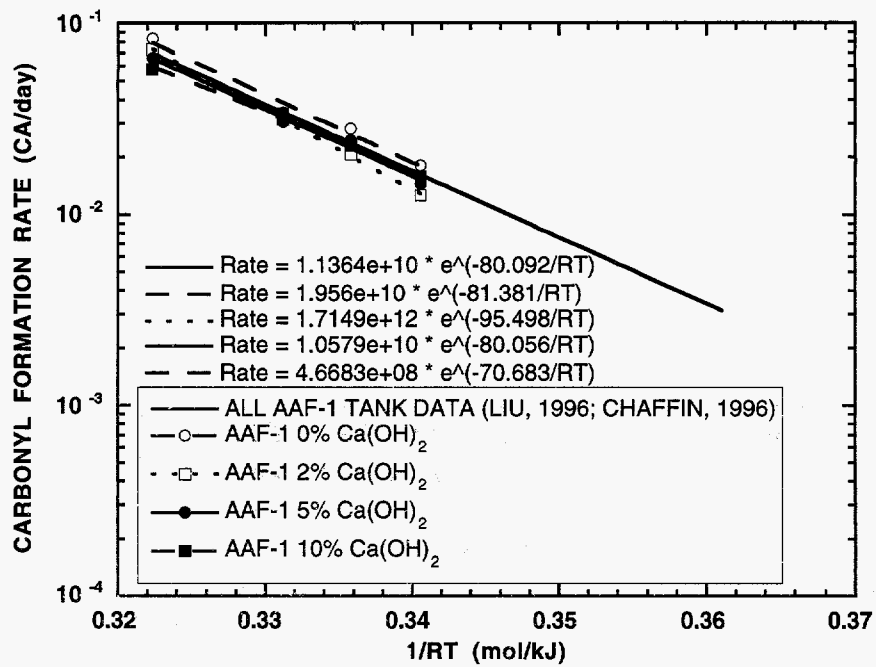


Figure 7-6. Arrhenius plots for AAF-1 materials.

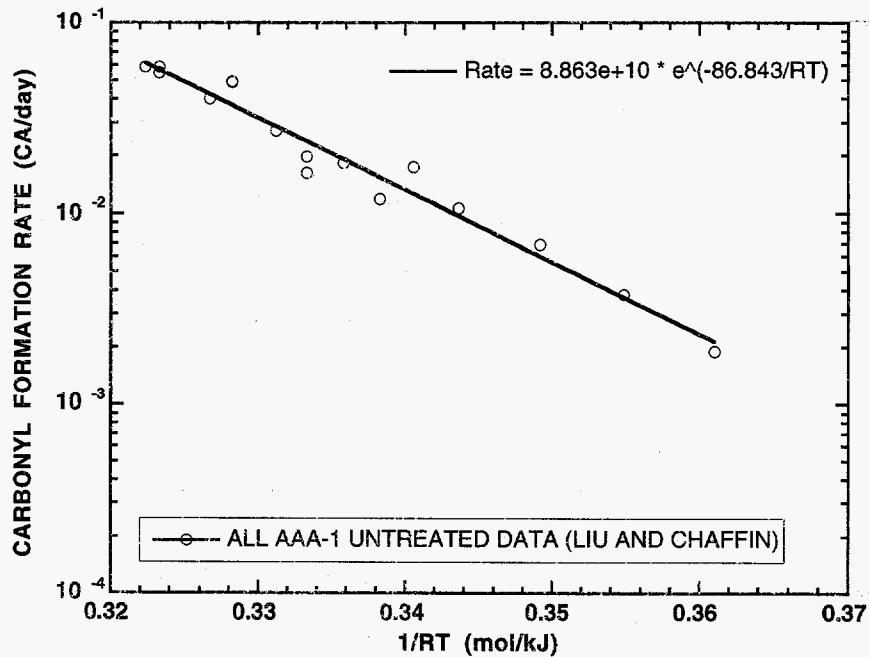


Figure 7-7. Arrhenius plot for all atmospheric untreated AAA-1.

content. This was also noted by Wisneski (1995) for lime-treated tank asphalts and Wisneski et al. (in press) for recycled asphalts, with a few exceptions. This is expected if one assumes that the lime serves only as a diluting agent. Using this assumption, one expects that the carbonyl formation rates for the lime-treated materials should be equal to weight fraction of asphalt times the carbonyl rate for the untreated asphalt. As can be seen in Figure 7-8, the scatter in the data indicate that, if anything, the lime is slightly increasing the rate over that expected for pure dilution. As such, it appears that any antioxidant effects that the lime imparts to the asphalt are strictly limited to the dilutory effects.

The hardening susceptibilities for the AAA-1 materials are shown in Figure 7-9. The data points used to generate the hardening susceptibilities (HS) have been omitted for clarity. In addition, only the data collected in this study were used to generate the HS plot for the untreated AAA-1 asphalt. It can be seen from Figure 7-8 that the HS values (slopes) are somewhat lower for the lime-treated materials when compared to the untreated asphalt. Similar trends exist for the AAB-1, AAD-1, and AAF-1 materials analyzed in this study. The HS values for all of the lime-treated materials examined in these experiments are tabulated in Table 7-6. Table 7-6 also includes previously reported atmospheric pressure HS values (Liu, 1996; Wisneski et al., in press). The data collected in this study support the conclusions of Wisneski et al. (in press) that the mere presence of lime lowers the HS but the amount of lime seems to have little or no effect on the HS value. In other words, addition of lime will decrease the HS, but the point of diminishing returns in terms of HS reduction is achieved with only small amounts of lime. Examining the data more closely, there is a general lack of agreement in HS value between the data collected in this study and the previous data. The one material showing any agreement in HS with the published data is the untreated AAA-1. Although the HS values collected in this study are not the same as the published values, the data are highly consistent between asphalts. Examining the data in Table 7-6 more closely, one sees that the average percent reductions in HS for all four asphalts with lime treatment of 8, 14, 11, and 16%, for AAA-1, AAB-1, AAD-1, and AAF-1, respectively are much more consistent than the percent reductions reported by Wisneski et al. (in press) of 29% and 13% for AAA-1, and AAF-1,

Prediction of Ambient Performance

The overall goal of any asphalt study, this one included, is to produce materials which will last

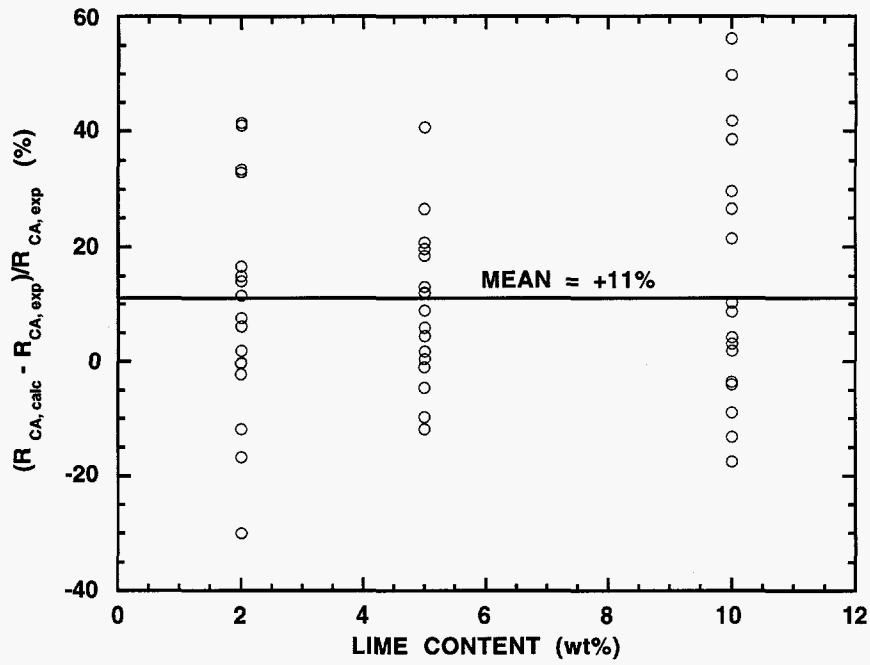


Figure 7-8. The dilutory effect of lime on the aging of tank asphalts.

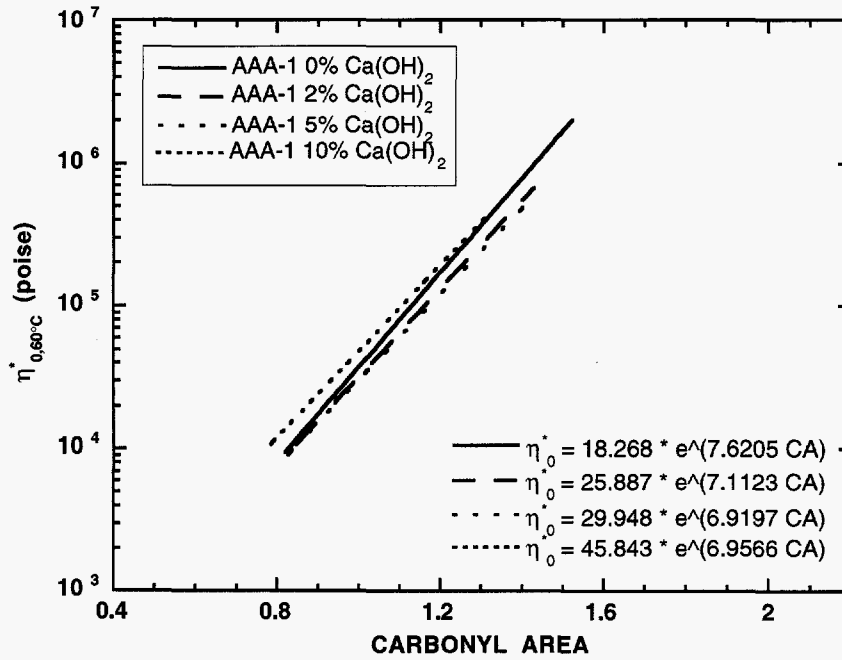


Figure 7-9. Lime-treated AAA-1 hardening susceptibility comparisons.

Table 7-6. Lime-Treated Tank Asphalt Atmospheric Pressure Hardening Susceptibilities

Asphalt	HS								
	0 ^a	0 ^b	2 ^b	5 ^b	10 ^b	0 ^c	2 ^c	5 ^c	10 ^c
Nominal Ca(OH) ₂ Content (wt%)									
AAA-1	6.93	7.60	5.20	5.60	5.50	7.62	7.11	6.92	6.96
AAB-1	6.18	-	-	-	-	6.52	5.58	5.40	5.87
AAD-1	8.00	-	-	-	-	9.82	8.67	8.54	9.03
AAF-1	4.47	4.30	3.90	3.70	3.60	5.09	4.35	4.44	4.09

^a Table III-5 Liu (1996), neat asphalt only

^b Wisneski et al. (in press)

^c This study

longer before failure occurs. The simplest way to do this is to determine the rate of increase in the viscosity (or $\ln \eta$) at road conditions through the use of Equation (1-8).

$$\frac{d \ln \eta^*_0}{dt} = \left(\frac{d \ln \eta^*_0}{dCA} \right) \cdot \left(\frac{dCA}{dt} \right) = HS \cdot R_{CA} \quad (1-8)$$

Thus, the rate of increase in viscosity can be obtained from the product of the HS and the carbonyl formation rate at the temperature of interest, 60°C (a reasonable pavement temperature in the summer). The theoretical oxidation rates and the theoretical increases in $\ln \eta^*_0$, further referred to as hardening rate (strictly only equivalent when comparing asphalts of similar viscosity), are shown in Table 7-7. The HS values collected in this study were used to determine the hardening rates for the untreated asphalts using all of the atmospheric data available. The data in Table 7-7 show several important items. First, the calculated rates obtained from the Arrhenius equation for all the atmospheric untreated asphalts are remarkably similar to the extrapolated rates obtained using only the high temperature aging data collected in this study, indicating that it may be possible to obtain an accurate value for the “true” activation energy from a limited amount of data. However, the extrapolated carbonyl rate for the untreated AAB-1 is approximately 50% higher than the carbonyl

**Table 7-7. Lime-Treated Tank Asphalt Extrapolated Road Condition
Oxidation and Hardening Rates**

Material	$R_{CA} \times 10^3$ at 60°C (CA/day)	$d \ln \eta_0^* / d t \times 10^3$ at 60°C
AAA-1 0% Ca(OH) ₂ ^a	2.15	16.3
AAA-1 0% Ca(OH) ₂	2.07	15.8
AAA-1 2% Ca(OH) ₂	1.32	9.39
AAA-1 5% Ca(OH) ₂	1.83	12.7
AAA-1 10% Ca(OH) ₂	1.63	11.3

AAB-1 0% Ca(OH) ₂ ^a	2.56	16.7
AAB-1 0% Ca(OH) ₂	3.69	24.0
AAB-1 2% Ca(OH) ₂	2.72	15.2
AAB-1 5% Ca(OH) ₂	1.92	10.4
AAB-1 10% Ca(OH) ₂	1.74	10.2

AAD-1 0% Ca(OH) ₂ ^a	1.76	17.2
AAD-1 0% Ca(OH) ₂	1.53	15.0
AAD-1 2% Ca(OH) ₂	3.66	31.7
AAD-1 5% Ca(OH) ₂	2.13	18.2
AAD-1 10% Ca(OH) ₂	2.81	25.4

AAF-1 0% Ca(OH) ₂ ^a	3.15	16.0
AAF-1 0% Ca(OH) ₂	3.40	17.3
AAF-1 2% Ca(OH) ₂	1.82	7.94
AAF-1 5% Ca(OH) ₂	2.97	13.2
AAF-1 10% Ca(OH) ₂	3.86	15.8

^a Using all experimental atmospheric data available (Liu, 1996)

rate calculated by using the Arrhenius parameters for all of the atmospheric data. This is likely a reasonable value for the error that can be expected to result from extrapolation of only the high temperature data collected in this study. The extrapolated carbonyl rates of 2.07, 3.69, 1.53, and 3.40×10^{-3} CA/day obtained using only the high temperature data collected in this study also compare favorably with the experimental 60°C rates reported by Liu (1996) of 1.95, 2.45, 1.51, and 2.58×10^{-3} CA/day for AAA-1, AAB-1, AAD-1, and AAF-1, respectively. These values further support the claim that the data collected in this study should provide extrapolated oxidation rates within 50% of the actual oxidation rate.

The second, and more important result that is illustrated in the data in Table 7-7 is that the extrapolated hardening rates are lower for the lime-treated AAA-1 and AAB-1 compared to the respective untreated materials. The extrapolated hardening rates for the lime-treated AAF-1 are also lower. The extrapolated rates for the AAD-1 materials are all higher for the lime-treated samples when compared to the untreated asphalt.

Unfortunately, any conclusions regarding the effect of lime on the road condition aging rates are ambiguous at best because the accuracy of the extrapolated rates is no better than $\pm 50\%$ of the actual rate. This is especially true for the AAD-1 and AAF-1 materials given the rate and activation energy problems previously noted for these materials. However, the data in Table 7-7 suggest that there is a strong possibility that lime will reduce the road condition hardening rate. At the very least, the data collected in the experiments described in this chapter indicate that addition of lime is not likely to be detrimental to the aging characteristics of tank asphalts.

Summary

The data collected in the experiments described in this chapter indicate that lime treatment of tank asphalts had little or no effect on any of the oxidation kinetic parameters of tank asphalts. The "initial jumps" and activation energies were largely unaffected by lime at levels up to 10% by weight. The viscosity temperature susceptibilities of the unaged samples were also largely unchanged, although there may be slight bias towards increased VTS with lime treatment. On the other hand, increased lime contents resulted in uniformly increased initial 60°C viscosities. Finally, lime treatment appeared to have a uniformly beneficial influence on the hardening susceptibilities.

However, increased lime contents did not result in increased improvement in the hardening susceptibility.

CHAPTER 8

RECYCLING STUDIES

Two separate recycling studies were performed. The first study was conducted with the primary purpose of comparing the aging performance of recycled blends produced using commercial recycling agents (CRAs), industrial supercritical fractions (ISCFs), and the Texas A&M supercritical fractions detailed in Appendix C (TAMU SCFs) as the rejuvenating agent. The second study was conducted to study the performance of recycled blends not only in terms of oxidative aging characteristics, but also in terms of strategic highway research program (SHRP) performance grading. The second study was also conducted to further investigate the use of lime as an additive in asphalt recycling and to investigate the accuracy involved in trying to extrapolate high temperature aging data to road-temperature conditions.

First Recycling Study Design

The first recycling study was conducted using AAF-AB1 as the aged asphalt and nine different rejuvenating agents. Three different CRAs, three ISCFs, and three TAMU SCFs were utilized as the rejuvenating agents. The viscosity of the aged asphalt was 55,000 dPa·s (poise). The properties of the rejuvenating agents are shown in Table 8-1. Table 8-1 also shows that the composition of the rejuvenating agents investigated in the first recycling study vary widely, with saturate contents ranging from 7 to 31% while all are very low in asphaltenes. Particularly noticeable are the high saturate contents of the ISCF B (30.8%) and the CRA C (28.0%). Table 8-1 also shows that the commercial recycling agents have extremely low viscosities (~1 poise) while the supercritical fractions are higher in viscosity. Thus, clearly it will take more supercritical fraction to reduce the viscosity of the aged asphalt to a like-new state. Lin et al. (1995b) and Peterson (1994) both suggested that dilution of the asphaltenes is desired in producing recycled blends.

The nine rejuvenating agents were blended with AAF-AB1 to obtain a viscosity ($\eta_{0,60^{\circ}\text{C}}^*$) $\pm 20\%$ of the viscosity of unaged SHRP AAF-1 asphalt with subsequent reblending to obtain a viscosity in the target range. The initial amount of rejuvenating agent was determined using the viscosity mixing rule developed in the studies described in Appendix H. In particular, the quantity

Table 8-1. First Recycling Study Rejuvenating Agent Properties

Rejuvenating Agent	$\eta_{0,60^{\circ}\text{C}}^*$	Saturates (wt%)	Asphaltenes	Aromatics (wt%) ^a
ISCF A	17.6	20.4	0.3	79.3
ISCF B	58.0	30.8	0.7	68.5
ISCF C	434.0	11.4	3.4	85.2
CRA C	1.0	28.0	0.5	71.5
CRA B	1.2	12.4	0.9	86.7
CRA A	2.4	8.7	0.7	90.6
AAF F3	67.1	14.3	0.4	85.3
YBF F3	137.4	11.0	0.1	88.9
ABM F3	627.3	7.7	0.0	92.3

^a determined by difference

of rejuvenating agent was determined using the dimensionless log viscosity (DLV) mixing rule shown in Figure H-13.

The recycled blends and the unaged SHRP AAF-1 were subjected to a slightly modified strategic highway research program (SHRP) pressure aging vessel (PAV) accelerated aging test as described in Appendix A. The slight modifications may significantly alter the absolute value of the viscosity obtained after the complete PAV test, but should not alter the relative comparison of the samples investigated in this first recycling study.

Pressure oxygen vessel (POV) aging was also conducted to investigate the effects that aging temperature may have on the ranking of the asphalts. Because only a limited amount of recycled asphalt was produced (~60 g), it was necessary to use the residues from the PAV test for the POV aging. Even so, the small amount of PAV residue limited the POV aging to three temperatures. The POV aging conditions consisted of atmospheric air pressure and temperatures of 80, 90, and 100°C. Because the samples had been previously aged in the PAV, it was assumed that the “initial jump” would not be a factor influencing the kinetics. Consequently, initial sampling times and sampling intervals of 4, 3, and 2 days were used, respectively. The properties of interest were the viscosities and the carbonyl areas.

First Recycling Study Unaged Blend Properties

A target viscosity for the recycled blends was chosen as $\pm 20\%$ of the viscosity of unaged SHRP AAF-1 so that the recycled blends could be compared not only against each other, but also against the original parent asphalt. The final recycling agent content and the final unaged blend viscosities are shown in Table 8-2. The target viscosity was obtained for four of the nine recycled blends on the first blending attempt as is indicated by the # in Table 8-2. The target viscosity was obtained after the second blending attempt for four of the remaining five recycled blends. This is a marked improvement over the results that would have been obtained using the mixing rule suggested in ASTM D4887. Figure 8-1 shows the location of blend dimensionless log viscosity (DLV) data points in relation to the data points collected in the viscosity mixing rules study described in Appendix H and the DLV data points obtained during the second set of recycling experiments which are detailed later in this chapter. The diagonal line represents the mixing rule suggested in ASTM D4887 for recycled blends. The data presented in Figure 8-1 clearly show that the data points generated in the first recycling study are well described by the DLV relationship discovered in Appendix H. Of particular importance is the fact that the ISCFs behave like CRAs and TAMU SCFs in terms of viscosity reduction.

First Recycling Study Aging Results

The aging indexes (AIs), which are calculated as the viscosity after aging divided by the viscosity before aging, for all materials after TFOT pretreatment and after subsequent PAV aging are shown in Table 8-3. The recycled blend using ISCF B was very problematic from the initial blending through the end of the PAV test. In fact, blending with this agent required multiple tries to obtain the correct initial viscosity and a low frequency limiting dynamic viscosity could not be obtained for the TFOT treated and PAV aged materials. This is likely the result of the extremely high saturate content of the AAF-AB1/ISCF B blend. Because the viscosities could not be determined for the TFOT and PAV aged ISCF B blends, the aging indexes could not be calculated.

The data in Table 8-3 show that all of the recycled blends have lower aging indexes than the parent asphalt SHRP AAF-1. Furthermore, the data show that the aging indexes of the recycled blends using CRAs are higher than the aging indexes of the blends which used supercritical fraction

Table 8-2. First Recycling Study Blend Compositions and Viscosities

Rejuvenating Agent	Composition (Asphalt/Agent) ^a	$\eta_{0,60^\circ\text{C}}^*$ (dPa·s)
NONE	N/A	1890
ISCF A	72/28 #	1900
ISCF B	61/39	2140
ISCF C	43/57	2080
CRA C	83/17	1900
CRA B	83/17	1850
CRA A	81/19	1840
AAF F3	67/33 #	2090
YBF F3	61/39 #	2000
ABM F3	44/56 #	1670

^a approximate composition (unless denoted by #)

Target viscosity achieved first attempt

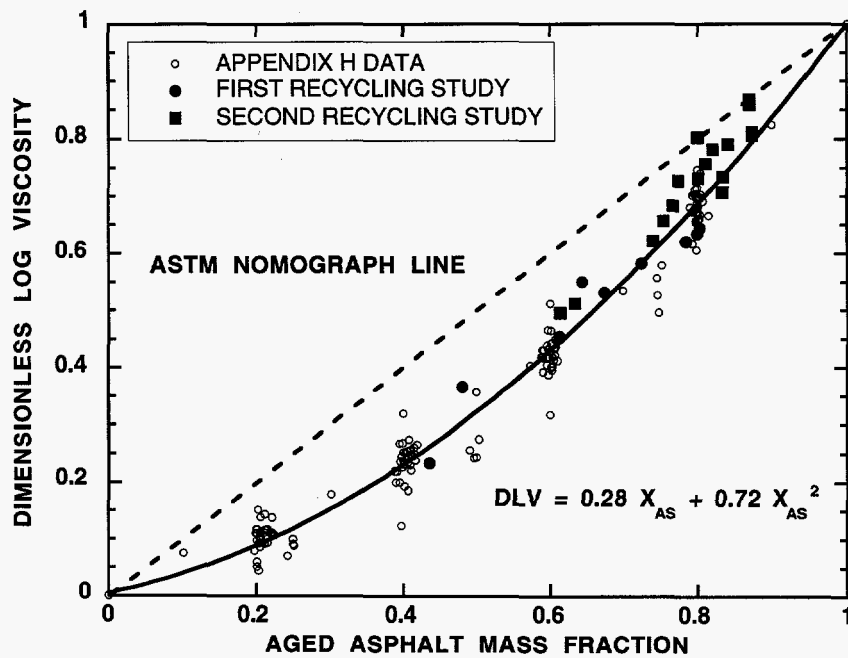


Figure 8-1. DLV plot for recycling studies.

Table 8-3. First Recycling Study Blend Aging Indexes

Rejuvenating Agent	Composition (Asphalt/Agent) ^a	Saturates (wt%) ^b	TFOT AI ^c	PAV AI ^c
NONE	N/A	12.6	2.80	12.42
ISCF A	72/28 [#]	14.5	1.68	4.21
ISCF B	61/39	19.7	N/A	N/A
ISCF C	43/57	11.9	1.67	3.89
CRA C	83/17	15.2	1.96	5.53
CRA B	83/17	12.6	1.70	4.46
CRA A	81/19	11.9	1.85	4.30
AAF F3	67/33 [#]	13.2	1.67	3.85
YBF F3	61/39 [#]	12.0	1.50	3.00
ABM F3	44/56 [#]	9.9	1.59	2.93

^a approximate composition (unless denoted by [#])

^b calculated as weighted sum of component saturate contents

^c AI = aging index, the viscosity after aging/unaged viscosity

[#] Target viscosity achieved first attempt

rejuvenating agents, either those obtained from industrial sources or those produced in the experiments detailed in Appendix C. Finally, the aging indexes for the TAMU SCF blends are the lowest of all the aging indexes.

The aging indexes, especially the PAV aging indexes, are strongly correlated with the rejuvenating agent content in the blends, regardless of what class of rejuvenating agent was used. The reasons for this are clear. The relatively larger proportion of supercritical fractions (more than 50% SCF in some blends examined in this study) in the recycled blends compared to the proportion of commercial recycling agents (approximately 18% CRA in all blends examined in this study) in the recycled blends results in much more dilution of the aged asphalt. Thus, the data indicate that dilution of the aged asphalt seems to play an important role in decreasing the hardening behavior of recycled asphalts, confirming the results of Lin et al. (1995b) and Peterson (1994). The aging indexes are also strongly correlated with the saturate content of the blends. However, the correlation with blend

saturate content is not “universal” across rejuvenating agent classes. The lower aging indexes for the recycled for the TAMU SCF blends compared to the ISCF blends are likely due to the narrower cuts that are obtained by fractionating into seven distinct fractions (eight total) rather than the two or three cuts that are produced industrially. Unfortunately, the extremely strong correlation between rejuvenating agent content and aging indexes suggest that the asphaltene dilution effects can not be separated from the composition effects such as the aromatic/saturate ratio in the rejuvenating agent.

The residues from the PAV aging test were then distributed into POV trays and subsequently aged at 80, 90, and 100°C using atmospheric air to determine aging kinetics. As discussed in Chapter 7, the use of atmospheric air pressure allows the use of the simplified kinetic expression shown in Equation (1-6).

$$R_{CA} = A e^{-E/RT} \quad (1-6)$$

Once again, an Arrhenius plot of the logarithm of the carbonyl formation rate (R_{CA}) versus the reciprocal of the product of the ideal gas constant times the aging (absolute) temperature ($1/RT$) should yield a straight line, the slope of which is the activation energy (E).

After aging, carbonyl area measurements were performed on all of the samples and viscosity measurements were performed on enough samples (approximately one-half of the samples) to determine HS values for each mixture. The one exception to this was the rejuvenated blend using ISCF B as the softening agent. Because viscosity measurements did not yield low frequency limiting values for the TFOT and PAV aged samples, viscosity measurements were not performed on the POV aged samples. As such, the HS was not determined for this blend. Although the new data obtained in the experiments described in Chapter 7 and the data previously reported (Liu et al., 1996; Liu, 1996) can be used to determine the POV time which is equivalent to the PAV aging for the AAF-1 asphalt, no such calculations can be performed for the recycled blends. As such, an accurate CA_0 value can not be determined for the recycled blends.

Figure 8-2 shows a plot of CA versus time (time = 0 arbitrarily set to be when the POV aging started) for the AAF-AB1/ISCF A blend. The slopes of each of the three lines are equal to the

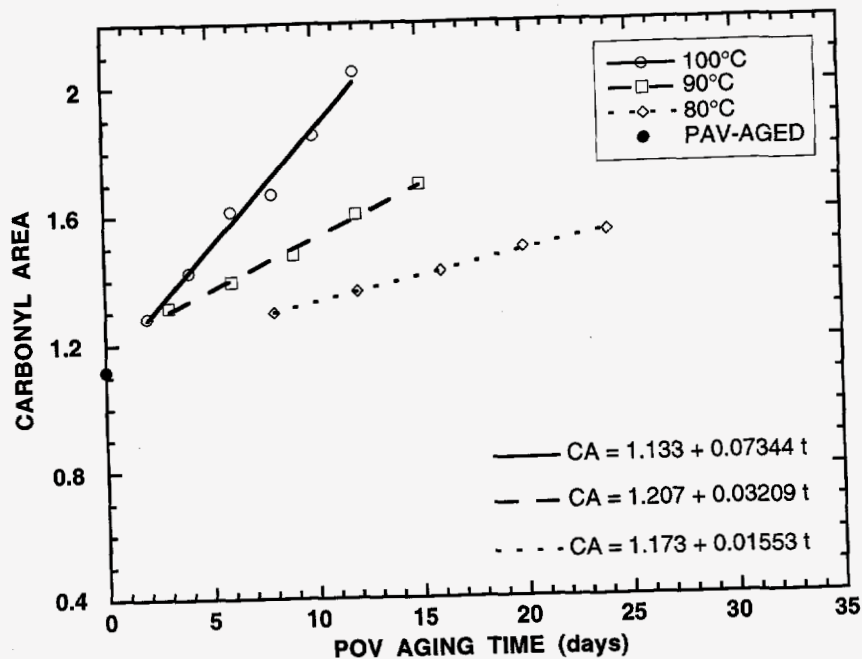


Figure 8-2. Carbonyl growth for AAF-AB1/ISCF A.

oxidation rate (as measured by CA) at the various temperatures. Figure 8-3 shows the Arrhenius plot for the AAF-AB1/ISCF blends. The limited data presented in Figure 8-3 are well described by Equation (1-7), within experimental scatter. Figure 8-4 is a hardening susceptibility plot for the PAV pre-aged AAF-AB1/ISCF blends. The slope of the line produced from the data in Figure 8-4 is the HS. The activation energies and HS values for all of the samples are reported in Table 8-4.

The data in Table 8-4 show that the activation energies vary widely for the AAF-1 materials investigated in this study. Of particular importance is the fact that the activation energy of the original asphalt is lower than the activation energies of all of the recycled blends. This will be manifested in higher oxidation rates at road conditions, as will be shown later. The data in Table 8-4 also show that the activation energies are not correlated with either the saturate content or the rejuvenating agent, and thus, the asphaltene content in the blends.

The HS values are more variable, with some recycled materials having higher (worse) HS

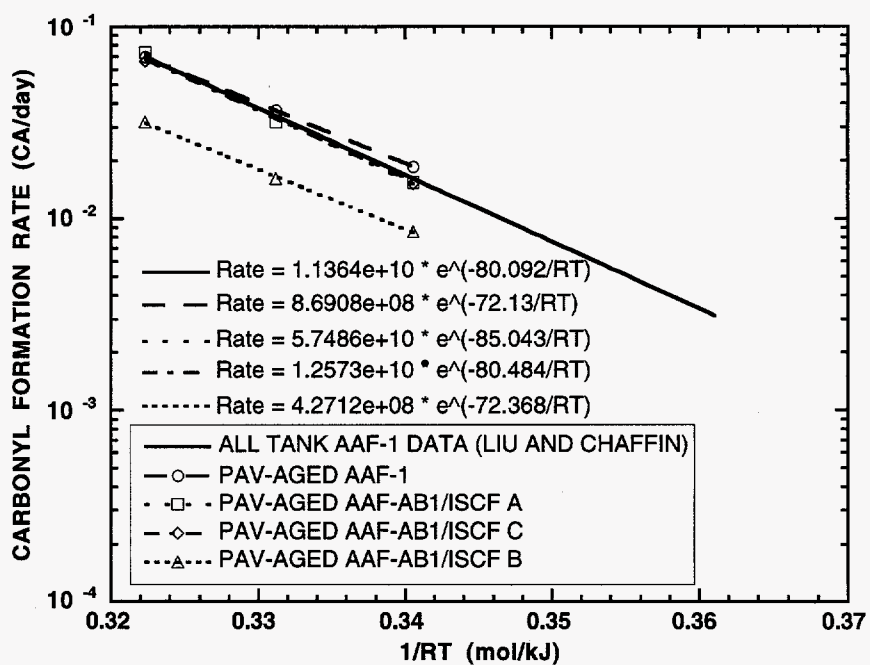


Figure 8-3. Arrhenius plots for AAF-AB1/ISCF blends.

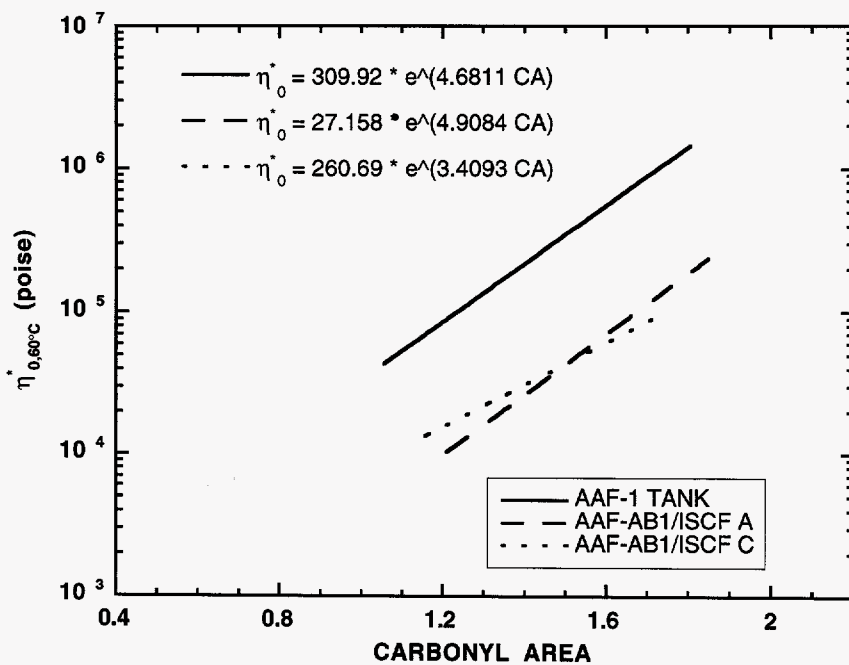


Figure 8-4. Hardening susceptibilities for AAF-AB1/ISCF blends.

Table 8-4. First Recycling Study Aging Parameters

Rejuvenating Agent	Composition (Asphalt/Agent) ^a	Saturates (wt%) ^b	E _A (kJ/mol)	HS
NONE	N/A	12.6	72.1	4.48
ISCF A	72/28 [#]	14.5	85.0	4.91
ISCF B	61/39	19.7	72.5	N/A
ISCF C	43/57	11.9	80.5	3.41
CRA C	83/17	15.2	83.3	5.11
CRA B	83/17	12.6	93.4	4.70
CRA A	81/19	11.9	88.9	3.49
AAF F3	67/33 [#]	13.2	74.4	3.53
YBF F3	61/39 [#]	12.0	98.3	3.20
ABM F3	44/56 [#]	9.9	83.1	2.22

^a approximate composition (unless denoted by #)

^b calculated as weighted sum of component saturate contents

values and some having lower (better) HS values than the original asphalt. Using the data in Tables C-1, 8-1, and 8-2, the approximate saturate contents in the materials were calculated. This is justified by the HPLC study conducted using several of the aged asphalt/softening agent pairs investigated in Appendix C which showed that the saturate content in blends is equal to the weighted sum of the saturate contents in the two blend components. The HS correlates well with the rejuvenating agent content for the various classes of rejuvenating agents. However, the variability in HS is strongly correlated with the saturate content in the material, regardless of rejuvenating agent. In fact, Figure 8-5 indicates that the correlation between HS and saturate content is also valid for the tank AAF-1 asphalt. The correlation seen in Figure 8-5 agrees with statements by several researchers (Epps et al., 1980; Peterson et al., 1994; Lin et al., 1996) that the saturate content should be minimized to produce good quality recycled blends.

The combination of HS and CA rate (extrapolated) at 60°C yields the extrapolated rate of ln η increase, or simply the hardening rate, at an aging temperature of 60°C. As was the case with the aging indexes determined from the TFOT and PAV tests, the data in Table 8-5 indicate that all of the

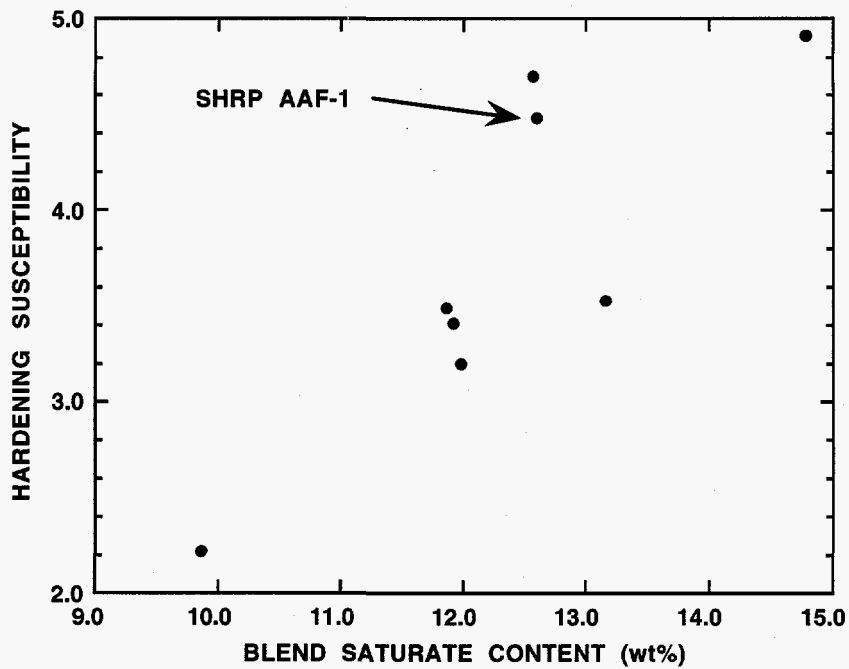


Figure 8-5. HS versus saturate content for the first recycling study materials.

Table 8-5. First Recycling Study Extrapolated Rates

Rejuvenating Agent	$R_{CA} \times 10^3$ at 60°C (CA/day) ^a	$d \ln \eta_0^* / d t \times 10^3$ at 60°C ^a
NONE	4.27	19.1
ISCF A	2.67	13.1
ISCF B	1.92	N/A
ISCF C	3.02	10.3
CRA C	2.61	13.3
CRA B	2.33	11.0
CRA A	2.41	8.40
TAMU SCF: AAF F3	3.56	12.6
TAMU SCF: YBF F3	1.62	5.18
TAMU SCF: ABM F3	2.80	6.21

^a subject to errors associated with extrapolation

recycled materials will harden more slowly than the original asphalt at road temperatures. This results mostly from the improvements in activation energy, which results in lower oxidation rates at 60°C road temperatures ($1/RT = 0.36 \text{ mol/kJ}$) as shown in Figure 8-6.

The data in Table 8-5 also indicate that the extrapolated hardening rates ($d \ln \eta_o^*/dt$) of the recycled asphalts which were softened with supercritical fractions are similar to the hardening rates of the recycled asphalts softened with commercial recycling agents. In fact, the two best hardening rates were obtained for recycled asphalts using TAMU SCFs. Once again, this can likely be attributed to the narrow cuts that are obtained by fractionation into seven fractions as opposed to two or three. The extrapolated hardening rates are correlated with rejuvenating agent content, but only for each class of rejuvenating agents. As discussed in Chapter 7, these results are presented with some caution due to the extreme variability that may result both from estimation of activation energy from only three temperatures and from significant extrapolation.

The relative rankings based on the TFOT and PAV aging indexes and the extrapolated hardening rates are given in Table 8-6. There are relatively minor differences between the actual values of the data, but the relative rankings might unnecessarily slight the CRA A and the CRA B. The reasonable agreement between the PAV relative rankings and the extrapolated hardening rate rankings implies that it may be possible to select the proper rejuvenating agent *for a given aged asphalt* based on the PAV aging index. This first recycling study reinforces the conclusions of Liu (1996) that the PAV test generally agrees with kinetic data. However, the stronger agreement between PAV aging index and ambient aging for recycled asphalts is likely due to the fact that the recycled asphalts from a given aged asphalt are much more similar than different tank asphalts.

Significance of Neat AAF-1 Data

The data collected on the original asphalt AAF-1 were compared to the atmospheric aging data reported for RTFOT pre-treated and neat AAF-1 by Liu (1996), and in Chapter 7. Notably, the carbonyl formation rates determined for the PAV pre-aged AAF-1 and the carbonyl rates obtained from atmospheric aging conditions reported by Liu et al. (1996), Liu (1996), and in the lime studies in Chapter 7 are all consistent as shown in Figure 8-7. Figure 8-7 clearly shows that the rate data for the PAV pre-aged AAF-1, RFTOT pre-treated material, and neat asphalt are highly consistent. The

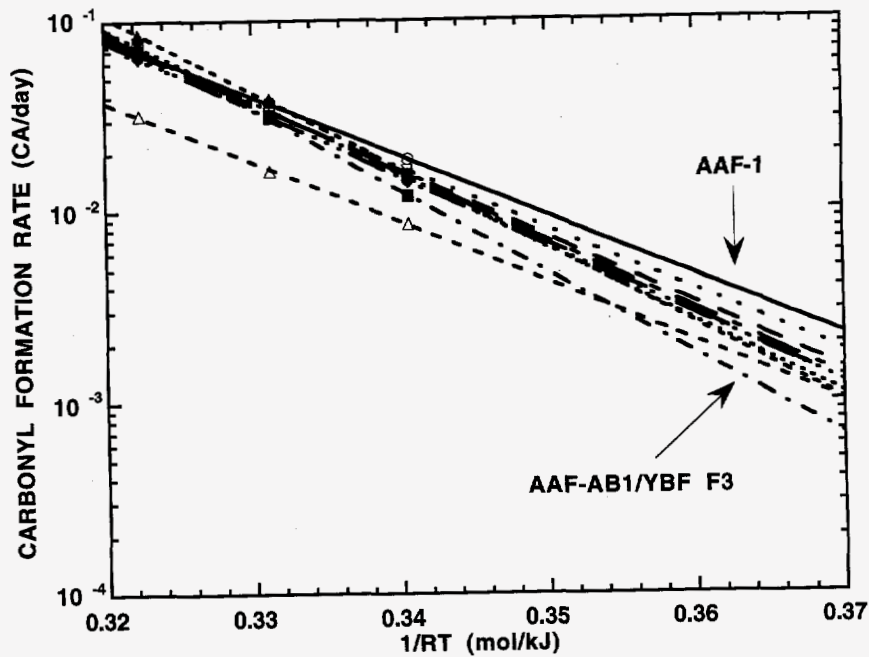


Figure 8-6. Arrhenius plots for all of the first recycling study materials.

Table 8-6. Relative Rankings of First Recycling Study Asphalts

Rejuvenating Agent	TFOT Aging Index (1 = lowest)	PAV Aging Index (1 = lowest)	$d \ln \eta^* / d t$ at 60°C (1 = lowest)
NONE	9	9	9
ISCF A	5	5	7
ISCF B	--	--	--
ISCF C	4	4	4
CRA C	8	8	8
CRA B	6	7	5
CRA A	7	6	3
AAF F3	3	3	6
YBF F3	1	2	1
ABM F3	2	1	2

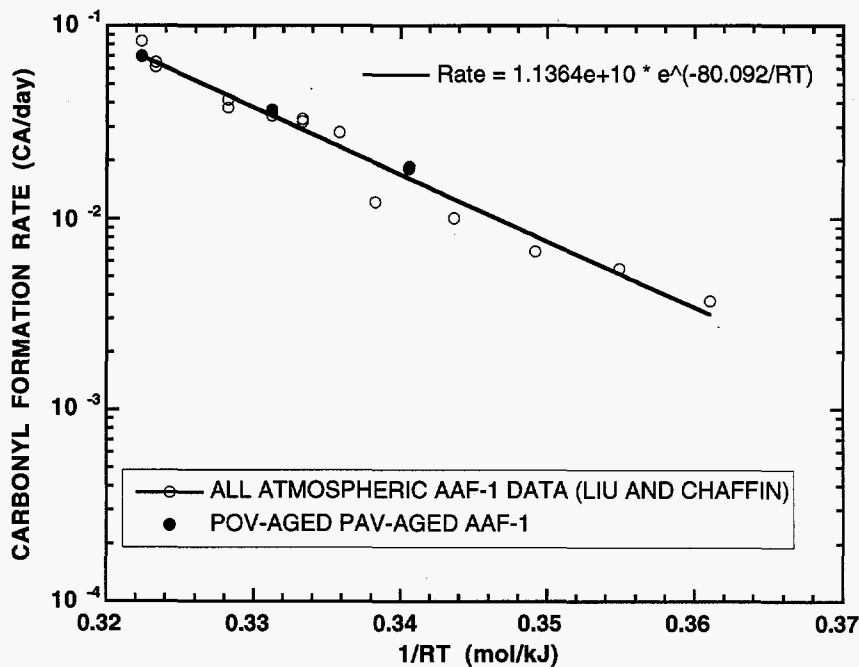


Figure 8-7. Arrhenius plot for all atmospheric AAF-1 aging experiments.

activation energy for the PAV pre-aged AAF-1 of 72.1 kJ/mol is similar to the activation energy of 80.2 kJ/mol determined using all of the atmospheric rate data available (Liu et al., 1996; Chapter 6 of this report). The 8 kJ/mol difference is rather small given the discussions presented in Chapter 7.

Additionally, the HS value of 4.48 for the PAV pre-aged AAF-1 in this experiment is within the range of HS values reported in Table 7-6 for tank AAF-1 and is similar to the HS value of 4.62 reported by Liu (1996) for RTFOT pre-treated. The consistency of the activation energy and the HS prove conclusively for the first time that the aging history of the material has little, if any, influence on the kinetic parameters. (Obviously, if the samples have ever been subjected to extreme oxidation conditions such as 500°F, this may alter this conclusion). This means that it may be *possible* to extract an asphalt from a pavement sample and subject it to the POV test to determine kinetic parameters. From these kinetic parameters and the HS, it may be possible to accurately predict the future condition of the pavement. This is a pleasing and expected, but unintended, result of this experiment.

Second Recycling Study Design

The second recycling study involved the same four asphalts studied in Chapter 7: AAA-1, AAB-1, AAD-1, and AAF-1. In addition, three different viscosity levels of aged AAB-1 were utilized. Thus, a total of six aged asphalts were used. Each aged asphalt was blended with at least two rejuvenating agents, and each viscosity level of aged AAB-1 was blended with three different viscosity level rejuvenating agents. The properties of the materials examined in the second recycling study are listed in Table 8-7. To examine the effects of lime on the properties of recycled asphalts, each aged asphalt/rejuvenating agent pair was also blended with 5% lime. However, instead of mixing one large batch of each recycled blend and then dividing the material for blending with lime, the lime blends were constructed separately from the control blends. Seventeen different recycled asphalts were produced at two different lime levels to yield a total of thirty-four recycled blends.

A viscosity of 5000 poise, a reasonable value of the viscosity of an AC-20 after rolling thin film oven treatment (RTFOT), and a likely target viscosity for a recycled asphalt in Texas was chosen as the target viscosity. The amount of rejuvenating agent was estimated using the DLV mixing rule developed in Appendix H. To make this set of experiments more realistic, no reblending was performed to obtain the target viscosity. That is, the recycled blend obtained from the initial blending was utilized regardless of what the viscosity of the unaged blend was. Blending was accomplished in ½ pint cans and mixing was accomplished using the drill press and mixing paddle.

A sufficient quantity (at least 150 g) of each blend was produced to perform both POV aging and PAV aging on the unaged recycled blends. In other words, it was not necessary to POV age the PAV aged residues. The standard PAV aging conditions of 300 psia air and 100°C for 20 hours were utilized. The samples were POV aged on a rotating schedule at 80, 85, 90, 95, and 100°C using atmospheric air pressure for varying time periods. In addition, six POV trays of each asphalt were aged in the environmental room controlled at 60°C to verify extrapolation of high temperature POV aging rates. The 60°C samples were pre-aged at 100°C for at least 5 days to insure that the "initial jump" would not be a factor. The typical atmospheric aging sampling times are shown in Table 8-8.

The primary properties of interest were the 60°C viscosities ($\eta_{0,60^\circ\text{C}}^*$) and the carbonyl areas. However, rheological properties were also measured on all of the unaged materials to determine if the choice of rejuvenating agent and/or the presence of lime greatly influences the viscosity

Table 8-7. Second Recycling Study Material Properties

Material	$\eta_{0.60^\circ\text{C}}^*$ (poise)	Saturates, %	Asphaltenes, %	Aromatics, %
AAA-AB8	37,000	11.2		
AAF-AB2	22,000	11.8	23.5	64.7
AAD-AB3	28,000	7.4		
AAB-AB1	114,000	12.5		
AAB-AB2	85,000	12.5		
AAB-AB3	38,000	12.5		
CRA D	2.0	19.0	0.0	81.0
CRA B	1.8	12.4	0.9	86.7
ISCF C	434.0	11.4	3.4	85.2
AAF F2	11.7	23.5	0.4	76.2
AAA F2	14.5	20.0	0.2	79.8
YBF F2	29.2	18.2	0.2	81.7
AAF F3	67.1	14.3	0.4	85.4
AAA F3	99.2	11.0	0.4	88.6
ABM F5	115.8	11.5	0.0	88.5
YBF F3	137.4	11.0	0.1	88.9

^a tank values except AAF-AB2

^b determined by difference

Table 8-8. Second Recycling Study Aging Conditions

Aging Temperature (°C)	Initial Sampling (days)	Sampling Interval (days)
80	12	4
85	10	3
90	10	3
95	5	2
100	5	2
60 ^a	21	21

^a Samples pre-aged at 100°C to overcome the “initial jump” region

temperature susceptibility (VTS) In addition, each blend was performance graded according to the SHRP high temperature $G^*/\sin \delta$ specifications for RTFOT residues and the SHRP low temperature $S(t)$ and m -value specifications for PAV residues.

Second Recycling Study Unaged Blend Properties

A target viscosity for the recycled blends was chosen as 5000 poise, a typical 60°C viscosity for RTFOT aged asphalt. The recycling agent content and the actual unaged blend viscosities are shown in Table 8-9. The data in Table 8-9 show that only four of the seventeen untreated recycled blends were within the typical acceptable error limits on viscosity specifications (at least for tank asphalts) of $\pm 20\%$ of the mean value. In fact, the average viscosity of the untreated recycled blends is 6910 poise. Two of the three highest viscosities were obtained for the AAD-AB3 blends with AAA F2 and AAF F2. The viscosity measurements of the lime-treated POV aged samples of these blends also resulted in highly scattered hardening susceptibilities (HS), as discussed later. While it is possible that there was some undetermined problem with the AAD-AB3 aged asphalt, it is likely that the high initial viscosities of these two blends result from the high saturate contents in the rejuvenating agents which results in poor maltene solvation, as suggested in the literature (Altgelt and Harle, 1975; Lin et al., 1996). Either way, the lack of success in achieving the target viscosity in the second recycling study is rather disappointing. However, the errors were on the side of caution (slightly more viscous than desired). Figure 8-1 shows the location of blend dimensionless log viscosity (DLV) data points in relation to the data points collected in the viscosity mixing rules study described in Appendix H and the DLV data points obtained during the first set of recycling experiments. The diagonal line represents the mixing rule suggested in ASTM D-4887 for recycled blends. Figure 8-1 shows that the DLV data points obtained during this study lie much closer to the ASTM nomograph line than do any of the previous data. The reasons for this are not clear.

Perhaps the most surprising trend shown in Table 8-9 is that the lime-treated blends had lower viscosities than the control blends for all of the blends which used aged AAA-1, AAD-1, and AAB-1. In fact, the addition of lime caused only minor increases in the viscosities for the blends using aged AAF-1. This is in stark contrast to the trends noted in Chapter 7 for lime-treated tank asphalts where the addition of lime caused the viscosities of the unaged asphalts to increase. The data Wisneski

Table 8-9. Second Recycling Study Blend Compositions and Viscosities

Blend	Composition (Asphalt/Agent)	Saturates (wt%) ^a	$\eta_{0,60^\circ\text{C}}^*$ (dPa·s)	
			0	5
Nominal Ca(OH) ₂ Content (wt%)				
AAA-AB8/AAA F3	80/20	11.2	7100	6930
AAA-AB8/YBF F3	77/23	11.2	7910	7470
AAAF-AB2/AAA F2	87/13	12.9	5330	5700
AAAF-AB2/YBF F3	82/18	11.7	7160	7400
AAD-AB3/AAAF F2	87/13	9.5	10,000	9450
AAD-AB3/AAA F2	87/13	9.0	9600	9070
AAD-AB3/ABM F5	81/19	8.2	7350	7200
AAD-AB3/YBF F3	80/20	8.1	9700	9180
AAB-AB1/CRA B	83/17	12.5	3730	3080
AAB-AB1/YBF F2	75/25	13.9	6700	5240
AAB-AB1/ISCF C	61/39	12.1	6820	6500
AAB-AB2/CRA D	83/17	10.4	4950	4070
AAB-AB2/AAAF F3	74/26	13.0	5670	4700
AAB-AB2/ISCF C	63/37	12.1	6430	6000
AAB-AB3/CRA D	87/13	10.9	5600	4860
AAB-AB3/AAAF F2	84/16	14.3	7100	5900
AAB-AB3/YBF F3	77/23	12.2	6280	5690

^a Calculated as weighted sum of component saturate contents

(1995) reported are inconclusive regarding the effect of lime on the viscosity of unaged recycled asphalts. The volume of data shown indicate that the lime likely will reduce the viscosity of unaged recycled asphalts. It has been suggested (Wisneski et al., in press) that the lime may hinder the association of oxidation products (aggregation of asphaltenes). In fact, the interference with

association is likely responsible for the lower HS values noted in Chapter 7 and by Wisneski et al. (In press) for lime-treated tank asphalts. The relation to the current observations is that it is possible that the lime is effectively breaking up the asphaltene aggregates present in the aged asphalt. Wisneski et al. (in press) did hypothesize this, but could not prove it.

Low frequency limiting dynamic viscosity (η_0^*) measurements at 0, 10, 25, and 40°C were also measured on the thirty-four unaged blends. The data were modeled using the Andrade equation (Andrade, 1930) as described in Chapter 1.

$$\ln \eta_0^* = A_{\text{vis}} + \frac{E_{\text{vis}}}{RT} \quad (1-9)$$

The slope of a plot of viscosity versus the reciprocal of the product of the ideal gas constant times the absolute temperature ($1/RT$) is the viscosity activation energy E_{vis} , one measure of the viscosity temperature susceptibility (VTS). The E_{vis} plot for all of the AAA-AB8 blends is shown in Figure 8-8. Similar plots were constructed for the other blends. The E_{vis} values for the unaged

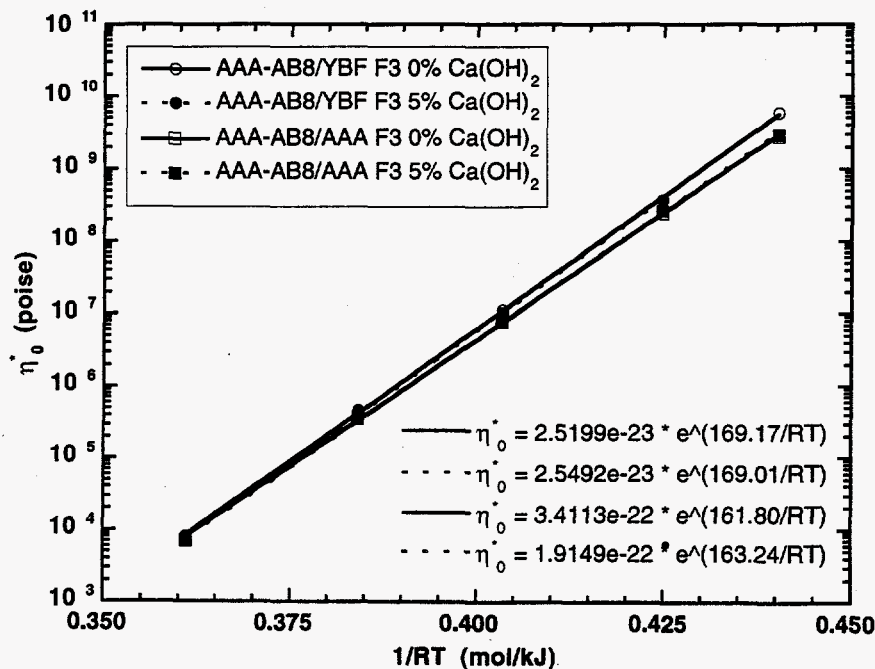


Figure 8-8. E_{vis} for second recycling study AAA-AB8 blends.

second recycling study blends are shown in Table 8-10 along with the aged asphalt content and the saturate content in the blend. Figure 8-8 and the data in Table 8-10 indicate that the E_{vis} varies only slightly between blends using the same aged asphalt, with the maximum deviation being less than 10%. However, it appears that E_{vis} generally increases (gets worse) for the untreated blends as the rejuvenating agent content increases for blends using the same aged asphalt. Note that as the recycling agent content increases, the asphaltene content decreases through dilution because all of the rejuvenating agents are virtually asphaltene free. Comparing the E_{vis} values in Table 8-10 for the unaged recycled asphalts to those reported in Table 7-3 for the unaged tank asphalts, it can be seen that the E_{vis} values for the recycled blends are much higher (worse) for the recycled blends. These results contradict statements made by Peterson et al. (1994). However, this trend is expected based on the data reported by Corbett (1979) that asphaltenes contribute to good temperature susceptibility. While the results contradict statements made by Peterson et al. (1994), analysis of their data indicate that they also measured worsening temperature susceptibility with increased rejuvenating agent content.

The data in Table 8-10 indicate that there is no apparent correlation between the blend saturate content and the E_{vis} . The direct correlation between rejuvenating agent content (asphaltene content) and the E_{vis} and the lack of an apparent correlation between saturate content and the E_{vis} might suggest that there is no correlation between the aromatic content and the E_{vis} . This is a highly surprising result of these experiments given that Liu (1996) reported differences of over 60 kJ/mol in the E_{vis} of aromatic fractions from AAA-1 and AAG-1. At least some of this 60 kJ/mol difference should have been manifested in the E_{vis} values for the AAD-AB3/AAA F2 and AAD-AB3/ABM F5 blends. However, the E_{vis} values for these two blends are the same, within experimental error. This apparent lack of correlation with aromatic content, and therefore aromatic composition, is also in direct contrast to the results reported by Corbett (1979) suggesting that the naphthene aromatics contribute to good temperature susceptibility. Furthermore, Corbett suggested that lower molecular weight naphthene aromatics and saturates, which the rejuvenating agents certainly contain (Table C-3), likely contribute to better temperature susceptibility. However, Corbett attributed the lower molecular weight effects to reduced dilution of asphaltenes rather than strictly composition influences. Thus, the VTS data indicate that dilution of the asphaltenes existing in the aged asphalt

Table 8-10. VTS Values for the Unaged Second Recycling Study Blends

Blend	Composition (Asphalt/Agent)	Saturates (wt%) ^a	E _{vis}	
			Nominal Ca(OH) ₂ wt%: 0	5
AAA-AB8/AAA	80/20	11.2	161.8	163.2
AAA-AB8/YBF	77/23	11.2	169.2	157.1
AAAF-AB2/AAA	87/13	12.9	174.5	188.6
AAAF-AB2/YBF	82/18	11.7	193.2	188.7
AAD-AB3/AAAF	87/13	9.5	177.5	183.5
AAD-AB3/AAA	87/13	9.0	166.8	172.4
AAD-AB3/ABM	81/19	8.2	164.2	164.7
AAD-AB3/YBF	80/20	8.1	175.3	174.1
AAB-AB1/CRA	83/17	12.5	175.3	174.1
AAB-AB1/YBF	75/25	13.9	177.3	179.6
AAB-AB1/ISCF	61/39	12.1	177.9	177.5
AB-AB2/CRA D	83/17	10.4	173.7	167.9
AAB-AB2/AAAF	74/26	13.0	180.3	183.8
AAB-AB2/ISCF	63/37	12.1	187.4	190.6
AAB-AB3/CRA	87/13	10.9	172.6	171.7
AAB-AB3/AAAF	84/16	14.3	179.3	180.4
AAB-AB3/YBF	77/23	12.2	181.9	188.7

^a Calculated as weighted sum of component saturate contents

may not be desirable.

The second trend noted in Table 8-10 is that the lime treatment has little if any influence on the E_{vis} of a particular recycled blend. This observation is in agreement with the observation noted in Chapter 7 for lime-treated tank asphalts. Thus, it appears that lime has little or no effect on the E_{vis} of unaged asphalts, either tank asphalts or recycled asphalts. In summary, the only influence on E_{vis} found in these experiments is a slight correlation between rejuvenating agent content and E_{vis} .

Second Recycling Study Aging Results

The recycled blends were subjected to the SHRP PAV aging test, high temperature POV aging, and 60°C environmental room aging. Because the viscosities of the recycled blends were all similar to the viscosities of RTFOT-aged AC-20 samples, the recycled blends were not subjected to RTFOT aging prior to being PAV-aged. The PAV aging indexes for the second recycling study are shown in Table 8-11. The aging indexes generally decrease with increasing rejuvenating agent content for each aged asphalt. Thus, the PAV aging indexes indicate, once again, that dilution of asphaltenes may be an important factor to consider in recycling. In addition, without exception, the lime-treated blends had lower aging indexes than the control samples. Although the initial viscosities were not equivalent, this indicates that the hardening rates for the lime-treated recycled blends are below those of the untreated blends, sometimes substantially so, at least at PAV conditions.

The recycled blends were also subjected to POV aging and aging at 60°C using atmospheric conditions. The main purposes of these aging experiments was to determine the kinetic parameters of the various asphalts and to determine how accurately the high temperature kinetic data could be used to predict the road condition aging (60°C). The carbonyl growth for the untreated AAA-AB8/YBF F3 blends aged at 80 to 100°C is shown in Figure 8-9. The 60°C carbonyl growth for both the untreated and 5% lime-treated AAA-AB8/YBF F3 blends is shown in Figure 8-10. It should be noted that the samples aged at 60°C had been pre-aged for approximately five days in the POVs at 100°C before being transferred to the 60°C environmental room. As such, the time at the origin has been arbitrarily set to be the time that the environmental room aging began.

Table 8-11. Second Recycling Study PAV Aging Indexes

Blend	Composition (Asphalt/Agent)	Saturates (wt%) ^a	PAV Aging Index ^b	
			0	5
Nominal Ca(OH) ₂ Content (wt%)			0	5
AAA-AB8/AAA F3	80/20	11.2	2.73	1.99
AAA-AB8/YBF F3	77/23	11.2	3.03	2.25
AAF-AB2/AAA F2	87/13	12.9	2.46	2.07
AAF-AB2/YBF F3	82/18	11.7	2.09	1.85
AAD-AB3/AAF F2	87/13	9.5	5.33	4.13
AAD-AB3/AAA F2	87/13	9.0	4.66	3.72
AAD-AB3/ABM F5	81/19	8.2	3.35	2.96
AAD-AB3/YBF F3	80/20	8.1	4.35	3.59
AAB-AB1/CRA B	83/17	12.5	3.51	2.09
AAB-AB1/YBF F2	75/25	13.9	3.43	2.00
AAB-AB1/ISCF C	61/39	12.1	3.08	2.37
AAB-AB2/CRA D	83/17	10.4	4.55	2.46
AAB-AB2/AAF F3	74/26	13.0	3.90	2.49
AAB-AB2/ISCF C	63/37	12.1	3.89	3.00
AAB-AB3/CRA D	87/13	10.9	3.50	2.28
AAB-AB3/AAF F2	84/16	14.3	3.66	2.47
AAB-AB3/YBF F3	77/23	12.2	3.14	2.21

^a Calculated as weighted sum of component saturate contents

^b AI = aging index, viscosity after aging/unaged viscosity

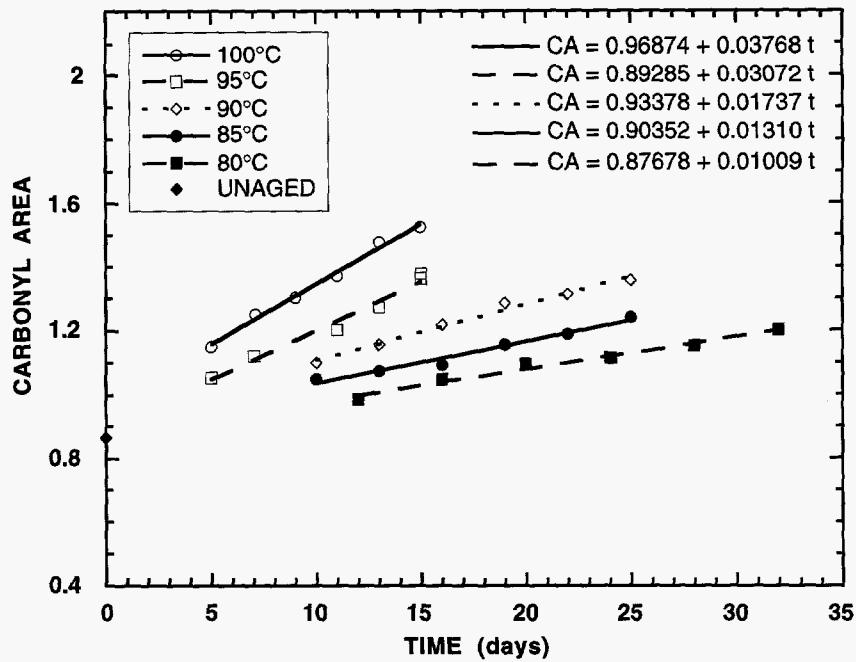


Figure 8-9. POV carbonyl growth for untreated AAA-AB8/AAA F3.

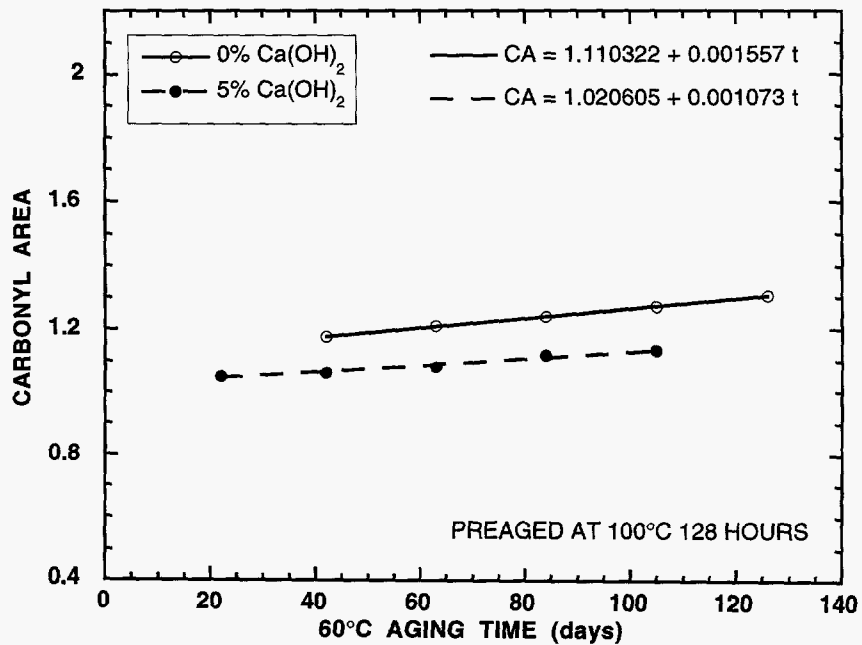


Figure 8-10. Road condition carbonyl growth for AAA-AB8/AAA F3 blends.

As expected, the carbonyl growth is linear with respect to time for all blends and at all temperatures. Furthermore, the linear regressions shown in Figure 8-9 indicate that the CA_0 values are temperature independent, within experimental scatter. The carbonyl areas of the unaged samples (CA_{unaged}), the average CA_0 values from the high temperature aging, and the difference between the two are shown in Table 8-12. If the data in Table 8-12 are compared to the data in Table 7-4, it is readily apparent that the "initial jumps" for the recycled blends are far smaller in magnitude than those for tank asphalts. This is expected because the old asphalt which makes up at least 61% of each blend has already undergone the aging responsible for its "initial jump" and only the rejuvenating agent will contribute to the "initial jump" in the recycled blend.

The data in Table 8-12 also indicate that the lime treatment has relatively little effect on the "initial jump" although there may be a slight bias towards a decrease in the initial jump. However, the scatter in the data prevent making firm conclusions, especially since the presence of 5% lime is not uniformly apparent from the carbonyl areas of the unaged blends. The general lack of an "initial jump" in the recycled blends indicates that PAV aging is not going to be greatly affected by the occurrence of an "initial jump". As a result, one might expect that relative rankings based on PAV aging indexes might be more accurate for recycled asphalts than for tank asphalts. However, the complications of pressure on the aging kinetics may still result in some differences.

The Arrhenius plots of both the untreated and 5% lime-treated AAA-AB8/YBF F3 carbonyl rates are shown in Figure 8-11 along with the Arrhenius plot of all of the AAA-1 tank atmospheric rate data. The reaction activation energies for all blends are tabulated in Table 8-13. At this time, a very important point should be noted. The activation energies reported in Table 8-13 have been determined using *only* the carbonyl rates for aging at 80, 85, 90, 95, and 100°C, as is noted on the Arrhenius plots. This is an important distinction because inclusion of the 60°C rates into the regression will severely overweight the 60°C rates, practically forcing the curve fit to pass through the 60°C data. This is undesirable because one of the main purposes of these experiments was to determine how accurately high temperature aging data can predict road condition aging.

The data in Table 8-13 indicate that the choice of rejuvenating agent can have an influence on the activation energies, as was the case in the first recycling study. This can be seen most clearly

Table 8-12. Second Recycling Study "Initial Jump" Data

Blend Nominal Ca(OH) ₂	CA _{0,ave}		CA _{unaged}		CA ₀ - CA _{unaged}	
	0	5	0	5	0	5
AAA-AB8/AAA F3	0.920	0.857	0.865	0.848	0.055	0.009
AAA-AB8/YBF F3	0.191	0.889	0.869	0.853	0.023	0.036
AAAF-AB2/AAA F2	0.929	0.921	0.841	0.808	0.088	0.113
AAAF-AB2/YBF F3	0.927	0.917	0.819	0.825	0.108	0.092
AAD-AB3/AAF F2	1.046	0.996	1.004	0.953	0.042	0.044
AAD-AB3/AAA F2	1.055	0.982	1.016	0.989	0.040	-0.007
AAD-AB3/ABM F5	1.066	1.045	1.042	1.001	0.024	0.044
AAD-AB3/YBF F3	1.020	0.971	0.991	0.970	0.029	0.002
AAB-AB1/CRA B	1.117	1.095	1.131	1.098	-0.014	-0.003
AAB-AB1/YBF F2	1.104	1.007	1.024	1.022	0.080	-0.014
AAB-AB1/ISCF C	1.051	0.967	0.948	0.940	0.103	0.028
AAB-AB2/CRA D	1.110	1.077	1.094	1.070	0.015	0.008
AAB-AB2/AAF F3	1.121	1.003	0.987	0.977	0.135	0.026
AAB-AB2/ISCF C	1.075	1.057	0.953	0.949	0.122	0.108
AAB-AB3/CRA D	1.093	1.069	1.002	0.977	0.091	0.092
AAB-AB3/AAF F2	1.050	0.992	0.922	0.920	0.128	0.072
AAB-AB3/YBF F3	1.020	0.969	0.919	0.912	0.101	0.057

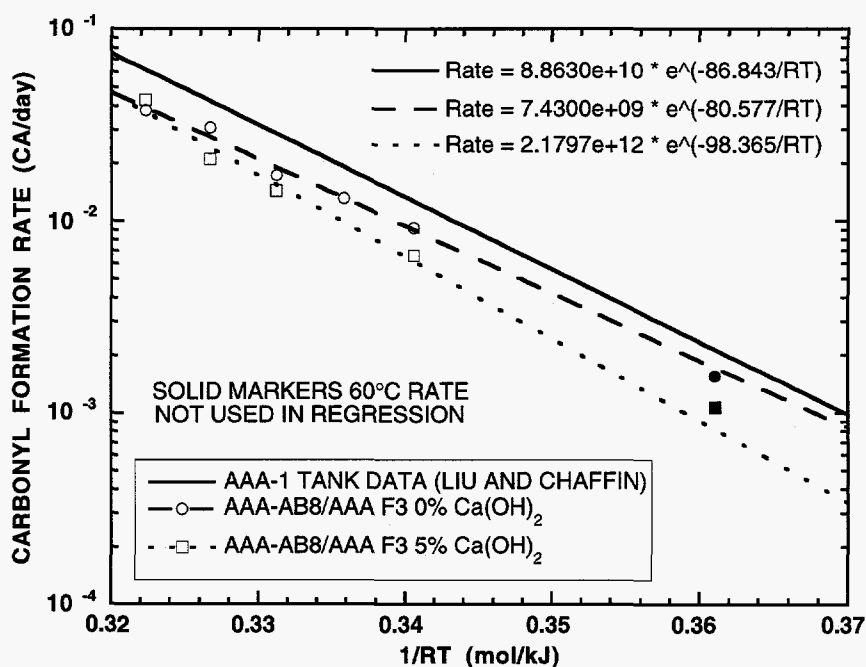


Figure 8-11. Arrhenius plots for AAA-AB8/AAA F3 blends.

with the AAB-AB1 blends, although the AAF-AB2 blends also show differences. The data in Table 8-13 also indicate that there is little correlation between activation energy and rejuvenating agent content for the untreated blends. For example, the activation energies decrease with decreasing aged asphalt content for the AAD-AB3 blends while the activation energies increase (substantially) with decreasing aged asphalt content for the AAF-AB2 and AAB-AB1 blends. The trends for the other three sets of untreated blends are mixed. There also appears to be no correlation between blend saturate content, asphaltene content, or aromatic content and the activation energies for the untreated blends.

Figure 8-11 and the data in Table 8-13 clearly show that the lime treatment generally results in increased activation energies for the recycled blends analyzed in these experiments. This is in stark contrast to the results reported in Table 7-5 for lime treatment of tank asphalts where lime treatment had little or no effect on the activation energies of tank asphalts. Wisneski et al. (in press) reported

Table 8-13. Second Recycling Study Activation Energies

Blend	Composition (Asphalt/Agent)	Saturates (wt%) ^a	E _A (kJ/mol)	
			0	5
Nominal Ca(OH) ₂ Content (wt%)				
AAA-AB8/AAA F3	80/20	11.2	80.6	98.4
AAA-AB8/YBF F3	77/23	11.2	78.6	105.0
AAF-AB2/AAA F2	87/13	12.9	79.0	79.3
AAF-AB2/YBF F3	82/18	11.7	96.0	101.9
AAD-AB3/AAF F2	87/13	9.5	95.3	76.4
AAD-AB3/AAA F2	87/13	9.0	98.6	82.9
AAD-AB3/ABM F5	81/19	8.2	90.2	83.7
AAD-AB3/YBF F3	80/20	8.1	89.6	96.4
AAB-AB1/CRA B	83/17	12.5	72.3	77.6
AAB-AB1/YBF F2	75/25	13.9	77.6	95.1
AAB-AB1/ISCF C	61/39	12.1	94.5	100.4
AAB-AB2/CRA D	83/17	10.4	88.4	99.9
AAB-AB2/AAF F3	74/26	13.0	87.6	93.9
AAB-AB2/ISCF C	63/37	12.1	90.4	117.8
AAB-AB3/CRA D	87/13	10.9	103.0	79.4
AAB-AB3/AAF F2	84/16	14.3	89.6	112.2
AAB-AB3/YBF F3	77/23	12.2	96.3	91.4

^a Calculated as weighted sum of component saturate contents

activation energies for lime-treated recycled asphalts indicating the general trend that the presence of lime increases the activation energy, although there is significant scatter in the data. The scatter in their data likely results from determining kinetic parameters from three aging temperatures. Three of the five exceptions to the general trend from Table 8-13 are AAD-AB3 blends. In contrast to the untreated blends, the activation energies for the lime-treated blends show much stronger correlation to the rejuvenating agent content. The only clear exception is the AAB-AB3 set of blends, although

the AAB-AB2 blends also show some deviation from the trend.

The previous discussions have been focused solely on the high temperature POV aging data and the Arrhenius activation energies. One of the main purposes of the second recycling study was to determine the accuracy associated with extrapolating the high temperature data to road conditions. To determine the accuracy, it was necessary to conduct actual experiments at road-like conditions and compare to the carbonyl rates predicted by extrapolation of high temperature reaction rates. The experimental 60°C reaction rates, extrapolated reaction rates, and the errors between the two are tabulated in Table 8-14. Of particular interest are the average errors between the extrapolated rates and the experimental rates for both the untreated and lime-treated recycled blends. The averages of 35.2% and 30.4% support the conclusion in Chapter 7 that the high temperature data can be used to extrapolate high temperature aging data to road conditions to within about 50% of the actual oxidation rate. However, there are several data points which exceed the $\pm 50\%$ range.

The data in Table 8-14 can also be used to see that lime treatment generally results in substantial reductions in the 60°C experimental rates. This can be seen graphically in Figure 8-10. In fact, the average reduction in 60°C carbonyl rate is 27%. This is much more than would be expected if the lime is acting as a diluent only. Looking at all of the carbonyl rates, it is evident that the lime treatment substantially reduces the reaction rates at all temperatures as shown in Figure 8-12. The increased scatter as aging temperature decreases is attributed to the narrower range of carbonyl areas obtained for aging at lower temperatures. For example, the change in carbonyl area for the AAA-AB8/YBF F3 blend at 80°C is approximately 0.1 units while the change at 100°C is more than 0.4 units, as shown in Figure 8-9.

Viscosity ($\eta_{0,60^\circ\text{C}}^*$) measurements were performed on approximately one-third of the aged samples at each temperature (2 trays). The hardening susceptibilities for the AAA-AB8/YBF F3 blends are shown in Figure 8-13. The HS relationships for the other asphalts were obtained and the HS values were tabulated in Table 8-15. As was the case in the first recycling study, the data indicate that the HS of the untreated recycled blends are generally correlated with the blend saturate content for the blends using a given aged asphalt with the exception of the AAB-AB2 and AAB-AB3 blends. Particularly noticeable are the extremely high HS values for the AAD-AB3 blends with AAF F2 and AAA F2. These two rejuvenating agents are, not coincidentally, the rejuvenating agents with the

Table 8-14. Second Recycling Study Road Condition Oxidation Rate Comparisons

Blend	Exper. $R_{CA} \times 10^3$		Extr. $R_{CA} \times 10^3$		Error ^a	
	(CA/day)		(CA/day)		(%)	
Nominal $Ca(OH)_2$ Content (wt%)	0	5	0	5	0	5
AAA-AB8/AAA F3	1.56	1.09	1.73	0.82	10.9	-24.8
AAA-AB8/YBF F3	1.78	0.56	2.22	0.51	24.7	-8.9
AAF-AB2/AAA F2	3.12	1.79	2.92	1.93	-6.4	7.8
AAF-AB2/YBF F3	1.03	0.95	1.79	1.03	73.8	8.4
AAD-AB3/AAF F2	1.46	1.70	1.17	1.29	-19.9	-24.1
AAD-AB3/AAA F2	1.18	0.89	1.10	1.35	-6.8	51.7
AAD-AB3/ABM F5	1.90	1.60	1.51	1.53	-20.5	-4.4
AAD-AB3/YBF F3	1.30	1.22	1.50	0.99	15.4	-18.9
AAB-AB1/CRA B	2.76	1.46	4.49	2.45	62.7	67.8
AAB-AB1/YBF F2	1.91	1.14	2.70	1.14	41.4	0.0
AAB-AB1/ISCF C	1.80	1.01	1.97	1.23	9.4	21.8
AAB-AB2/CRA D	2.21	0.98	2.83	1.02	28.1	4.1
AAB-AB2/AAF F3	1.35	1.22	2.18	1.40	61.5	14.8
AAB-AB2/ISCF C	1.40	1.66	2.16	0.67	54.3	-59.6
AAB-AB3/CRA D	1.42	1.43	1.58	1.51	11.3	5.6
AAB-AB3/AAF F2	1.72	0.78	2.00	0.59	16.3	-24.4
AAB-AB3/YBF F3	1.65	0.87	1.83	1.24	10.9	42.5
Root Mean Square Error					35.2	30.4

^a %Error = (Extr. - Exp.) / Exp. × 100

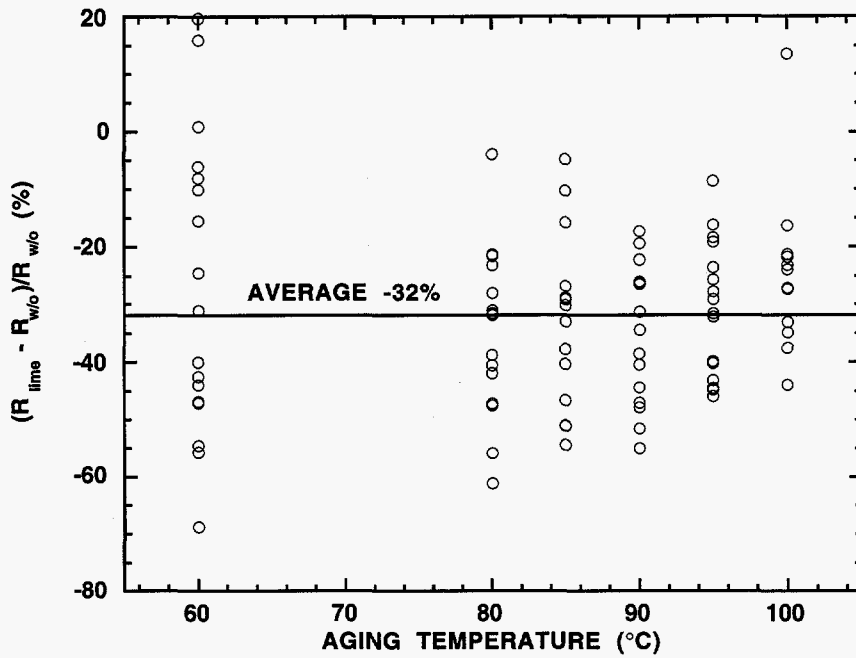


Figure 8-12. The effect of lime on the oxidation rates of recycled asphalts.

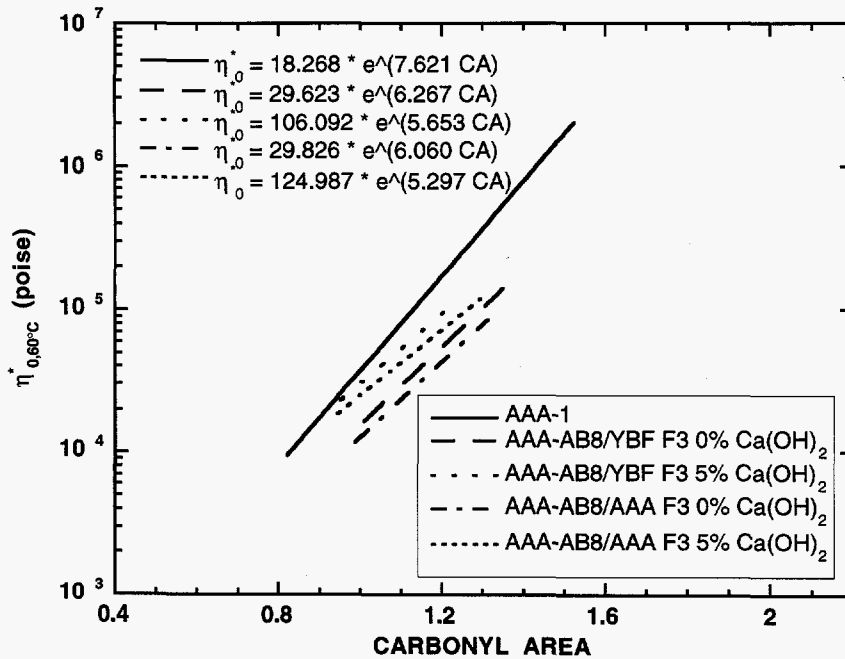


Figure 8-13. Hardening susceptibilities for recycled AAA-AB8 blends.

Table 8-15. Second Recycling Study Hardening Susceptibilities

Blend	Composition (Asphalt/Agent)	Saturates (wt%) ^a	HS	
			0	5
Nominal Ca(OH) ₂ Content (wt%)				
AAA-AB8/AAA F3	80/20	11.2	6.06	5.30
AAA-AB8/YBF F3	77/23	11.2	6.27	5.65
AAF-AB2/AAA F2	87/13	12.9	3.98	3.57
AAF-AB2/YBF F3	82/18	11.7	3.89	3.64
AAD-AB3/AAF F2	87/13	9.5	11.35	8.27
AAD-AB3/AAA F2	87/13	9.0	11.81	8.91
AAD-AB3/ABM F5	81/19	8.2	8.91	7.62
AAD-AB3/YBF F3	80/20	8.1	8.90	8.38
AAB-AB1/CRA B	83/17	12.5	5.47	4.47
AAB-AB1/YBF F2	75/25	13.9	6.11	5.00
AAB-AB1/ISCF C	61/39	12.1	5.01	3.99
AAB-AB2/CRA D	83/17	10.4	6.28	5.32
AAB-AB2/AAF F3	74/26	13.0	6.66	5.62
AAB-AB2/ISCF C	63/37	12.1	4.82	4.86
AAB-AB3/CRA D	87/13	10.9	6.78	6.16
AAB-AB3/AAF F2	84/16	14.3	6.55	6.50
AAB-AB3/YBF F3	77/23	12.2	5.47	4.60

^a Calculated as weighted sum of component saturate contents

highest saturate contents. This illustrates the need to use rejuvenating agents with low saturate contents, particularly when recycling an asphalt with an already poor HS.

The data in Table 8-15 indicate a general correlation between rejuvenating agent content and HS, with HS decreasing with increasing rejuvenating agent content. This trend is clearest for the AAD-AB3. This is not surprising since the HS of the tank AAD-1 asphalt is so poor. This is yet another indication that dilution of the asphaltenes existing in the aged asphalt is highly desirable, if

not essential, in order to produce recycled asphalts with excellent properties. There correlation between blend saturate content and HS for the blends using a given aged asphalt is much stronger than the correlation between HS and rejuvenating agent content, as was the case in the first recycling study. However, the correlation is aged asphalt specific, and not universal.

The effect of lime on the hardening susceptibility is much more conclusive. With only the one exception for the AAB-AB2/ISCF C blend (4.82 versus 4.86), the HS is lower for the lime-treated recycled asphalts compared to the untreated blends. This is consistent with the results from the lime-treated tank asphalt experiments detailed in Chapter 7 and the results reported by Wisneski et al. (in press) for lime-treated recycled asphalts. The two largest reductions in HS were 27% and 25% for the AAD-AB3 blends with the AAF F2 and the AAA F2, respectively. Recall from Table 8-7 that these two rejuvenating agents have the highest saturate contents of the agents investigated in the second recycling study. Unfortunately, any conclusions regarding the effect of lime on these blends would be highly speculative as the HS plots for these asphalts are highly scattered as shown in Figure 8-14. The carbonyl areas were measured and remeasured for these blends. Furthermore, viscosity measurements were performed on several additional AAD-AB3/AAF F2 samples. The problems with the AAD-AB3 blends are not limited to the HS only. In fact, for almost every property analyzed in the second recycling study, at least one of the AAD-AB3 blends showed anomalous behavior, from the large deviation from the DLV mixing rules to the reduction in reaction activation energies for the lime-treated blends. Whether this is a result of asphalt specific interactions, or potential problems with the aged asphalt is not clear. In any event, any conclusions about the AAD-AB3 blends should be treated with due caution.

The hardening susceptibilities were then combined with the 60°C *extrapolated* reaction rates to obtain the predicted hardening rates which are shown in Table 8-16 together with the reduction in hardening rate for the lime-treated blends compared to the untreated recycled blends. Comparing the road condition oxidation rates in Table 8-14 and the hardening rates in Table 8-16 to the rates reported in Table 7-7, it can be seen that recycling alone can significantly reduce both rates relative to the tank asphalt. The two blends with higher hardening rates have two things in common: AAB-1 is the base asphalt and the rejuvenating agents are both commercial recycling agents. The first major

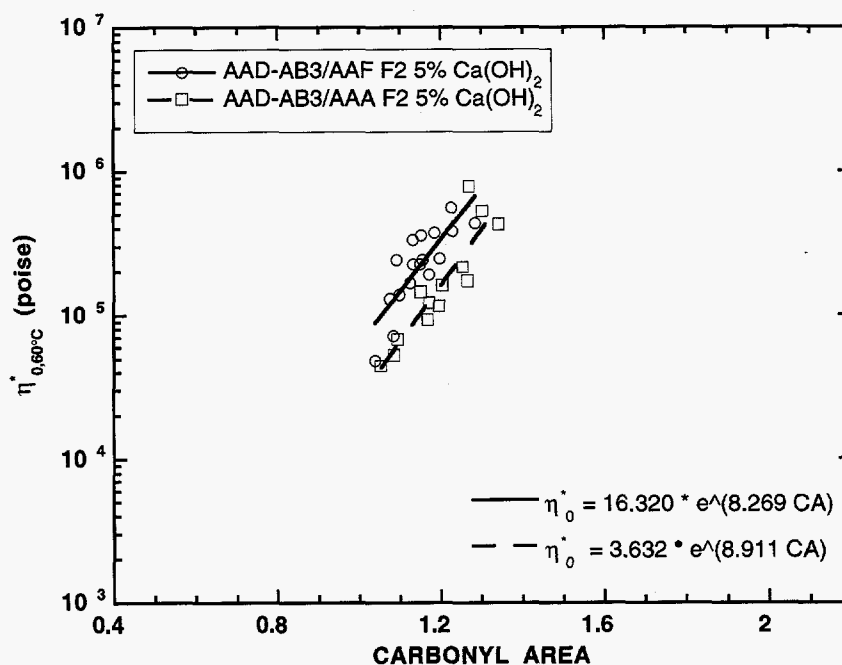


Figure 8-14. Anomalous HS relationships of lime-treated AAD-AB3 blends.

implication of these observations is that a binder with superior aging characteristics can be produced through recycling. The second major implication is that the rejuvenating agents isolated through supercritical fractionation of asphalts are at least as good as, if not better than, the commercial recycling agents. Recall that this conclusion was reached in the first recycling study, as well. These two results were, *the* main goals of this study.

The data in Table 8-16 also show without exception that lime treatment reduces the road aging condition hardening rates. In fact, the average reduction in the rate of increase is more than 45%. Once again, the data indicate that lime treatment will significantly reduce the hardening rate. Furthermore, the average reduction in rate of viscosity increase is at least a factor of two higher than the average error resulting from extrapolating the high temperature aging data to road conditions. Thus, a firm conclusion can be drawn that lime treatment will reduce the rate of viscosity increase of recycled asphalts at road conditions.

**Table 8-16. Second Recycling Study Extrapolated Road Condition
Hardening Rates**

Blend	$d \ln \eta_{0,60^\circ\text{C}}^* / dt \times 10^3$		Reduction (%)
	Nominal Ca(OH) ₂ Content (wt%)		
	0	5	
AAA-AB8/AAA F3	10.5	4.3	58.5
AAA-AB8/YBF F3	13.9	2.9	79.3
AAAF-AB2/AAA F2	11.6	6.9	40.7
AAAF-AB2/YBF F3	7.0	3.7	46.2
AAD-AB3/AAF F2	13.3	10.7	19.7
AAD-AB3/AAA F2	13.0	12.0	7.4
AAD-AB3/ABM F5	13.5	11.7	13.3
AAD-AB3/YBF F3	13.4	8.3	37.9
AAB-AB1/CRA B	24.6	11.0	55.4
AAB-AB1/YBF F2	16.5	5.7	65.4
AAB-AB1/ISCF C	9.9	4.9	50.3
AAB-AB2/CRA D	17.8	5.4	69.5
AAB-AB2/AAF F3	14.5	7.9	45.8
AAB-AB2/ISCF C	10.4	3.3	68.7
AAB-AB3/CRA D	10.7	9.3	13.2
AAB-AB3/AAF F2	13.1	3.8	70.7
AAB-AB3/YBF F3	10.0	5.7	43.0

The relative rankings based on the extrapolated road condition hardening rates and the PAV aging index are tabulated in Table 8-17. The relative rankings were determined independently for each aged asphalt and includes the lime-treated blends. The data in Table 8-17 show excellent agreement between the relative rankings based on kinetic data and PAV aging data. In fact, the only blend showing a difference of more than two relative ranking points between the comparison properties is the untreated AAD-AB3/ABM F5 blend. This supports the previous assertion that the lack of an "initial jump" for the recycled blends might make the PAV aging index more representative of the road condition aging properties. The general agreement between PAV rankings and hardening rates was also noted in the first recycling study.

Additional Kinetic Analyses

Liu (1996) conducted aging experiments using the supercritical fractions of AAF-1. The kinetic data obtained by Liu can be used, together with the kinetic information for the tank asphalts AAD-1 and AAB-1, in an effort to perform preliminary analyses to determine if the kinetics of the recycled blends can be determined from the kinetics of the aged asphalt and the rejuvenating agent. Specifically, the atmospheric aging rates for the AAF F2 and AAF F3, or F2F and F3F as Liu referred to them, were used to generate the Arrhenius parameters for these fractions. The newly determined AAF F2 and AAF F3 Arrhenius parameters and the Arrhenius parameters for the AAD-1 and AAB-1 asphalts were then weighted according to their weighting in the blends investigated in this work. The calculated blend Arrhenius parameters are shown in Table 8-18 together with the untreated blend Arrhenius parameters determined experimentally.

The data in Table 8-18 indicate that fairly accurate guesses for the Arrhenius parameters can be obtained by weighting the Arrhenius parameters of the aged asphalt and the rejuvenating agent properly. However, the 60°C aging rates calculated using the weighted Arrhenius parameters are 4.36×10^{-3} , 2.46×10^{-3} , and 2.45×10^{-3} CA/day for the AAD-AB3/AAF F2, AAB-AB2/AAF F3, and AAB-AB3/AAF F2 blends, respectively. These amount to errors of 195%, 82%, and 42%, respectively when compared to the actual experimentally determined reaction rates reported in Table 8-14. These errors compare to the 20%, -62%, and -16% extrapolation errors shown in Table 8-14. This preliminary analysis indicates the components may age faster separately than they do in

Table 8-17. Relative Rankings for Second Recycling Study Blends

Blend	d ln $\eta_{0,60^\circ\text{C}}^* / dt$ relative ranking		PAV Aging Index relative ranking	
	0	5	0	5
Nominal Ca(OH) ₂ Content (wt%)	0	5	0	5
AAA-AB8/AAA F3	3	2	3	1
AAA-AB8/YBF F3	4	1	4	2
AAAF-AB2/AAA F2	4	2	4	2
AAAF-AB2/YBF F3	3	1	3	1
AAD-AB3/AAAF F2	6	2	8	5
AAD-AB3/AAA F2	5	4	7	4
AAD-AB3/ABM F5	8	3	2	1
AAD-AB3/YBF F3	7	1	6	3
AAB-AB1/CRA B	6	4	6	2
AAB-AB1/YBF F2	5	2	5	1
AAB-AB1/ISCF C	3	1	4	3
AAB-AB2/CRA D	6	2	6	1
AAB-AB2/AAAF F3	5	3	5	2
AAB-AB2/ISCF C	4	1	4	3
AAB-AB3/CRA D	5	3	5	2
AAB-AB3/AAAF F2	6	1	6	3
AAB-AB3/YBF F3	4	2	4	1

Table 8-18. AAF-1 Supercritical Fraction Blend Arrhenius Parameter Comparisons

Blend	Calculated		Experimental	
	A (CA/day)	E _A (kJ/mol)	A (CA/day)	E _A (kJ/mol)
AAD-AB3/AAAF F2	3.922 × 10 ¹¹	89.0	1.021 × 10 ¹²	98.3
AAB-AB2/AAAF F3	6.356 × 10 ¹⁰	85.6	1.160 × 10 ¹¹	87.6
AAB-AB3/AAAF F2	8.186 × 10 ¹⁰	86.3	2.203 × 10 ¹¹	89.6

the blend. Liu (1996) came to the same conclusion when trying to reconstruct the aging rate of the aromatics fraction based on the weighted averaged of the reaction rates of the naphthene and polar aromatics. Thus, it appears unlikely that an accurate prediction of blend kinetic properties can be made based on the kinetic parameters of the two components.

All of the kinetic data collected in this study, lime-treated tank asphalts, and recycled asphalts with and without lime, were analyzed to check for the existence of an isokinetic temperature, or a temperature at which the oxidation rates of all of the asphalts are the same. Liu (1996) reported the occurrence of such a phenomenon for asphalts. Furthermore, Liu reported an isokinetic temperature of 86.6°C for the ten asphalts studied. A plot of the pre-exponential factor A versus activation energy E_A from the Arrhenius equation (Equation 1-6) should be linear if such a relationship exists for the lime-treated asphalts. Figure 8-15 shows that this is indeed the case for both the lime-treated tank asphalt aging experiments described in Chapter 7 and for the recycling experiments described in this chapter.

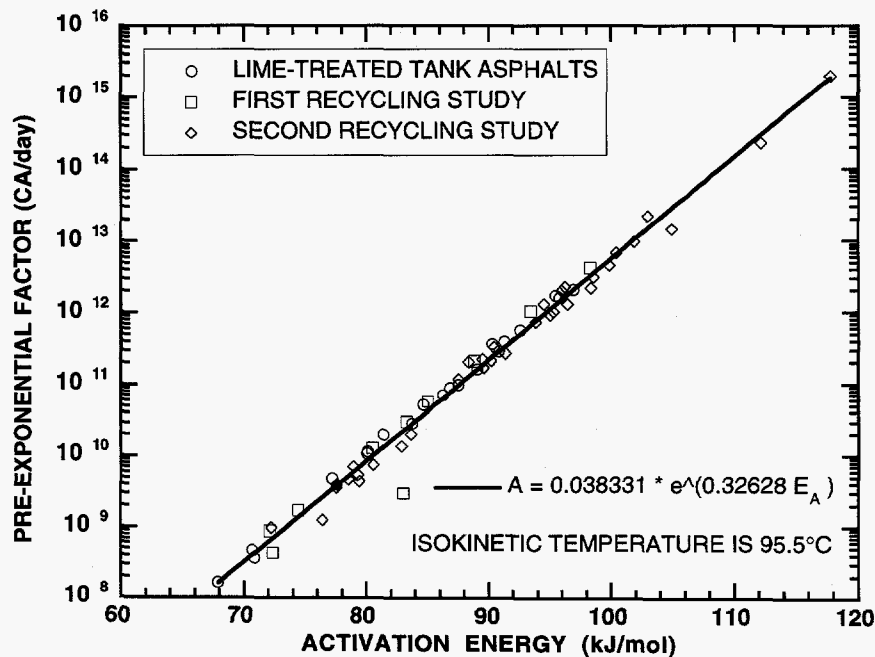


Figure 8-15. Isokinetic plot for all of the materials studied.

SHRP Performance Grading

The recycled asphalts in the second recycling study were graded according to a slightly modified SHRP performance grading procedure. The full SHRP grading procedure entails testing the rheological properties of both unaged and RTFOT-aged samples at high temperature using a dynamic shear rheometer, testing the low temperature rheological properties of the PAV-aged residue using a bending beam rheometer, and testing the room temperature rheological properties of the PAV-aged residue. However, because the recycled asphalts under investigation all had 60°C viscosities similar to that of an RTFOT-aged AC-20, the performance grading described here treats the unaged materials as if they were the RTFOT-aged materials. Furthermore, because asphalts rarely, if ever, fail the room temperature specifications, these measurements were not performed. As such, the performance grading criteria used to grade the recycled asphalts are that the high temperature value of $G^*/\sin\delta$ must be greater than 2.2 kPa at the respective measurement temperature and the creep stiffness, $S(t)$, at 60 seconds and the so-called m-value must be below 300 MPa and above 0.3, respectively at the test measurement temperature.

The high temperature testing was accomplished by performing a torque sweep at 10 rad/s and taking an average value of G^* and δ over the range where they were constant. The measurement temperatures investigated were 64 and 70°C. A few of the blends did not pass specifications at 64°C. However, during routine viscosity testing, they all passed at 60°C and these samples will be listed as having passed at 58°C although measurements at 58°C were not performed. The SHRP grading criteria require testing of multiple beam specimens at each bending beam measurement temperature. However, given the limited amount of recycled material that was produced, only three beams could be produced for each recycled blend. To be able to test multiple beam specimens at each measurement temperature would have required approximately twice as much material as was produced if the POV tests were not conducted. To conduct POV tests and to be able to test multiple beam specimens would have required approximately three times as much material for each blend. This quantity of material is almost prohibitively high, especially if testing is to occur on recycled asphalts using aged asphalts extracted from pavement samples.

The values of $G^*/\sin\delta$ at 64°C are shown in Table 8-19 and the $S(t)|_{t=60s}$ and m-values at a measurement temperature of -18°C are shown in Table 8-20 to illustrate several important trends.

Table 8-19. 64°C G*/sinδ Values for Second Recycling Study Blends

Blend	Composition (Asphalt/Agent)	Saturates (wt%) ^a	G*/sinδ (kPa)	
			0	5
Nominal Ca(OH) ₂ Content (wt%)				
AAA-AB8/AAA F3	80/20	11.2	2790	2710
AAA-AB8/YBF F3	77/23	11.2	2870	2770
AAF-AB2/AAA F2	87/13	12.9	2530	2510
AAF-AB2/YBF F3	82/18	11.7	3090	3300
AAD-AB3/AAF F2	87/13	9.5	3290	3290
AAD-AB3/AAA F2	87/13	9.0	3380	3280
AAD-AB3/ABM F5	81/19	8.2	2770	2720
AAD-AB3/YBF F3	80/20	8.1	3450	3310
AAB-AB1/CRA B	83/17	12.5	1630	1370
AAB-AB1/YBF F2	75/25	13.9	2690	2270
AAB-AB1/ISCF C	61/39	12.1	3040	2970
AAB-AB2/CRA D	83/17	10.4	2220	1820
AAB-AB2/AAF F3	74/26	13.0	2350	2040
AAB-AB2/ISCF C	63/37	12.1	2880	2780
AAB-AB3/CRA D	87/13	10.9	2460	2180
AAB-AB3/AAF F2	84/16	14.3	2830	2480
AAB-AB3/YBF F3	77/23	12.2	2730	2620

Table 8-20. -18°C Bending Beam Parameters for Second Recycling Study Blends

Blend	Composition (Asphalt/Agent)	Saturates (wt%) ^a	S(t) @ 60s (MPa)		m-value @ 60s	
			0	5	0	5
Nominal Ca(OH) ₂ Content (wt%)			0	5	0	5
AAA-AB8/AAA F3	80/20	11.2	152.1	158.8	0.360	0.378
AAA-AB8/YBF F3	77/23	11.2	178.2	190.5	0.355	0.352
AAF-AB2/AAA F2	87/13	12.9	358.1	426.5	0.276	0.269
AAF-AB2/YBF F3	82/18	11.7	520.5	487.2	0.260	0.258
AAD-AB3/AAF F2	87/13	9.5	182.2	200.0	0.335	0.339
AAD-AB3/AAA F2	87/13	9.0	139.3	179.0	0.344	0.357
AAD-AB3/ABM F5	81/19	8.2	211.4	237.1	0.361	0.351
AAD-AB3/YBF F3	80/20	8.1	218.4	239.1	0.336	0.329
AAB-AB1/CRA B	83/17	12.5	145.8	149.9	0.331	0.353
AAB-AB1/YBF F2	75/25	13.9	192.1	211.0	0.321	0.332
AAB-AB1/ISCF C	61/39	12.1	322.1	455.2	0.283	0.263
AAB-AB2/CRA D	83/17	10.4	146.5	175.0	0.325	0.348
AAB-AB2/AAF F3	74/26	13.0	250.1	262.3	0.304	0.308
AAB-AB2/ISCF C	63/37	12.1	362.3	422.7	0.227	0.273
AAB-AB3/CRA D	87/13	10.9	202.2	221.0	0.327	0.334
AAB-AB3/AAF F2	84/16	14.3	217.9	247.8	0.309	0.308
AAB-AB3/YBF F3	77/23	12.2	294.7	294.5	0.304	0.292

First, in nearly every case, the lime-treated blend had a $G^*/\sin\delta$ value less than that of the untreated blend as shown in Table 8-19. This is expected because G^* (kPa) at 10 rad/s is numerically equivalent to the viscosity (poise). As discussed previously, the viscosities for the lime-treated samples were uniformly lower, with the exception of the AAF-AB2 blends. This is important because this can and does lead to diverging SHRP performance grades for the lime-treated and untreated samples. In fact, the performance grades, which are shown in Table 8-21, indicate that this is indeed the case for the AAB-AB2/CRA D, AAB-AB2/AAF F3, and the AAB-AB3/CRA D blends, although the latter two are clearly borderline asphalts which may pass the specifications at 64°C with only minor modifications. Second, there is no general correlation between either recycling agent content or blend saturate content and the high temperature SHRP parameter values.

The low temperature data in Table 8-20 are much more interesting. First, for every aged asphalt/rejuvenating agent pair, the creep stiffness increases with increasing recycling agent content for both the untreated and lime treated blends. The second trend that should be noted is that the m -value decreases with increasing rejuvenating agent content, with a few exceptions. Once again, the one exception to the $S(t)$ trend is the AAD-AB3/AAA F2 blend. Because two beams of this blend were tested at this temperature, it is safe to infer that this is a continuation of the anomalous behavior noted previously for the AAD-AB3 blends. In addition, the only blends showing deviation from the correlation between m -value and rejuvenating agent content are the AAD-AB3 blends. Increased stiffness and decreased m -value are both undesirable. Thus, the bending beam parameters confirm the VTS conclusions regarding the effects of asphaltene dilution. In short, the rheological properties indicate that dilution of the aged asphalt, and thus, the asphaltenes, is not desirable while the kinetic parameters indicate that dilution is desirable. Clearly, some tradeoffs must be investigated.

Because the correlations between recycling agent content and $S(t)$ and m -value are so strong, there is no noticeable correlation between blend saturate content and the bending beam parameters. This doesn't mean that such a correlation doesn't exist. It simply means that the correlations with rejuvenating agent content are strong enough to mask any potential correlations with rejuvenating agent composition.

The data in Table 8-20 also show that in nearly every case, the creep stiffness values are higher, sometimes significantly higher, in the lime-treated samples than for the untreated samples.

Table 8-21. SHRP Performance Grades for the Second Recycling Study Blends

Blend	Performance Grade		Temperature Span (°C)	
	0	5	0	5
Nominal Ca(OH) ₂ Content (wt%)				
AAA-AB8/AAA F3	64-28	64-28	92	92
AAA-AB8/YBF F3	64-28	64-28	92	92
AAF-AB2/AAA F2	64-22	64-22	86	86
AAF-AB2/YBF F3	64-22	64-22	86	86
AAD-AB3/AAF F2	64-28	64-28	92	92
AAD-AB3/AAA F2	64-28	64-28	92	92
AAD-AB3/ABM F5	64-28	64-28	92	92
AAD-AB3/YBF F3	64-28	64-28	92	92
AAB-AB1/CRA B	58-28	58-28	86	86
AAB-AB1/YBF F2	64-28	64-28	92	92
AAB-AB1/ISCF C	64-22	64-22	86	86
AAB-AB2/CRA D	64-28	58-28	92	86
AAB-AB2/AAF F3	64-28	58-28	92	86
AAB-AB2/ISCF C	64-22	64-22	86	86
AAB-AB3/CRA D	64-28	58-28	92	86
AAB-AB3/AAF F2	64-28	64-28	92	92
AAB-AB3/YBF F3	64-28	64-22	92	86
AAA-1 ^a	58-28		86	
AAF-1 ^a	64-10		74	
AAD-1 ^a	58-28		86	
AAB-1 ^a	58-22		80	

^a Data taken from Mortazavi and Moulthrop (1993)

The lime appears to be acting as a filler in the binder at these temperatures. As was the case with the high temperature SHRP parameter, this could potentially lead to different performance grades for the untreated and lime-treated blends. In fact, the AAB-AB3/YBF F3 lime-treated and untreated blends do have different low temperature grades as shown in Table 8-21. Thus, the data collected in these experiments indicate that lime treatment may adversely affect either performance grade temperature or under the proper circumstances lime could adversely affect both temperatures simultaneously, reducing the temperature span by 12°C. The data presented here indicate that it is unlikely that the addition of lime to the recycled binder will affect the span by more than 12°C.

It is clear the performance grades and temperature span data in Table 8-21 that the performance grades and temperature spans for the untreated recycled asphalts are superior to the performance grades and temperature spans for the original tank asphalt. This is true even though the S(t) and m-values are negatively impacted by rejuvenating agent content. This illustrates that the specification temperature ranges are too wide. Any improvement in the high temperature (first temperature) results solely from too high of an initial blend viscosity. The goal was to obtain an initial 60°C viscosity of 5000 poise, the viscosity of a TFOT or RTFOT treated AC-20. Because nearly all of the viscosities exceeded this target viscosity and because the TFOT viscosity for the tank asphalts are reported (Mortazavi and Moulthrop, 1993) as less than 5000 poise, it is clear that the improvements in the high temperature grades result solely from the relatively hard initial viscosities. To substantiate this claim, one need not look any further than the AAB-AB1/CRA B blend. This is the one blend with an initial viscosity (3730) within 10% of a published value (3420) for the TFOT treated tank asphalt. Not coincidentally, the high temperature grades are the same for these two asphalts. The low temperature grades on the other hand can be improved dramatically by recycling. For example, the low temperature grades of the AAF-AB2 blends are 12°C better than that of the tank AAF-1 asphalt. As discussed previously, the temperature spans indicate that recycling can be a highly beneficial to the SHRP performance grading.

Summary

Two separate recycling studies were conducted. The viscosity mixing rules described in Appendix H were utilized with limited success to predict the quantity of rejuvenating agent to use in

order to achieve the target viscosities. In the first recycling study, the aging indexes, Arrhenius activation energies, and extrapolated road condition hardening rates of recycled asphalts all were superior to the tank asphalt values indicating that binders with superior aging properties can be obtained through recycling deteriorated pavements. The performance grades for the second recycling study blends confirmed this observation. However, the second recycling study showed that the viscosity temperature susceptibility of the unaged recycled blends were generally much worse than those of the original asphalts. The data from both studies indicated that the number one factor affecting the properties of the recycled asphalts is dilution of the aged asphalt. Increased rejuvenating agent content generally resulted in superior aging properties such as activation energy, aging index, and hardening susceptibility, but worse rheological properties such as viscosity temperature susceptibility, creep stiffness, and m-value. The correlations between rejuvenating agent content and the blend properties were so strong that any possible compositional influences were masked. The exception to this was the hardening susceptibility. The hardening susceptibility was shown to be strongly dependent on the saturate content in the blends.

The second study also showed that lime treatment of recycled asphalts resulted in little or no effect on the "initial jump", which was shown to be small for the recycled asphalts in general, or the viscosity temperature susceptibility of the unaged asphalts. Lime treatment of recycled asphalts resulted in dramatically reduced oxidation rates, improved activation energies, and hardening susceptibilities. However, the data showed that lime treatment could possibly result in a two grade reduction in performance grade over an untreated recycled blend.

Finally, the data from both recycling studies indicate that the PAV aging index is in strong agreement with the predicted road condition hardening rates. Given that the PAV aging index requires far less effort, time, and equipment, obtaining the PAV aging index is much more preferable than obtaining complete kinetic information or even the hardening susceptibility.

CHAPTER 9

HIGHLY AROMATIC RECYCLING AGENTS

The experiments presented in Chapter 8 along with the work of Peterson et al., (1993) have focused on determining what types of materials are suitable for use as asphalt recycling (softening) agents. Both works have suggested that recycling agents should have a high concentration of aromatics and possess few, if any, asphaltenes or saturates. The high aromatic content helps replace the aromatic materials that have been consumed during oxidation. The low asphaltene criterion helps maintain a low viscosity for the softening agent and is important because the aged asphalt is already high in asphaltenes. Low saturate content is important because of the incompatibility between the saturate molecules in the recycling agent and the asphaltene molecules in the aged asphalt.

The recycling agents of Peterson et al., (1993) were low in asphaltenes, less than 0.7wt%; however they possessed in excess of 20wt% saturates. The recycling agents of Chapter 8 were also low in asphaltenes, less than 3.5wt%, however they contained saturates in excess of 10wt%. Both studies utilized recycling agents that were very low in asphaltenes. However, the rejuvenating agents were relatively high in saturate content.

The experiment described in this chapter was undertaken to determine how the hardening susceptibility (HS) of an aged asphalt would be affected when the aged asphalt is reblended (rejuvenated) with a highly aromatic recycling agent. This recycling study is different from the experiments discussed above in that the recycling agents used in this study are not only low in asphaltenes, but also are essentially saturate free.

Experimental Design

Three industrial supercritical fractions (ISCFs), two commercial recycling agents (CRAs) along with five top fractions from the Texas A&M University supercritical unit (TAMU SCFs) were selected as the recycling agents. The ISCFs and CRAs are products from a commercial deasphalting unit and are essentially asphaltene free. The three ISCFs and two CRAs utilized in this study have been given the arbitrary designations: ISCF 1, 2, 3, and CRA 1, 2; to protect the identities of the company supplying the materials. Four asphalts were fractionated in the supercritical pilot unit at

Texas A&M from which the top fractions were selected as recycling agents. The top fractions are the lightest (lowest boiling point) components and as such are asphaltene free. Three of the four asphalts: AAA-1, AAF-1, and ABM-1, were obtained from the Strategic Highway Research Program's (SHRP) Materials Reference Library (MRL). One asphalt, an AC-20, was obtained from a local paving contractor and is given the designation YBF. The five TAMU SCFs are AAF F1, YBF F1, ABM F1 and AAA F1 #15 and AAA F1 #21. Asphalt AAA-1 was fractionated at two different operating conditions, hence two different top fractions were obtained: AAA F1 #15 and AAA F1 #21.

The compositions of these ten recycling agents were determined following the Corbett fractionation procedure (ASTM D-4124, 1994; Corbett, 1969) as detailed in Chapter 1. The recycling agents were then fractionated into aromatic (AR) and saturate (SA) fractions by the "Giant" Corbett procedure developed by Peterson (1993). Thus, a total of twenty different fractions, ten aromatic and ten saturate fractions, were produced.

The ten aromatic fractions (recycling agents) were then blended in controlled amounts with an aged asphalt. SHRP AAA-1 was aged in the air bubbling apparatus described in Appendix A. This aged asphalt was aged to a final viscosity of 55,000 dPa·s (poise). This sample is referred to as AAA-AB11. The recycled blends were then POV-aged at 100°C and atmospheric pressure. Samples were periodically removed from the POV and η_0^* at 60°C, and carbonyl areas were measured as described in Appendix A. From these measurements, the hardening susceptibility (HS) was calculated.

Experimental Methods

Recycled Asphalt Blending

The amount of softening agent added to the aged asphalt was determined using the dimensionless log viscosity (DLV) mixing rule discussed in Appendix H. The target viscosity for the recycled blends was selected to be 5000 dPa·s (poise) at 60°C. Blending was performed in a manner similar to that suggested in specification ASTM D-4887.

POV-Aging

Six trays, each containing 1.5 ± 0.1 g of a particular reblended asphalt (6 trays x 10 blends=60 total trays) were then POV-aged at 100°C and atmospheric pressure. The work of Liu et al., (1996) was utilized to determine both the length of time (3 days) necessary to overcome the "initial jump" and the appropriate sampling intervals (every two days).

Results and Discussion

The focus of this study was to determine how a highly aromatic recycling agent would affect the HS of an aged asphalt. The first step was to produce several aromatic recycling agents. Table 9-1 lists the compositions and viscosities ($\eta_{0,60^\circ\text{C}}^*$) of all the recycling agents utilized in this study. From Table 9-1, it can be concluded that the "Giant" Corbett procedure removed all saturates along with a small quantity of light aromatics. This fact is demonstrated by comparing the "Giant" Corbett aromatic masses to the actual aromatic masses. All the "Giant" Corbett aromatic masses, except for AAA F1 #21 and ISCF 2, are less than the actual aromatic masses. This indicates that some aromatics were "carried-over" to the saturate phase, which is desirable, since this resulted in essentially pure aromatic recycling agents. For the AAA F1 #21 and ISCF 2 recycling agents, the mass differences between the "Giant" Corbett aromatics and actual aromatics are minimal. These two agents were considered essentially saturate free.

The next step was to blend the "Giant" Corbett aromatic fractions (recycling agents) with an aged asphalt. Table 9-2 lists the weight percentages (wt%) of both recycling agent and aged asphalt used for each blend, along with the resulting blend viscosities. The desired blend viscosity was originally set at 5000 poise. However, as can be seen from Table 9-2, the resulting blend viscosities were lower than this value. A small amount of aged asphalt could have been added to increase the blend viscosity. However, this was not done, because the resulting blend viscosities were within the range of commercially available asphalts.

The reblended asphalt samples were then POV-aged to determine the HS. After aging, carbonyl area measurements and viscosities at 60°C were performed. Figures 9-1 and 9-2 show plots of carbonyl area (CA) versus the natural log of the viscosity ($\ln \eta_0^*$) for the TAMU SCFs and ISCFs.

Table 9-1. Recycling Agent Compositions and Viscosities

Recycling Agent	Actual Saturate Mass Weight %	Giant Corbett Saturate Mass Weight %	Actual Aromatic Mass Weight %	Giant Corbett Aromatic Mass Weight %	Aromatic Fraction $\eta_{0,60^\circ\text{C}}^*$ (poise)
TAMU SCFs					
AAF F1	51.2	52.9	48.8	47.1	40
AAA F1 #21	64.3	63.8	35.6	36.2	28
YBF F1	53.1	55.2	47.0	44.8	227
AAA F1 #15	66.2	70.5	33.8	29.5	89
ABM F1	52.8	54.3	47.2	45.7	559
ISCFs & CRAs					
CRA 1	57.8	65.7	42.1	34.3	55
CRA 2	49.9	62.0	50.1	38.0	430
ISCF 1	22.3	43.2	77.7	56.8	1645
ISCF 2	47.9	45.4	52.2	54.6	385
ISCF 3	22.6	51.2	77.4	48.8	929

Table 9-2. Compositions and Viscosities of Recycled Blends

Recycled Blend	Weight % Recycling Agent	Weight % Aged Asphalt	Recycled Blend Viscosities $\eta_{0,60^{\circ}\text{C}}^*$ (poise)
TAMU SCFs			
AAF F1/AAA-AB11	21.4	78.6	2929
AAA F1 #21/AAA-AB11	20.2	79.8	3133
YBF F1/AAA-AB11	28.7	71.3	2619
AAA F1 #15/AAA-AB11	24.2	75.8	2585
ABM F1/AAA-AB11	36.1	63.9	2010

ISCFs & CRAs			
CRA 1/AAA-AB11	22.1	77.9	2672
CRA 2/AAA-AB11	34.2	65.8	1904
ISCF 1/AAA-AB11	50.6	49.4	2691
ISCF 2/AAA-AB11	32.6	67.4	3503
ISCF 3/AAA-AB11	41.0	59.0	3165

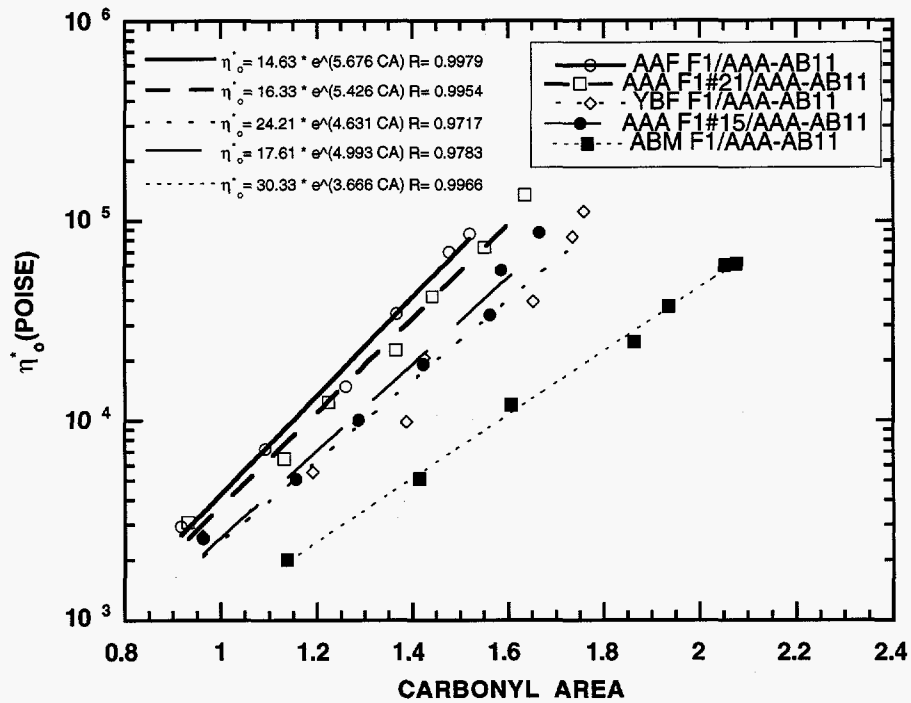


Figure 9-1. Hardening susceptibilities of TAMU SCFs.

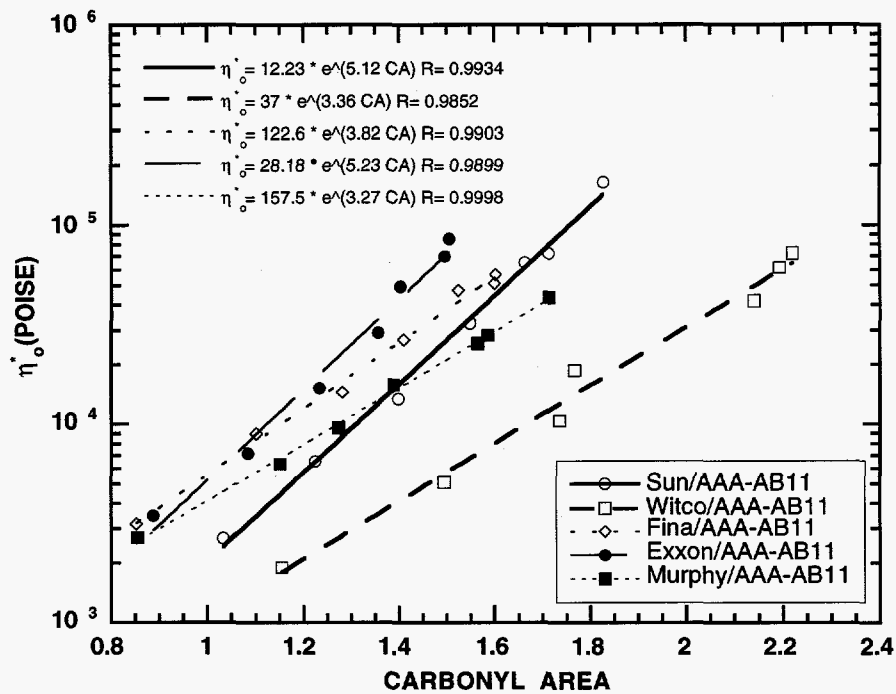


Figure 9-2. Hardening susceptibilities of ISCFs.

The HS (slope of $\ln \eta_0^*$ versus CA) of each blend along with the mass percentages (mass%) of recycling agent added are listed in Table 9-3. Also listed in this table are the HS values and mass % of recycling agents for the softening agents studied in Chapter 8.

Table 9-3. HS Values of AAA-AB11 Blends and Chapter 8 Blends

Blend	AAA-AB11 Blends ^a		Chapter 8 Blends ^b	
	HS	Mass % of Recycling Agent	HS	Mass % of Recycling Agent
CRA 1	5.12	22.1	-	-
CRA 2	3.36	34.2	-	-
ISCF 1	3.27	50.6	-	-
ISCF 2	5.23	32.6	-	-
ISCF 3	3.82	41.0	-	-
AAA F1 #15	4.99	24.2	-	-
AAA F1 #21	5.43	20.2	-	-
YBF F1	4.63	28.7	3.20	39
ABM F1	3.67	36.1	2.22	56
AAF F1	5.68	21.4	3.53	33
ISCF A	-	-	4.91	28
ISCF C	-	-	3.41	57
CRA A	-	-	3.49	19
CRA B	-	-	4.70	17
CRA C	-	-	5.11	17

^aHS of AAA-AB11 is 7.0

^bHS of Chapter 8 asphalt is 4.48

From the data listed in Table 9-3, it appears that the HS did not improve for the overlapping blends. However, the recycling agents and aged asphalts used in the two studies possessed varied compositions and a direct comparison is not correct. Rather, a plot of the HS ratio (the recycled blend HS is divided by the HS of the aged asphalt used in the blend) versus the mass % of recycling agent was determined to provide an unbiased comparison of the two studies. Figure 9-3 shows such a plot. Figure 9-3 clearly indicates that the highly aromatic recycling agents had a significant impact on lowering the HS ratio of the aged asphalt in this study as compared to the recycling agents of Chapter 8.

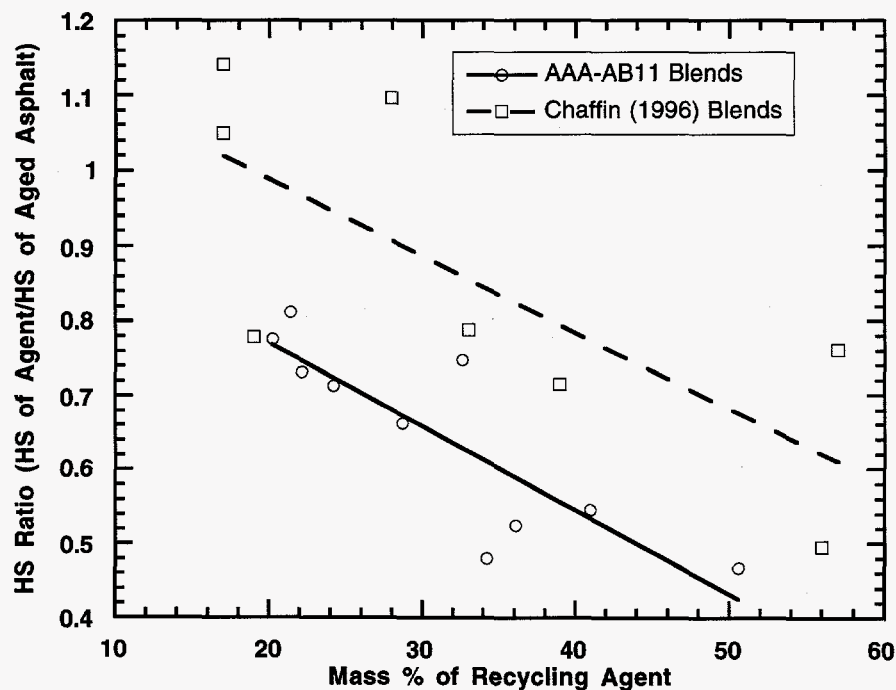


Figure 9-3. HS ratio versus mass percent of recycling agent.

Conclusions

The data collected in this study indicate that an asphaltene-free, highly aromatic (saturate-free) recycling agent significantly lowered the HS ratio of the aged asphalt. Furthermore, it can be concluded from the experimental data that the concept of fractionating an asphaltene-free recycling agent one step further to remove the saturates will make for an improved recycling agent. In fact, many of the commercial recycling agents are actually aromatic extract by-products of lube oil manufacturing, and high in saturate content. If these agents could be fractionated one more step to remove the saturates, an improved recycling agent would result.

CHAPTER 10

PROCESSING SCHEMES AND IMPLEMENTATION

The research conducted in this project has indicated that recycling agents from lighter asphalt fractions can produce blends with hardened asphalt which have superb resistance to age hardening, generally much better than the original asphalt. These results are reported in Chapter 8 and 9 although results given throughout the report support the use of these fractions. These data suggest that recycling agents should be very low in asphaltenes, low in saturates and comprised principally of lighter naphthene and polar aromatics. The data in Chapters 8 and 9 indicate that material meeting these requirements can be separated from asphalt by supercritical extraction (SCE) or more particularly from deasphalted oil (DAO) separated by any method.

Though SCE is a promising procedure most units are 2-stage and only produce a DAO that would need further processing. Even a 3-stage unit will only produce a satisfactory agent if the unit is operated for this purpose which will likely increase asphaltene production and decrease DAO production. Otherwise, the desired resin fraction will be too hard and contain too much asphaltene.

The original plan outlined in the project proposal was to obtain more detailed information about SCE costs from Kerr-McGee, the licensee of the ROSE™ process. However, this technology has been sold to M.W. Kellogg, and this capital cost and utility consumption must be based on what is available in the literature.

Processing Schemes and Cost

In this section five processing options will be discussed along with cost estimates for each.

These options are:

1. Use existing 3-stage SCE unit.
2. Construct a 3-stage unit.
3. Add a 2 or 3-stage unit to an existing DAO facility.
4. Construct a 4 or 5-stage unit.
5. Add a solvent extraction (SX) unit to an existing DAO unit.

The operating costs will be based on factors recommended by Peters and Timmerhaus (1991). This

factor, 15% of fixed capital investment as working capital, is probably high for a refinery addition such as this. Consequently, we have reduced this to 10%. Because of the uncertainty in both capital and operating costs, it is pointless to use any but the simplified definition of return on investment. Therefore a return of 25% before taxes on total capital investment will be assumed with no regard for the time value of money. Thus, each dollar of total capital invested is tantamount to an annual cost of 25 cents.

Use Existing 3-Stage SCE Unit

The simplified alternative is to use an existing facility to produce a satisfactory agent. There are several drawbacks, the greatest being that there are only a few of these in existence. Most of these are operating much as a 2-stage unit in that the principle product is DAO, which generally comprises catalytic cracker feed. This does produce a cleaner DAO in that a 2-stage precipitation prior to DAO recovery gives better metal and other heteroatom removal. This leaves resin and asphaltene fractions that may be of little use beyond low grade fuel oil. By changing operating conditions, i.e., lower first stage temperature to produce more asphaltenes and probably lower the second stage temperature to produce more resin, a good agent could be produced from many feeds. The economics would depend on the relative increase in value of the resin fraction with respect to some loss in DAO volume, though accompanied by some improvement in DAO quality. This situation is only possible at a few refineries and the tradeoff would require specific and unavailable cost and operating data. However, if feasible, it would be quite profitable in that it would require no capital investment.

Construct a 3-Stage Unit

There are refineries that now make no or little asphalt, and feed the vacuum tower bottoms to a coker. This is relatively low grade material and in many instances a much more valuable product could be recovered by SCE. Obviously the practicality, including product yield and composition depend on the value and composition of the feed. It will therefore be necessary to make some assumptions. For this calculation, it will be assumed that a coker feed is available having a flow rate of 30,000 Bbl/day and having a composition typical of asphalt. The SCE unit will separate 10,000

Bbl/day (BPD) of a resin fraction having a satisfactory composition for recycling and the remaining light and heavy fractions are still fed to the coker. Therefore the value of the feed is the value of coker feed which is similar to the value of asphalt.

Capital cost data and utility consumption for a 30,000 Bbl/day ROSE™ unit are given in a recent issue of Hydrocarbon Processing (Nov. 1996, p. 106). A diagram of the 3-stage unit is given in Figure 10-1. The composition data in Appendix C indicate that it is reasonable to assume that 1/3 of the feed can be recovered in the second stage, and that it will make a good recycling agent. Therefore, we will assume a 30,000 BPD unit producing 10,000 BPD of agent. Depreciation will be straight line over 10 years and 330 operating days per year will be assumed. The results are shown in Table 10-1. The capital cost is given as \$1250 per BPD for a fixed cost of \$37.5 million.

Table 10-1. Conventional 3-Stage SCE Unit Economics

Feed Capacity	30,000 BPD
Product Capacity	10,000 BPD
Fixed Capital Investment	\$37.5 x 10 ⁶
Total Capital Investment	\$41.25 x 10 ⁶
Operating Costs:	
Utilities	\$ 3.5 x 10 ⁶
Labor and Supervision	\$ 1.0 x 10 ⁶
Maintenance and Supplies	\$ 2.1 x 10 ⁶
Other	\$ 2.3 x 10 ⁶
Depreciation	\$ 3.75 x 10 ⁶
	\$12.65 x 10 ⁶
Cost/Bbl of feed	\$ 1.28
Cost/Bbl of Product	\$ 3.83
Selling Price with 25% Return	\$ 6.96

Incidentally, this price is very close to that obtained from an internal rate of return of 20% after taxes.

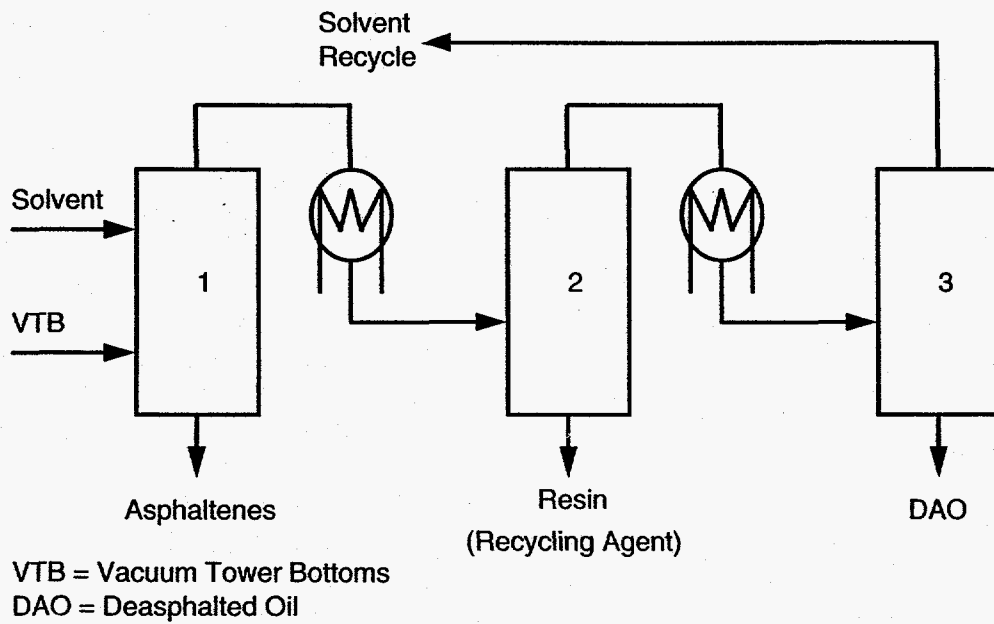


Figure 10-1. Conventional 3-stage SCE unit.

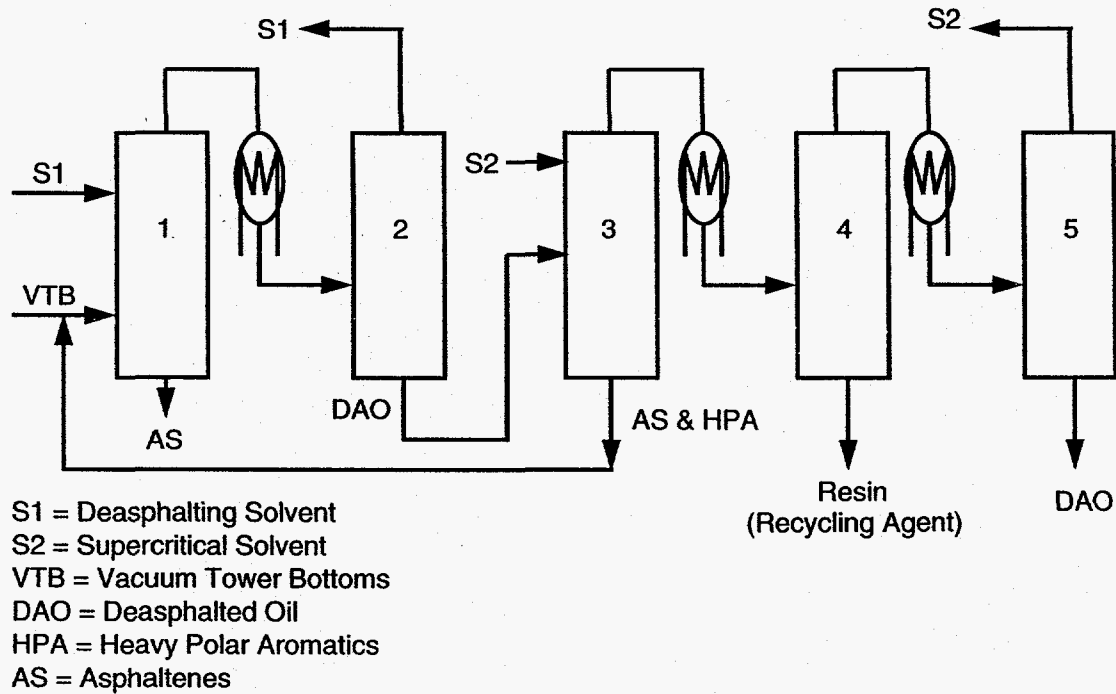


Figure 10-2. Deasphalting unit with 2 or 3-stage SCE unit.

Add a 2 or 3-Stage Unit to an Existing 2-Stage Facility

Because of the added stages, the original system can cut deeply into the feed sending perhaps 75% from stage 2, Figure 10-2 to the new unit. With the extra stages, probably half of this material can be recovered as recycling agent. Thus a 30,000 BPD original unit will send 22,500 BPD to the new unit producing 11,250 BPD of product. We will assume this unit scales as the 0.7 power so the cost of the new unit will be $\$30.7 \times 10^6$ for a TCI of $\$33.7 \times 10^6$. Utilities should be proportional to the feed and incremental labor should be small. We will assume half the stand alone arrangement. With these assumptions, the costs in Table 10-2 are obtained. Incidentally, if this is an add on to a SCE unit, the incremental utilities will be less as only one stripper is added.

Table 10-2. Deasphalting Unit Plus a 2 or 3-Stage SCE Unit Economics

Product Capacity	11.250 BPD
Fixed Capital	$\$30.7 \times 10^6$
Total Capital	$\$33.7 \times 10^6$
Operating Costs	
Utilities	$\$2.6 \times 10^6$
Labor and Supervision	$\$0.5 \times 10^6$
Maintenance and Supplies	$\$1.8 \times 10^6$
Other	$\$1.7 \times 10^6$
Depreciation	$\$3.1 \times 10^6$
	<hr/>
	$\$9.7 \times 10^6$
Cost/Bbl of Product	\$2.61
Selling Price/Bbl of Product	\$4.88

Build a 4 or 5-Stage Unit

This corresponds to Figure 10-2. It is similar to case 2 except that with more stages it can produce more and probably better recycling agent. It is like case 2 in structure so a feed of 30,000 BPD will be assumed to produce 11,250 BPD of product. The utility cost will increase somewhat

because of two solvent recycle sections, but both have 3 strippers and operate through essentially the same temperature range. We will assume an increased utility cost of \$1 million/yr. Labor cost should only slightly increase. From a capital standpoint, there are one or two extra separators and heat exchangers. It is doubtful if the fixed capital investment will increase 20% and the working capital not at all. This will be assumed. This yields the results in Table 10-3. This indicates that a 4 or 5-stage unit would cost only a little more to operate than a 3-stage unit, case 2. At the same time, it would be expected to produce more product of higher quality.

Table 10-3. 4 or 5-Stage SCE Unit Economics

Feed = 30,000 BPD

Product = 11,250 BPD

Fixed Capital Investment = $\$45 \times 10^6$

Total Capital Investment = $\$48.75 \times 10^6$

Operating Cost

Utilities	$\$ 4.5 \times 10^6$
Labor and Supervision	$\$ 1.3 \times 10^6$
Maintenance and Supplies	$\$ 2.6 \times 10^6$
Other	$\$ 2.9 \times 10^6$
Depreciation	$\$ 4.5 \times 10^6$
Total Cost	$\$15.8 \times 10^6$
Cost/Bbl of Product	$\$ 4.25$
Selling Price/Bbl	$\$ 7.54$

Add a Solvent Extraction Unit to an Existing DAO Unit

There are a number of solvent extraction (SX) processes used to remove aromatics from lube oil fractions. A largely light aromatic fraction is produced as a by-product and this material is sometimes used as a recycling agent. Sometimes these materials contain too much saturates, but more importantly, the viscosity is so low that not much can be used and the results of incompatible

mixing could be quite serious if only this material is used to soften the hard material. If however, a DAO were fed to a unit such as this, a recycling agent very similar to those studied in the work reported in Chapter 9 could be produced.

One of the best solvents now in use is n-methyl-2-pyrrolidone (NMP). A system combining this process with a DAO unit is shown in Figure 10-3. This figure shows the feed above the tower bottom and a stream of separated product returned to the bottom of the tower. This may not be necessary with a selective solvent, but it allows a very pure product to be produced.

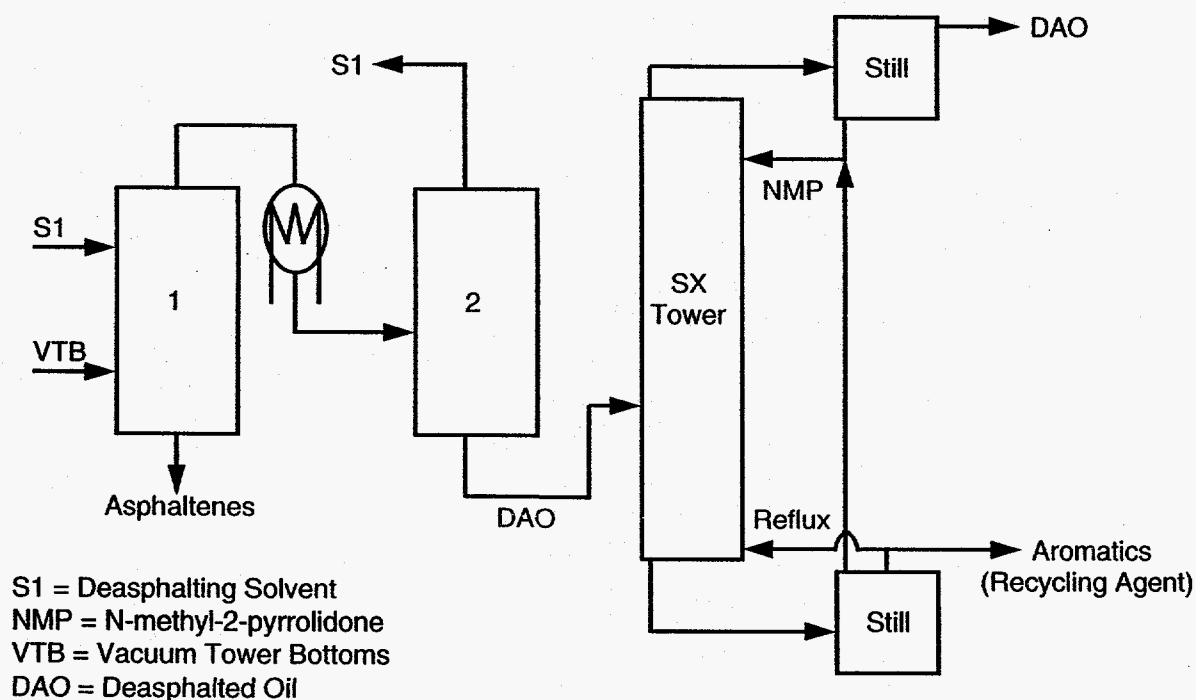


Figure 10-3. Deasphalting unit with solvent extraction unit.

In this design, the DAO unit cannot be integrated with the SX unit, so the cost will be estimated on a stand alone basis. We have a rough cost estimate for a 25,000 Bbl per day unit producing 12,000 Bbl/day of a recycling agent containing less than 10% saturates or recycling agent. The capital cost and utilities for this unit are given below (source, Bechtel Corporation process licensing department).

Capital Cost Estimate (order of magnitude - 30% + 50%)

U.S. Gulf Coast 4th quarter 1996

\$60 million inclusive of pilot testing and process technology fees

Estimated Utility Consumption

Fuel 120 MM BTU/hr

Steam 30 M lb/hr

Electric 1400 kw

Cooling Water 3500 GPM (20°ΔJ)

Solvent Makeup 550 lb/day

Using the procedures applied to the previous processes, the results shown in Table 10-4 were obtained. However, the working capital was taken as \$4 million as there is little reason for the higher capital cost to be reflected in working capital. This is the highest cost, but there is considerable uncertainty, and it could probably make a product that more nearly meets the desired composition.

In each instance, the cost and price given is without feed cost which may be DAO cracker feed, asphalt, or coker feed. No credit is assumed here, but in each case a very high grade DAO is produced as a light product.

Implementation

The costs of producing these agents are not excessive if viewed in the light of the considerable savings in money, energy, and waste. Reblended materials produced with these agents have superb resistance to oxidation hardening. Work reported in Chapter 8 also indicates that recycled asphalts can achieve Superpave performance grades that equal those of new asphalts.

Table 10-4. Conventional DAO Unit Plus Solvent Extraction Unit Economics

Labor and Supervision	\$ 1.3 x 10 ⁶
Utilities and Solvent	\$ 4.6 x 10 ⁶
Maintenance and Supplies	\$ 3.4 x 10 ⁶
Other	\$ 3.2 x 10 ⁶
Depreciation	\$ 6.0 x 10 ⁶
	<hr/>
	\$18.5 x 10 ⁶
Cost/Bbl of Product	\$ 4.67
Selling Price/Bbl	\$ 8.71

It must also be noted that equal Superpave grades can often be achieved simply by using a low viscosity asphalt. In these instances, probably no more than 25% of old material will be used, but this corresponds to usual practice. Road builders feel confident that if relatively small amounts of old material are used that the introduction of this material will not seriously affect the mix design.

In fact a reluctance to use large amounts of old material arises from the uncertainty of the uniformity of asphalt content and gradation of the old material. This can result from past repair work on sections of the road that will affect the composition of recycled material, and the process of digging up the old material can affect the aggregate gradation. These fears can be addressed, but until they are large scale, recycling will be inhibited.

Actually, the introduction of Superpave specifications is a further inhibition. Almost all state agencies are intent on meeting these specifications, and if they can be met with a recycled mix which uses a conventional asphalt, they are not likely to spend \$35-\$40 a ton more for a recycling agent even if it does show superior aging properties.

The fact is that Superpave specifications are relatively insensitive to aging so that the superb hardening properties of the recycling agents produced in this research are not sufficiently reflected in the Superpave grade. This is a serious shortcoming, because, if one believes that those specifications reflect long term performance, then one believes age hardening does not affect long term performance. In our view, the Superpave specifications must be viewed as only a first step and must be modified to reflect long term aging. Until then, recycling as envisioned in this report will be inhibited.

REFERENCES

- "AASHTO Designation PP1, Standard Practice for Accelerated Aging of Asphalt Binder Using a Pressurized Air Vessel (PAV)," *AASHTO Provisional Standards*, AASHTO, Washington, DC (1994).
- "AASHTO Designation TP1, Standard Test Method for Determining the Flexural Creep Stiffness of Asphalt Binder Using the Bending Beam Rheometer (BBR)," *AASHTO Provisional Standards*, AASHTO, Washington, DC (1994).
- Ali, M.A. and W.A. Nofal, "Application of High Performance Liquid Chromatography for Hydrocarbon Group Type Analysis of Crude Oils," *Fuel Sci. Technol. Int.*, **12**, 21-33 (1994).
- Altgelt, K.H. and E. Hirsh, "GPC Separation and Integrated Structural Analysis of Petroleum Heavy End," *Separation Science*, **5**, 855 (1970).
- Altgelt, K.H. and T.H. Gouw, "Chromatography of Heavy Petroleum Fractions," in *Advances in Chromatography*, Eds. J.C. Giddings and R.A. Keller, **13**, Marcel Dekker, New York, 71 (1975).
- Altgelt, K.H. and O.L. Harle, "The Effect of Asphaltenes on Asphalt Viscosity," *Ind. Eng. Chem. Prod. Res. and Dev. (now Ind. Eng. Chem. Res.)*, **14**, 240-246 (1975).
- Anderson, A.P., F.H. Stross, and A. Ellings, "Measurement of Oxidation Stability of Road Asphalts," *Ind. and Eng. Chem. Anal. Ed.*, **14**, 45 (1942).
- Anderson, D.I, D.E. Peterson, and M. Wiley, *Characteristics of Asphalts as Related to the Performance of Flexible Pavements*, Utah Department of Transportation Final Report UDOT-MR-76-6 (1976).
- Andrade, E.N., "The Viscosity of Liquids," *Nature*, **125**, 309 (1930).
- Arrhenius, S., "The Viscosity of Aqueous Mixtures (In German)," *Z. Phys. Chem.*, **1**, 285 (1887).
- Asphalt Hot-Mix Recycling*, Report MS-20, The Asphalt Institute, Lexington, KY (1981).
- "ASTM D-1754, Standard Test Method for Effect of Heat and Air on Asphaltic Materials", *Annual Book of ASTM Standards*, **04.03**, ASTM, Philadelphia, 158 (1994).
- "ASTM D-2872, Standard Test Method for Effect of Heat and Air on a Moving Film of

- Asphalt (Rolling Thin-Film Oven Test)," *Annual Book of ASTM Standards*, **04.03**, ASTM, Philadelphia, 245 (1994).
- "ASTM D-4124, Standard Test Methods for Separation of Asphalt into Four Fractions," *Annual Book of ASTM Standards*, **04.03**, ASTM, Philadelphia, 423 (1994).
- "ASTM D-4887, Standard Test Method for Preparation of Viscosity Blends for Hot Recycled Bituminous Materials," *Annual Book of ASTM Standards*, **04.03**, ASTM, Philadelphia, 509 (1994).
- Beg, S.A., F. Mahmud, and D.K. Al-Harbi, "Hydrocarbon Group Analysis of Arabian Crude Oils TBP-Fractions," *Fuel Sci. Technol. Int.*, **8**, 125-134 (1990).
- Bishara, S.W. and E. Wilkins, "Rapid Method for the Chemical Analysis of Asphalt Cement: Quantitative Determination of the Naphthene Aromatic and Polar Aromatic Fractions Using High Performance Liquid Chromatography," *Transp. Res. Rec.*, **1228**, 183-190 (1989).
- Blokker, P.C., and H. van Hoorn, "Durability of Bitumen in Theory and Practice," *5th World Petroleum Congress*, 417-429 (1959).
- Boduszynski, M.M., J.F. McKay, and D.R. Latham, "Asphaltenes, Where are You?," *Proc. Assoc. Asphalt Paving Technol.*, **49**, 123-143 (1980).
- Boudart, M., *Kinetics of Chemical Process*, Butterworth-Heinemann, Stoneham (1991).
- Branthaver, J.F., M. Nazir, J.C. Petersen, and S.M. Dorrence, "The Effect of Metalloporphyrins on Asphalt Oxidation. I. The Effect of Synthetic Chelates," *Liq. Fuels Technol. (now Fuel Sci. Technol. Int.)*, **1**, 355-369 (1983).
- Branthaver, J.F., M. Nazir, J.C. Petersen, S.M. Dorrence, and M.J. Ryan, "The Effect of Metalloporphyrins on Asphalt Oxidation. II. The Effect of Vanadyl Chelates Found in Petroleum," *Liq. Fuels Technol. (now Fuel Sci. Technol. Int.)*, **2**, 67-89 (1984).
- Branthaver, J.F., J.C. Petersen, J.J. Duvall, and P.M. Harnsberger, "Compatibilities of Strategic Highway Research Program Asphalts," *Transportation Research Record*, **1323**, 22 (1991).
- Brons, G. and J.M. Yu, "Solvent Deasphalting Effects on Whole Cold Lake Bitumen," *Preprints, Division of Petroleum Chemistry, American Chemical Society*, **40**, 785 (1995).
- Brown, A.B., J.W. Sparks, and O. Larsen, "Rate of Change of Softening Point, Penetration, and Ductility of Asphalt in Bituminous Pavement," *Proc. Assoc. Asphalt Paving Technol.*, **26**, 66 (1957).

- Brule, B., G. Ramond, C. Such, "Relationships Between Composition, Structure, and Properties of Road Asphalts: State of Research at the French Public Works Central Laboratory," *Transportation Research Record*, **1096**, 22 (1986).
- Burr, B.L., R.R. Davison, C.J. Glover, and J.A. Bullin, "Solvent Removal from Asphalt," *Transp. Res. Rec.*, **1269**, 1-8 (1990).
- Burr, B.L., R.R. Davison, H.B. Jemison, C.J. Glover, and J.A. Bullin, "Asphalt Hardening in Extraction Solvents," *Transp. Res. Rec.*, **1342**, 50-57 (1991).
- Burr, B.L., *Improved Methods for Extracting and Recovering Asphalts from Pavement Samples*, Ph.D. Dissertation, Texas A&M University, College Station, TX (1993).
- Burr, B.L., R.R. Davison, C.J. Glover, and J.A. Bullin, "Softening of Asphalts in Dilute Solutions at Primary Distillation Conditions," *Transp. Res. Rec.*, **1436**, 47-53 (1994).
- Button, J.W., M. Jawle, V. Jagadam, and D.N. Little, "Evaluation and Development of a Pressure Aging Vessel for Asphalt Cement," *Trans. Res. Rec.*, **1391**, 11 (1993).
- Bynum, D., Jr. and R.N. Traxler, "Gel Permeation Chromatography Data on Asphalts Before and After Service in Pavements," *AAPT*, **39**, 683 (1970).
- Carbognani, L. and A. Izquierdo, "Preparative Compound Class Separation of Heavy Oil Vacuum Residua by High Performance Liquid Chromatography," *Fuel Sci. Technol. Int.*, **8**, 1-15 (1990).
- Chaffin, J.M., R.R. Davison, C.J. Glover, and J.A. Bullin, "Viscosity Mixing Rules for Asphalt Recycling," *Transp. Res. Rec.*, **1507**, 78-85 (1995).
- Chaffin, J.M., *Characterization of Asphalt Recycling Agents and Evaluation of Recycled Asphalt Binder Aging Properties*, Ph.D. Dissertation, Texas A&M University, Department of Chemical Engineering, College Station, TX (1996).
- Chaffin, J.M., M. Liu, R.R. Davison, C.J. Glover and J.A. Bullin, "Supercritical Fractions as Asphalt Recycling Agents and Preliminary Aging Studies on Recycled Asphalts," *Ind. Eng. Chem. Res.*, **36**(3), 656-666 (1997).
- Choquest, F.S., and A.F. Verhasselt, "Natural and Accelerated Aging of Bitumens: Effects of Asphaltene," *Asphaltene Particles in Fossil Fuel Exploration, Recovery, Refining, and Production Processes*, M.K. Sharma and T.F. Yen, ed., Plenum Press, New York, p. 13 (1994).
- Corbett, L.W. and R.E. Swarbick, "Clues to Asphalt Composition," *Proc. Assoc. Asphalt Paving*

- Technol.*, **27**, 107 (1958).
- Corbett, L.W. and R.E. Swarbrick, "Composition Analysis Used to Explore Asphalt Hardening," *Proc. Assoc. Asphalt Paving Technol.*, **29**, 104 (1960).
- Corbett, L.W., "Densimetric Method for Characterizing Asphalt," *Analytical Chemistry*, **36**, 1967 (1964).
- Corbett, L.W., "Composition of Asphalt Based on Generic Fractionation, Using Solvent Deasphalting, Elution-Adsorption Chromatography, and Densimetric Characterization," *Anal. Chem.*, **41**, 576-579 (1969).
- Corbett, L.W., "Relationship Between Composition and Physical Properties of Asphalt," *Proc. Assoc. Asphalt Paving Technol.*, **39**, 481 (1970).
- Corbett, L.W. and P.E. Merz, "Asphalt Binder Hardening in the Michigan Test Road After 18 Years of Service," *Transportation Research Board*, **544**, 27 (1975).
- Corbett, L.W., "Reaction Variables in the Air Blowing of Asphalt," *Ind. Eng. Chem. Proc. Des. Dev.*, **14**, 181 (1975).
- Corbett, L.W., U. Petrossi, "Differences in Distillation and Solvent Separated Asphalt Residue," *Ind. Eng. Chem. Prod. Res. Dev.*, **17**, 342 (1978).
- Corbett, L.W., "Dumbbell Mix for Better Asphalt," *Hydrocarbon Process.*, **58**, 173-177 (1979).
- Corbett, L.W., and H.E. Schwyer, "Composition and Rheology Considerations in Age Hardening of Bitumen," *AAPT*, **50**, 571 (1981).
- Corbett, L.W., "Refinery Processing of Asphalt Cement," *Trans. Res. Rec.*, **999**, 1 (1984).
- Dark, W.A., "Crude Oil Hydrocarbon Group Separation Quantitation," *J. Liq. Chromatogr.*, **5**, 1645-1652 (1982).
- Dark, W.A., "Shale Oil Separation by High Performance Liquid Chromatography," *J. Liq. Chromatogr.*, **6**, 325-342 (1983).
- Dark, W.A. and W.H. McFadden, "The Role of HPLC and LC-MS in the Separation and Characterization of Coal Liquefaction Products," *J. Chromatogr. Sci.*, **16**, 289-293 (1978).
- Dark, W.A. and R.R. McGough, "Use of Liquid Chromatography in The Characterization of Asphalts," *J. Chromatogr. Sci.*, **16**, 610-615 (1978).

- Davidson, D.D., W. Canessa, and S.J. Escobar, "Recycling of Substandard or Deteriorated Asphalt Pavements - A Guideline for Design Procedures," *Proc. Assoc. Asphalt Paving Technol.*, **46**, 496 (1977).
- Davison, R.R., J.A. Bullin, C.J. Glover, B.L. Burr, H.B. Jemison, H.B., A.L.G. Kyle, and C.A. Cipione, *Development of Gel Permeation Chromatography, Infrared and Other Tests to Characterize Asphalt Cements and Correlate with Field Performance*, Research Report No. FHWA/TX-90/458-1F, Texas Transportation Institute, College Station, TX (1989).
- Davison, R. R., J. A. Bullin, C. J. Glover, J. R. Stegeman, H. B. Jemison, B. L. Burr, A. L. G. Kyle, and C. A. Cipione, *Design and Manufacture of Superior Asphalt Binders*, Texas Department of Transportation Final Report No. 1155 (1991).
- Davison, R. R., J. A. Bullin, C. J. Glover, H. B. Jemison, C. K. Lau, K. M. Lunsford, and P. L. Bartnicki, *Design and Use of Superior Asphalt Binders*, Texas Department of Transportation Final Report No. 1249 (1992).
- Davison, R.R., J.A. Bullin, C.J. Glover, J.M. Chaffin, G.D. Peterson, K.M. Lunsford, M.S. Lin, M. Liu, M., A. Ferry, *Verification of an Asphalt Aging Test and Development of Superior Recycling Agents and Asphalts*, Texas State Department of Highways and Public Transportation Final Report No. 1314-1F (1994).
- Davison, R.R., C.J. Glover, B.L. Burr, and J.A. Bullin, "SEC of Asphalts," in *Handbook of Size Exclusion Chromatography*, Ed. Chi-San Wu, Marcel-Dekker, Inc., New York, NY, 211-247 (1995).
- Dickinson, E.J., and J.H. Nicholas, "The Reaction of Oxygen with Tar Oils," *Road Research Technical Paper No 16*, 1 (1949).
- Dickinson, E.J., J.H. Nicholas, and S. Boas-Traube, "Physical Factors Affecting the Absorption of Oxygen by Thin Film of Bitumen Road Binders," *J. Appl. Chem.*, **8**, 673-687 (1958).
- Dunning, R.L., and R.L. Mendenhall, "Design of Recycled Asphalt Pavements and Selection of Modifiers," *Recycling of Bituminous Pavements, ASTM STP 662*, Ed. L.E. Wood, Philadelphia, PA, 35 (1978).
- Ebberts, A.R., "Oxidation of Asphalt in Thin Films," *Ind. And Eng. Chem.*, **34**, 1048 (1942).
- Eilers, H.J., "The Colloidal Structure of Asphalt," *J. Phys. Colloid Chem.*, **53**, 1195-1211 (1948).
- Epps, J.A., D.N. Little, R.J. Holmgreen, and R.L. Terrel, *Guidelines for Recycling Pavement Materials*. NCHRP-224 (1980).

- Ferry, J., *Viscoelastic Properties of Polymers*, John Wiley and Sons, 4th ed., New York, NY (1985).
- Gannon, C.R., R.H. Wombles, C.A. Ramey, J.P. Davis, and W.V. Little, "Recycling Conventional and Rubberized Bituminous Concrete Pavements Using Recycling Agents and Virgin Asphalt as Modifiers (A Laboratory and Field Study)," *Proc. Assoc. Asphalt Paving Technol.*, **49**, 95 (1980).
- Gayla, L.C. and J.C. Suatoni, "Rapid SARA Separations by High Performance Liquid Chromatography," *J. Liq. Chromatogr.*, **3**, 229 (1980).
- Gearhart, J.A. and L. Garwin, "ROSE Process Improves Resid Feed," *Hydrocarbon Processing*, **55**, 125 (1976a).
- Gearhart, J.A. and L. Garwin, "Resid-Extraction Process Offers Flexibility," *Oil and Gas Journal*, **75**, 63 (1976b).
- Gearhart, J.A., "Solvent Treat Resids," *Hydrocarbon Processing*, **59**, 5 (1980).
- Girdler, R.B., "Constitution of Asphaltenes and Related Studies," *Proc. Assoc. Asphalt Paving Technol.*, **34**, 45-79 (1965).
- Glover, C.J., J.A. Bullin, J.W. Button, R.R. Davison, G.R. Donaldson, M.W. Hlavinka, and C.V. Philip, *Characterization of Asphalts Using Gel Permeation Chromatography and Other Methods*, Research Report No. FHWA/TX-87/53+419-1F, Texas Transportation Institute, College Station, TX (1987).
- Goodrich, J.L., J.E. Goodrich, and W.J. Kari, "Asphalt Composition Tests: Their Application and Relation to Field Performance," *Transp. Res. Rec.*, **1096**, National Research Council, Washinton, D.C., 164-167 (1986).
- Grunberg, L. and A.H. Nissan, "Mixture Law for Viscosity," *Nature*, **164**, 799-800 (1949).
- Halstead, W.J., F.S. Rostler, and R.M. White, "Properties of Highway Asphalts-Part III, Influence of Chemical Compositon," *Proc. Assoc. Asphalt Paving Technol.*, **35**, 91 (1966).
- Halstead, W.J., "Relation of Asphalt Chemical Composition to Physical Properties and Specifications," *Proc. AAPT*, **54**, 91 (1985).
- Handbook of Chemistry and Physics*, Editors R.C. Weast, M.J. Astle, and W.H. Beyer, **68** (1987).
- Harsberger, P.M., J.M. Wolf, and J.C. Petersen, "Oxidation of SHRP Asphalts at Different

- Temperatures Using the TFAAT Method," *Proceeding of the International Symposium Chemistry of Bitumens, Vol II.*, Rome, Italy, 706 (1991).
- Heukelom, W. and P.W.O. Wijga, "Viscosity of Dispersions as Governed by Concentration and Rate of Shear," *Proc. Assoc. Asphalt Paving Technol.*, **40**, 418-437 (1971).
- Hoiberg, A.J. and W.E. Garris Jr., "Analytical Fractionation of Asphalts," *Ind. Eng. Chem. Anal. Ed.*, **16**, 294 (1944).
- Hubbard, R.L. and K.E. Stanfield, "Determination of Asphaltenes, Oils, and Resins in Asphalts," *Anal. Chem.*, **20**, 460 (1948).
- Hughes, F.J., "Asphalt Oxidation Studies at Elevated Temperatures," *I&EC Product Research and Development*, **1**, 290 (1962).
- Huh, J.D. and R.E. Robertson, "Modeling of Oxidative Aging Behavior of Asphalts from Short Term, High Temperature Data as a Step Toward Prediction of Pavement Aging," Preprint 961112, 75th Annual Meeting of the Transportation Research Board, Washington, DC (1996).
- Hveem, F.N., Zube, E., and Skog, J., "Proposed New Tests and Specifications for Paving Grade Asphalts," *Proc. Assoc. Asphalt Paving Technol.*, **32**, 271-327 (1963).
- Hydrocarbon Processing*, **71**:11, 159 (Nov. 1992).
- Irving, J.B., *Viscosities of Binary Liquid Mixtures: A Survey of Mixture Equations*, Report 630, National Engineering Laboratory, U.K. Department of Industry (1977a).
- Irving J.B., *Viscosities of Binary Liquid Mixtures: The Effectiveness of Mixture Equations*, Report 631, National Engineering Laboratory, U.K. Department of Industry (1977b).
- Ishai, I., "A Suggested Methodology for the Analysis of Asphalt Age-Hardening," *Journal of Testing and Evaluation*, **15**, 127 (1987).
- Ishai, I., B. Brule, J.C. Vaniscote and G. Ramond, "Some Rheological and Physico-Chemical Aspects of Long-Term Asphalt Durability", *AAPT*, **57**, 65 (1988).
- Jamieson, I.L. and M.M. Hattingh, "The Correlation of Chemical and Physical Properties of Bitumens with Their Road Performance," *Proc. Australian Road Research Board*, **5**, 293 (1970)
- Jemison, H.B., R.R. Davison, C.J. Glover, and J.A. Bullin, "Evaluation of Standard Oven Tests for Hot-Mix Plant Aging," *Transportation Research Record*, **1323**, 77 (1991).

- Jemison, H.B., *Supercritical Refining of Asphalts*, PhD Dissertation, Texas A&M University, Department of Chemical Engineering, College Station, TX, (1992).
- Jemison, H.B., B.L. Burr, R.R. Davison, J.A. Bullin, and C.J. Glover, "Application and Use of the ATR, FT-IR Method to Asphalt Aging Studies," *Fuel Sci. Technol. Int.*, **10**, 795-808 (1992).
- Jemison, H.B., R.R. Davison, C.J. Glover, and J.A. Bullin, "Fractionation of Asphalt Materials by Using Supercritical Cyclohexane and Pentane," *Fuel Sci. Technol. Int.*, **13**, 605-638 (1995).
- Jennings, P.W., "Workshop-Prediction of Asphalt Performance by HP-GPC," *Proc. Assoc. Asphalts Paving Technol.*, **54**, 635 (1985).
- Jones, G.M, *The Effect of Hydrated Lime on Asphalt in Bituminous Pavements*, Paper prepared for presentation at the National Lime Association Meeting, Colorado Springs, CO, May 22, 1971.
- Kandhal, P.S. and W.C. Koehler, "Significant Studies on Asphalt Durability: Pennsylvania Experience," *Transportation Research Record*, **999**, 41 (1984).
- Kemp, G.R., and N.H. Predoehl, "A Comparison of Field and Laboratory Environments on Asphalt Durability," *AAPT*, **50**, 492 (1981).
- Kleinschmidt, L.R., "Chromatographic Method for the Fractionation of Asphalt into Distinctive Groups of Components," *J. of Res. NBS*, **54**, 163 (1955).
- Knotnerus, J., "Bitumen Durability-Measured by Oxygen Absorption", *Ind. Eng. Chem. Prod. Res. Develop.*, **11**, 411 (1972).
- Lau, C.K., K.M. Lunsford, C.J. Glover, R.R. Davison, J.A. and Bullin, "Reaction Rates and Hardening Susceptibilities as Determined from POV Aging of Asphalts," *Transp. Res. Rec.*, **1342**, 50-57 (1992).
- Lee, A.R., and E.J. Dickinson, "The Durability of Road Tar," *Road Research Technical Paper No. 31*, 1 (1954).
- Lee, D.Y., "Development of a Laboratory Durability Test for Asphalt," *Hwy. Res. Board Bulletin*, **231**, 34 (1968).
- Lee, D.Y. and R.J. Huang, "Weathering of Asphalts as Characterized by Infrared Multiple Internal Reflectance Spectra," *Appl. Spectrosc.*, **27**, 435-440 (1973).

- Lin, M.S., *The Formation of Asphaltenes and Its Impact on the Chemical and Physical Properties of Asphalts*, Ph.D. Dissertation, Texas A&M University, College Station, Texas (1995).
- Lin, M.S., K.M. Lunsford, C.J. Glover, R.R. Davison, and J.A. Bullin, "The Effects of Asphaltenes on the Chemical and Physical Characteristics of Asphalts," In *Asphaltenes: Fundamentals and Applications*, Eds. E. Y. Sheu and O.C. Mullins, Plenum Press, New York, 155 (1995a).
- Lin, M.S., C.J. Glover, R.R. Davison, and J.A. Bullin, "The Effect of Asphaltenes on Asphalt Recycling and Aging," *Transp. Res. Rec.*, **1507**, 86-95 (1995b).
- Lin, M.S., J.M. Chaffin, M. Liu, C.J. Glover, R.R. Davison, and J.A. Bullin, "The Effect of Asphalt Composition on the Formation of Asphaltenes and Their Contribution to Asphalt Viscosity," *Fuel Sci. Technol. Int.*, **14**(1&2), 139-162 (1996).
- Liu, M., *The Effects of Asphalt Fractional Composition on Properties*, PhD Dissertation, Texas A&M University, Department of Chemical Engineering, College Station, TX, (1996)
- Liu, M., K.M. Lunsford, R.R. Davison, C.J. Glover, and J.A. Bullin, "The Kinetics of Carbonyl Formation in Asphalt," *AIChE J.*, **42**, 1069 (1996).
- Low, J.Y., R.L. Hood, and K.Z. Lynch, "Valuable Products from the Bottom of the Barrel Using ROSE Technology," *Preprints, Division of Petroleum Chemistry, American Chemical Society*, **40**, 780 (1995).
- Lundanes, E. and Tyge Greibrokk, "Quantitation of High Boiling Fractions of North Sea Oil After Class Separation and Gel Permeation Chromatography," *J. Liq. Chromatogr.*, **8**, 1035-1051 (1985).
- Lunsford, K.M., *The Effect of Temperature and Pressure on Laboratory Oxidized Asphalt Films with Comparison to Field Aging*, PhD Dissertation, Texas A&M University, Department of Chemical Engineering, College Station, TX, (1994).
- Manheimer, J., "The Effects of Paraffins on Asphalt," *Proceeding of The First World Petroleum Congress*, Vol 2, 553-556 (1933).
- Martin, K.L., R.R. Davison, C.J. Glover, and J.A. Bullin, "Asphalt Aging in Texas Roads and Test Sections," *Transp. Res. Rec.*, **1269**, 9-19 (1990).
- McHugh, M. and V. Krukoni, *Supercritical Fluid Extraction: Principles and Practice*, Butterworths, Boston, MA (1986).
- Mehrotra, A.K., "Development of Mixing Rules for Predicting the Viscosity of Bitumen and

- Its Fractions Blended with Toluene," *Can. J. Chem. Eng.*, **68**, 839 (1990).
- Mehrotra, A.K., "Mixing Rules for Predicting the Viscosity of Bitumens Saturated with Pure Gases," *Can. J. Chem. Eng.*, **70**, 165 (1992).
- Mortazavi, M. and J.S. Moulthrop, *The SHRP Materials Reference Library*, SHRP-A-646 (1993).
- Newcomb, D.E., B.J. Nusser, B.M. Kiggundu, and D.M. Zallen, "Laboratory Study of the Effects of Recycling Modifiers on Aged Asphalt Cement," *Transportation Research Record*, **968**, 66 (1984).
- Noureldin, A.S. and L.E. Wood, "Evaluating Recycled Asphalt Binders by the Thin-Film Oven Test," *Transportation Research Record*, **1269**, 20 (1990).
- Pal R. and E. Rhodes, "Viscosity/Concentration Relationship for Emulsions," *J. Rheol.*, **33**, 1021-1045 (1989).
- Pearson, C.D., G.S. Huff, and S.G. Gharfeh, "Technique for the Determination of Asphaltenes in Crude Oil Residues," *Anal. Chem.*, **58**, 3266-3269 (1986).
- Peters, M.S. and K.D. Timmerhaus, *Plant Design and Economics for Chemical Engineers*, 4th edition, McGraw-Hill, Inc., New York, 210 (1991).
- Petersen, J.C., *Relationships Between Asphalt Chemical Composition and Performance-Related Properties*, Prepared for presentation at the annual meeting of the Asphalt Emulsion Manufacturers Association, Las Vegas, Nevada, March 16-19, 1982.
- Petersen, J.C., "Chemical Composition of Asphalt as Related to Asphalt Durability: State of the Art," *Transportation Research Record*, **999**, 13 (1984).
- Petersen, J.C., "Quantitative Functional Group Analysis of Asphalts Using Differential Infrared Spectrometry and Selective Chemical Reactions-Theory and Application," *Trans. Res. Rec.*, **1096**, 1 (1986).
- Petersen, J.C., H. Plancher, and P.M. Harnsberger, "Lime Treatment of Asphalt to Reduce Age Hardening and Improve Flow Properties," *Proc. Assoc. Asphalt Paving Technol.*, **56**, 632-653 (1987).
- Petersen, J.C., J.F. Branthaver, R.E. Robertson, P.M. Harnsberger, J.J. Duvall, and E.K. Ensley, "Effects of Physicochemical Factors on Asphalt Oxidation Kinetics," *Transp. Res. Rec.*, **1391**, 1-10 (1993).

- Peterson G.D., *Relationship Between Composition and Performance of Asphalt Recycling Agents*, MS Thesis, Department of Chemical Engineering, Texas A&M University, College Station, TX (1993).
- Peterson, G.D., R.R. Davison, C.J. Glover, and J.A. Bullin, "The Effect of Composition on Asphalt Recycling Agent Performance," *Transp. Res. Rec.*, **1436**, 38-46 (1994).
- Plancher, H., E.L. Green, and J.C. Petersen, "Reduction of Oxidative Hardening of Asphalts by Treatment with Hydrated Lime - A Mechanistic Study," *Proc. Assoc. Asphalt Paving Technol.*, **45**, 1-19 (1976).
- Que, G., W. Liang, Y. Chen, C. Liu, and Y. Zhang, "Relationships Between Chemical Composition and Performance of Paving Asphalt," *Proceeding of the International Symposium: Chemistry of Bitumens*, Rome, Italy, **2**, 517-527 (1991).
- Reerink, H. and J. Lijzenga, "Molecular Weight Distributions of Kuwait Asphaltenes as Determined by Ultracentrifugation. Relation with Viscosity of Solutions," *J. Inst. Pet.*, **59**, 211 (1973).
- Reerink, H. and J. Lijzenga, "Gel-Permeation Chromatography Calibration Curve for Asphaltenes and Bituminous Resins," *Analytical Chemistry*, **47**, 2160 (1975).
- Roberts, F.L., P.S. Kandahl, E.R. Brown, D.-Y. Lee, and T.W. Kennedy, *Hot Mix Asphalt Materials, Mixture Design, and Construction*, NAPA Education Foundation, Lanham, MD (1991).
- Rostler, F.S. and H.W. Sternberg, "Compounding Rubber and Petroleum Products," *Ind. Eng. Chem.*, **41**, 598-608 (1949).
- Rostler, F.S., and R.M. White, *Influence of Chemical Composition of Asphalt on Performance, Particularly Durability*, ASTM STP 277, Symposium on Road and Paving Materials, 64-88 (1959).
- Rostler, F.S. and R.M. White, "Composition and Change in Composition of Highway Asphalts, 85-100 Penetration Grade," *Proc. Assoc. Asphalt Paving Technol.*, **31**, 35 (1962).
- Rostler, F.S., "Fractional Composition: Analytical and Functional Significance," in *Bituminous Materials: Volume II-Asphalts*, Ed. A.J. Hoiberg, Robert E. Kreiger, Huntington, NY, 151 (1979).
- Rostler, F. and K.S. Rostler, "Basic Considerations in Asphalt Research Pertaining to Durability," *Proc. Assoc. Asphalt Paving Technol.*, **50**, 582 (1981).

- Savastano, C.A., "The Solvent Extraction Approach to Petroleum Demetallization," *Fuel Sci. Technol. Int.*, **9**, 855-871 (1991).
- Sheu, E.Y., M.M. De Tar, and D.A. Storm, "Rheological Properties of Vacuum Residue Fractions in Organic Solvents," *Fuel*, **70**, 1151-1156 (1991).
- Shiau, J.-M., M. Tia, B.E. Ruth, and G.C. Page, "Characterization of Age-Hardening Potential of Asphalts by Using Corbett-Swarbick Asphalt Fractionation Test," *Transportation Research Record*, **1323**, 53 (1991).
- SHRP Binder Specification, Draft No. 7G., SHRP, Federal Highway Administration, Washington, DC (1992).
- Skog, J. and E. Zube, "Durability of Paving Asphalts Part II.," State of California Dept. of Public Works Div. Of Highways, Materials and Research Dept. Research Report M & R 633134-2 (1966).
- Stegeman, J.R., R.R. Davison, C.J. Glover, and J.A. Bullin, "Supercritical Fractionation and Reblending to Produce Improved Asphalts," in *Proceedings of the International Symposium: Chemistry of Bitumens*, Rome, Italy, **1**, 336-381 (1991).
- Stegeman, J.R., A.L. Kyle, B.L. Burr, H.B. Jemison, R.R. Davison, C.J. Glover, and J.A. Bullin, "Compositional and Physical Properties of Asphalt Fractions Obtained by Supercritical Extraction," *Fuel Sci. Technol. Int.*, **10**, 767-794 (1992).
- Storm, D.A. and E.Y. Sheu, "Rheological Studies of Ratawi Vacuum Residue at 366K," *Fuel*, **72**, 233 (1993).
- Strieter, O.G., and H.R. Snoke, "A Modified Accelerated Weathering Test for Asphalts and Other Materials," *Journal of the Research of the National Bureau of Standards*, **16**, 481 (1936).
- Suatoni, J.C., H.R. Garber, and B.E. Davis, "Hydrocarbon Group Types in Gasoline-Range Materials by High Performance Liquid Chromatography," *J. Chromatogr. Sci.*, **13**, 367-371 (1975).
- Suatoni, J.C. and R.E. Swab, "Rapid Hydrocarbon Group-Type Analysis by High Performance Liquid Chromatography," *J. Chromatogr. Sci.*, **13**, 361-366 (1975).
- Suatoni, J.C. and H.R. Garber, "Hydrocarbon Group-Type Analysis of Petroleum Fractions [b.p. 190°-360°C] by High Performance Liquid Chromatography," *J. Chromatogr. Sci.*, **14**, 546-548 (1976).
- Suatoni, J.C. and R.E. Swab, "Preparative Hydrocarbon Compound Type Analysis by High

- Performance Liquid Chromatography," *J. Chromatogr. Sci.*, **14**, 535-537 (1976).
- Such, C. and B. Brule, "Characterization of a Road Asphalt by Chromatographic Techniques (GPC and HPLC)," *J. Liq. Chromatogr.*, **2**, 437 (1979).
- Thenoux, G., C.A. Bell, and J.E. Wilson, "Evaluation of Asphalt Physical and Fractional Properties and Their Interrelationship," Paper No.870531 presented at the Transportation Research Board 67th Annual Meeting, Washington D.C., January 11-14 (1988).
- Traxler, R.N. and H.E. Schweyer, "How to Make Component Analysis," *Oil and Gas Journal*, **52**, 158 (1953).
- Traxler, R. N., "Relation Between Hardening and Composition of Asphalt," *American Chemical Society Division of Petroleum Chemistry*, **5**, A71-A77 (1960).
- Traxler, R.N., "Relation Between Asphalt Composition and Hardening by Volatilization and Oxidation," *Proc. Assoc. Asphalt Paving Technol.*, **36**, 359-377 (1961).
- Van Oort, W.P., "Durability of Asphalt, Its Aging in the Dark," *Ind. Eng. Chem.*, **48**, 1196-1201 (1956).
- Verhasselt, A.F., and F.S. Choquet, "A New Approach to Studying the Kinetics of Bitumen Aging," *Proceedings of the International Symposium Chemistry of Bitumens*, Rome, Italy, **2**, 686 (1991).
- Verhasselt, A.F., and F.S. Choquest, "Comparing Field and Laboratory Aging of Bitumens on a Kinetics Basis," *Trans.Res. Rec.*, **1391**, 30 (1993).
- Way, P.J., H.I. Fuller, T. Les, and A. Winward, "Road and Laboratory Experiments on Bitumens from Western Hemisphere and Middle East Crudes," *5th World Petroleum Conference*, 433 (1959).
- White, R.M., W.R. Mitten, and J.B. Skog, "Fractional Components of Asphalts-Compatibility and Interchangeability of Fractions Produced from Different Asphalts," *Proc. Assoc. Asphalt Paving Technol.*, **39**, 492 (1970).
- Wisneski, M.L., *The Effects of Lime and Amines on the Aging of Asphalts and Recycling Agents*, M.S. Thesis, Texas A&M University, Department of Chemical Engineering, College Station, TX, (1995).
- Wisneski, M.L., J.M. Chaffin, R.R. Davison, J.A. Bullin, and C.J. Glover, "The Use of Lime in Recycling Asphalt," *Transp. Res. Rec.*, **1535**, 117-123 (1996).

ABBREVIATIONS

AB	air-bubbling
AI	aging index
AS	asphaltenes
ASTM	American Society for Testing and Materials
ATR	attenuated total reflectance
n-C ₇	n-heptane
CRA	commercial rejuvenating agent
DAO	deasphalted oil
DLV	dimensionless log viscosity
DMA	dynamic mechanical analysis
DOE-OIT	Department of Energy, Office of Industrial Technologies
EtOH	ethanol
FTIR	Fourier transform infrared spectroscopy
GPC	gel permeation chromatography
HPLC	high performance liquid chromatography
IRR	internal rate of return
ISCF	industrial supercritical fraction
MeOH	methanol
MRL	materials reference library
NA	naphthene aromatic
PA	polar aromatic
PAV	pressure aging vessel
PB	payback
POV	pressure oxygen vessel
PTFE	poly tetrafluoroethylene
RA	rejuvenating agent
RAP	recycled asphalt pavement
RI	refractive index
ROSE	residual oil supercritical extraction
RTFOT	rolling thin film oven test
SA	saturates
SCF	supercritical fraction
SHRP	Strategic Highways Research Program
SPP	solvation power parameter
TAMU	Texas A&M University
TCE	trichloroethylene
TFOT	thin film oven test
THF	tetrahydrofuran
VTS	viscosity temperature susceptibility

NOTATION

A	frequency factor for oxidation
AS%	weight percentage of asphaltenes
AFS	asphaltene formation susceptibility
A_{vis}	frequency factor for viscosity dependence on temperature
CA	infrared carbonyl peak area
CA_0	carbonyl peak area zero-time intercept
CA_{tank}	infrared carbonyl peak area of virgin asphalt
Ca_{unaged}	carbonyl area of unaged fractions
E	activation energy for oxidation
E_{vis}	activation energy for viscosity dependence on temperature
G^*	complex dynamic shear modulus
$HS_{60^\circ C}$	hardening susceptibility at 60°C
HS_T	hardening susceptibility at temperature T
HS_{T_0}	hardening susceptibility at reference temperature T_0
m	model parameter in equation 1-7a and 3-4; the η_0^* zero CA intercept
O%	oxygen content in weight percentage
P	aging pressure
R	universal gas constant
R_{CA}	oxidation rate
RF_s	response factor of saturates
t	time or aging time
T	absolute temperature

Greek letters

α	pressure reaction order with respect to oxygen
β	model parameter defining initial jump pressure dependence
γ	pressure dependence factor of initial jump
Δ	change in
δ	pressure dependence factor of HS
η	viscosity
η_0^*	low frequency limiting viscosity
θ	model parameter defining HS pressure dependence

APPENDIX A

EXPERIMENTAL METHODS

SUPERCRITICAL FRACTIONATION

The supercritical fractionation unit has been described in Study 1155 (Davison et al., 1991) and Study 1249 (Davison et al., 1992). A brief description of the process, operating conditions, and apparatus modifications follow.

Process Description

The following description is taken primarily from the TxDOT Study 1249 (Davison et al, 1992) report with appropriate modifications. The unit operates at a constant pressure above the critical pressure of the solvent. The SC fractionation unit separates heavy petroleum products into up to four fractions according to solubility in SC solvents. The temperatures of the separators determine the density of the solvent and, consequently, the solvent power in each vessel. Components of the feed precipitate when no longer soluble in the solvent. The lightest, most-soluble materials are removed by decompression during solvent recovery.

Figures A-1 and A-2 illustrate schematically the SC unit. The solvent is pumped to the operating pressure in S1-S3 by MP1. Several hours are required to bring the temperatures to the desired steady-state values. The steady-state operating temperature in S4 determines the steady state pressure for S4. Once steady-state conditions are achieved, MP2 is activated, introducing feed material into the circulating solvent stream. The temperature in each separator determines the solubility in the SC solvent. The insoluble material is transferred from the separator to its corresponding collector periodically to avoid potential plugging problems while the soluble material travels to the next separator. Finally, the overhead mixture from S3 passes through the control valve, where the pressure is reduced to significantly subcritical value. At these gaseous conditions, none of the asphaltic material is soluble and complete separation of the solvent is achieved. The solvent then passes overhead, is condensed in WC1 and flows back into the

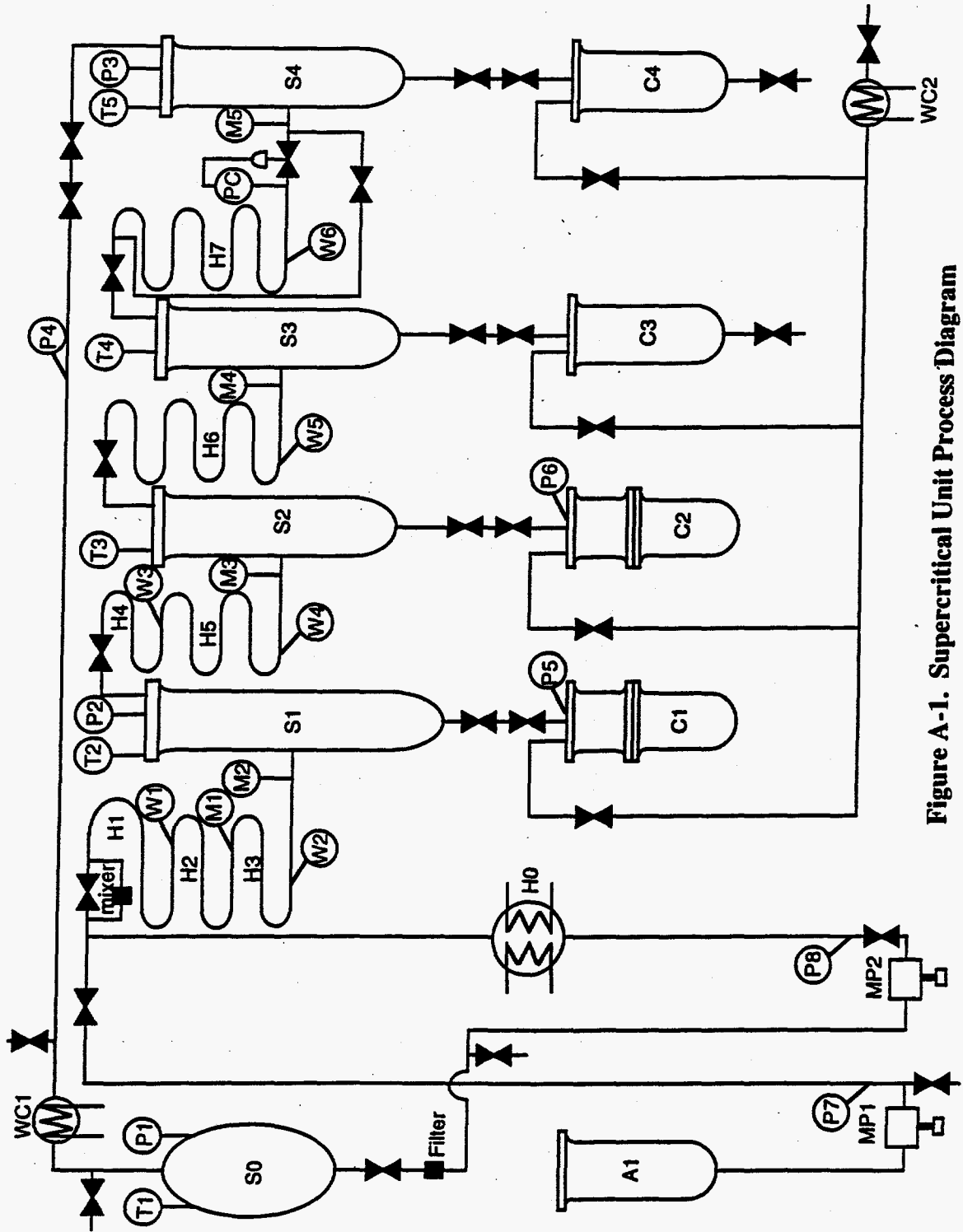


Figure A-1. Supercritical Unit Process Diagram









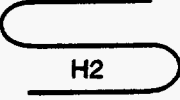

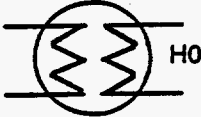

S0	Solvent Tank	S1-S4	Separators
C1-C4	Collectors	A1	Asphalt Tank
	In-line Filter/mixer		Valve
	Control Valve		Thermocouple
	Tubing Wall Temperature Thermocouple		Temperature Monitor and Controller
	Pressure Controller		Pressure Gauge
	Heating Tape Heater		Metering Pump
	Dual Purpose Heater/Cooler		Water Cooled Condenser

Figure A-2. Legend for Supercritical Extraction Unit Diagram

solvent reservoir. For this DOE project, n-pentane is the solvent used for supercritical fractionation.

The four asphalts fractionated during the first year of this DOE project were fractionated in two passes through the unit. The lightest fraction from the first pass was fed through the unit a second time yielding eight fractions that may be analyzed. The lightest fraction from the second pass is designated as fraction F1 and the heaviest fraction from the first pass is designated as fraction F8 (fraction F5 is the feed material for the second pass through the unit).

AGED ASPHALT PRODUCTION

During the first year of this DOE project, a new apparatus was developed for aging a large quantity of asphalt by bubbling air through a well mixed asphalt sample at moderate temperature. The apparatus consists of a variable speed 1/4 horsepower motor which drives a 2" diameter mixing shaft placed in a half full gallon can of asphalt. Another, less powerful mixer (1/15th horsepower) is also available for use. The can is wrapped with a heating tape connected to a variable transformer and a thermocouple actuated on/off controller.

Building air passes through a surge tank, filter, and a copper coil placed in a mineral oil temperature bath before being fed to the asphalt. The air is introduced to the asphalt through a 5" diameter sparging ring made from 1/4" stainless steel tubing with 14 nearly uniformly spaced 1/16" holes. The inlet air temperature is controlled by adjusting both the temperature of the oil bath and the air flow rate. The operating temperature of the air-bubbled reaction vessel must be high enough for the oxidation to proceed at an appreciable rate, but not so high as to drastically alter the reaction mechanism or reaction products. To produce pavement-like materials, the reaction temperature is targeted at 93.3°C (200°F), initially. However, as the asphalt ages, the temperature begins to rise due to increased viscous dissipation. This is not critical, but the temperature should not be allowed to exceed 110°C (230°F).

PRESSURE OXYGEN VESSEL (POV)

The original unit is described by Lau (1992) and Davison et al. (1992). In order to improve on aging simulation capacity, four additional units were constructed and a central control panel was installed as shown in Figure A-3. Later, to eliminate temperature gradient problems with the initial design, the vessels were placed in glycol/water baths.

Figure A-4 shows a schematic of one of the POVs. The vessels are located behind a steel wall in an explosion proof hood. Each vessel is contained in an aluminum barrel filled to the bottom of the top flange with a mixture of triethylene glycol and water. The vessel is monitored and controlled from a panel outside the explosion proof hood. The control panel houses a compound pressure gauge to monitor the pressure, a variable transformer to control the amount of electrical power to the heating elements in the water/triethylene glycol bath, a temperature controller which controls the temperature of the bath, and a recorder to monitor the temperature within the POV. A stirrer is employed in the bath to insure that the temperature distribution in the bath is uniform. A vacuum pump is used to evacuate the vessels before charging with oxygen or to remove oxygen depleted air once per day. Three valves per vessel, as labeled in Figure A-3, are used for venting to atmospheric pressure, evacuating to low pressure to remove the gas inside the vessel, and charging with oxygen. The oxygen feed valve isolates the POVs from the oxygen cylinder when closed.

Asphalt samples are prepared in aluminum trays. The dimensions of the tray are 7.0 cm (2.75 in) by 3.5 cm (1.38 in). Typical film thicknesses of less than 1 mm (0.039 in) are used to minimize potential diffusion problems at low pressure; however, diffusion studies may be performed with thicker films. After preparing the asphalt samples, loading the sample rack, and allowing the temperature in the POV to reach equilibrium, the operator places the rack inside the POV and bolts the cover flange to the top. The vent valves, oxygen feed valves, and vacuum valves are closed. A vacuum pump evacuates the air in the vessel to a pressure of 0.03 atm absolute. The vessels are slowly pressurized to the desired level by manipulating the oxygen cylinder regulator and oxygen feed valves for pure oxygen aging, or by slowly opening the atmospheric venting valve for aging with air (note 0.2 atm oxygen is equivalent to atmospheric

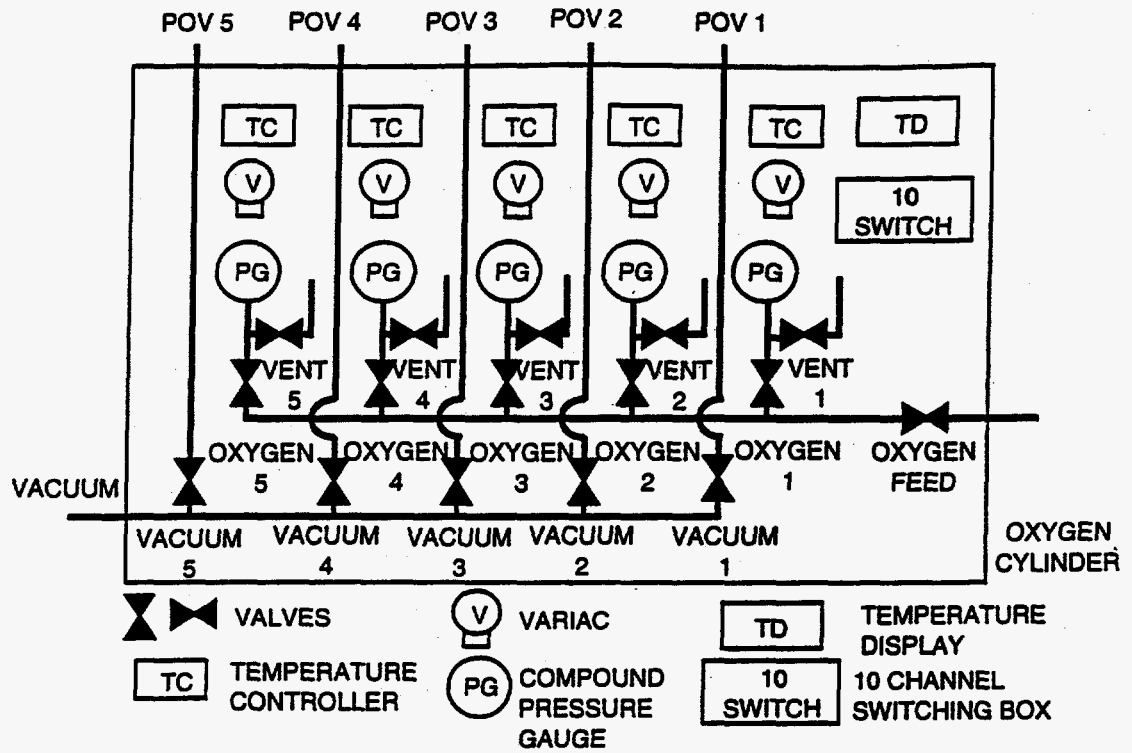


Figure A-3. Pressure Oxygen Vessel Control Panel

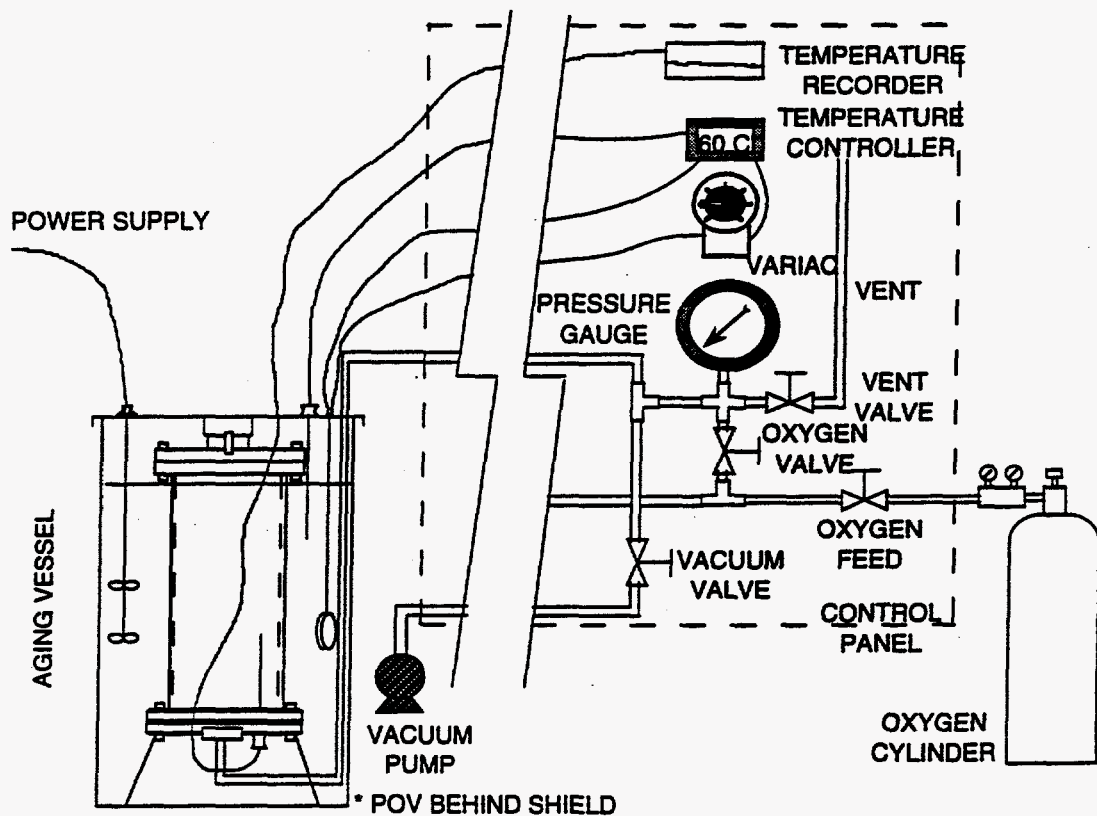


Figure A-4. Pressure Oxygen Vessel and Control Panel

air aging). Once the desired oxygen pressure is reached, the cylinder, regulators, and feed valves are closed.

During the experiment, samples are periodically removed. To obtain samples, the pressure in the vessel is decreased by slowly venting off the oxygen to the atmosphere until the pressure gauge reads zero. The operator removes the top insulation, unbolts the cover flange, and collects the samples. Samples to be aged further are loaded back into the vessel, and the process is repeated. The aged samples are saved for chemical and physical analysis.

CORBETT ANALYSIS

A description of the traditional Corbett (1969) analysis can be found in the standard method ASTM D4124. However, detailed descriptions of the traditional Corbett analysis and the modifications used in this DOE effort can be found in Chapter 2. In addition, a brief description may be found in Chapter 5.

CORBETT ANALYSIS USING N-HEXANE PRECIPITATION AND HIGH PERFORMANCE LIQUID CHROMATOGRAPHY (HPLC)

As described by Pearson et al. (1986) asphalt or a similar sample is weighed to 0.2 ± 0.01 gram in a scintillation vial and mixed with 20 mL of n-hexane. The asphalt/n-hexane solution are then sonicated for 5 minutes to insure good mixing and set overnight. The asphaltenes are removed by filtering the solution through a dried preweighed $0.45 \mu\text{m}$ PTFE membrane syringe filter. After filtering, the filter is further dried in an oven at 100°C (212°F) for an hour and the filtered solution is analyzed using HPLC. The weight difference between the filter before and after filtering is the weight of the asphaltene and the asphaltene content is equal to the weight of asphaltene divided by the weight of the asphalt sample.

A detailed investigation into the use of HPLC for analyzing the saturate content of asphalt and related petroleum materials can be found in Chapter 5. The total aromatic content, the sum of the naphthene aromatic and polar aromatic contents, is determined by difference.

FOURIER TRANSFORM INFRARED SPECTROSCOPY (FTIR)

A Mattson Galaxy series 5020 Spectrometer at 4 cm^{-1} resolution and 64 scans is used to measure the infrared absorbance spectra of asphalt samples. In particular, the Attenuated Total Reflectance, ATR, method with a Zinc Selenide prism is used (Jemison et al., 1992). To quantify the changes in the spectra, the carbonyl content is defined as the integrated absorbance from 1820 to 1650 cm^{-1} with respect to the baseline at the absorbance of 1820 cm^{-1} . This area is called the Carbonyl Area or CA. The range of wave numbers includes the following carbonyl compounds: esters, ketones, aldehydes, and carboxylic acids. The primary absorbance peak for the oxidized asphalt is located at 1700 cm^{-1} and corresponds to ketone formation.

At low aging pressures of 2 and 0.2 atm oxygen and for thick ($\approx 1\text{mm}$) films, oxygen diffusion may be significant. To partially eliminate this diffusion problem, only the exposed surface, ES, of the film is analyzed for kinetic data. For analysis, a quarter of the material in the aluminum tray is removed and the ES placed on the prism face. For samples that have been aged in thinner films, diffusion is probably not significant, so it is possible to measure the spectra of a stirred sample. To insure good contact at the sample/prism interface, the sample is compressed. Heating of the sample is avoided, if possible.

For measuring the spectrum of asphaltenes, the material is dissolved in THF and the solution deposited on the ATR prism drop by drop allowing the THF to evaporate. When the film on the prism is sufficiently thick it is further dried with a heat gun.

DYNAMIC MECHANICAL ANALYSIS (DMA)

The rheological properties of neat and aged asphalt are measured using a Carri-Med 500 Controlled Stress Rheometer. The primary property of interest is the low frequency limiting complex viscosity, η_0^* . This limiting value of the viscosity is obtained at the point where the viscosity of the material becomes independent of frequency or shear rate (Lau et al., 1992). For the more viscous materials (most of the materials), a 2.5 cm (1 in) parallel plate geometry with a 0.5 mm (0.02 in) gap is used at temperatures above 60°C and a 1.5 cm parallel plate is used at

temperatures below 40°C. For low viscosity materials several sizes of cone-and-plate geometry may be used. For materials for which the limiting viscosity can not be obtained at the measurement temperature of interest, additional measurements are performed at elevated temperature. The data are then manipulated according to the time-temperature superposition principle, as described by Ferry (1985) and η_0^* can be calculated.

GEL PERMEATION CHROMATOGRAPHY (GPC)

A WATERS 600E multisolvent delivery system is utilized for gel permeation chromatography (GPC) analyses. Injection is accomplished with a WATERS 700 WISP autoinjector. A WATERS 410 differential refractometer (RI) is utilized for sample detection. Data acquisition and processing are performed using Baseline 810 software.

For GPC analyses, helium-sparged HPLC grade tetrahydrofuran (THF) is used as the mobile phase at a flow rate of 1 mL/min. Three columns of decreasing pore size of 1000, 100, and 50 Å are utilized in series to accomplish separation. The 1000 and 100 Å columns are 7.8 mm ID × 300 mm long and are packed with 7 μm ultrastyrigel particles. The 50 Å column is 7.8 mm ID × 600 mm long and is packed with 5 μm PLGel particles. Samples are prepared by dissolving 0.2 ± 0.01 g of sample in 10 mL of THF. The samples are then filtered through 0.45 μm PTFE membrane syringe filters and 100 μL aliquots are injected onto the columns. Samples are analyzed within 2 days of preparation to reduce potential solvent aging (Burr et al., 1991). Molecular weight distributions are then determined from calibration with polystyrene standards at a concentration of 0.025 g/mL. This is possible because the retention times for the asphalt samples are in the range of the PS standards. The columns and detector are operated isothermally at 313.2 K.

MICRODUCTILITY MEASUREMENTS

A detailed description of the microductility measurements can be found in Chapter 9.

APPENDIX B

THE USE OF HPLC TO DETERMINE THE SATURATE CONTENT OF HEAVY PETROLEUM PRODUCTS

Chaffin, J.M., M.S. Lin, M. Liu, R.R. Davison, C.J. Glover and J.A. Bullin, "The Use of HPLC to Determine the Saturate Content of Heavy Petroleum Products," J. of Liq. Chromatogr. & Rel. Technol., Vol. 19, No. 10, pp. 1669-1682, 1996.

Abstract

The refractive index response factors for several pure saturate fractions isolated from heavy petroleum products were determined using a μ -Bondapak aminopropylmethylsilyl bonded amorphous silica HPLC column. The response factors for saturates obtained from asphalts had an average refractive index response factor of 1.06 ± 0.096 V/g and the saturates obtained from industrial supercritical fractions had an average refractive index response factor of 1.13 ± 0.048 V/g. The difference between these two values can probably be attributed to the fact that different researchers prepared the pure saturates. Based on this assumption, it was possible to obtain an overall response factor for saturates from high boiling petroleum materials. The overall average response factor for the saturates from these heavy petroleum products was determined to be 1.10 ± 0.079 V/g. The data collected in this study indicate that petroleum jelly, with a response factor of 1.05 V/g, may be used as an adequate saturate calibration standard for asphalt and asphalt related materials.

Conclusions

All the previous work on HPLC calibration has relied on the tacit assumption that the saturate data from the standard open column separation methods are correct and that the HPLC saturate contents must be determined in such a way as to minimize the difference between the two values even if this requires obtaining the saturate content by difference. This belief that the open column saturate contents represent the true saturate contents has undoubtedly hindered development of HPLC as an analytical tool in characterization of heavy petroleum products even though it has been known for over ten years that bonded phase HPLC provides better separation of the naphthene aromatics from

the saturates. A natural consequence of this is that the saturate contents determined by HPLC should be more representative of the "true" saturate content. Even with improved and/or complete resolution of the saturate and naphthenic fractions, accurate quantitation of the saturate *character* in the asphalt may never be possible as a molecule containing a benzene ring with an aliphatic side chain with thirty carbon atoms will be grouped as a naphthene aromatic even though it probably exhibits entirely saturate-like behavior in the material.

It has been shown in this study that the refractive index response factors for saturates obtained from heavy petroleum products are similar to each other and to the response factor for petroleum jelly. Therefore, petroleum jelly, with a response factor of 1.05 V/g, may be an *adequate* saturate calibration standard for asphalt and asphalt related materials.

APPENDIX C

SUPERCRITICAL FRACTIONS AS ASPHALT RECYCLING AGENTS AND PRELIMINARY AGING STUDIES ON RECYCLED ASPHALTS

Chaffin, J.M., M. Liu, R.R. Davison, C.J. Glover, J.A. Bullin, "Supercritical Fractions as Asphalt Recycling Agents and Preliminary Aging Studies on Recycled Asphalts," Ind. Eng. Chem. Res., in press.

Abstract

Several asphalts were fractionated using supercritical pentane. These fractions were analyzed by gel permeation chromatography and high-performance liquid chromatography, and their viscosities were measured. The properties of these fractions vary not only among the fractions of a given asphalt but also for the same fraction produced from different asphalts. These widely varied fractions previously have been shown to have potential for reblending to produce superior asphalts. This study investigates the potential for using some of the fractions as asphalt recycling agents. A modified strategic highway research program (SHRP) pressure aging vessel (PAV) test and kinetics studies were conducted on nine recycled asphalts and the original asphalt. The aging indexes of eight of the recycled asphalts are superior to the aging index of the original asphalt. Two of the blends using industrial supercritical fractions and the three blends using laboratory supercritical fractions have lower aging indexes than blends using commercial recycling agents. The kinetics investigation also indicates that at road conditions the recycled asphalts will harden more slowly than the original asphalt. The degree of hardening for a given amount of oxidation in the recycled binders was found to be a strong function of the total saturate content in the recycled binder.

Conclusions

It has been shown that the properties of supercritical fractions produced from fractionation of asphalt vary not only among the fractions of a given asphalt but also for the same fraction produced from different asphalts. Several of the supercritical fractions produced in this study have low enough saturate and asphaltene contents to restore an aged asphalt to a like-new compositional

state. Furthermore, several of the fractions produced in this study also have viscosities suitable for blending with an aged asphalt to restore it to a like-new consistency state.

One aged asphalt was blended with three of the laboratory supercritical fractions, three industrial supercritical fractions, and three commercial recycling agents. The aging indexes after thin film oven test (TFOT) treatment, the aging indexes after pressure aging vessel (PAV) aging, and the extrapolated road conditions hardening rates all indicate that supercritical fractions can be used to produce recycled blends with properties superior to those of the original asphalt. Furthermore, the TFOT and PAV aging indexes from the blends using supercritical fractions are superior to those of the blends produced by using commercial recycling agents. The hardening susceptibilities of the supercritical fraction blends are also generally superior to those of the commercial recycling agent blends. The lower aging indexes for the recycled blends using supercritical fraction rejuvenating agents indicate that using a higher viscosity rejuvenating agent is desirable and that asphaltene dilution is a key factor in asphalt recycling. The hardening susceptibilities for the materials examined in this study are correlated strongly with the saturate content, indicating that minimized saturate content is also important. The generally superior performance of the laboratory supercritical fraction recycled blends can thus be attributed to the narrower cuts produced in the laboratory compared to industrial operation.

This limited study indicates that a supercritical fraction constituting as much as 30% of the asphalt from which it was produced may be useful as a recycling agent. Through proper selection of operating conditions and feedstocks, this percentage could be dramatically increased. Obviously, this could have tremendous impact on asphalt processing and economics.

APPENDIX D

THE EFFECTS OF ASPHALTENES ON THE CHEMICAL AND PHYSICAL CHARACTERISTICS OF ASPHALT

Lin, M.S., K.M. Lunsford, C.J. Glover, R.R. Davison and J.A. Bullin, "The Effects of Asphaltene on the Chemical and Physical Characteristics of Asphalt," In Asphaltene: Fundamentals and Applications, Eds. E.Y. Sheu and O.C. Mullins, Plenum Press, New York, 155, 1995.

Brief Introduction

There are about two million miles of asphalt pavement in this country and billions of dollars are spent annually on building and repairing them. Asphalt roads are constructed with layers of graded crushed stone glued together with asphalt. There are several properties that an asphalt must possess to be a good glue. Obviously it must have good adhesion to the stone. It must set up in a reasonable time and it must be sufficiently ductile to resist cracking under stresses from traffic and temperature changes.

Asphalts vary considerably in these properties, but in general they perform satisfactorily when first laid down in new roads. However, oxidation results in progressive hardening characterized by decreasing ductility and increasing viscosities. This hardening is almost entirely due to the formation of asphaltene, generally defined as paraffin insolubles with heptane, hexane or pentane most commonly used as the solvent.

Conclusions

Our studies conclude

1. With oxidative aging, n-hexane asphaltene content increases in whole asphalts and maltene as a result of carbonyl formation. The presence of the original asphaltene has no effect on the formation of the produced asphaltene per unit oxidation in the whole asphalt until high levels of aging.
2. The produced asphaltene have the very similar rheological effect as the original asphaltene even though they are chemically quite different.

3. A modified Pal-Rhodes model successfully describes the viscosity/asphaltene behavior of both whole asphalts and maltenes.
4. The Hardening Susceptibility is a weak function of asphaltene content for whole asphalts. For maltenes, the HS increases to that of whole asphalt when the %AS content reaches that of whole asphalt.

APPENDIX E

EFFECTS OF ASPHALTENES ON ASPHALT RECYCLING AND AGING

Lin, M.S., R.R. Davison, C.J. Glover and J.A. Bullin, "The Effects of Asphaltenes on Asphalt Recycling and Aging," Transportation Research Record, Vol. 1507, pp. 86-95, 1995.

Abstract

Blends made using n-hexane asphaltenes from asphalts, SHRP AAG-1, AAD-1, and AAK-2 and maltenes from SHRP AAG-1 and AAD-1 were laboratory-aged to study the effects of asphaltenes on rheological properties. For comparison, maltenes from SHRP AAG-1 and AAD-1 as well as their parent asphalts were aged at the same aging conditions as those of blends. The laboratory oxidation conditions were pure oxygen pressure at 20.7 bar absolute, temperatures of 71.1, 82.2, and 93.3°C with aging time from 1 to 24 days depending on aging temperature. The changes due to oxidative aging were monitored by asphaltene precipitation in n-hexane, Fourier transform infrared spectroscopy, and dynamic mechanical analysis at 60°C. Oxidative aging of asphalts and maltenes results in the formation of carbonyl compounds, the production of asphaltenes, and an increase in viscosity. The change in asphaltene content with respect to the change in carbonyl content is quantified by defining the asphaltene formation susceptibility (AFS). The type of asphaltenes, regardless of their sources, have no effect on AFS. Therefore, it appears that AFS is a strong function of maltene composition. However, the effect of asphaltenes on viscosity is only moderately dependent on the asphalt source of the asphaltenes. The results of this study show that the maltene composition has the dominant effect on the oxidation behavior of an asphalt. For recycling of road pavement, the results suggest that a recycling agent should be chosen so that the mixture of the recycling agent and the maltene from the old pavement possesses good oxidation properties.

Conclusions

Based on the research, the following conclusions can be made:

1. With oxidative aging, n-hexane asphaltene content increases in whole asphalts as maltenes as a result of carbonyl formation. The presence of asphaltenes has no effect on the AFS of a

given maltene.

2. The asphaltenes produced by aging exhibit rheological effects very similar to those of the original asphaltenes present in a given maltene, regardless of the asphaltene source. However, the relative viscosity is a strong function of asphaltene content. This implies that maltene solvation power is much more important than asphaltene source.
3. AFS is an extremely important property to consider in asphalt recycling.
4. Asphaltene dilution also should be a major goal in asphalt recycling.

APPENDIX F

**THE EFFECT OF ASPHALT COMPOSITION ON THE FORMATION OF
ASPHALTENES AND THEIR CONTRIBUTION TO ASPHALT
VISCOSITY**

Lin, M.S., J.M. Chaffin, M. Liu, C.J. Glover, R.R. Davison and J.A. Bullin, "The Effect of Asphalt Composition on the Formation of Asphaltenes and Their Contribution to Asphalt Viscosity," Fuel Sci. and Technol. Int'l., Vol. 14, No. 1&2, pp.139-162, 1996.

Abstract

Interactions among asphalt components have significant effects on the performance of asphalt binder. To understand those interactions, four asphalts, SHRP AAA-1, AAD-1, AAF-1 and AAG-1, were fractionated into three generic fractions according to Corbett's procedure and reblended into asphaltenes/aromatics/saturates ternary mixtures in various ratios. Mixtures were oxidatively aged with atmospheric air at temperatures of 87.7, 93.3, and 98.8°C for 5 to 33 days. The changes in chemical composition and physical properties were monitored using Fourier transform infrared spectroscopy (FT-IR) and dynamic mechanical rheometry.

The formation of asphaltenes is a major factor in the hardening of asphalt with aging. The data collected in this study indicate that the saturate content in the maltene phase has a profound impact on the contribution that asphaltenes have on the viscosity of aged asphalt. The data also suggest that the aromatics fraction is solely responsible for the formation of asphaltenes as an asphalt oxidizes.

Conclusions

It has been demonstrated in this study that composition has significant effects on the aging performance of asphalts. The data collected in this study support other researchers findings that asphaltenes and saturates are incompatible. Furthermore, the data collected in this study suggest that asphaltene/saturate incompatibility increases as either asphaltene or saturate content increases. Several specific conclusions that can be drawn from this study follow:

1. The AFS, or asphaltene formation as a function of carbonyl formation, is not affected by the presence of saturates. This, in combination with the previous study on the influence of asphaltenes on the AFS, implies that the AFS is a function of the composition of reactive aromatics.
2. Asphaltenes, both original and those produced through oxidation, increase the viscosity activation energy (E_{vis}). For aged asphalt, the increase in E_{vis} with the increase in asphaltene content through aging can be characterized using $\left(\frac{dE_{vis}}{dCA}\right)$ which is a characteristic aging parameter of an asphalt.
3. Saturates increase $\left(\frac{dE_{vis}}{dCA}\right)$, indicating that high saturate content does serious damage to the performance of asphalt at low temperatures.
4. The $(\log_{10}\eta/\%A)$ function is strongly dependent on the solvent power of the maltene phase. The presence of saturates reduces the solvation power of a maltene, which causes $\log_{10}\eta$ to increase sharply with increasing asphaltene content. This effect is more pronounced as the initial asphaltene content increases.

APPENDIX G

INTERSTATE 45 RECYCLING

Bullin, J.A., C.J. Glover, R.R. Davison, J.M. Chaffin and M.S. Lin, "Development of Superior Asphalt Recycling Agents," Technical Progress Report, DOE/AL/94460-1, pp. 43-54, 1995.

Background

A section of Interstate 45 (I-45) near Madisonville, Texas that was recycled in September and October of 1993 was chosen as a recycling test section. The section of I-45 that was recycled starts at 1993 mile marker 137 and extends to mile marker 141. A two mile stretch between mile marker 141 and mile marker 143 was not recycled and then recycling continued for four miles between mile marker 143 and mile marker 147 using Hot-In-Place-Recycling (HIPR). Hot-In-Place-Recycling is a process where the existing material is heated in place, a set depth of the pavement is roto-milled, fresh hot mix and/or rejuvenator is added, and the mixture is replaced on the road through the screed. All of this takes place in a continuous train of equipment. Addition of fresh hot mix allows the aggregate gradation of the pavement to be altered and slightly softens the pavement. Addition of rejuvenator reduces the viscosity and increases the penetration value. The final mixture should result in a pavement with desired gradation and a viscosity similar to that of a fresh hot mix pavement.

Conclusions

Several samples were collected and analyzed along the 8 mile section of I-45. A total of 42 core samples, along with at least 0.0076 m³ (2 gal) of post-heater (PH) material, at least 0.0038 m³ (1 gal) of add hot mix, and at least 0.0038 m³ of pre-screed (PS) material were obtained. The core samples were tested to determine the void content along with extracting and recovering the asphalt binder. The PH material was also extracted and analyzed similar to the core binders. From the core and PS extractions, it was clear that TxDOT probably under estimated the viscosity (over estimated the pen) of the binder to be recycled. This would result in recycled asphalt that is hard and brittle. To examine this possibility, PS materials were also extracted. Upon comparison of the viscosities between PS Extraction #1 material (10,000 poise) and the TxDOT target viscosity (3,800 poise), it

was confirmed that either TxDOT underestimated the viscosity of the binder to be recycled or the contractor did not add enough of the add-mix (rejuvenating agent).

Several recycling studies were then conducted where the extracted PH materials were blended with five softening agents. Two of the recycling agents were supercritical fractions, two were commercial recycling agents and the last was an AC-3 asphalt. Five samples of the five lab blends and the contractor's blend for each of the four I-45 locations (24 total blends, 120 total samples) were aged in the POV at 82.2°C (180°F) and 20.7 bar O₂ (300 psia). The hardening susceptibility (HS) for each recycled blend was determined by measuring carbonyl areas and blend viscosities. The blends made using commercial agents and those produced using supercritical fractions followed no systematic pattern. Although the HS for the contractor's blends are similar to those of the other recycling agents, the single point viscosity comparison show that using only recycling agents is superior to using an asphalt in combination with a rejuvenating agent. However, no clear distinction between the supercritical fractions and the commercial agents exists using these limited analyses. Clearly some additional criterion for comparison is needed in the future.

Based on the HS obtained from the aging of the laboratory recycled blends and the single point viscosity comparison, two recycling agents were chosen for further study. One supercritical fraction and one commercial recycling agent were blended with the remaining unextracted PH material from all four I-45 locations. Three cores were made for each recycled material. The cores were tested to determine the air voids, they were also subjected to indirect tension, resilient modulus, and Hveem stability tests. Typical values for the void content were near 3.0%, with only 4 cores out of 36 having voids above 3.0% while several had values of 2.0% or lower. The low voids are an indication that the mixes were over-asphalted. The resilient moduli and average tensile strength at failure results were within normal values. All of the cores had non-passing initial Hveem stability values. These poor Hveem stabilities indicate that the aggregate used was of poor quality, or of the wrong gradation. The results of the core tests indicate that mixes made with the supercritical fraction recycling agent and the commercial agent, although over-asphalted, are no worse than those made from the contractor's mix in terms of physical properties and may be better in terms of the limited aging data collected.

APPENDIX H

VISCOSITY MIXING RULES FOR ASPHALT RECYCLING

Chaffin, J.M., R.R. Davison, C.J. Glover, J.A. Bullin, "Viscosity Mixing Rules for Asphalt Recycling," Transportation Research Record, Vol. 1507, pp. 78-85, 1995.

Abstract

Forty-seven aged asphalt-softening agents pairs were blended at multiple levels of aged material content. The relationship between 60°C low-frequency limiting viscosity and aged material mass fraction for 45 of the asphalt-agent pairs can be described using the Grunberg model. The value of the viscous interaction parameter is a strong function of the viscosity difference between the aged asphalt and the softening agent. A normalized Grunberg model was developed to eliminate this dependency. An average normalized interaction parameter can be used to generate a "universal" mixing rule for commercial-type recycling agents. This new mixing rule was compared to the Epps mixing rule and the mixing rule specified in ASTM D4887. Comparison was based on the ability of each mixing rule to predict the quantity of softening agent required to produce blends with a specific target viscosity. It was concluded that for low-viscosity asphalt softening agents, the method specified in ASTM D4887 should be used. However, for supercritical fractions and commercial recycling agents, the universal normalized Grunberg mixing rule developed in this study is superior to the other two mixing rules.

Conclusions

Forty-seven aged asphalt-softening agent pairs were blended at multiple levels of aged material content. For each asphalt-agent pair, 60°C low-frequency limiting viscosities were measured at each aged material content.

The relationship between mixture viscosity and aged material mass fraction for 45 of the asphalt-agent pairs can be described using the Grunberg model. Blends using low-viscosity asphalts as the softening agents exhibited significantly different behavior from blends using commercial recycling agents and supercritical fraction recycling agents. The low-viscosity asphalt softening

agents had viscous interaction parameters close to or greater than zero. All of the blends using supercritical fraction and commercial recycling agents had interaction parameters less than zero.

The value of the interaction parameter G_{12} is a strong function of the viscosity difference between the aged asphalt and recycling agent. Normalizing viscosity in terms of the DLV reduces the difference between recycling agents. In fact, DLV data for all of the recycling agent blends show strikingly little variation between recycling agents regardless of chemical composition or aged asphalt used.

An average normalized interaction parameter was obtained by fitting all of the aged asphalt-recycling agent data. This overall fit was compared to the mixture rule of Epps and the mixing rule specified by ASTM. Comparison was based on the ability of each mixing rule to predict the quantity of softening agent required to produce blends with a specific target viscosity. If a low-viscosity asphalt is to be used as the softening agent to recycle an asphalt, the method specified in ASTM D4887 should be used. However, for prediction of the amount of recycling agent needed to produce the target viscosity, the DLV mixing rule developed in this study is superior to the other two mixing rules.

APPENDIX I

USE OF LIME IN RECYCLING ASPHALT

Wisneski, M.L., J.M. Chaffin, R.R. Davison, J.A. Bullin and C.J. Glover, "The Use of Lime in Recycling Asphalt," Transportation Research Record, Vol. 1535, pp. 117-123, 1996.

Abstract

Two Strategic Highway Research Program asphalts were aged in a pressure oxygen vessel (POV) with and without admixture of CaO and Ca(OH)₂ at several concentrations. These same asphalts were then aged by low-temperature air blowing, and the resulting materials were softened by mixing with three recycling agents obtained by supercritical extraction of asphalts. These rejuvenating asphalts were mixed with varying amounts of CaO and aged in the POV. Oxidation rates and hardening were measured at various temperatures, and the resulting kinetic parameters were used to estimate hardening at road conditions. The hardening rate was always reduced by lime addition. The oxidation rate was sometimes reduced. The recycling agents alone reduced the hardening rates relative to those of the original asphalts, but the effect was further enhanced by CaO additions.

Conclusions

The data indicate that as far as oxidative hardening is concerned and for the limited sample of asphalts and blends studied in this work, lime addition during recycling has a uniformly beneficial effect. For most of the materials, the oxidation rate was also reduced although this may only be a dilution effect. Using the Arrhenius equation to extrapolate to road temperatures, it appears that the improvement in aging rates might be even greater at road conditions than indicated by higher-temperature aging measurements. For the rejuvenating agents used in this study, blending aged asphalt with recycling agent alone (without the addition of lime) improved the HS relative to the original asphalt.

APPENDIX J

ECONOMIC SUMMARY

Bullin, J.A., C.J. Glover, R.R. Davison, M.S. Lin, J.M. Chaffin, M. Liu, and C. Eckhardt, "Development of Superior Asphalt Recycling Agents," Technical Progress Report, DOE/AL/94460-2, pp.114-123 and pp. 142-186, 1996.

Introduction

An economic analysis for using superior asphalt binder in original construction and for using recycling agents with reclaimed asphalt pavement (RAP) to construct overlays is provided. Both of these applications envision the use of a supercritical refinery process to produce an optimal material, either asphalt binder or rejuvenating agent, at added cost (relative to conventional asphalt binder).

Three types of evaluation are considered. The first addresses the incentive for the refiner (as producer) to construct a ROSE unit for producing the recycling agent and/or superior asphalt binder. The second type of evaluation addresses the incentive for departments of transportation (as users) to construct pavements using supercritically-refined asphalt binder. The third addresses the incentive for departments of transportation to recycle pavements using a supercritically-refined rejuvenating agent to mix with reclaimed asphalt pavement (RAP) to produce a viable pavement material.

Conclusions

The annualized cost of producing a recycling agent (RA) from a single residual oil supercritical extraction (ROSE) refinery process with a capacity of handling 30,000 bbl/day of feed to produce 10,000 bbl/day of superior asphalt or recycling agent is \$3.40/bbl. An economic analysis using the DOE-OIT spreadsheet, assuming a sale price for the superior asphalt/rejuvenating agent of \$6.25/bbl, resulted in an internal rate of return (IRR) of 26% for the ROSE process, with a discounted payback period of 4.4 years. This resulted in a superior asphalt binder (or rejuvenating agent) cost of approximately \$135/ton.

In comparing the relative cost and benefit of a superior asphalt pavement to that of a conventional asphalt binder pavement, it was assumed that a new overlay is placed which is 4 inches thick, 30 feet wide (2 lanes), contains 5 wt% binder and 95 wt% aggregate and has a density

approximately twice that of water. With these assumptions, there are 3,270 tons of pavement per mile, which corresponds to 164 tons of asphalt binder/mile (5 wt% binder). The in-place cost of a conventional pavement is approximately \$30/ton of pavement which is approximately \$98,100/mile of pavement. Whereas, the in-place cost of a superior asphalt pavement, assuming a cost of \$135/ton of superior binder, is approximately \$6000/ton of pavement more or \$103,823/mile of pavement. For both the conventional and superior asphalt pavement, a baseline maintenance cost was approximated as one-fourth of the original capital cost (including construction) distributed over the life of the pavement. For the conventional pavement (average service life of 12 years) the cost is \$2,040/mile/year. For the superior-asphalt pavement, assuming a service life of 15 years for example, the cost is \$1,730/mile/year. Several superior-asphalt pavement performance levels were considered in the analysis. Each level represented a different pavement life (15, 18, and 24 years) and was compared to an average life of 12 years for a conventional pavement. The cost to replace the conventional pavement was prorated over its expected life, multiplied by the additional number of years needed to meet the projected life of the superior pavement, and then this amount was distributed over the entire performance period as additional maintenance cost. For each level analyzed, the capital cost of the superior asphalt was larger than that of the conventional asphalt, however, the maintenance cost, energy usage, and waste production values for the superior asphalt were appreciable lower than those of the conventional pavement.

To compare the relative cost and benefit of a recycled asphalt pavement to that of a conventional asphalt binder pavement, the same assumptions as mentioned previously were utilized. This resulted in 3,270 tons of pavement per mile, or 164 tons of asphalt binder/mile (5 wt% binder). The in-place cost of a conventional pavement is approximately \$30/ton of pavement which is approximately \$100,000/mile. The in-place cost of a recycled asphalt pavement, assuming the same costs except for \$135/t for the rejuvenating agent (RA) instead of \$100/t for conventional asphalt and that one ton of the recycled pavement consists of 2/3 ton RAP and 1/3 ton RA/fresh aggregate mixture, is approximately \$8,200/mile of pavement less than the conventional pavement or approximately \$89,900/mile of pavement. The baseline maintenance cost for each pavement is \$24,960/mile. As before, several recycled-asphalt pavement performance levels were considered: 12, 15 and 18 years of pavement life. For each level analyzed, the capital cost, maintenance cost,

energy usage, and waste produced were substantially lower for the recycled asphalt pavement versus values for the conventional asphalt pavement.